

**THE UTILISATIONS OF ENGINEERING SOLID MECHANICS
AND COMPUTATIONAL FLUID DYNAMICS IN ART AND
DESIGN**

BY
HAN LIU

A thesis submitted to
the University of Birmingham
for the degree of
DOCTOR OF PHILOSOPHY

Department of Mechanical Engineering
School of Engineering
College of Engineering and Physical Science of
The University of Birmingham

July 2023

UNIVERSITY OF
BIRMINGHAM

University of Birmingham Research Archive

e-theses repository

This unpublished thesis/dissertation is copyright of the author and/or third parties. The intellectual property rights of the author or third parties in respect of this work are as defined by The Copyright Designs and Patents Act 1988 or as modified by any successor legislation.

Any use made of information contained in this thesis/dissertation must be in accordance with that legislation and must be properly acknowledged. Further distribution or reproduction in any format is prohibited without the permission of the copyright holder.

ABSTRACT

This thesis presents a PhD study that explores the utilisations of engineering solid mechanics and Computational Fluid Dynamics (CFD) in art, engineering and design. In this study, three approaches are presented: (1) the use of Non-uniform Rational B-spline (NURBS) and CFD in art appreciation and art creation; (2) the rigidity of NURBS and its utilisation in Chinese calligraphy; and (3) the practical applications in product and visual design.

The combination of NURBS and CFD can accurately and conveniently draw streamlines to reflect original shapes in art and closely analyse existing ones. Raphael's oil painting *Jacob's Encounter with Rachel* and Ingres' *La Source* were analysed using mathematical and engineering techniques with Computer-Aided Design (CAD), CFD and NURBS as tools. In the analysis, 2D scenes are converted into a 3D model based on perspective projection and CAD. Then the fluid flows are simulated using the Volume of Fluid (VoF) method. The discrepancy in the artworks is shown in the simulation results. In a sketch of a painting, a hypothetical scene with a fluid flow is simulated by CFD, and the streamline of fluid flow is expressed by the NURBS. The method provides a

reliable reference for art appreciation and art creation, especially for realistic artworks.

The research has also explored the rigidity of NURBS mathematically and used it in the study of Chinese calligraphy. The cubic NURBS and beam bending are connected using the dimensionless quantity. The connection represents the rigidity of NURBS and explains why cubic NURBS makes the curve or outline look powerful and soft. Based on the study of the NURBS curve and its rigidity, a piece of calligraphy artwork by Ji Zhao (Song Huizong) is analysed. The results show a surprising similarity between the strokes in the calligraphy and cubic NURBS curves. That means Huizong's calligraphy -Shou Jin Ti- looks slim but strong and powerful because the strokes have a certain rigidity and toughness. The research additionally provides a new approach to guiding artists in drawing a powerful and energetic line more skilfully. This enables people to improve their understanding of and draw the core of Chinese calligraphy with an academic approach.

Some practical cases demonstrate how product and visual design can benefit from the proposed engineering approach using NURBS and CFD. As the samples for product design, pipes, the inlet air duct of TREx, and the sedan

design are discussed. One significant result shows that the working efficiency can be stable if the shape of the pipe is made of NURBS, even if there is a 40° change in angle. The inlet air duct is redesigned using NURBS and CFD, resulting in an easy approach to designing the shape of some components, and making the product meet the functional requirements at the same time. The application of NURBS and CFD also provides a convenient guideline for sedan design. It is shown that the profile of the sedan drawn by cubic NURBS easily meets both the functional requirements and the general aesthetic and reduces the drag by over 20%, compared to that of a simple rounded corner design. For the cases of visual design, the redesign of the casing of TREx and a poster design about TREx are discussed. The redesign of the casing represents the specialisations and technical advantages of TREx, including being environmentally friendly, high-performance, and innovative. A poster showing TREx's technical advantages of energy saving and environmental protection, designed for an international conference, has been highly evaluated by experts in popular design competitions. NURBS plays a significant role in both cases.

ACKNOWLEDGEMENTS

First and foremost, I would like to express my sincere appreciation to my supervisor Professor Kyle Jiang for providing me with the PhD opportunity, giving me support and guidance, and sharing his knowledge and expertise throughout my PhD research. I also want to appreciate my second supervisor, Dr Carl Anthony, for his guidance and help during my study.

I would like to thank Dr Vincent Van Bever Donker for his patient guidance, help, and excellent proofreading. Any remaining errors, of course, are my own. I want to thank Dr Zhongyang He, Dr Tianchu Jiang and Dr Guang Pu for their countless help and valuable advice during my study. Special thanks belong to Miss Qiaoyu Chen, Mr Zhuqiang Xiao and Dr Xiaowei Zhang for their support and help in my study and life. I also appreciate my friends: Mr Hui Dong, Dr Yongsheng Ge and his family, Dr Xianfeng Chen and his family, Mr Zhuowei Guan, Mr Chen Zheng, Mr Yuchen Liang, Mr Guan Wang, Mr Kai Zhu, Mr Chao Liu, Dr. Danying Wang, Mr Chu Yan Wong, Dr Yunluo Yu, Dr Hanyang Xu and Mr Wuyang Zhuge for their companionship. Many thanks belong to my badminton coach: Mrs Lorraine Cole for her patient guidance and training. Also,

I want to thank everyone in our university badminton team for the unforgettable happy time and competitive games they have given me.

Finally, I want to appreciate Dr Jian Cao and his family, and my family. Their unconditional support and encouragement have sustained me to persevere with my research till completion.

TABLE OF CONTENTS

ABSTRACT.....	II
ACKNOWLEDGEMENTS	V
TABLE OF CONTENTS	VII
LIST OF PUBLICATIONS DURING THE PHD STUDY.....	XIII
LIST OF SELECTED AWARDS AND HONOURS DURING THE PHD STUDY	XVI
LIST OF PATENTS	XV
LIST OF TABLES.....	XVI
LIST OF FIGURES	XIX
LIST OF ABBREVIATIONS	XXIX
LIST OF SYMBOLS	XXX
CHAPTER 1. INTRODUCTION	1
1.1. Introduction to the research project.....	1
1.2. Background and motivation.....	2
1.3. Aims and objectives	4
1.4. Thesis outline	5
CHAPTER 2. LITERATURE REVIEW.....	8
2.1. Introduction	8

2.2.	Scientific studies in classic western arts	9
2.3.	The applications of CFD in engineering and art	13
2.4.	CAD in engineering, design and art	16
2.5.	Scientific studies in Chinese calligraphy	21
2.6.	Design and NURBS	26
2.7.	Dimensionless Quantity	29
2.8.	Conclusion	31
CHAPTER 3. CFD AND NURBS FOR THE DESIGN OF FLUID COMPONENTS IN CLASSIC PAINTINGS		33
3.1.	Introduction	33
3.2.	Fluid in traditional realistic fine art	35
3.3.	The two traditional paintings as research samples and their creators.....	37
3.4.	Raphael's <i>Jacob's Encounter with Rachel</i>	46
3.4.1.	Using perspective to model the pond.....	46
3.4.2.	Using CFD to simulate the water flowing out of the pond from the main outlet.....	54
3.5.	Ingres' <i>La Source</i>	57
3.5.1.	Using perspective to model the fluid containers	57
3.5.2.	Using CFD to simulate the water flow.....	62

3.6.	Results	63
3.6.1.	Raphael's Jacob's Encounter with Rachel	63
3.6.2.	Ingres' La Source.....	66
3.7.	Discussion, extensions, and implications	70
3.8.	Method testing and practising in art creation.....	73
3.8.1.	Designing and modelling the liquid container	74
3.8.2.	The simulation of the water flow	76
3.8.3.	The sketch of the artwork produced with the method	77
3.9.	Conclusion	79
CHAPTER 4. THE RIGIDITY OF NURBS AND ITS APPLICATION IN CHINESE CALLIGRAPHY		80
4.1.	Introduction	80
4.2.	The rigidity of NURBS and the dimensionless quantity	82
4.2.1.	Using NURBS to fit beam bending in visual.....	86
4.2.2.	Using dimensionless quantity to bridge NURBS and beam bending in mathematics.....	92
4.3.	Application of the rigidity of NURBS in art (Chinese calligraphy) 108	
4.3.1.	The power and toughness in Chinese calligraphy	108
4.3.2.	The rigidity of strokes in Huizong's Shou Jin Ti.....	113

4.4.	Results	137
4.4.1.	The rigidity of NURBS and dimensionless quantity	137
4.4.2.	Application of the rigidity of NURBS in art (Chinese calligraphy)	149
4.5.	Conclusions.....	162
4.6.	Discussion, extensions, and implications	165
CHAPTER 5. METHOD APPLICATIONS IN DESIGNS		172
5.1.	Introduction	172
5.2.	NURBS and CFD in pipe design	175
5.3.	NURBS, CFD, and the design of industrial product components 183	
5.4.	A guide to the sedan design.....	189
5.4.1.	Using NURBS to fit the outline of the car and build the model via CAD.....	190
5.4.2.	Using CFD to simulate the running and calculate the drag 194	
5.5.	The other cases of design using the application of NURBS	202
5.5.1.	The redesign of the casing of TREx.....	202
5.5.2.	A poster design about TREx.....	208
5.6.	Results	212

5.6.1.	NURBS and CFD in pipe design.....	212
5.6.2.	NURBS, CFD, and the design of industrial product components	214
5.6.3.	A guide to the sedan design	214
5.6.4.	The other cases of design using the application of NURBS	
	215	
5.7.	Conclusions, extensions, and implications	217
CHAPTER 6. CONCLUSIONS AND FUTURE WORK.....		221
6.1.	Introduction	221
6.2.	Conclusions.....	221
6.3.	Summary of novel contributions to knowledge	223
6.4.	Proposal for future work	225
APPENDIX.....		227
1.	The code in the analysis of approximation of Cantilever beam with NURBS	227
2.	The code in the analysis of cantilever beam of Case 2&6 and NURBS	231
3.	The code in the analysis of simply supported beam of Case 4 and NURBS	235
4.	The code in the analysis of the rigidity of strokes in Huizong's Shou	

Jin Ti 238

REFERENCES241

LIST OF PUBLICATIONS DURING THE PHD STUDY

1. **Han Liu**, Vincent Van Bever Donker, Kyle Jiang. “CFD and NURBS for the Drawing of Fluid Flow in Classic Painting”, 2023 IEEE Smart World Congress (SWC)
2. **Han Liu**, Vincent Van Bever Donker, Kyle Jiang. “A scientific study of La Source by Jean Auguste Dominique Ingres”, “CONNECTIONS: EXPLORING HERITAGE, ARCHITECTURE, CITIES, ART, MEDIA” in Canterbury 2020
3. Junchao Yi, Xiaowei Zhang, Guozheng Liu, Jeremy H. Rao, **Han Liu***. “Microstructure and dynamic microhardness of additively manufactured (TiB₂+TiC)/AlSi10Mg composites with AlSi10Mg and B₄C coated Ti powder”, April 2023 Journal of Alloys and Compounds 939:168718
4. Yibo Han, Xiaowei Zhang, **Han Liu**, Meng Xu, Guochao Gao. “Structural design, numerical examination and experimental approach of the multi-powder mixer for directed energy deposition”, Powder Technology, Volume 398, January 2022, 117144

5. Yibo Han, Xiaowei Zhang, Mingzong Wang, **Han Liu**, Guochao Gao, Meng Xu, Jingxuan Ao, Yaozeng Cai, Jinzhe Wang. “ Numerical Examination and Experimental Approach of L-Pbfed Vortex Mixer for Directed Energy Deposition”, SSRN Electronic Journal, November 2022

6. Guochao Gao, Xiaowei Zhang, Yibo Han, Meng Xu, **Han Liu**, Jingxuan Ao, Yaozeng Cai, Jinzhe Wang, Mingzong Wang. “Structural design of a coaxial-jet vortex powder mixer for multi-material directed energy deposition”, April 2023 Powder Technology 425:118586

LIST OF PATENTS

1. Han Liu, Kaichun Jiang. 2023. Unmanned Aerial Vehicle. China. (submitted)
2. Kaichun Jiang, Han Liu. 2021. Gas Turbine (Micro). China. Patent ZL 2020 3 0464923. 9, filed August 14, 2020, and issued January 5, 2021.

LIST OF SELECTED AWARDS AND HONOURS DURING THE PHD STUDY

1. Silver Prizes x 3 of “A’ Design Award” 2019-2020 (one of the top levels of international design competitions in Italy)
2. Was invited to and exhibited in “Chinese Rat Year Digital Design Exhibition” 2020 (international design exhibition)
3. Was invited to and exhibited in “The 2019 San Jose International Digital Design” (international design exhibition)
4. Silver and Bronze Prizes of the Novum Design Award 2019 (international design competition)
5. Was invited to and exhibited “The 2019 Spring International Digital Design Invitation Exhibition” (international design exhibition)
6. Winner of “German Design Award” 2019 x4 (one of the top levels of international design competitions in Germany)
7. Designs are included in “JOSEPH BINDER AWARD BOOK”
8. Winner of “The Red-dot Award” 2018-2019 (the most popular international design competition)
9. Golden Prize of “MUSE Creative Awards 2018-2019 (one of the top levels of international design competitions in USA)
10. Was invited to and exhibited in “The 2018 GIRONA International Digital Design Invitation Exhibition”

11. Bronze Prize of "A' Design Award" 2018
12. Winner of "The Red-dot Award" 2017-2018
13. Golden Prize of "MUSE Creative Awards 2017-2018
14. Bronze Prize of "The 11th Annual IDA Design Award" 2017-2018

LIST OF TABLES

Table 5-1. The working efficiency of the pipe changes while the length increases.....180

Table 5-2. The working efficiency of the pipe changes while the angle increases.181

Table 5-3. The working efficiency of the pipe changes while the diameter increases.182

LIST OF FIGURES

Figure 2-1. The six processes of designing include Recognition of need, Definition of problem, Synthesis, Analysis and optimization, Evaluation and Presentation. “The synthesis of a scheme connecting possible system elements is sometimes called the invention of the concept or concept design, and it shows that synthesis and analysis and optimization are intimately and iteratively related. Evaluation is a significant phase of the total design process and the final proof of a successful design “, usually involving the testing of a prototype in the laboratory. Presentation is the step of communicating or selling a job in design. It is the final with a different challenge because the designers or engineers need to prove that their solution is a better one, compared to the others.

..... 17

Figure 2-2. The simplified processes of designing..... 18

Figure 2-3. Application of CAD to the design process..... 18

Figure 2-4. the three vertices of the product design triangle 27

Figure 3-1. ‘A Mediterranean beach’ by Han Liu. The artwork is produced by coding written with Python, a high-level, general-purpose programming language..... 36

Figure 3-2. The School of Athens painted by Raphael. 39

Figure 3-3. The Last Supper painted by Leonardo. 39

*Figure 3-4. Jacob’s Encounter with Rachel (pixel 926*608, 300 DPI) 42*

Figure 3-5. La Source..... 43

Figure 3-6. The stone pond in Jacob’s Encounter with Rachel..... 47

Figure 3-7. The Matlab code for showing all the pixels of the JPEG file. There are two steps: the first is importing the image to Matlab, and the second is putting the parameter in pixels on the image. Then the coordinate axis is drawn in markable units (pixels). 48

Figure 3-8. The image is displayed with the data of pixel axes..... 49

Figure 3-9. The key points of the man and stone pond. 49

Figure 3-10. The central axis, the key points of the water and the main outlet. 52

Figure 3-11. The points of (xo, yo1) and (xo, yo2) show the height of (xo, yo1) on the exterior wall of the water pond..... 53

Figure 3-12. The top view of the 3D model of the pond. 53

Figure 3-13. The 3D model of the pond, the water and the main outlet. 54

<i>Figure 3-14. The model for CFD analysis includes the water (the blue zone), the air (the grey zone), the wall of the pond (the white zone) and the passage of the water flowing out from the main outlet (the orange tunnel).</i>	55
<i>Figure 3-15. The start of the water flows out from the pond.</i>	56
<i>Figure 3-16. In the process, the water flows out from the pond.</i>	56
<i>Figure 3-17. The pitcher in a digital grid graph.</i>	58
<i>Figure 3-18. The schematic diagram of the opening</i>	59
<i>Figure 3-19. The outline is fitted by quadratic NURBS.</i>	60
<i>Figure 3-20. The outline is fitted by cubic NURBS.</i>	61
<i>Figure 3-21. The outline is fitted by quartic NURBS.</i>	61
<i>Figure 3-22. The outline is fitted by quintic NURBS.</i>	61
<i>Figure 3-23. The digital model of the pitcher</i>	62
<i>Figure 3-24. The start of the water flow.</i>	63
<i>Figure 3-25. The end of the water flow.</i>	63
<i>Figure 3-26. The comparison of Raphael's water flow and the simulation result</i>	64
<i>Figure 3-27. The red track is the water flow in Raphael's painting, the blue zone is the track of the water flow in simulation with more reasonable conditions.</i>	65
<i>Figure 3-28. According to the simulation results, it is inferred that the red zone will be the more reasonable passageway for the water track from Raphael's painting.</i>	66
<i>Figure 3-29. The model was built by quadratic NURBS.</i>	67
<i>Figure 3-30. The model was built by cubic NURBS.</i>	67
<i>Figure 3-31. The comparison of the painting-pitcher and the converted 3D model.</i>	68
<i>Figure 3-32. In the comparison of the simulation and the original painting, the red track is the water flow in Ingres' painting, the blue zone is the track of the water flow in the simulation.</i>	69
<i>Figure 3-33. The left view of the liquid container</i>	74
<i>Figure 3-34. The front view of the liquid container</i>	75
<i>Figure 3-35. The top view of the liquid container</i>	75
<i>Figure 3-36. The bottom view of the liquid container</i>	75
<i>Figure 3-37. The start of the water flow</i>	76
<i>Figure 3-38. The water flow at 2.9999 seconds</i>	76
<i>Figure 3-39. The scene is the water flowing out from the liquid container and the blue zone is the track of the water flow. The water flow path changes when the view angle changes.</i>	77
<i>Figure 3-40. Susanna at her Bath by Han LIU (draft)</i>	78
<i>Figure 4-1. Case NO. 1 (the loading at the end)</i>	84
<i>Figure 4-2. Case NO. 2 (the loading on the top surface)</i>	84
<i>Figure 4-3. Case NO. 3</i>	84

Figure 4-4. Case NO. 4 (the loading at the middle).....	84
Figure 4-5. Case NO. 5 (the loading at a random point).....	85
Figure 4-6. Case NO. 6 (the loading on the top surface).....	85
Figure 4-7. Case NO. 7.....	85
Figure 4-8. A NURBS with second order.....	86
Figure 4-9. The platform is bent because of the load on the endpoint. (The image was found from the Internet on 23rd June 2021.).....	87
Figure 4-10. The platform is simplified using Photoshop.	88
Figure 4-11. A quadratic NURBS curve is drawn in UG-NX.....	88
Figure 4-12. This is an example - the sketch by Han Liu - of the simply supported beam with Fixed hinge support and Sliding hinge support in engineering. The types of Sliding hinge support are various in practical applications. In this example, there is a corridor between the two buildings. Since the deformation of the two buildings is not consistent, the corridor is made into a simply supported beam, one end is Fixed hinge support, and the other end is Sliding hinged support.....	89
Figure 4-13. The simulation result of the steel beam.....	90
Figure 4-14. The curve is drawn by directional deformations of the beam. A is the third directional deformation.....	91
Figure 4-15. The comparison of the deformations and quadratic NURBS.....	91
Figure 4-16. This is the comparison of the deformations and cubic NURBS. Because the deformation curve is a parabola, the locations of the control points need to be mirrored.....	92
Figure 4-17. The Beam Deflection and Slopes.....	93
Figure 4-18. The comparison of fitted NURBS and deflection curve for Case NO. 2. The blue and red lines overlap.....	105
Figure 4-19. The comparison of fitted NURBS and deflection curve for Case NO. 4. The blue and red lines overlap.....	106
Figure 4-20. The comparison of fitted NURBS and deflection curve for Case NO. 6. The blue and red lines overlap.....	108
Figure 4-21. The eight components of the character Yung.....	110
Figure 4-22. Both straight and curvy strokes were used in He Yang Ling Cao Quan Bei made in Han Dynasty (185 A.D.). In its rubbing, the characters represent both power and rigidity. The curvy strokes do not seem to follow certain rules of change, and the straight strokes had not been curved much.....	111
Figure 4-23. The straight strokes were used in Han Gu Gu Cheng Chang Dang Yin Ling Zhang Jun Biao, also called Zhang Qian Bei, made in Han Dynasty (186 A.D.). In its rubbing, straight strokes show the power and hardness of the characters. Every word looks approximately square.....	112

Figure 4-24. In this piece of Hui Zong's calligraphy named Run Zhong Qiu Yue Tie (1110 A.D.), every stroke seems curved, and the changes in the strokes seem to follow specific rules. All the changes make the characters represent the beauty of slimness and elegance. The work is now preserved in the Palace Museum in Beijing.....112

Figure 4-25. In the character "Zhong" from Run Zhong Qiu Yue Tie, the basic strokes "—" and " | " have been highlighted in red.114

Figure 4-26. In the character "Qiu", the basic strokes "—", " J " and " \ " have been highlighted in red.114

Figure 4-27. In the character "Di", the basic strokes "—", " | " and " / " have been highlighted in red.115

Figure 4-28. The beam in Case NO.1 fitted by cubic NURBS with a -0.05-unit deformation.....117

Figure 4-29. In the character of Zhong, the first basic stroke "—" is extracted and highlighted in orange.....118

Figure 4-30. The second basic stroke " | " is extracted and highlighted in orange.119

Figure 4-31. In the character of Qiu, the third and fourth basic strokes " J ", and " \ " are extracted and highlighted.....119

Figure 4-32. In the character of Di, the fifth basic stroke " / " is extracted and highlighted in orange.....120

Figure 4-33. To simulate Cases NO.1 and NO.2, the basic stroke "—" is put in a Cartesian coordinate and the approximate deformation shows as -0.37 unit.122

Figure 4-34. To simulate Cases NO.4 and NO.6, the basic stroke "—" is put in a Cartesian coordinate and the approximate deformation shows as 0.05 unit.122

Figure 4-35. In Case NO.1, the cubic NURBS curve is produced based on the given deformation (-0.37).123

Figure 4-36. In Case NO.2, the cubic NURBS curve is produced based on the given deformation (-0.37).123

Figure 4-37. In Case NO.4, the cubic NURBS curve is produced based on the given deformation (0.05).....124

Figure 4-38. In Case NO.6, the cubic NURBS curve is produced based on the given deformation (0.05).....124

Figure 4-39. To simulate Cases NO.1 and NO.2, the basic stroke " | " is put in a Cartesian coordinate and the approximate deformation shows as -0.10 unit.125

Figure 4-40. To simulate Cases NO.4 and NO.6, the basic stroke “ ” is put in a Cartesian coordinate and the approximate deformation shows as 0.02 unit.	125
Figure 4-41. In Case NO.1, the cubic NURBS curve is produced based on the given deformation (-0.10).....	126
Figure 4-42. In Case NO.1, the cubic NURBS curve is produced based on the given deformation (-0.10).....	126
Figure 4-43. In Case NO.4, the cubic NURBS curve is produced based on the given deformation (0.02).....	127
Figure 4-44. In Case NO.6, the cubic NURBS curve is produced based on the given deformation (0.02).....	127
Figure 4-45. To simulate Cases NO.1 and NO.2, the basic stroke “ J ” is put in a Cartesian coordinate and the approximate deformation shows as -0.265 unit.....	128
Figure 4-46. To simulate Cases NO.4 and NO.6, the basic stroke “ J ” is put in a Cartesian coordinate and the approximate deformation shows as 0.055 unit.	128
Figure 4-47. In Case NO.1, the cubic NURBS curve is produced based on the given deformation (-0.265).....	129
Figure 4-48. In Case NO.2, the cubic NURBS curve is produced based on the given deformation (-0.265).....	129
Figure 4-49. In Case NO.4, the cubic NURBS curve is produced based on the given deformation (0.055).....	130
Figure 4-50. In Case NO.6, the cubic NURBS curve is produced based on the given deformation (0.055).....	130
Figure 4-51. To simulate Cases NO.1 and NO.2, the basic stroke “ \ ” is put in a Cartesian coordinate and the approximate deformation shows as -0.62 unit.	131
Figure 4-52. To simulate Cases NO.4 and NO.6, the basic stroke “ \ ” is put in a Cartesian coordinate and the approximate deformation shows as 0.17 unit.	131
Figure 4-53. In Case NO.1, the cubic NURBS curve is produced based on the given deformation (-0.62).....	132
Figure 4-54. In Case NO.2, the cubic NURBS curve is produced based on the given deformation (-0.62).....	132
Figure 4-55. In Case NO.4, the cubic NURBS curve is produced based on the given deformation (0.17).....	133
Figure 4-56. In Case NO.6, the cubic NURBS curve is produced based on the given deformation (0.17).....	133

Figure 4-57. To simulate Cases NO.1 and NO.2, the basic stroke “↗” is put in a Cartesian coordinate and the approximate deformation shows as -0.11 unit.134

Figure 4-58. To simulate Cases NO.4 and NO.6, the basic stroke “↗” is put in a Cartesian coordinate and the approximate deformation shows as 0.035 unit.134

Figure 4-59. In Case NO.1, the cubic NURBS curve is produced based on the given deformation (-0.11).135

Figure 4-60. In Case NO.2, the cubic NURBS curve is produced based on the given deformation (-0.11).135

Figure 4-61. In Case NO.4, the cubic NURBS curve is produced based on the given deformation (0.035).136

Figure 4-62. In Case NO.6, the cubic NURBS curve is produced based on the given deformation (0.035).136

Figure 4-63. The comparison between the platform and the fitted quadratic NURBS curve.138

Figure 4-64. The comparison between the platform and the fitted cubic NURBS curve.138

Figure 4-65. The comparison between the platform and the fitted quartic NURBS curve.139

Figure 4-66. The output shows the cubic curve (NURBS), the curve of the bent cantilever beam, and the control points. In this image, the blue line is the theoretical beam bending curve, the blue squares are the control points (there are four in total), and the red cross is the points of the cubic spline (NURBS) fitting.140

Figure 4-67. The zoomed-in Figure 4-66 shows the fitting is very good visually. From this image, it is clear that all the red cross points - the points of the cubic spline (NURBS) fitting - are on the theoretical beam bending curve.141

Figure 4-68. The comparison has shown the equivalence between the y- coordinates of the theoretical beam bending curve (the group A of the parameter) and the y- coordinates of the cubic fitting curve (the group B of the parameter). Here for the parameter comparison, only a small group of the units is selected because there are 1000 points, and it is not necessary to show all the numbers.142

Figure 4-69. The output shows the cubic curve (NURBS), the curve of the bent cantilever beam, and the control points. In this image, the blue line is the theoretical beam bending curve, the green triangle is the points of the cubic NURBS without weight fitting and the error is 3.5521e-07, the red triangle is the points of the cubic NURBS with weight fitting and the error is 1.6724e-07, and the blue star means the control points of the cubic NURBS curve. This image shows the fitting is very good

visually. From this image, it is clear that all the green and red triangles look appear to overlap, and on the theoretical beam bending curve.....143

Figure 4-70. The comparison has shown the similarity between the y- coordinates of the theoretical beam bending curve (the group A of the parameter) and the y- coordinates of the cubic fitting curve (no weight) (the group B of the parameter). Here for the parameter comparison, only a small group of the units is selected because there are 100 points. So, it is not necessary to show all the numbers.144

Figure 4-71. The comparison has shown the similarity between the y- coordinates of the theoretical beam bending curve (the group A of the parameter) and the y- coordinates of the cubic fitting curve (with weight) (the group B of the parameter). Same to the previous comparison, only a small group of the units is selected.145

Figure 4-72. The output shows the cubic curve (NURBS), the curve of the bent simply supported beam, and the control points. In this image, the blue line is the theoretical beam bending curve, the green triangle is the points of the cubic NURBS without weight fitting and the error is $8.294e-07$, the red triangle is the points of the cubic NURBS with weight fitting and the error is $4.7357e-07$, and the blue star means the control points of the cubic NURBS curve. This image shows the fitting is very good visually. In this image, all the green and red triangles look appear to overlap, and on the theoretical beam bending curve.146

Figure 4-73. The comparison has shown the similarity between the y- coordinates of the theoretical beam bending curve (the group A of the parameter) and the y- coordinates of the cubic fitting curve (no weight) (the group of B the parameter). Here for the parameter comparison, only a small group of the units is selected because there are 100 points. So, it is not necessary to show all the numbers.147

Figure 4-74. The comparison has shown the similarity between the y- coordinates of the theoretical beam bending curve (the group A of the parameter) and the y- coordinates of the cubic fitting curve (with weight) (the group B of the parameter). Same to the previous comparison, only a small group of the units is selected.148

Figure 4-75. In Case NO.1, the basic stroke “—” is fitted by the cubic NURBS curve with the given deformation (-0.37).....150

Figure 4-76. In Case NO.2, the basic stroke “—” is fitted by the cubic NURBS curve with the given deformation (-0.37).....150

Figure 4-77. In Case NO.4, the basic stroke “—” is fitted by the cubic NURBS curve with the given deformation (0.05).....151

Figure 4-78. In Case NO.6, the basic stroke “—” is fitted by the cubic NURBS curve with the given deformation (0.05).....151

Figure 4-79. In Case NO.1, the basic stroke “|” is fitted by the cubic NURBS curve with the given deformation (-0.10).....152

Figure 4-80. In Case NO.2, the basic stroke “ ” is fitted by the cubic NURBS curve with the given deformation (-0.10).....	153
Figure 4-81. In Case NO.4, the basic stroke “ ” is fitted by the cubic NURBS curve with the given deformation (0.02).....	153
Figure 4-82. In Case NO.6, the basic stroke “ ” is fitted by the cubic NURBS curve with the given deformation (0.02).....	154
Figure 4-83. In Case NO.2, the basic stroke “ ” is fitted by the cubic NURBS curve with the given deformation (-0.095).....	155
Figure 4-84. In Case NO.1, the basic stroke “ J ” is fitted by the cubic NURBS curve with the given deformation (-0.265).....	155
Figure 4-85. In Case NO.2, the basic stroke “ J ” is fitted by the cubic NURBS curve with the given deformation (-0.265).....	156
Figure 4-86. In Case NO.4, the basic stroke “ J ” is fitted by the cubic NURBS curve with the given deformation (0.055).....	156
Figure 4-87. In Case NO.6, the basic stroke “ J ” is fitted by the cubic NURBS curve with the given deformation (0.055).....	157
Figure 4-88. In Case NO.1, the basic stroke “ \ ” is fitted by the cubic NURBS curve with the given deformation (-0.62).....	158
Figure 4-89. In Case NO.2, the basic stroke “ \ ” is fitted by the cubic NURBS curve with the given deformation (-0.62).....	158
Figure 4-90. In Case NO.4, the basic stroke “ \ ” is fitted by the cubic NURBS curve with the given deformation (0.17).....	159
Figure 4-91. In Case NO.6, the basic stroke “ \ ” is fitted by the cubic NURBS curve with the given deformation (0.17).....	159
Figure 4-92. In Case NO.1, the basic stroke “ / ” is fitted by the cubic NURBS curve with the given deformation (-0.11).....	160
Figure 4-93. In Case NO.2, the basic stroke “ / ” is fitted by the cubic NURBS curve with the given deformation (-0.11).....	161
Figure 4-94. In Case NO.4, the basic stroke “ / ” is fitted by the cubic NURBS curve with the given deformation (0.035).....	161

Figure 4-95. In Case NO.6, the basic stroke “/” is fitted by the cubic NURBS curve with the given deformation (0.035).....	162
Figure 4-96. A part of Xizhi Wang’s calligraphy work “Lan Ting Ji Xu” in 353.....	167
Figure 4-97. A part of Zhenqing Yan’s calligraphy work “Duo Bao Ta Bei” in 752.....	168
Figure 4-98. Two pieces of handwriting by Moruo Guo.....	169
Figure 4-99. From the comparison between the generated Huizong-style font (left) and Huizong’s art (right), it is not difficult to find the difference. In the characters generated by a computer program, the strokes look different from Huizong’s calligraphy, especially in curves relevant to the basic strokes which have been highlighted in orange. The differences make the generated characters miss the core and the most important “soul” of Huizong’s art.	171
Figure 5-1. The shape of the pipe is made of quadratic NURBS. The plane where the point P1 is located and the plane where the point P2 are the inlet and outlet of the pipe. Because $\Delta P1P2P3$ is an isosceles right triangle, so the length of P1P2 is equivalent to that of P2P3, the $\angle P1P2P3=90^\circ$	177
Figure 5-2. The image shows both the inlet air duct and the main body of TREx have curvy shapes.....	185
Figure 5-3. The side view of the previous design of the inlet air duct.....	185
Figure 5-4. The simulation result of the previous design of the compressor inlet air duct.....	186
Figure 5-5. The side view of the optimised design of the inlet air duct.....	187
Figure 5-6. The simulation result of the optimised design of the compressor inlet air duct.....	188
Figure 5-7. The general structure of the sedan is shown. In this image, the engine and relevant components, the dashboard, the steering wheel, the wheels, the seats, the people with an appropriate ratio, the chassis and a general casing are found. The positions of all the essential components of the car are reliable and ergonomic.....	191
Figure 5-8. The blue boxes are the approximate necessary space for a car. The orange dots are the key inflexion points.....	191
Figure 5-9. The general outline is fitted by quadratic NURBS.....	192
Figure 5-10. The general outline fitted by cubic NURBS.....	193
Figure 5-11. The general outline is fitted by quartic NURBS.....	193
Figure 5-12. The general outline fitted by quintic NURBS.....	193
Figure 5-13. In the model for the simulation, the green area is the room for airflow; there is a gap between the chassis of the sedan and the ground; the air comes from the left and goes through to the right. The profile of the sedan in this image is drawn with cubic NURBS. Then the model now meets the requirements of the simulation.....	195

<i>Figure 5-14. The velocity of the quadratic outline.....</i>	196
<i>Figure 5-15. The velocity of the cubic outline.....</i>	196
<i>Figure 5-16. The velocity of the quartic outline.....</i>	196
<i>Figure 5-17. The velocity of the quintic outline.....</i>	197
<i>Figure 5-18. The total pressure of the quadratic outline.....</i>	197
<i>Figure 5-19. The total pressure of the cubic outline.....</i>	197
<i>Figure 5-20. The total pressure of the quartic outline.....</i>	198
<i>Figure 5-21. The total pressure of the quintic outline.....</i>	198
<i>Figure 5-22. The sedan's body with a right-angle design.....</i>	200
<i>Figure 5-23. The sedan's profile with a rounded design.....</i>	200
<i>Figure 5-24. The velocity of the rounded design outline.....</i>	200
<i>Figure 5-25. The pressure of the rounded design outline.....</i>	201
<i>Figure 5-26. The comparison of the 2018 PORSCHE 911 and cubic outline (yellow line).</i>	201
<i>Figure 5-27. From the main view of the new casing of TReX, the inlet air duct, the upper and lower half of the main body, the concave structures and the bolts for assembling can be found. The outlet air duct is not shown due to the angle of the view.</i>	205
<i>Figure 5-28. The image of the front display.....</i>	205
<i>Figure 5-29. The image of the top display.....</i>	206
<i>Figure 5-30. The image of the bottom display.....</i>	206
<i>Figure 5-31. The inlet air duct, the main body of the casing and the outlet air duct are shown in this image.....</i>	207
<i>Figure 5-32. The image of the status of use.....</i>	207
<i>Figure 5-33. Page one of the designs of TReX posters.....</i>	209
<i>Figure 5-34. Page two of the designs of TReX posters.....</i>	210
<i>Figure 5-35. Page three of the designs of TReX posters.....</i>	211
<i>Figure 5-36. The assembled casing.....</i>	216
<i>Figure 5-37. The inlet air duct (left) and outlet air duct (right).....</i>	216

LIST OF ABBREVIATIONS

2.5D	2.5-dimensional
2D	Two-dimensional
3D	Three-dimensional
B-Spline	Basic Spline
CAD	Computer-Aided Design
CFD	Computational Fluid Dynamics
NURBS	Non-Uniform Rational B-Splines
TREx	Turbo Range Extender
VoF	Volume of Fluid

LIST OF SYMBOLS

P_x	Control point [-]
C	Curve [-]
x	Displacement components in x directions [-]
y	Displacement components in y directions [-]
p	Load
L	Length of a beam
E	Young's modulus
I	Intersection shapes
α_x	Constant term
t	Variable
a_x	Constant term
b_x	Constant term
M	Torque
y_{NURBS}	NURBS curve

CHAPTER 1. INTRODUCTION

1.1. Introduction to the research project

Leonardo da Vinci once said that “He who loves practice without theory is like the sailor who boards a ship without a rudder and compass and never knows where he may cast.”¹ Similarly, scientific theory plays an important role in both figurative Western classical painting and abstract Chinese calligraphy art.

This thesis explores the utilisations of engineering solid mechanics and Computational Fluid Dynamics (CFD) in art, engineering and design. CFD, Computer-aided design (CAD) and NURBS are used in the analysis of classic artworks. The rigidity of NURBS is explained by the dimensionless quantity which links beam bending and the NURBS curve. Several practical applications in product and visual design benefit from the method.

In this PhD project, Raphael's classic oil painting and Ingres' *Neoclassical artwork* were analysed using mathematical and engineering techniques with CAD, CFD and NURBS as tools. Then, the cubic NURBS and beam bending

are connected using the dimensionless quantity and based on that, a piece of calligraphy artwork by Song Huizong is analysed. Following that, the cases of industrial product designs and digital visual designs are used to demonstrate how design can benefit from the proposed engineering approach using NURBS and CFD.

This chapter first presents the study's background, which supports the motivation, in Section 1.2. Then, section 1.3 demonstrates the aim and objectives of the research in order to define the scope of the study and section 1.4, lastly to the focus of each chapter.

1.2. Background and motivation

Many studies focus on the link between art and science and many scientific theories are used in art and design. The relationship between art and scientific theory has changed more and more, and their connection has become closer.

From ancient Greece to today, artistic creation has been influenced by the development of scientific theories. In Ancient Greece *techne* inspired art and the artworks symbolized the alliance of science with beauty.² Ancient Greek

sculptures had high requirements for the accuracy of modelling.³ Later, the classical oil paintings, murals and sculptures of the Renaissance also attached great importance to accuracy. Not only that, more scientific theories such as anatomy, perspective and geometry are used in painting teaching and artistic creation.⁴ Martin Kemp discusses how classic western art benefits from perspective, mechanical engineering and optics.⁵ The development of scientific theories allows more mathematical theories, physical theories and chemical research results to be integrated into artistic creation. Some Chinese researchers proposed an approach to shape description for Chinese calligraphy characters using the cubic Bezier curve which is a NURBS-like piecewise curve function described via four control points.^{6 7 8} Graphic design -a sort of visual art- and illustration have evolved in tandem with the methods of scientific research.⁹ Also, people try to discover the foundations of product and visual design thinking in the fine arts, the natural sciences, or the social sciences.¹⁰ Today, the concept of the metaverse enables even more art forms, through Virtual Reality (VR) and Augmented reality (AR) technologies.¹¹

The applications of scientific theory in the arts have been developed in a variety of ways. However, the utilisations of engineering solid mechanics and CFD in art, engineering and design are worth continuing to expand and develop. The

links between solid mechanics or CFD and art-related creations are required, particularly for studying classic artworks and Chinese calligraphy. These issues are addressed in this thesis.

1.3. Aims and objectives

This PhD project aims to progress the research of the utilisations of engineering solid mechanics and CFD in art, engineering and design, which involves: the use of NURBS and CFD in art appreciation and art creation; the rigidity of NURBS and its utilisation in Chinese calligraphy; and the practical applications in product and visual design. Furthermore, the study links cubic NURBS and beam bending with the dimensionless quantity.

In order to achieve its aims, the project's objectives are planned as follows:

1. Verify the accuracy of fluid flows in Raphael's *Jacob's Encounter with Rachel* and Ingres' *La Source* using NURBS and CFD. Then sketch an artwork to test the feasibility of the method.
2. Find the link between beam bending functions and cubic NURBS using the dimensionless quantity.
3. Analyse the core of Chinese calligraphy and explain its strength and

tenacity scientifically.

4. Analyse the utilisation of NURBS in pipe design.
5. Redesign and test the air duct of TREx for its improved performance with the NURBS shape.
6. Redesign the profile of TREx using NURBS in the modelling of the casing for a better visual impression.
7. Design an artwork about TREx for influential visual communication and see how the experts or professionals value it.
8. Validate the proposal using simulation and practice.

1.4. Thesis outline

There are six chapters in this thesis. Chapter 1 is the introduction, and it presents the study's fundamental background and motivations, followed by the aims and objectives. A chapter-by-chapter overview of the thesis is also presented.

Chapter 2 presents a comprehensive literature review of the history and current research on the scientific studies in arts, engineering and design, clarifying the

study's motivation. It starts by reviewing the scientific studies in classic western art. Following that, it covers CFD and its application in the study of Leonardo da Vinci and Ingres and his artwork. The relevant studies of CAD and art are discussed. After that, the studies of Chinese calligraphy are reviewed. Then the chapter addresses some applications of NURBS used in designs. Finally, the studies of dimensionless quantity and its applications are summarised.

Chapter 3 introduces the research into using CFD and NURBS to accurately and conveniently draw the profiles of streamlines in arts and analyse existing ones. To begin, the combination of CFD and NURBS is discussed. Raphael's oil painting *Jacob's Encounter with Rachel* and Ingres' *La Source* were analysed using mathematical and engineering techniques, utilising CFD and NURBS. In the process of the analysis, the 2D scenes are converted into a 3D model based on perspective projection and CAD. Then the fluid motions are simulated using the Volume of Fluid method and CFD. The simulation results were compared with the original artworks.

Chapter 4 presents how the rigidity of NURBS can be explained mathematically, and how it can be used to study and appreciate, as well as create Chinese calligraphy. There are seven different beam bending cases, and Cases NO. 1,

2, 3, 4, 6 and 7 are analysed and linked with cubic NURBS using the dimensionless quantity. The fundamental Chinese strokes in Song Huizong's calligraphy are fitted by cubic NURBS and discussed. Other handwriting and generated artistic fonts are compared with Huizong's art.

Chapter 5 gives details of the relevant practical design tasks using the findings in this thesis. This chapter introduces why and how the combination of CFD and NURBS can benefit product development and visual design. The combination of CFD and NURBS is used in the analysis of pipe design. Then the study proved that the application of the combination can benefit the design of simple industrial product components. After that, the method is utilised in car design and visual design.

Chapter 6 provides the conclusions and contributions of this PhD study, followed by some suggestions for future research.

CHAPTER 2. LITERATURE REVIEW

2.1. Introduction

This chapter reviews the scientific studies in classic western painting, traditional Chinese arts, design and research activities relevant to the use in these areas of Computational Fluid Dynamics (CFD), Computer-Aided Design (CAD), NURBS, and the dimensionless quantity.

This review systematically works through the fields analysed in subsequent chapters. It begins with research in classical western paintings in section 2.2. Then CFD and its application in the study of Leonardo da Vinci and Ingres and his artwork in section 2.3. In section 2.4, the relevant studies of CAD and art are reviewed. After that, the studies of Chinese calligraphy - a visual art in Chinese culture-¹² are reviewed in section 2.5. Section 2.6 addresses some applications of NURBS used in designs, while section 2.7 reviews the studies of dimensionless quantity and its applications. The summary of this chapter is given in section 2.8.

From ancient times to the present, various applications of scientific approaches in the arts have received a lot of attention. As Kemp has pointed out, there is a clear change in the shape of the relationship between art and science, and more scientific approaches are used in art creation and aesthetics.¹³

2.2. Scientific studies in classic western arts

In art, “whether we are discussing how materials combine or resist, how and why colours interact, or how structures assume their shape and structural integrity, we are engaging some aspect of physics, maths, or engineering”.¹⁴ The appreciation of classic art includes several aspects, one of which is the element of physical representation. In European art, an emphasis on representational accuracy started to become dominant in the art workshops in the 15th century, during which the artists paid increasing attention to the physical sciences in the process of creating beauty – a focus that would remain central until the time of Monet.^{15 16}

From the chronology of developments in both art and anatomy during the fifteenth and early sixteenth centuries, the sixteenth century was called “the century of anatomy”. To represent the human body, the sources of anatomical knowledge used in art were from its scientific application. The collaboration between science and art has been significant from Polyclitus' principles of proportion to the golden ratio.^{17 18} Painting and sketching became accurate because of the rise of academic approaches such as perspective and, before that, pinhole imaging. Until the late fifteenth century in Florence, drawing was

taught almost exclusively in the tradition of workshop training, in which young artists studied theoretical subjects called “academies” “such as anatomy, perspective, proportion and architecture” to ensure their sketching was accurate.¹⁹ The increasing importance of academic approaches is also evidenced in architectural and engineering diagrams of the time, for instance, in the work of Leonardo da Vinci²⁰ and Giotto.²¹ More importantly for present purposes, there was also the study of many sorts of flow in artworks, including the flow of air, water, oil, blood and other fluids, as well as the vitality and movement of life itself. In Martin Kemp’s study of Leonardo da Vinci’s “innovative experimental models for the motion of water and blood”, he points out that among “the vast range of phenomena that Leonardo explored and depicted was the behaviour of liquids”.²²

Similar to Leonardo da Vinci, the scientific study of Raphael have received increasing attention. Younger than Leonardo and older than Michelangelo, Raphael's work reflects the influence of academy and science on fine art during the Renaissance, and 1800s.^{23 24 25} Many researchers use Raphael’s artworks as samples in their study, but the significant limitation is the focus on the two sides, science and art. For example, the material makeup of *Between Raphael and Galileo* suggests that its author, Alexander Marr, is more at home with art history than with the culture of mathematics and its historians. That may account for some repetitiveness and flatness in the treatment of mathematical artefacts.²⁶ The work of Raphael nevertheless remains influential. Jean-Auguste-Dominique Ingres (Ingres), a Neoclassical artist, himself wrote that a

copy of the Madonna della Sedia seen when he was a boy in his master's studio in Toulouse began his life-long veneration of Raphael.²⁷

Ingres is a master of Neoclassical painting. In the nineteenth century, he was one of the finest painters of the female nude. His forte, in particular, is “the arrangement”, the selection and balancing of elements within the painting. “His best works are exciting plastic units in which line, space, and mass are perfectly balanced, and the colour is subtly used to reinforce linear effects and to delineate forms”.²⁸ Historical paintings in the neoclassical style of Ingres and his circle, moreover, had a sustained impact on the art market of the time. This was due to “their works [being] repeatedly purchased by the same government, shaping the taste of the public”.²⁹ In short Ingres' artworks are a symbol of the times and a model of realistic paintings.

“La Source”, the painting by Ingres analysed in Chapter 3, is one of his most famous paintings. The work was begun in Florence around 1820 and was not completed until 1856, in Paris. Sir Kenneth Clark notes that “La Source” “was immediately popular and has been called the most beautiful figure in French painting”.³⁰ “La Source” reflected Ingres' “Raphaellesque obsession, his scale, and his larger sense of form”.³¹ Unlike most representations of the female nude,

in the paintings such as “La Source” “the male viewer is not the centre of the work. The figures in these paintings attend to the sights and sounds of their own world; they are intent on their own pleasures”.³² Most of the previous research on this painting revolves around the figure of the nude, but there is no research on the pitcher and the water flow. Most of the arguments are related to statics, not fluid dynamics, and people usually judge the accuracy of the painting according to the structure of the objects within it. The water flow in “La Source” looks natural and smooth. That may reflect Ingres' deep observation and outstanding technics. Oppositely, as Bear comments, there is a suspicion “that Ingres used a camera lucida to facilitate the making of drawn likenesses of visitors to Rome in the second decade of the nineteenth century”.³³

It is worth noting that Raphael and Ingres created artworks with high accuracy. That means they all use academic approaches such as perspective and anatomy during art creation. All the academic approaches in classic art are to provide scientific support – accuracy - in art creation. Because art is essential to accurately describe organisms in natural history, accuracy is a part of the importance of classic painting.³⁴

2.3. The applications of CFD in engineering and art

Computational fluid dynamics (CFD) uses computers and applied mathematics to model fluid flow situations. CFD, as a developing science, has received much attention throughout the international community since the advent of computers. Now it has grown from a mathematical curiosity to become an essential tool in almost every branch of fluid dynamics.³⁵

Generally, CFD is widely used more in Engineering than in art. Since the late 1960s, the development and application of CFD has seen considerable growth in all aspects of fluid dynamics.³⁶ As a result, CFD has become an integral part of engineering design.³⁷ So, to improve the quality of the design, designers and engineers are increasingly using CFD to analyse the fluid flow and performance of products, because CFD can provide a reasonable simulation or analysis result and save much testing time.³⁸ To boost the utilisation of CFD in engineering applications, Wilcox created seven main algebraic models and turbulence energy equation models for CFD. The models include the channel and pipe flow which is used in pipe design and channel testing in engineering.³⁹ A research group from NASA notes that the ability to simulate aerodynamic

flows using CFD has progressed rapidly during the last several decades and has fundamentally changed the aerospace design process.⁴⁰ Some researchers from the UK combine CFD and other methods to improve the structural design of a high-performance air bearings product and the working efficiency is enhanced significantly.⁴¹ Recently, CFD has been utilised in an optimised design of a new 3D printer device in China, resulting in high performance and turbulence reduction in transferring of raw material.⁴² Additionally, CFD is also used in the design of energy transfer products such as heat exchangers.^{43 44} All of this shows that CFD is a good aid for fluid analysis.

In art, people use CFD to test the accuracy of drawings or paintings created hundreds of years ago. Leonardo's model of the motion of blood in the human body has been constructed and verified by fluid-dynamics specialist Morteza Gharib, who, as Kemp phrases, it "used modern imaging techniques" to do so.⁴⁵ CFD, the method used by Gharib, provides numerical methods and algorithms to solve and analyse fluid flow, heat transfer, and related phenomena through computer-based simulation. His work opened up a new approach to evaluating the accuracy of representations. Although "Art and CFD are such distinctly different metiers that one would not naturally see a connection between the two subjects", Gharib's work makes it clear that some common features do exist

between them in the uses of “colour and shape”.⁴⁶ In both, colour is carefully manipulated to reflect changing light or motion, “making the results clear”, and “distinctive and visually pleasing”.⁴⁷ For example, in artworks, colour changes due to the light; in ANSYS, the CFD simulation software, different colours show different pressure, velocity, temperature, and sometimes thermal energy in simulation results. In a recent study, the present author tried to show Ingres’s outstanding skills and accuracy in *La Source* using CFD.⁴⁸ The results represent the water flowing out from the pitcher and seem believable. However, the tracks of the water in *La Source* and the CFD simulation results have not been put together for comparison.

CFX and Fluent are two common CFD software and can be found in ANSYS WORKBENCH. Several researchers have used CFX to study the local surface heat and energy transfer coefficient during food processing.⁴⁹ ⁵⁰ Fluent is one of the largest providers of CFD software and has been used to optimise air-flow conditions during chilling and storage.⁵¹ In addition, a research group utilised Fluent to develop the model of an air-bearing system with active electromagnetic assistance.⁵² It is noticeable that both CFX and Fluent are the software of CAD.

2.4. CAD in engineering, design and art

Generally, CAD is used in product design and engineering. CAD techniques are applied in many kinds of industries including aviation, aerospace, machinery, electronics, textile, architecture, and petrochemical .

Before considering the applications of CAD in engineering, design and art, the process of design and the functions of CAD in design need to be introduced.

Design is an innovative and highly iterative process. The process of designing, especially for engineering or product design, consists of six identifiable steps or phases and is often outlined from start to finish as in Figure 2-1.⁵³ With the consideration of CAD in design, the processes are simplified as in Figure 2-2.

Shigley explained why the six phases are logical and indispensable in designing.

The various design-related tasks which are performed by a modern CAD system can be grouped into four functional areas, including Geometric modelling, Engineering analysis, Design review and evaluation, and Automated drafting.⁵⁴ The connection between the six phases of designing and the functions of CAD is as in Figure 2-3.

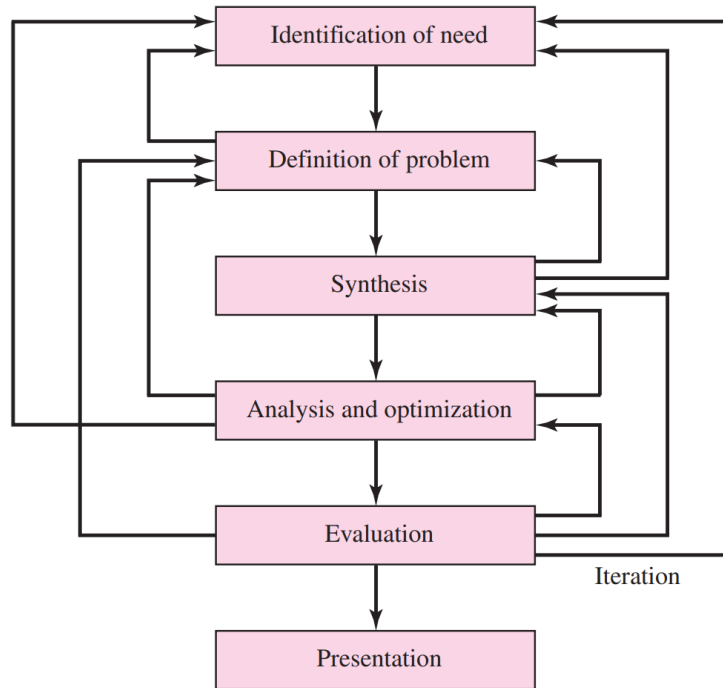


*Figure 2-1. The six processes of designing include Recognition of need, Definition of problem, Synthesis, Analysis and optimization, Evaluation and Presentation. "The synthesis of a scheme connecting possible system elements is sometimes called the invention of the concept or concept design, and it shows that synthesis and analysis and optimization are intimately and iteratively related. Evaluation is a significant phase of the total design process and the final proof of a successful design", usually involving the testing of a prototype in the laboratory. Presentation is the step of communicating or selling a job in design. It is the final with a different challenge because the designers or engineers need to prove that their solution is a better one, compared to the others.*⁵⁵

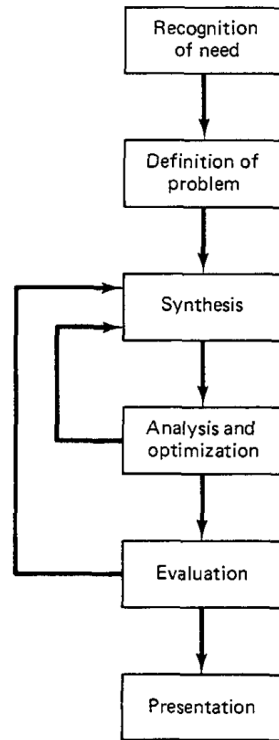


Figure 2-2. The simplified processes of designing.⁵⁶

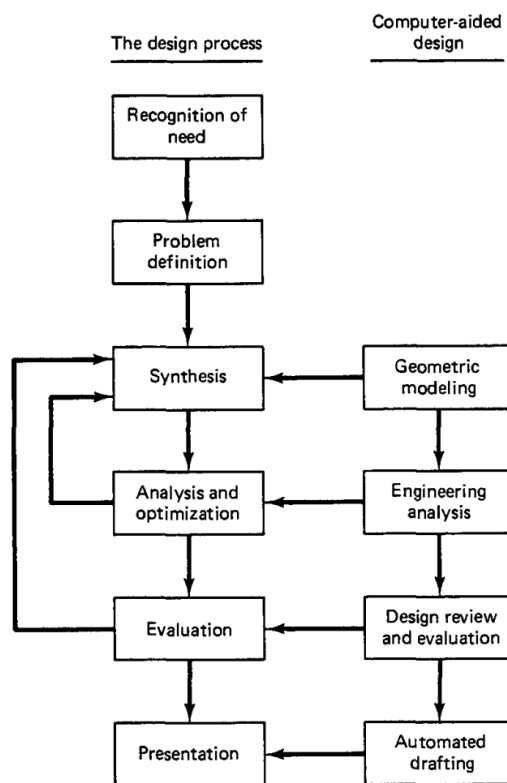


Figure 2-3. Application of CAD to the design process.⁵⁷

Mikell explained how the design steps of Synthesis and the other three benefit from four functional areas. For example, “in computer-aided design, geometric modelling is concerned with the computer-compatible mathematical description of the geometry of an object.” Both the functions of Synthesis in design and Engineering analysis in CAD can benefit from Geometric modelling. Also, CAD can play a key role in checking the accuracy of the design because some CAD software has the function of a graphics terminal. ⁵⁸ That also means it is very possible that CAD can be used in art too, such as art appreciation and art creation.

CAD has been seen as an important innovation in this era and it has been widely used in engineering and product design. The first major push toward computer-aided software systems occurred in 1969 and now CAD has changed the face of the design industry and has influenced the lives of designers and engineers worldwide.⁵⁹ Apart from design and engineering, the applications of CAD increasingly emerge in the relevant studies of art.

CAD, which draws on both NURBS and CFD, has a wide range of applications within the research into and preservation of various artworks. “Computer modelling for spatial analysis and digital recording techniques” was used in a

study of Atlantic Rock Art.⁶⁰ Similarly, in a study of Pre-Magdalenian cave art in the central area of the Cantabrian region (Spain), the “precise output of images was achieved using computer-aided image processing software”.⁶¹ The production of visual art itself has changed significantly because of the development of CAD. Middlesex University’s Centre for Electronic Arts opened in 1985, then known as the Centre for Advanced Studies in Computer Aided Art and Design, and “has seen several projects which explore alternative rendering methods, the most influential being the work of Simon Schofield in the late 1980s.”, namely his work which creatively used “the post-processing of images” to create “a variety of expressive styles”.⁶² Nowadays, design studios and factories create and produce 3D models and souvenirs from 2D objects from artworks. People use perspective rules and data analysis to translate 2D paintings into tactile models, like bas-reliefs art, to break down the vision barrier, resulting in more possibilities for the visually impaired touching visual arts. ⁶³ The elements in a scene can be reconstructed and the transition differences of surfaces can be shown in a 2.5D or 3D form, where the CAD always plays a key role.⁶⁴ In China, CAD dominates the application of Computer Graphics (CG).⁶⁵ Despite this broad applicability in art, CAD, and CFD in particular, have not been applied together to the evaluation of Raphael’s paintings and Neoclassical paintings such as Ingres’s artwork.

Even though there are many challenges during development, CAD has become an essential tool in engineering and design.⁶⁶ Further, in art creation, it also starts to play a more and more important role. Not only limited to western classical paintings, the utilization of CAD to the analysis of Chinese art is also being expanded.

2.5. Scientific studies in Chinese calligraphy

Both Chinese calligraphy and Chinese painting are traditional cultures and arts in China. Even though the Chinese painters did not pay much attention to perspective like the west, they use axonometry -a scientific valuable alternative to photorealistic imagery- in composition.⁶⁷ Compared to Chinese painting, despite fields such as anatomy and perspective not being utilised in Chinese calligraphy, geometry and other scientific methods are involved.

As a traditional art, Chinese calligraphy can, in some respects, be considered the soul of Chinese culture . It is also called one of the six arts (rites, music, archery, charioteering, calligraphy, and mathematics) in ancient China.⁶⁸ Yee Chiang observes that most countries or nations rarely considered calligraphy

to be an art as in China.⁶⁹ The history of Chinese calligraphy appears to be as long as that of China itself. Chinese calligraphy has its own characteristics in each period, and they are all very beautiful. Written words can be formed to liberate visual beauty, and this is possible with Chinese characters to a greater degree than with the scripts of other languages, because art, not science or religion, was the prime goal of those responsible for their development. A good Chinese character is an artistic thought.⁷⁰

Chinese calligraphy has been inherited and continued for thousands of years and most of the people who are affected by Chinese culture learn it. Similar to Europeans learning drawing in Italy during Renaissance, the non-elites in China have references for learning calligraphy too. In the period of the late Ming - around 1590 and also akin to the Renaissance - calligraphy is one of the popular subjects in encyclopaedias. In addition, medical prescriptions, divination formulas, ancient lore, astrology and geomantic almanacks are also included.⁷¹ The importance of western handwriting resides much more in its message, whereas that of Chinese calligraphy is predominantly its visual beauty. From Song Dynasty to Qing Dynasty, the civil service examinations were central to China's political and cultural life.⁷² During the examination, the candidates need to use their handwriting to write an article about the given title.

So, from a very early age, students would start practising calligraphy, giving rise to a powerful intelligentsia whose skills in composition and calligraphy were highly valued. Consequently, in traditional China, excellence in learning, superb handwriting, and an official post were a common combination.⁷³ This tradition is carried on in modern China. Today, during important events or official inspection tours, government officials often write or are asked to write words of encouragement and commemoration in calligraphy to be presented to the public. Even a person's learning is judged, at least in part, by his or her handwriting.⁷⁴

Now, learning and practicing Chinese calligraphy is mechanized, and the lack of innovation is obvious. I agree with Yee Chiang's theory which explained why copying is important and that a perfect copy would require a lifetime's practice.⁷⁵ Copying from popular copybooks is the predominant approach to learning and practising Chinese calligraphy. For example, Li Qi Bei and Zhang Qian Bei are copies of two gravestones from the time of the East Han. The books about these two gravestone copies show how to mimic the writing and move the brush.^{76 77} Except for the copybooks, for practice, there is a dictionary of about 7000 Chinese characters in five popular styles and people can use it as a guide.⁷⁸ People can find almost any daily used Chinese characters in this dictionary.

However, Yee Chiang also mentioned that there are three stages of learning Chinese calligraphy, and the students need to find their own way and personal style after a long period of being discouraged from doing so.⁷⁹ Even though, generally speaking, good practice can produce skilfulness, in this fast-paced era, writing Chinese calligraphy well is time-consuming, at least much slower than generating Chinese characters with high-tech aids.

Despite it having been called Art for thousands of years, studying it scientifically also plays a significant role in the inheritance and continuation of Chinese calligraphy. Many researchers have paid attention to discovering the method of learning and teaching calligraphy. For example, some Chinese researchers propose an approach to extract strokes using the geometric properties of the contour(s) of a character.⁸⁰ That means the basic strokes in Chinese calligraphy can be extracted with scientific methods and the styles of handwriting can be classified. Similarly, some researchers try to use modern techniques to create and automatically generate original Chinese calligraphy that meets visually aesthetic requirements. A virtual brush model is created to simulate Chinese calligraphy and painting, and it works well.⁸¹ Another virtual brush is designed by analysing the change of the contact surface between the brush and the paper during the movement.⁸² Similar digital brushes can be

found in Photoshop and other graphics editing software. A Chinese research group analysed the strokes on Chinese characters and the track of the brush moving, resulting in an intelligent system for the automatic generation of artistic Chinese calligraphy.^{83 84} The contribution proposes an intelligent system that can automatically create novel, aesthetically appealing Chinese calligraphy from a few training examples of existing calligraphic styles. Using mechanical system hardware, some people designed a generative adversarial nets-based calligraphic robotic framework, and the results show the system allows a calligraphic robot to successfully write fundamental Chinese strokes with good quality in various styles.⁸⁵ In art appreciation, Xizhi Wang's *Lan Ting Ji Xu* was studied and an effective Chinese calligraphy reconstruction and assessment method was proposed, using Photometric Stereo and the Iterative Closest Point (ICP) algorithm. The method can give people's handwriting a score to evaluate their work.⁸⁶ Even though many researchers have proposed various methods to try to truly understand the powerful significance and beauty of the art of Chinese calligraphy, the strength and power inside the characters have not been explained scientifically.

There are an incredible number of many fonts or different ways that people can choose when typing or generating Chinese characters with computers or

smartphones. Different to the official ones such as Kai Ti, Xing Ti and Fang Song, some Chinese fonts have their unique styles and people call them “artistic fonts”. Those generated “artistic fonts” look different from the official ones and may be more similar to famous handwriting.

2.6. Design and NURBS

In the balance between art and mechanical engineering, artists, designers and engineers always attempt to probe into the equilibrium and put forward an approach to benefit both sides, especially in product design, ever since the first world design conference was held in the UK 60 years ago.⁸⁷

The design process of function, manufacture, and aesthetics of a product builds up three vertices of the product design triangle,⁸⁸ and these three aspects of product design interact with each other, strengthening the manufacturing quality and functionality will contribute to aesthetic enhancement.^{89 90 91 92} Figure. 2.4 shows the three vertices of the product design triangle. Aesthetics in product design consists of visual and non-visual (hearing, smell, taste, touch, and thinking) aspects.^{93 94 95} Related design methodology could be utilised by researchers in order to get the design process right by evaluating the related

issues more objectively, assisting researchers in eliminating subjective interpretation, and laying the artistic foundation for engineering design methods to enhance their capabilities. ⁹⁶

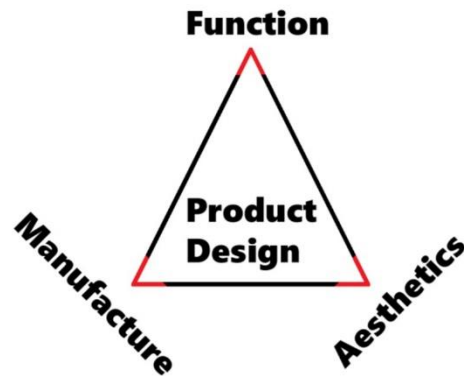


Figure 2-4. the three vertices of the product design triangle

Nowadays, computer-aided industrial design or mechanical engineering has become an important method that is used in product design. Also, computers are not props but materials, and they can be used to develop a rational world.⁹⁷ In the Iron Age, iron's hard and tough properties as a medium can be perceived as a catalyst for activities such as agriculture and war.⁹⁸

In the modern world, NURBS has played a significant role in computer modelling and design, which has become the standard curve and surface description.^{99 100} NURBSs - Non-uniform rational basis splines – are piecewise functions and have various mathematic properties.¹⁰¹ A p^{th} degree NURBS curve function can be defined as a *Function (NURBS)*. The curve of NURBS

changes according to alterations in its key points, and with lines made of dots and bodies made of lines, people can easily change the NURBS curve by changing the location of the key points with software or code writing. In product design, like computer modelling NURBS is widely used as a handy tool due to its easy control.¹⁰² ¹⁰³ This increases the possibilities for building and modifying a model. It also enables the creation of almost any model by using NURBS. NURBS not only has high controllability but is also likely to obtain better surfaces as it benefits the generation of numerical grids, usually the most labour-intensive part of any CFD application.¹⁰⁴ There is a property of continuity in NURBS, and the cubic NURBS has C_2 (Curvature continuity, describing two curves having a common point, tangent vectors lying along the same direction, and having the same curvature).¹⁰⁵ Because of the continuity, the higher order the NURBS has, the smoother the curve will be.¹⁰⁶ In the studies of NURBS surfaces, it has been proven that the cubic NURBS can play a key role in the finite-element implementation of continuous contact surfaces and keep the smoothness, resulting in the possibility of creating an overly natural, flat and beautiful complex surface.¹⁰⁷ Meshing, this process of grid generation, is an important step in the computational simulation, and time can be saved by using NURBS when modelling before gridding. This makes it very suitable for CFD modelling and simulation of blood flow.¹⁰⁸

$$C(u) = \frac{\sum_{i=0}^n N_{i,p(u)} w_i P_i}{\sum_{i=0}^n N_{i,p(u)} w_i} \quad a \leq u \leq b \quad \text{Equation 2-1}$$

In visual design, the movements or emotions of the elements need to be represented abstractly. Before visual design, painting was a dominant visual medium and, “before the eighteenth century”, animals used to be illustrated in picture “books of the world’s fauna generally as specimens, rarely in action. But Jean Baptiste Oudry (1686–1755), famous in the 18th century for his paintings of animals, introduced “not only [...] vitality in traditional genres, but also [...] movements, mental states and emotions of animals”.¹⁰⁹ NURBS is a good tool for showing the movements and emotions of creatures and objects abstractly. Because NURBS has been successfully utilised in modelling objects for the visual arts, including entertainment industries, fine art, and sculpture, NURBS are now also being used for modelling scenes for virtual reality applications.¹¹⁰

2.7. Dimensionless Quantity

The history of the dimensionless quantity started in the 1800s and many mathematicians and physicists boosted its development. The developments in the modern concepts of dimension and unit were led by French mathematician

Joseph Fourier and Scottish physicist James Clerk Maxwell in the nineteenth century. After that, British physicists Osborne Reynolds and Lord Rayleigh contributed to the understanding of dimensionless numbers in physics. Then Edgar Buckingham proved the π theorem to formalize the nature of these quantities, independent of French mathematician Joseph Bertrand's previous work and building on Rayleigh's method of dimensional analysis.¹¹¹

The dimensionless quantities can be divided into several groups. The most important group - generalized variable quantities - consists of the physical similarity criteria obtained by some of the similarity theory methods. The dimensionless physical constants belong to another group. In addition, the approximate ratio quantities can also be included among the dimensionless quantities. Other dimensionless ratio quantities can be created as well, which do not have any full-value importance from the modelling point of view.¹¹² The dimensionless quantity is almost utilised in every area of engineering, including physics and physical chemistry, fluid mechanics, solid mechanics, thermomechanics, electromagnetism, geophysics and ecology.¹¹³ That means dimensionless quantity can be written and used to represent an abstract mathematic relationship between two equations or functions. For example, it is possible to link a physics formula and a curve function.

2.8. Conclusion

This review has considered scientific studies in classic western art, Chinese calligraphy, the connection between scientific methods or tools and art, and other research that is relevant to the present study. In light of this, it can be concluded, firstly, that many scientific approaches are found in classic western art. Hundreds of years ago, artists bring science into drawing or painting learning and teaching. With the development of technology, more and more scientific methods have been used in art appreciation and creation such as CFD. As an essential tool in engineering and industrial design, CAD plays a significant role in the academic research of art. However, these tools have not been used in combination to analyse the accuracy of flow in realist painting, and this is the focus of Chapter 3.

Compared to western art, even though the sense of space, the ratio in proportion, and the accuracy of illustration are important in Chinese art, fewer academic methods are proposed, especially in Chinese calligraphy. Many researchers focused on the study of calligraphy history, the relationship between Chinese culture and calligraphy, and generating artistic “calligraphy” using coding and other modern high-tech approaches. However, few people

study its essence and the core through the look. That means the strength and softness in Chinese calligraphy are rarely analysed and explained scientifically. Chapter 4 seeks such an explanation. It has become clear from the review that the potential application of the dimensionless quantity in art analysis is feasible. For instance, it may explain the strength of calligraphy, using dimensionless quantity to link the curves in characters and mathematic functions. If the relationship between the features of characters or parts of it and physics functions can be found, then maybe the reason why good Chinese calligraphy works look strong but slim can be explained scientifically. Chapter 4 does so through the combination of the dimensionless quantity and the rigidity of NURBS.

The studies between design and NURBS show how engineering, product development and visual design also benefit from NURBS. Although NURBS is a piecewise function, and it cannot be directly used in modern design and engineering projects, NURBS is used in much CAD-based software. For example, in modelling software and image processing software, there are tools created based on NURBS. Nowadays, SolidWorks, GU-NX and Photoshop are common ones and are often used in various sorts of design. The use of NURBS in engineering and design is the focus of Chapter 5.

CHAPTER 3. CFD AND NURBS FOR THE DESIGN OF FLUID COMPONENTS IN CLASSIC PAINTINGS

3.1. Introduction

This chapter introduces the research into using Computational Fluid Dynamics (CFD) and Non-uniform rational B-spline (NURBS) to accurately and conveniently draw the profiles of streamlines in arts and analyse existing ones.

In general, streamlines in painting that is, the lines or tracks which a stream of liquid follows – are aesthetically pleasing and frequently praised, but it is hard to evaluate the accuracy of fluid flows in painting without modern high-tech scientific aids, especially for the artworks created before the invention of the camera. Examples of streamlines in the classic painting are prolific. For example, the water flows in *La Source* by Jean Auguste Dominique Ingres (Ingres), *The Birth of Venus* by Alexandre Cabanel (Cabanel), or *Jacob's Encounter with Rachel* by Raffaello Sanzio da Urbino (Raphael). In these famous paintings, all the liquid flowing appears good and natural. The water

flows show the painters' masterly skills and expressions of beauty. People praise their artworks highly and admire their techniques, including their accuracy and the use of colour. Peter Cooke, for instance, observes Ingres's unrivalled mastery of drawing,¹¹⁴ while Janis Bell notes that Raphael's use of colour is an underrated aspect of his art.¹¹⁵ However, unlike the anatomy used in art from the fifteenth century, the accuracy of fluid from artworks could not be calculated or measured with tools or machines before. So, the evaluation and appreciation of art have been limited regarding the depiction of flowing liquid. Even nowadays, people struggle to draw a liquid flow accurately without a camera or images as a reference. However, often in artistic creation not every item in a painting or drawing can be found in real life. Then what can be done to draw an accurate streamline in art?

The method presented in this chapter provides a new approach to benefit art appreciation and creation with CFD and NURBS, resulting in a production satisfied with both scientific rules and public aesthetics. To begin, the combination of CFD and NURBS is discussed. CFD can be used to simulate the flowing scenes and to analyse the flow. NURBS can easily provide streamlines because of its mathematical properties. Two famous widely recognized artworks, Raphael's oil painting *Jacob's Encounter with Rachel* and

Ingres' *La Source*, were analysed using mathematical and engineering techniques, utilising CFD and NURBS. In the process of the analysis, the 2D scenes are converted into a 3D model based on perspective projection and CAD. Then the fluid motions are simulated using the Volume of Fluid (VoF) method and CFD. The simulation results were compared with the original artworks. The results show the two famous artists' mistakes and inaccuracies in their artworks.

To test whether the approach is practical and feasible, a fluidic scene is created to aid art creation. The example presents the application and advantages of the method.

3.2. Fluid in traditional realistic fine art

It is not difficult to find fluidic scenes in traditional realistic fine art. However, it is hard to say the fluid flows in realistic paintings are very accurate, even for the famous ones. Accuracy is a characteristic of Western classic painting. In the depiction of scenes, especially ones including architecture, the application of calculable scientific approaches such as perspective and geometry are ubiquitous for both artists and their critics. Consequently, accuracy has become

an important standard for evaluating the quality of a work of art, for which a scientific method of verification is essential. Also, accuracy is an important indicator of art appreciation, particularly for realistic artworks. This part of the study is an attempt to apply NURBS and CFD to the appreciation of realistic art in order to demonstrate their potential impact on art criticism and art creation. The approach has the potential to open up a new scientific channel to study classic paintings and create realistic art with high accuracy. Although the application of science in art has been studied over the centuries, new methods emerge with the development of modern technology. For example, digital arts are well-known nowadays and more and more young people have started to use professional hi-tech tools such as tablets in their art creations. People use Artificial Intelligence (AI) to aid their artistic endeavours, especially in landscape art or painting the background of portraits (See Fig 3-1). Virtual reality and 3D printing have also played a significant role in art and design.



Figure 3-1. 'A Mediterranean beach' by Han Liu. The artwork is produced by coding written with

Python, a high-level, general-purpose programming language.

Flowing water is a typical type of fluidic scene. It is not uncommon for flowing water to be found in scenes in classic art; previous evaluations of water flow, however, were made based on individual experience and subjective feelings and not scientifically. This chapter introduces an analysis of the famous oil painting *Jacob's Encounter with Rachel* by Raffaello Sanzio da Urbino (Raphael), and *La Source*¹¹⁶ by Jean Auguste Dominique Ingres (Ingres) using a scientific approach to verify the painting's accuracy. This evaluation contributes to the debate on Raphael and Ingres's artistic process, and presents the possibility of using NURBS, CFD and CAD to produce highly accurate scenes with flowing water based on mathematics and physics. Before detailing the method and results of the study, however, it is necessary to establish some of the contexts for the paintings under consideration.

3.3. The two traditional paintings as research samples and their creators

Raphael was an Italian painter and architect of the High Renaissance and is an ideal artist for this research. Together with Michelangelo and Leonardo da Vinci, he forms the traditional trinity of great masters of that period.^{117 118} Until the

later 19th century, Raphael was regarded as the greatest painter who had ever lived. 'He became the ideal of all academies', Reynolds said.¹¹⁹ During that period, one of the key metrics to evaluate the artwork is accuracy. At the height of his career/powers, Raphael created visions of unequalled grandeur and serenity in the golden moment of Rome.¹²⁰ When *The School of Athens* (see Fig 3-2) had been finished, Raphael was only 27 years old.¹²¹ In *the School of Athens*, Raphael's composition is extremely complex. There are 52 figures in as many different poses, but it keeps the sense of symmetry and achieves the same unification.¹²² From the variation in posture and complexity of space, *The School of Athens* tests the artist's more academic drawing skills, even more than in *Last Supper* by Leonardo (See Fig 3-3). It is a big challenge to maintain the balance with dozens of different poses in one scene. That means the artist needs to be well trained in skills including the understanding of perspective, the utilisation of anatomy in art creation and the representation of movement.



Figure 3-2. The School of Athens painted by Raphael.¹²³



Figure 3-3. The Last Supper painted by Leonardo.¹²⁴

The study of Raphael and his works is comprehensive and includes his biography, the stories of the paintings,^{125 126} anatomical studies¹²⁷, his architectural achievement^{128 129 130}, and studies of art and religious culture^{131 132}, but there are no studies considering the scientific connection between his

artworks, CFD and NURBS. Similarly, despite having broad applicability in art, CAD and CFD have not been applied together to the evaluation of Neoclassical paintings, of which Ingres, the second focus of this chapter, was a master.¹³³ In the nineteenth century, he was one of the finest painters of the female nude. His forte, in particular, is “the arrangement”, the selection and balancing of elements within the painting. As Werner comments, “His best works are exciting plastic units in which line, space, and mass are perfectly balanced, and the colour is subtly used to reinforce linear effects and to delineate forms”.¹³⁴ Historical paintings in the neoclassical style of Ingres and his circle, moreover, had a sustained impact on the art market of the time. This was due to “their works [being] repeatedly purchased by the same government, shaping the taste of the public”.¹³⁵ In short Ingres' artworks are a symbol of his time and a model of realistic paintings.

La Source is one of Ingres' most famous works and it is a good sample to be analysed due to its scene of flowing water and Ingres' artistic ideals. The painting was begun in Florence around 1820 and was not completed until 1856, in Paris. In numerous works on Ingres, *La Source* is the most celebrated and most attractive to the general public. It has, perhaps, been more popularised than any other of his artworks, due to it being “the most harmonious in its purity

of line, the refinement and breadth of its modelling, its delicate colouring, and its perfection of form.”¹³⁶ Sir Kenneth Clark notes that *La Source* “was immediately popular and has been called the most beautiful figure in French painting”.¹³⁷ *La Source* reflected Ingres’ “Raphaelesque obsession, his scale, and his larger sense of form”.¹³⁸ Unlike most representations of the female nude, in *La Source* “the male viewer is not the centre of the work. The figures in these paintings attend to the sights and sounds of their own world; they are intent on their own pleasures”.¹³⁹ Most of the previous research on this painting revolves around the figure of the nude, but there is no research on the pitcher and the water flow. Most of the arguments are related to statics, and people usually judge the accuracy of the painting according to the structure of the objects within it, but there is little attention to fluid dynamics.

Classic painters paid great attention to accuracy. For very famous painters, the accuracy of their paintings remains a hotly debated topic. Even the famous artist, Raphael (Raffaello Sanzio da Urbino) of the Renaissance, made slight and easily overlooked mistakes in the accuracy of his paintings, especially in his depiction of fluid motion. Ingres is one of the most famous neoclassical painters in Europe from the 19th century. He studied Raphael and demanded of himself extreme accuracy in his scenes and character’s emotions. People

may be able to discern the inaccuracy of fluid movement in the scene of a painting, but it is difficult to describe precisely how inaccurate these visual dissonances are in words.

As detailed above, this chapter explores the possibilities and specific methods of utilising mathematical and CFD in the appreciation of *Jacob's Encounter with Rachel* (see Fig. 3-4) and *La Source* (see Fig. 3-5). Raphael and Ingres's works were chosen as the samples for several reasons.



*Figure 3-4. Jacob's Encounter with Rachel (pixel 926*608, 300 DPI)*



Figure 3-5. La Source

There were more than 184 artworks that were archived during Raphael's life from *Self Portrait* (1499) to *Vision of the Cross* (1520). Of these 184 artworks, only 7 paintings, including *Miraculous Draught of Fishes* (1500), *The Parnassus*, from the *Stanza delle Segnatura* (1510-1511), *The Triumph of Galatea* (1512), *Miraculous Draught of Fishes* (1515), *Jacob's Encounter with Rachel* (1518-1519), *Moses Saved from the Water* (1518-1519), and *The Separation of Land and Water* (1518-1519) used water as an obvious and significant part of the

whole composition.¹⁴⁰ Of these 7 paintings, only the *Miraculous Draught of Fishes*, *Jacob's Encounter with Rachel* and *Moses Saved from the Water* show the phenomenon of water flow, and it is only *Jacob's Encounter with Rachel* that meets the conditions for the study. The water-flow scenes in the other paintings are difficult to analyse due to too many uncertain and unquantifiable factors. Also, *Jacob's Encounter with Rachel* is one of Raphael's works and it was created from 1518 to 1519, after *The School of Athens* (1509-1510).^{141 142} That means anatomy had been used in art creation very well by Raphael in his time. Furthermore, in scenes of the water flowing in *Jacob's Encounter with Rachel*, the water flowing out from the stone pond reflects a natural phenomenon and is suitable for CFD simulation. The story comes from the Bible and consequently, Raphael was not painting a pre-existing scene. The whole picture needed to be imaginatively created. While there might have been models or references utilised for the poses of the characters, the water-flow could not hold a static pose in the same way as human beings or objects. Artists can represent the movement of water accurately in life drawings, but it would be extremely difficult to create a scene with water-flow relying on imagination only, even for famous painters such as Ingres.

Indeed, for Ingres, as a painter within the realist movement, accurate

representation is central. Furthermore, as a neo-classical painter, Ingres' work can suggest implications for paintings beyond the Realism movement. Most crucially, however, *La Source* provides an example of water flow that is both limited in quantity and controlled, as it flows from the pitcher – compared to, for instance, the sea in Alexandre Cabanel's *The Birth of Venus*.¹⁴³ As such, *La Source* serves as an excellent test case for this approach.

The study involves numerical modelling of the water containers and simulation of the water flowing out of the containers. First, the 2D water tank and jar in the paintings are converted into a 3D model based on perspective projection and CAD. Next, water flowing out of the containers is simulated using the volume of fluid (VoF) method and CFD. In Ingres' case, the NURBS model of the pitcher in *La Source* is used as the boundary.

Raphael's *Jacob's Encounter with Rachel* and Ingres' *La Source*, then, are two exemplary instances of realistic paintings, epitomising their quest for accuracy and often praised for their successful realism. They are, therefore, the perfect test cases to answer a few key questions. First, although NURBS, CAD, and CFD are widely used in modelling, computer simulation, and the creation of modern art, they are not deployed in art criticism and the creation of realistic

artworks; what is the feasibility of utilising these approaches in the field of classic art appreciation and creation? Second, for all their praise, how accurate are Raphael's *Jacob's Encounter with Rachel* and Ingres' *La Source*, and what are the possible implications of them being accurate? Is there anything inaccurate and why? Finally, by extension, can the average person and the beginner in art draw an accurate scene with fluid elements via the combined application of NURBS, CAD and CFD?

3.4. Raphael's *Jacob's Encounter with Rachel*

3.4.1. Using perspective to model the pond

Nowadays, design studios and factories create and produce 3D models and souvenirs from 2D objects and artworks. People use perspective rules and data analysis to translate 2D paintings into tactile models, like bas-reliefs art, to break down the vision barrier, resulting in more possibilities for the visually impaired touching visual arts. ¹⁴⁴ The whole scene can be reconstructed, and the transition differences of surfaces can be shown in a 2.5D or 3D form.¹⁴⁵ Using the rules of perspective, it is not difficult to translate architectures and objects from a 2D image into a 3D model with industrial design software such

as UG NX, Solidworks or Rhinoceros. Unlike the study of helping blind people to access inherently bi-dimensional works of art, the pond made of stone in *Jacob's Encounter with Rachel* can be translated into a 3D form easily, due to the simple ring-column-like structure (see Fig. 3-6). In the time of Raphael, the ponds were normally made round. It is reasonable to make a hypothesis that the stone pond in the painting is a ring column.

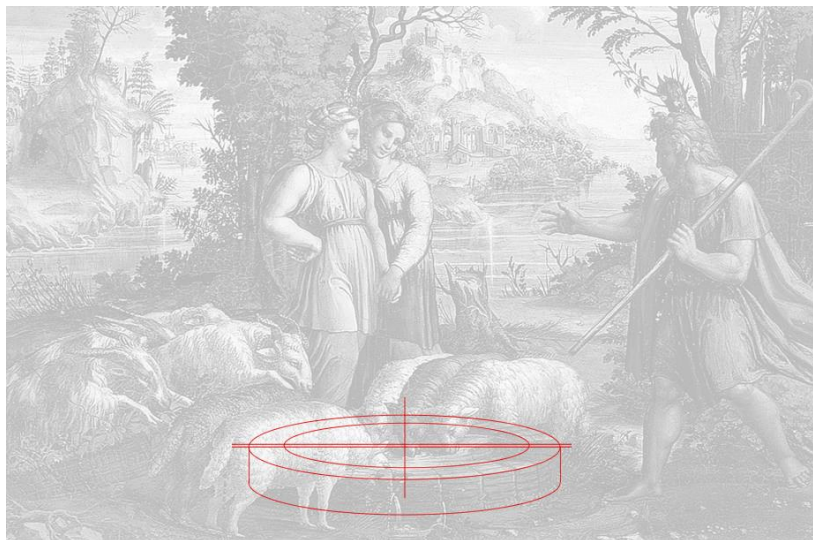


Figure 3-6. The stone pond in Jacob's Encounter with Rachel.

Here we have the JPEG file of the painting, and all the JPEG files are made of pixels. That means if the image is an 800×600 JPEG file, then there will be 800×600 pixels. After calculation in pixels, the ratio of every single item or element in the painting can be calculated and noted. Here Figure 3 is 926×608 pixels, and the DPI is 300, which means the image is high quality, with all the details easily recognisable. As a result, it will be straightforward to

precisely measure the distances from any point to another.

Firstly, to measure the sizes of the objects or elements in the image, it is needed to find a way how to target and lock the key points such as poles. Better than using human eyes, the data analysis can provide a practical and precise approach utilising Matlab. The code can be written as below (see Fig. 3-7):

```
%Proportion calculation on Jacob's encounter with rachel 1519 black&white  
  
d=imshow('D:\HAN LIU\UoB\PhD\Case of Raphael\JPEGs\jacob-s-encounter-with-rachel-1519-20211124.jpg')  
  
impixelinfo(d)
```

Figure 3-7. The Matlab code for showing all the pixels of the JPEG file. There are two steps: the first is importing the image to Matlab, and the second is putting the parameter in pixels on the image.

Then the coordinate axis is drawn in markable units (pixels).

Secondly, after running the code, the image quantized in pixels is displayed (see Fig. 3-8). Then it is a simple matter to locate the key points and have the data, like the coordinates of pixels. So, we have the key points of the man and stone pond including (x_1, y_1) , (x_2, y_2) , (x_{R1}, y_{R1}) , (x_{R2}, y_{R2}) , (x_{r1}, y_{r1}) , (x_{r2}, y_{r2}) , (x_{h1}, y_{h1}) and (x_{h2}, y_{h2}) . In these points, (x_1, y_1) and (x_2, y_2) define the height of the man; (x_{R1}, y_{R1}) and (x_{R2}, y_{R2}) define the outer

diameter of the pond; (x_{r1}, y_{r1}) and (x_{r2}, y_{r2}) define the inside diameter of the pond; (x_{h1}, y_{h1}) and (x_{h2}, y_{h2}) define the visible depth of the pond (see Fig. 3-9).



Figure 3-8. The image is displayed with the data of pixel axes.

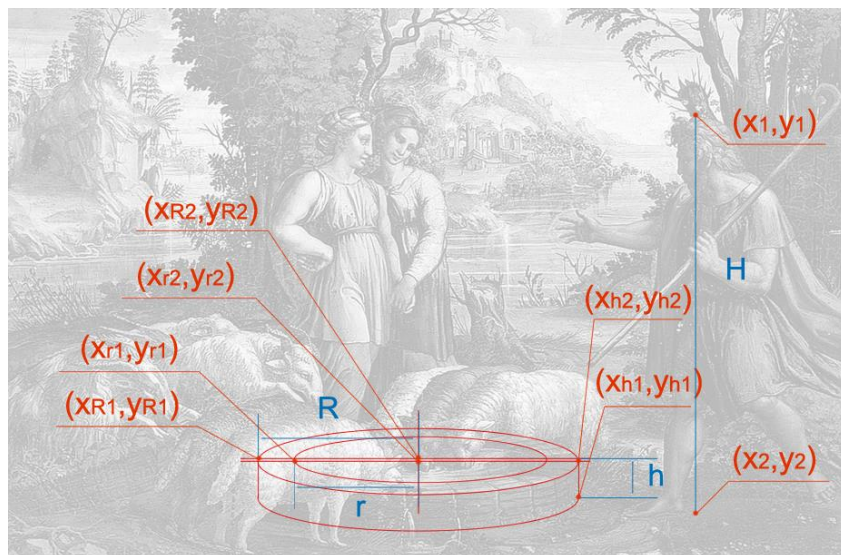


Figure 3-9. The key points of the man and stone pond.

The axes of (x_1, y_1) and (x_2, y_2) are $(748, 554)$ and $(748, 126)$. Because the x-axes of the two points are the same and the height is defined by the data of y-axes, so the height of the man in the image will be $(H_m = (x_1, y_1) - (x_2, y_2) = (748, 554) - (748, 126) = (0, 428) = 428$. If $1 \text{ pixel} = a$, then the height of the man is $428a$.

However, $428a$ is not a valuable number for describing height. The relevant research shows that the average human height in Europe fell from 173.4 centimetres in the early Middle Ages (476–800) to a low of roughly 167 centimetres during the 17th -18th centuries.¹⁴⁶ In the early modern period (1453-1789), in England, the average height was around 164cm and the soldiers in Galicia averaged 171 cm around 1740.¹⁴⁷ Raphael (1483 – 1520) was an artist in the period of the High Renaissance and he used normal people as the model reference in Jacob's Encounter with Rachel – the ratio of the size of the sheep relative to the people proves this, if there was any reason to doubt it. So, a height of 170 centimetres would be reasonable as the reference for the calculation. If the height of the man, Jacob from the painting, is 170 cm, then we have $170\text{cm} = 1700\text{mm} = 428a$. So, $a = 1700/428(\text{mm})$.

The axes of (x_{R1}, y_{R1}) and (x_{R2}, y_{R2}) are $(276, 500)$ and $(452, 500)$.

Because the y-axes of the two points are the same and the outer diameter of the pond (R) is defined by the data of x-axes, we have $(R) = (x_{R1}, y_{R1}) - (x_{R2}, y_{R2}) = (276,500) - (452,500) = (-176,0) = 176$. So, the outer diameter of the pond $(R) = 176a = 176 \times (1700/428)mm \approx 700mm$. The axes of (x_{r1}, y_{r1}) and (x_{r2}, y_{r2}) are (316,497) and (452,479). Similar to the outer diameter of the pond, we have the inside diameter of the pond $(r) = (x_{r1}, y_{r1}) - (x_{r2}, y_{r2}) = (316,497) - (452,497) = (-136,0) = 136$. So, $(r) = 136a = 136 \times (1700/428)mm \approx 540mm$. The axes of (x_{h1}, y_{h1}) and (x_{h2}, y_{h2}) are (630,540) and (630,500). Following the same method, then we have the height of the pond $(Hp) = (x_{h1}, y_{h1}) - (x_{h2}, y_{h2}) = (630,540) - (630,500) = (0,40) = 40$. So, $(Hp) = 40a = 40 \times (1700/428)mm \approx 160mm$.

The next step is to collect and analyse the data of the water in the pond and the main outlet on the wall of the pond. We deem that there is no gap between the stone pond and the water in it. So we have the radius of the space of water (R_w) equal to the inside radius of the pond (r), then $R_w = r = 540mm$. From the painting, we can see that the visible depth of the water is less than the height of the pond. So, the visible depth of the water (D) is the height of the pond (Hp) minus the height difference (HD). The point of (x_{hp}, y_{hp}) is the top of the pond, and the point of (x_{hw}, y_{hw}) is the top of the water. The x-axis of

(x_{hp}, y_{hp}) and (x_{hw}, y_{hw}) are the same. The y-axes of (x_{hp}, y_{hp}) and (x_{hw}, y_{hw}) , y_{hp} and y_{hw} , are 480a and 473a. So, the $HD = (x_{hp}, y_{hp}) - (x_{hw}, y_{hw}) = (480 - 473) \times a = 7 \times (1700/428)mm \approx 28mm$. Then we have $D = Hp - HD = (160 - 28)mm = 132mm$. The points of (x_{ol1}, y_{ol1}) and (x_{ol2}, y_{ol2}) are the two endpoints of the diameter, and the corresponding axes are (437,553) and (442,553). So, the diameter of the main outlet is: $D_m = x_{ol2} - x_{ol1} = (442 - 437) \times a = 5 \times (1700/428)mm \approx 20mm$ (see Fig. 3-10). The points of (x_o, y_{o1}) and (x_o, y_{o2}) are the two dots on the pond with the same x-axes as (x_o, y_o) . Because the axes of (x_o, y_{o1}) and (x_o, y_{o2}) are (439,536) and (439,576), and the axis of (x_o, y_o) is (439,553), the height of the main outlet is: $h_o = y_{o2} - y_o = (576 - 553) \times a = 23 \times (1700/428)mm \approx 91mm$ (see Fig. 3-11).

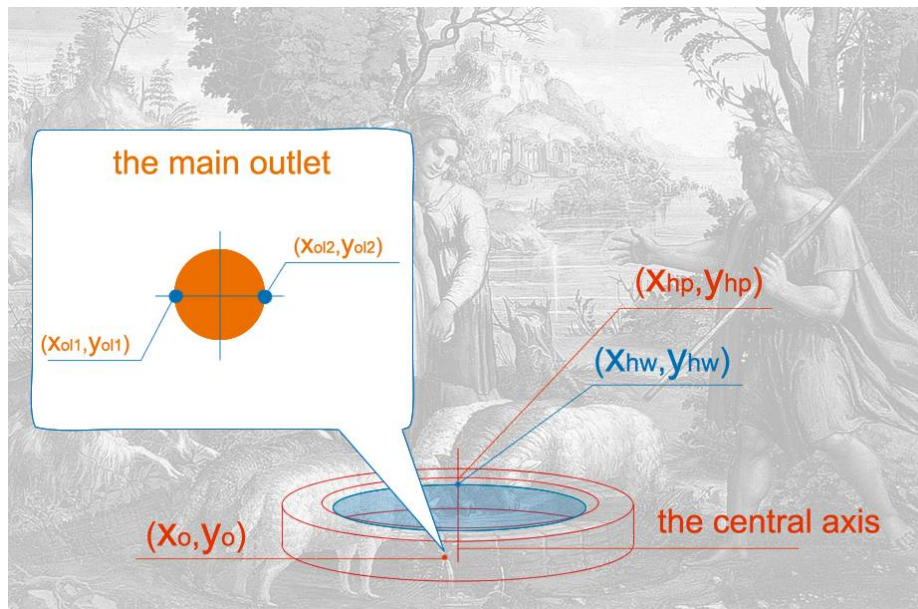


Figure 3-10. The central axis, the key points of the water and the main outlet.

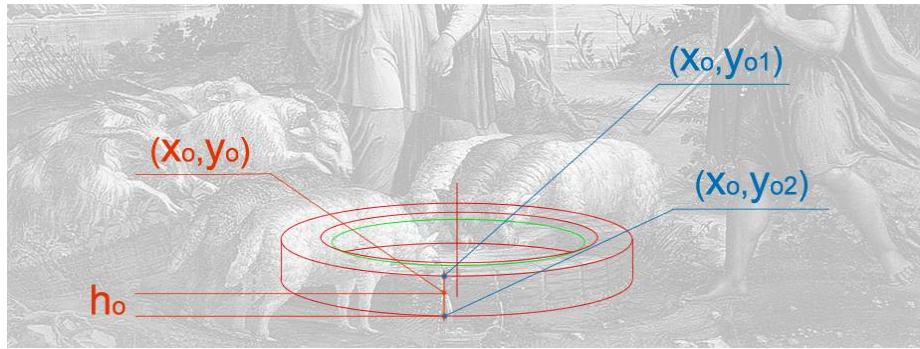


Figure 3-11. The points of (x_o, y_{o1}) and (x_o, y_{o2}) show the height of (x_o, y_{o1}) on the exterior wall of the water pond.

The pond is made of bricks and the main outlet is coming out of the cracks of the bricks. There are around 28 sets of bricks in the pond. So the structure of the pond can be envisaged to be a ring composed of multiple sectors, and the passage of the main outlet runs through the wall along the straight edge of two sectors (see Fig. 3-12).

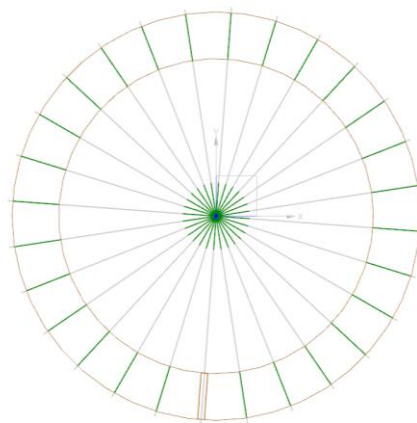


Figure 3-12. The top view of the 3D model of the pond.

Based on all the relevant data about the man, the pond, the water and the main outlet. We can draw a 3D model in UG-NX (see Fig. 3-13).

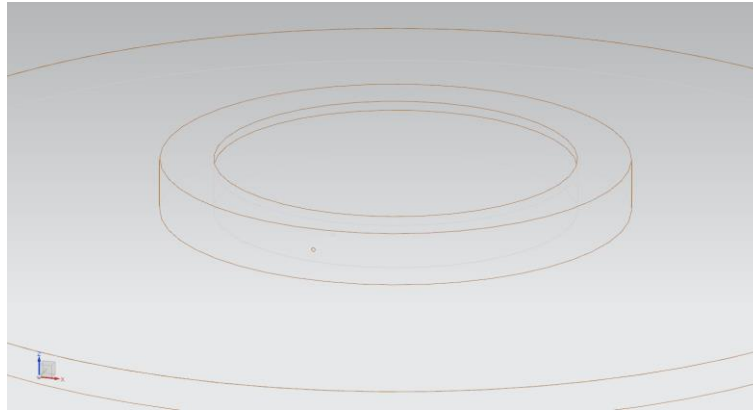


Figure 3-13. The 3D model of the pond, the water and the main outlet.

3.4.2. Using CFD to simulate the water flowing out of the pond from the main outlet

In CFD, the volume of fluid (VoF) method is a free-surface modelling technique, i.e. a numerical technique for tracking and locating the surface of the water. VoF takes various forms in what is termed two-phase flow: (1) Gas-liquid two-phase flow, such as the flow of air and water within a closed drainage pipe; (2) Gas-solid two-phase flow, such as airflow carrying powder or dust through the atmosphere; (3) Liquid-solid two-phase flow, such as sandy water flowing in natural river channels.¹⁴⁸

In the scene of *Jacob's Encounter with Rachel*, the water flow fits the air-water two-phase flow, as just two sorts of fluid are considered, the air and the water flowing out of the main outlet. Consequently, it is suitable for the VoF simulation method in Ansys software. In the simulation, the model for calculation needs to be built first (see Fig. 3-14). In simulation, the water flow can be shown (see Figs. 3-15 and 3-16).

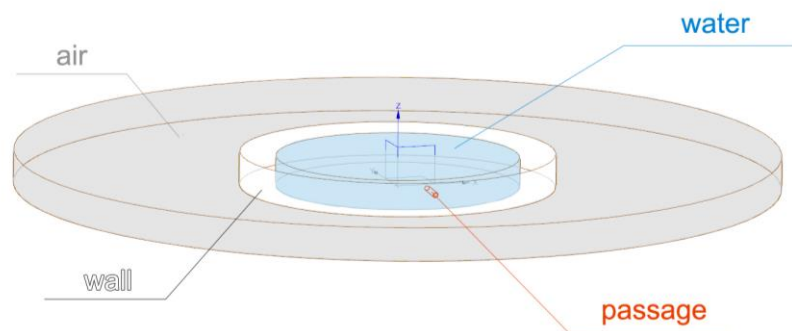


Figure 3-14. The model for CFD analysis includes the water (the blue zone), the air (the grey zone), the wall of the pond (the white zone) and the passage of the water flowing out from the main outlet (the orange tunnel).

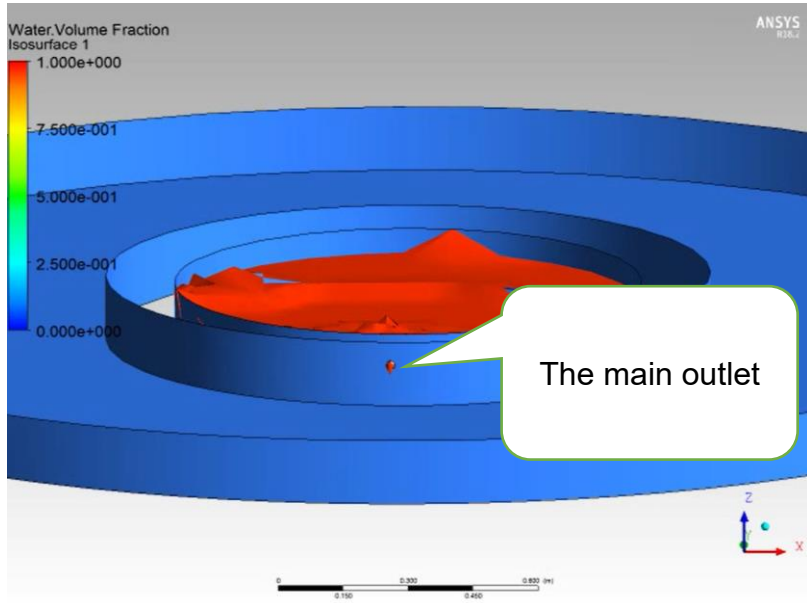


Figure 3-15. The start of the water flows out from the pond.

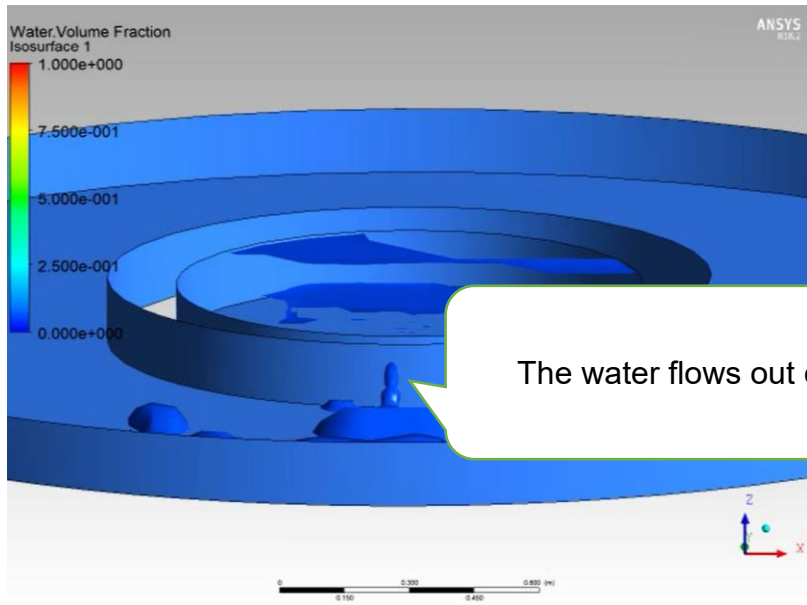


Figure 3-16. In the process, the water flows out from the pond.

3.5. Ingres' La Source

3.5.1. Using perspective to model the fluid containers

Following the method utilised in the study of *Jacob's Encounter with Rachel*, the key data in *La Source* can be collected and analysed. Through the method of Perspective and Trigonometric Functions, the key sizes of the pitcher can be calculated, including the length of the pitcher as a whole, the length of the bottleneck, the size of the opening, the diameters, and the slope.

The only thing that needs to be modelled in *La Source* is the pitcher, so it is not needed to measure the size in the same way as Raphael's painting. As with the analysis of *Jacob's Encounter with Rachel*, computer software (Matlab) can provide a more accurate measure of specific size than that taken by hand. To make the whole process easier, the pitcher was put in a digital grid graph in Matlab. All the key points of the pitcher were then located and the whole length and width were measured in the grid graph including points F, G, H, I, J and so on (see Fig. 3-17). The image is cut into sections and each section is a square. The squares are surfaces made of pixels. Having measured within the painting, we had the proportion between the length and width of the pitcher. Taking the

length of each square to be 'a', the length and width of the opening are around 3.45a and 5.00a respectively.

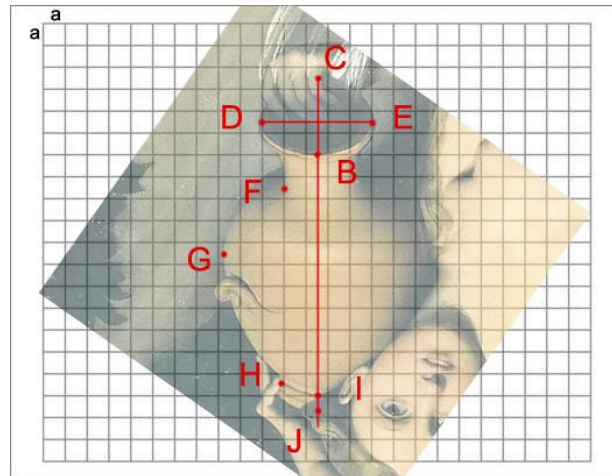


Figure 3-17. The pitcher in a digital grid graph

Second, based on the proportions above, the slope of the pitcher was calculated to be 44 degrees via the Trigonometric function. Here the opening of the pitcher should be a circle and the width should be the diameter. If the width is 5.00a and the length is 3.45a, by Trigonometric function the width = the diameter = BC = DE = 5.00a. The length = AB = 3.45a. So, $\text{Sin} \angle ACB = \frac{3.45a}{5.00a} = 0.69$ (see Fig. 3-18). By the Trigonometrical ratios table of Sin, it is clear that $\angle ACB$ is around 44 degrees.

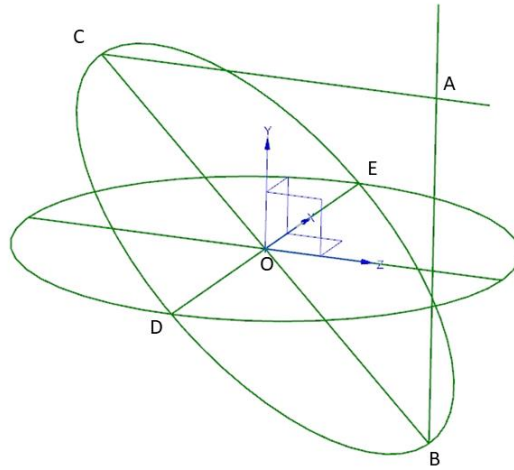


Figure 3-18. The schematic diagram of the opening

Following the geometric rules of perspective, all the key proportions can then be known, and the digital modelling is built through UG NX, the CAD software used in this case.

NURBS, as has been explained, is often used in industrial design, especially in sketching. Generally, product designers use Quadratic NURBS, Cubic NURBS, Quartic NURBS and Quintic NURBS to draw the profile of the object being designed. Undeniably, there are many functions and curves that can fit an outline or the profile of an object, but the NURBS function (see Equation 3-1) can tackle the task much more easily. It is also the reason why NURBS is often used in digital design, product design and reversing modelling.

$$C(u) = \sum_{i=1}^k \frac{N_{i,n} w_i}{\sum_{j=1}^k N_{j,n} w_j} \mathbf{P}_i = \frac{\sum_{i=1}^k N_{i,n} w_i \mathbf{P}_i}{\sum_{i=1}^k N_{i,n} w_i} \quad \text{Equation 3-1}$$

Here

In *La Source*, the pitcher can be seen as a combination of cone and cylinder. “In order to represent circles, cylinders and spheres, rational polynomials of at least quadratic order are necessary”.¹⁴⁹ This means that fitting the curve of the pitcher by NURBS is both possible and preferable. If the outer contour of the pitcher is fitted with a quadratic NURBS, a cubic NURBS, a quartic NURBS, and a quintic NURBS, different degrees of alignment are obtained (see Figs 3-19 to 3-22). From the figures, it is clear that the pitchers made by quadratic, quartic and quintic NURBS cannot cover the original one in *La source* well.



Figure 3-19. The outline is fitted by quadratic NURBS.



Figure 3-20. The outline is fitted by cubic NURBS.



Figure 3-21. The outline is fitted by quartic NURBS.



Figure 3-22. The outline is fitted by quintic NURBS.

By controlling the position of the key points, it became clear that the outline of the pitcher is best fitted by cubic NURBS and the model can be built via UG NX (see Fig. 3-23).

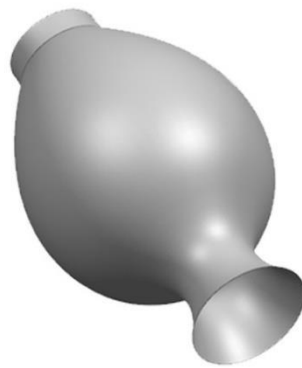


Figure 3-23. The digital model of the pitcher

3.5.2. Using CFD to simulate the water flow

To assure the quality and accuracy of the simulation and analysis, the pitcher has been scaled to a reasonable size – that is, kept in proportion to the woman’s head (the pitcher being two times as long as her head). Similar to the study of *Jacob’s Encounter with Rachel*, in the scene of *La Source* the water flow fits the air-water two-phase flow. There are two sorts of fluid considered, the air and the water flowing out of the pitcher. So, it is suitable for the VoF simulation method. Having simulated via CFD, the water flow can be shown (see Figs. 3-24 and 3-25).

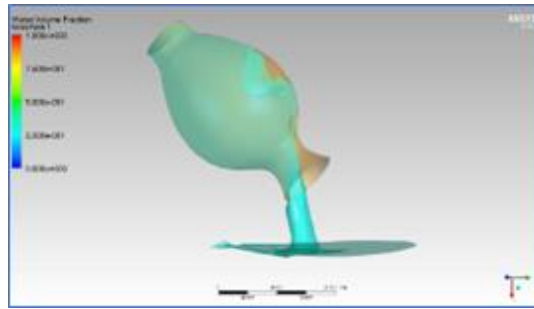


Figure 3-24. The start of the water flow

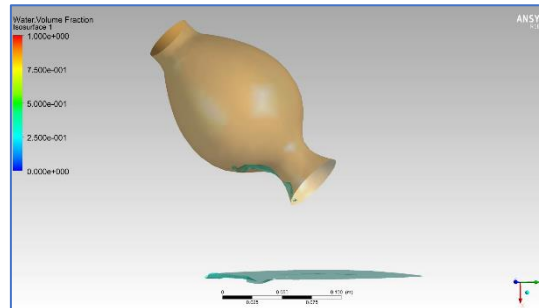


Figure 3-25. The end of the water flow

3.6. Results

3.6.1. Raphael's Jacob's Encounter with Rachel

The scene in Raphael's *Jacob's encounter with Rachel* has been reverted and simulated with reasonable conditions, i.e. the size calculation, analysis, the boundary conditions, and so on. The result shows the artist's 'unrealistic imagination' of water flows. Raphael is one of the three most influential artists (with Leonardo DaVinci and Michealangelo di Lodovico Buonarroti Simoni) in the period of the Renaissance. He is also a realism artist. For realism artists,

the accuracy of the drawing, sculpture or painting is important and cannot be ignored. The difference between the simulation results and the scene in the painting is significant if we put them together to compare from the same angle of view (see Fig. 3-26).

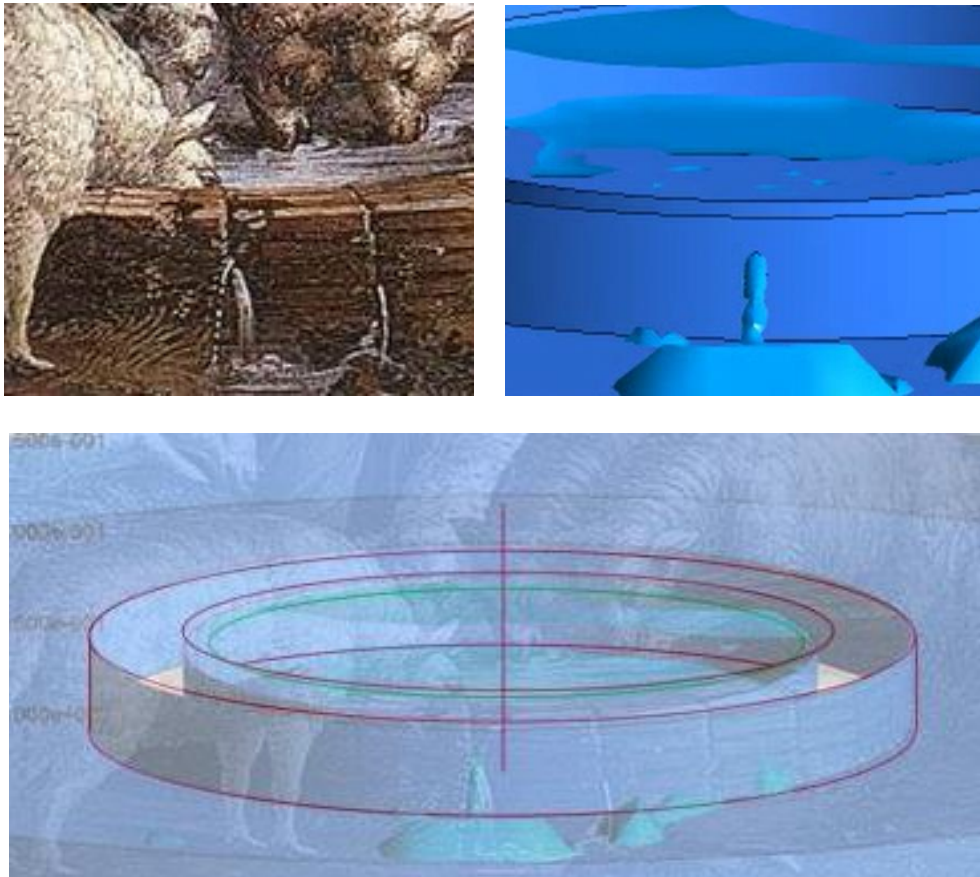


Figure 3-26. The comparison of Raphael's water flow and the simulation result

When compared with the painting, the simulation shows that the track of the water flowing out of the main outlet does not match the track in the painting. For easy comparison, cubic NURBS is used to draw the track of the water flow due to its higher continuity, resulting in a more natural and smoother surface

(see Figure. 3-27).

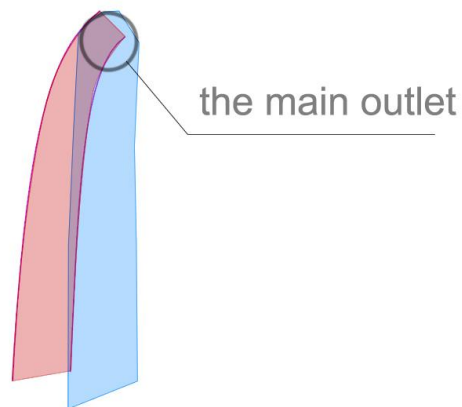


Figure 3-27. The red track is the water flow in Raphael's painting, the blue zone is the track of the water flow in simulation with more reasonable conditions.

Figure. 3-27 shows a result that came from more reasonable conditions because of the more possible assumption of the passageway of the water. The track from the simulation result shows the water passing through the straight edge of two sectors. However, the red track in Figure 3-27 represents the angle of the passageway should be different, which means the tilt angle should be smaller (see Figure. 3-28). Actually, the passageway may be more complicated than a straight tunnel. But still, if the water comes out with the track in Raphael's painting, the part connecting the main outlet should hold a smaller tilt angle, even if the tunnel is a curve.

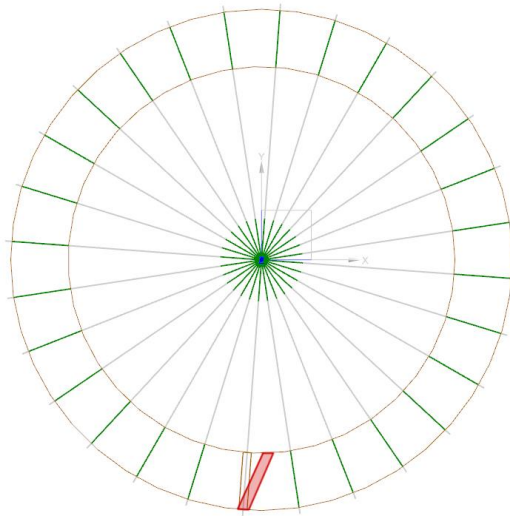


Figure 3-28. According to the simulation results, it is inferred that the red zone will be the more reasonable passageway for the water track from Raphael's painting.

3.6.2. Ingres' La Source

NURBSs of different orders were tested to ascertain which of them fit the profile of the 3D pitcher model the best, showing that it most accurately matches the cubic NURBS model, which is also the easiest curve to create. Since the quadratic NURBS have G1 and Cubic NURBS have G2 (that is, different orders of the functions which create the curves connecting the key points of the pitcher), it directly affects the profile of the pitcher and the shifts between light and dark on its surface (see Figure. 3-29 and 3-30). In this case, it is clear that

the Cubic NURBS is more suitable for fitting the pitcher from Ingres' painting.



Figure 3-29. The model was built by quadratic NURBS.

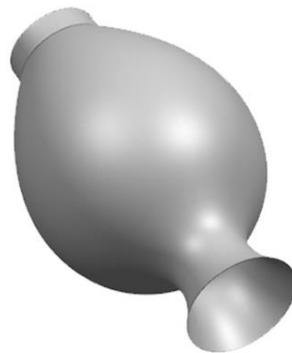


Figure 3-30. The model was built by cubic NURBS.

Secondly, from the digital representation of the scene in ANSYS and the water simulation with CFD, it was found that the projectile motion of the water from the pitcher doesn't match the numerical simulation precisely – that is, the simulation, which represents the flow of water from its start until its end when the pitcher is empty, does not contain within it the flow depicted in the painting. Ingres, in short, has very accurately captured the look and texture of the water's

flow, but there is a limitation in representing the movement of the liquid. On the other hand, as the water jar is positioned at a delicate angle to enable the water to flow out of the pitcher smoothly, without hindrance or choking, we would expect the water's fall to look gentle and comfortable, which is precisely what it does. In short, Ingres got everything correct in the water flow, with the exception of the streamline itself.

Thirdly, by controlling the position of the key points, it became clear that the outline of the pitcher is best fitted by cubic NURBS, and the model is built via UG NX. The results show that NURBS may provide a handier way to convert curved objects from paintings. Also, even the water flow cannot be presented beautifully by the simulation result, but based on the simulation, it can be tracked and fitted with NURBS very easily (see Figure. 3-31).



Figure 3-31. The comparison of the painting-pitcher and the converted 3D model

When compared with the original painting, the blue track, the simulation result, looks more natural and smoother. Unlike the case of Raphael's painting, the scene in *La Source* is easier to analyse. Also, the thickness of the pitcher does not have much of an impact. If we put the simulation result and the painting together, it is visibly clear how different they are. In reality, the water track is hardly like the painting. Even taking into account the hand holding the opening of the pitcher: if there is less water, the track will be like the blue zone, and if there is a lot more water, the track should not change to vertical that soon due to the greater pressure from the water and the speed of the water flow (see Figure. 3-32).



Figure 3-32. In the comparison of the simulation and the original painting, the red track is the water flow in Ingres' painting, the blue zone is the track of the water flow in the simulation.

3.7. Discussion, extensions, and implications

This part of the study has found the inaccuracy of the water flow scenes in Raphael and Ingres' paintings and the usefulness of the method introduced. In Raphael's case, due to the thickness, there are too many uncertainties inside the wall of the water tank. The water tunnel in the wall of the water tank has been presumed with an ideal state. The result shows Raphael's water flow might be possible, but it will be very difficult to match the state conditions of the water tunnel. In Ingres' case, NURBSs of different orders are tested to ascertain which of them fit the profile of the 3D pitcher model the best, showing that the pitcher's profile matches the cubic NURBS model most accurately. It is found that the pitcher is positioned at such a delicate angle to enable the water to flow out of the pot completely, without hindrance or choking. As a result, the water fall looks gentle and comfortable, but the projectile motion of the water from the jar doesn't match the numerical simulation very well. To produce a water flow the same as in Ingres's painting, the pitcher would need to change its angle, which means that it would need to rotate the body of the pitcher to the right with the diameter of the opening of the pitcher perpendicular to the painting as the axis.

Compared with the case of Ingres, Raphael's case is more complicated in the process of reverting and situation analysis. Nevertheless, the results demonstrate that there are some inaccuracies in the painting. This is mainly reflected in the parts related to fluids.

The study has shown that Ingres' representation of the track of the water flowing out of the pitcher does not correspond to the results of the scientific analysis. The flow of the water is smooth and gentle as would be expected as the simulation show, only it is along an inaccurate path. As such, it has also demonstrated that the combination of NURBS, CAD and CFD is a powerful tool for analysing artworks. It is also possible to extend the application of this approach and to state that so long as a painting – whether realistic or fantastic – aspires to give an effect of mimesis, the approach used in this paper can be applied to evaluate the accuracy of the flow of any fluids within it.

The accuracy of Ingres' painting, however, presents certain implications. One thing this study has not verified is how Ingres created *La Source*. Ingres and his students may have finished the painting through repeated practice in life drawing. The accuracy of the water flow, in this case, would be evidence of their profound talents in observation. Alternatively, they can have copied from a

photo, as Ingres is suspected to have used a camera in other works. As Martin Kemp notes, there is an “intuition” that “Ingres used a camera lucida to facilitate the making of drawn likenesses of visitors to Rome in the second decade of the nineteenth century”.¹⁵⁰ The use of a camera for this painting would make the achievement of accuracy more feasible, though arguably less impressive. Without evidence, either way, it is difficult to say for certain, though the texture and the look of the water flow can lend weight to arguments for a camera having been used. Further study is required to draw more decisive conclusions.

In addition to the value of this approach in the evaluation of artworks, it is clear that the approach can be used in the creation of art. In creating paintings without natural references, e.g., in fantastic or religious art, artists can utilise scientific calculations and simulations similar to the method above. Especially when describing a scene with water flow, or other fluids, people can simulate the scene via CFD and then use the simulation results as a reliable reference for creation. It is a method that can thus potentially influence the future development of art.

The study concludes, therefore, that both Raphael and Ingres’s masterpieces have produced impressive, one might say beautiful, representations of water

flow. On the other hand, the scenes lack the degree of accuracy seen in the simulations. The two artworks cannot withstand the rigorous examination of modern science. Both the two cases show that scenes with fluid are very difficult to represent with a high degree of accuracy, even for talented classic and realistic painters. However, having utilised CFD methods, NURBS and CAD, we can get a strong reference to guide us in art creation.

3.8. Method testing and practising in art creation

To test the practicality of the method and the application of the approach seeing how it benefits and guides art creation, a scene is designed and drawn. Like *Jacob's Encounter with Rachel* and *La Source*, the artwork is a realistic drawing and there is a human being and water flow in the picture. According to the method, the 3D model of the fluid container will be drawn first. Then following the simulation results, the track of the water flow will be drawn with cubic NURBS, which has C^2 and fit on water flowing easily, to ensure the accuracy and smoothness of the movement. At last, the whole picture will be drawn accurately.

3.8.1. Designing and modelling the liquid container

To test the method, the liquid container should be an object which has an irregular hyperboloid shape. This is so that people cannot imagine how water should flow out. Also, it is better if the opening of the container is not a circle or a square. Besides, the angle of view should be random and not be 100% front, 100% back, 100% left, 100% right, 100% bottom, and 100% top. Then it will be a big challenge for everyone to draw the container and the track of the water flow accurately.

Here the shape of the container has been drawn by cubic NURBS. The opening of it is oval. The bottom of the container is bigger than the top. The designed container meets all the conditions and has been drawn with UG NX (see Figure. 3-33 to 3-36).

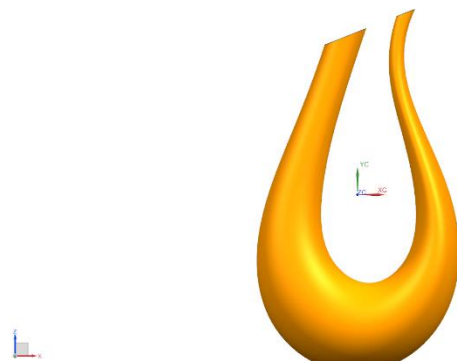


Figure 3-33. The left view of the liquid container



Figure 3-34. The front view of the liquid container



Figure 3-35. The top view of the liquid container



Figure 3-36. The bottom view of the liquid container

3.8.2. The simulation of the water flow

The liquid container has been scaled to a reasonable size (170 mm x 280 mm), which means the quality and accuracy of the simulation and analysis can be insured. Also, the angle of view is put irregularly. The water flow in the scene fits the air-water two-phase flow and it is suitable for the VoF simulation method. Having simulated via CFD, the water flow can be shown (see Figures. 3-37 and 3-38).

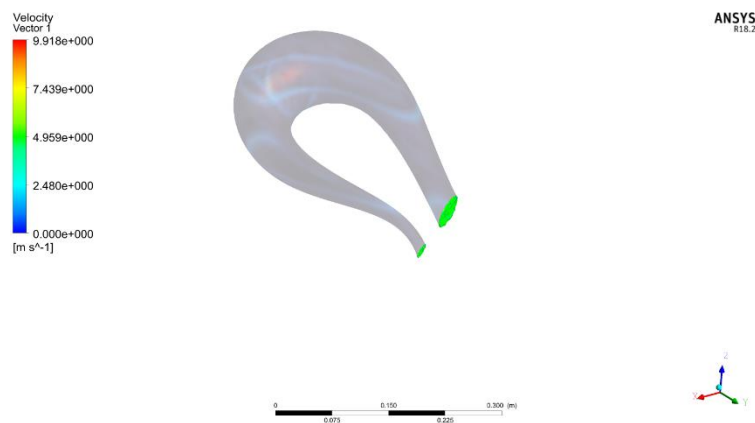


Figure 3-37. The start of the water flow

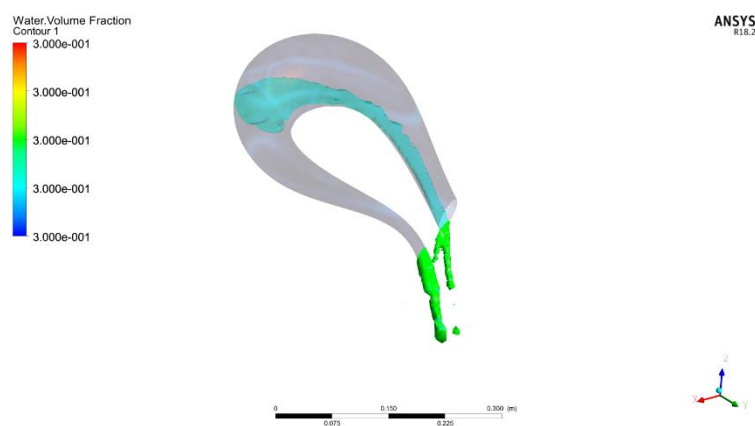


Figure 3-38. The water flow at 2.9999 seconds

Changing the view angle, we have the paths of the water flow with different looks. Obviously, the simulation result can not present the water flow very beautifully. With cubic NURBS, the track of the water flow is drawn smoothly and easily (see Figure. 3-39).

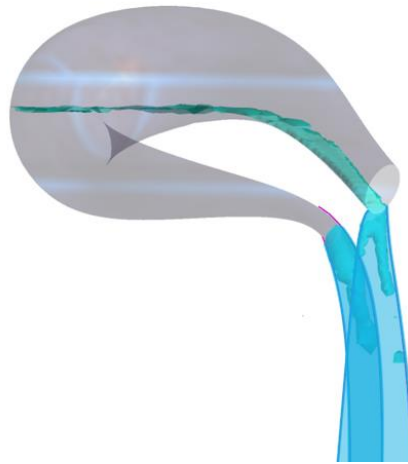


Figure 3-39. The scene is the water flowing out from the liquid container and the blue zone is the track of the water flow. The water flow path changes when the view angle changes.

3.8.3. The sketch of the artwork produced with the method

From the results, we can find that it is very difficult to imagine the water flowing if the structure of the container is complicated, especially the sort of surface made by hyperboloids. However, based on the design and analysis results, we

can use NURBS to draw the water flow easily and accurately. If combined with other different elements like the human body together, a realistic artwork can be created with high accuracy (see Figure. 3-40).

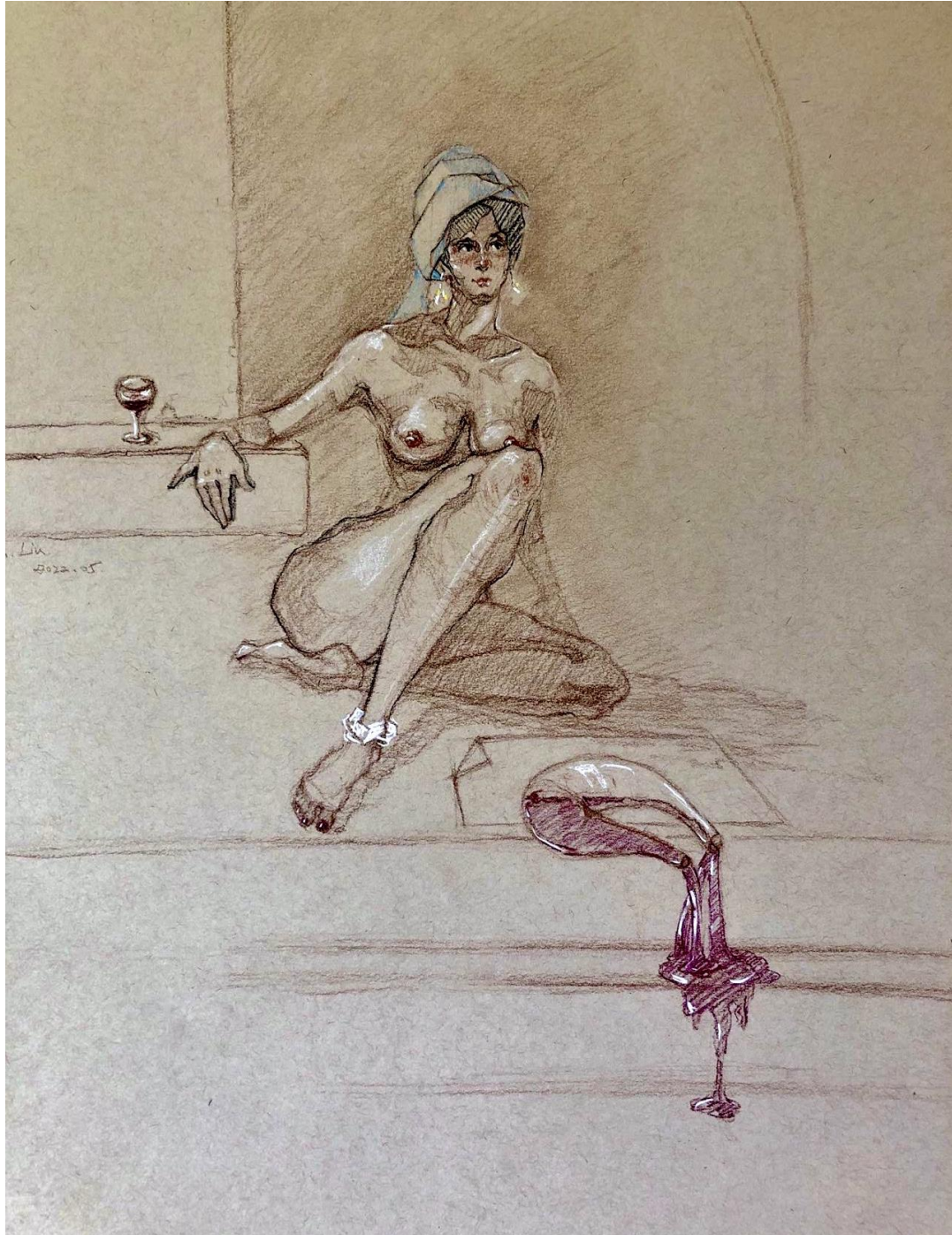


Figure 3-40. Susanna at her Bath by Han LIU (draft)

3.9. Conclusion

The method provides a reliable reference for product design and art creation, and it can be used to create realistic artwork and abstract artwork both. There will be no limitation in designing the liquid container, which means people do not have to find a real object as the container and draw it in life or take photos for reference. This theory provides infinite possibilities for the artist's creation. With the innovation of VR and AR technology, modelling will become easier and easier, and this approach will also allow metaverse art to be better developed too.

CHAPTER 4. THE RIGIDITY OF NURBS AND ITS APPLICATION IN CHINESE CALLIGRAPHY

4.1. Introduction

NURBS, combined with CFD, has been demonstrated as a useful tool for the scientific evaluation of flow in realistic art as well as the creation of new works with realistic fluidic scenes. This chapter now turns to a different area of art – striking, or powerful, lines – and shows how the rigidity of NURBS can be explained mathematically, and how it can be used to study and appreciate, as well as create, Chinese calligraphy in particular. There is a connection between NURBS and beam bending functions, resulting in a dimensionless quantity that can help people to learn what might be termed the spirit of Chinese calligraphy. Key to this is the rigidity of NURBS.

NURBS has 14 properties that designers and mathematicians use often in their work or research, including local support (easy to control and change the NURBS curve and surface) and continuity.¹⁵¹ However, the rigidity of NURBS

has still rarely been discussed. Apart from the two properties above, rigidity is another important property of NURBS, even though there are few studies that try to explain it mathematically. In art, people use anatomy to draw bones, muscles, or movements normatively and use perspective to show the space and different locations academically. But it is little known that the rigidity of NURBS can be used in art creation too. The dimensionless quantity bridges NURBS and beams bending, contributing to a relationship between abstract and reality. The Dimensionless quantity is a mathematical concept and is completely abstract.¹⁵² But in this chapter, this abstract concept has been utilised to explain the rigidity of NURBS and why NURBS makes the curve or outline look powerful or energetic. Power and energy are two things in reality and people can feel or recognise them in the real world. Artists often attempt to represent and show power or energy in their artworks, with dots, lines or planes. Based on the rigidity of NURBS, the research discussed in this chapter provides a new approach to guiding artists in drawing a powerful and energetic line more skillfully.

As a good sample to test this use of NURBS Chinese calligraphy. Good Chinese calligraphy artwork has two unmissable features: beauty and power.¹⁵³ The beauty of Chinese calligraphy depends on the structure of the word, including

the location of the strokes, the size difference of the strokes, the balance, the shape, the rhythm, and so on.^{154 155} The power of Chinese calligraphy is shown by the track of the strokes, in other words, the strokes' bones. Significantly, for human beings and animals, bones always show power and energy, for plants, the stem is the bone. So, it is in Chinese calligraphy. Using NURBS and the dimensionless quantity, people can improve their understanding and draw the soul and spirit (power and energy) of Chinese calligraphy with an academic approach.

4.2. The rigidity of NURBS and the dimensionless quantity

Rigidity, also sometimes called stiffness, is a physical concept. Here it means the property of a solid body to resist deformation. Solid objects like beams have rigidity. When a beam is bent, a common physical phenomenon, its rigidity can be reflected. For example, beams are deformed due to load, stress, or twist. People can point out if the beams are stiff or soft based on the extent of the deflections. From this perspective, the beam's rigidity can be recognized visually with some simple conditions, which means the rigidity is visible. But people cannot know the specific rigidity parameters of the beams by their

observations only because the parameters need to be obtained by calculation in a mathematical way.

Bent beams are used for study in this chapter because of their generality and simplicity. Generally, bent beams exist around us, including man-made ones and natural ones. For instance, people bend wooden or metal beams to meet the requirements of design or manufacture. Similarly, bridge engineers pay careful attention to the bending of the bridge. In nature, the branches of the willow tree are bent due to gravity as well as strong wind. For a simple bending, the straight beam becomes a simple curve. And such a bent beam looks like a NURBS curve. So, compared with complicated deformation, simple bending are easier to analyse and there is the possibility to connect NURBSs and beam bending.

There are seven different cases of beam bending and, in this chapter, most of them are analysed (see Figures. 4-1 to 4-7).¹⁵⁶

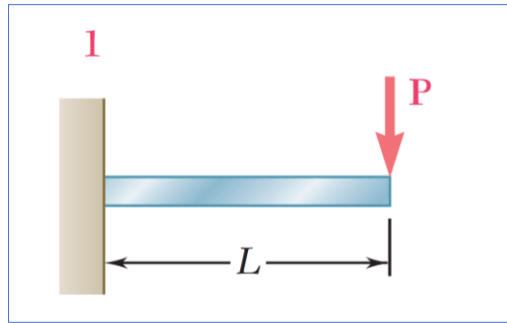


Figure 4-1. Case NO. 1 (the loading at the end)

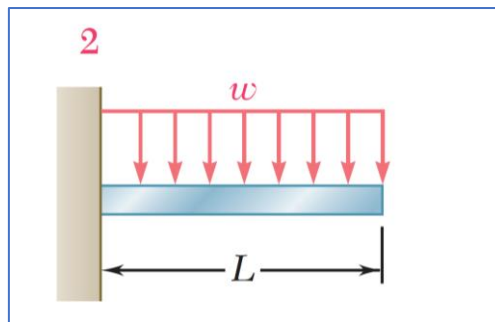


Figure 4-2. Case NO. 2 (the loading on the top surface)

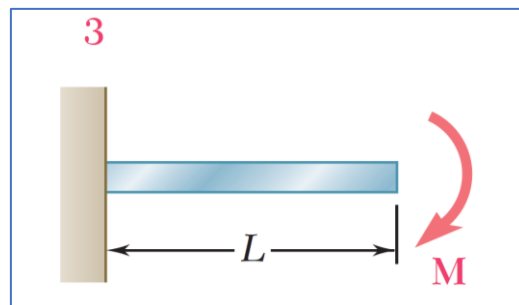


Figure 4-3. Case NO. 3

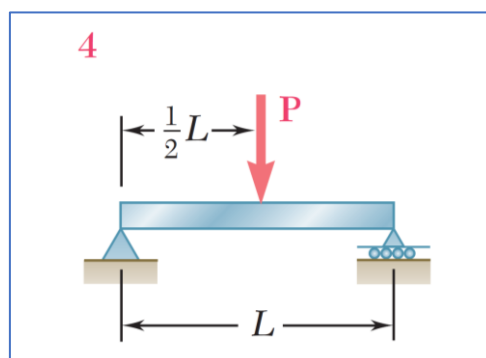


Figure 4-4. Case NO. 4 (the loading at the middle)

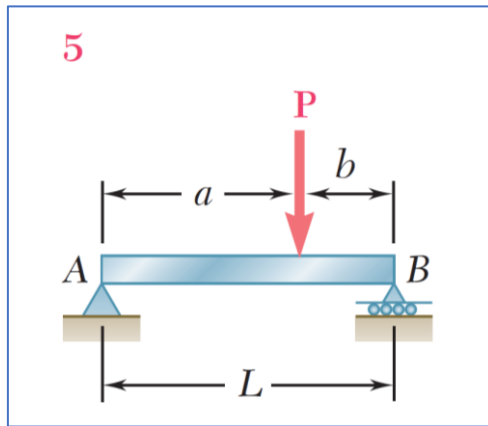


Figure 4-5. Case NO. 5 (the loading at a random point)

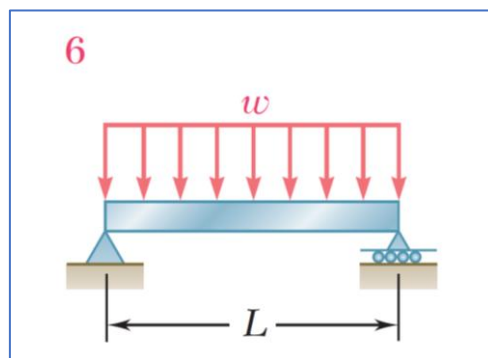


Figure 4-6. Case NO. 6 (the loading on the top surface)

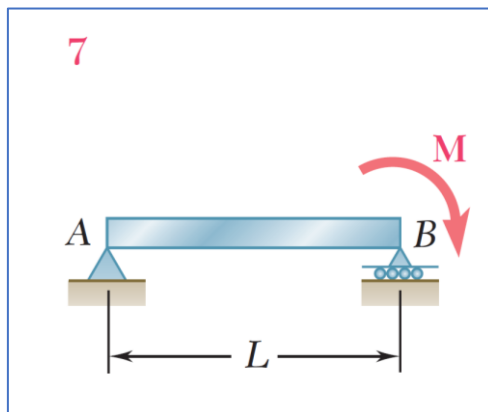


Figure 4-7. Case NO. 7

The three –cases – No.1, No.2 and No.4 - are the most common ones and can be easily found in nature, art creation, design or our daily life. Also, compared

with the other four, they are the simpler three deformation cases of the beam.

4.2.1. Using NURBS to fit beam bending in visual

Visually, a beam bent in a simple way looks like a NURBS of degree three or more. The NURBS curve is represented mathematically by a polynomial of degree one less than the order of the curve. Hence, second-order curves (which are represented by linear polynomials) are called linear curves, third-order curves are called quadratic curves, and fourth-order curves are called cubic curves. That means that when a beam like a Cantilever beam or a simple supported beam is bent, it looks like a quadratic NURBS or NURBS with a higher degree. It does not look like NURBS with second order because NURBSs are piecewise functions and the two degrees of NURBSs are made of straight-line segments -linear functions-, not curves (see Figure. 4-8).

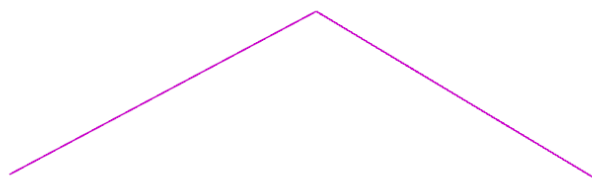


Figure 4-8. A NURBS with second order

For example, in Case No. 1, the platform - the one in the springboard diving - is a good sample for the analysis because the start point is fixed, and the load is at the endpoint of the beam. In springboard diving, the load from the athlete causes deformation and makes the platform change from a flat face to a curved face. From the side, the platform changes from straight to curved. So, at this time, the platform becomes a sort of cantilever beam, and it looks like a NURBS curve (see Figure. 4-9). The platform is simplified using Photoshop and the NURBS curves are drawn in UG-NX (see Figures. 4-10 and 4-11). The bent platform has been compared with NURBS in different orders, including quadratic NURBS, cubic NURBS and quartic NURBS.

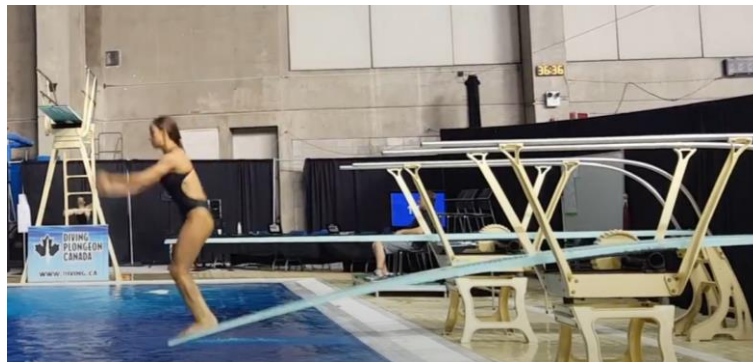


Figure 4-9. The platform is bent because of the load on the endpoint. (The image was found from the Internet.)



Figure 4-10. The platform is simplified using Photoshop.

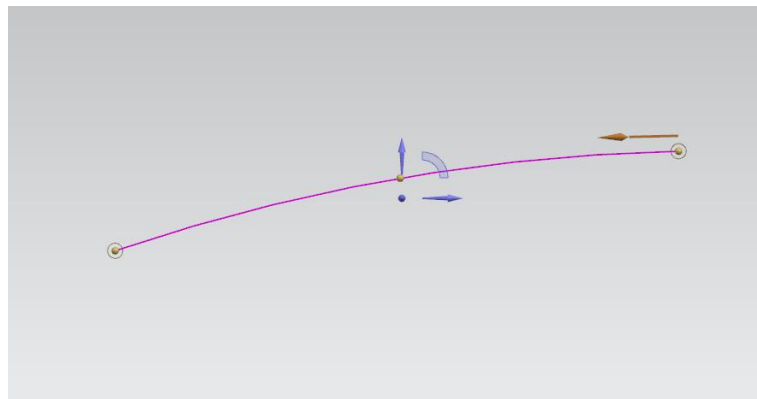


Figure 4-11. A quadratic NURBS curve is drawn in UG-NX

The second example is Case No. 4. Case No. 4 is a sort of simply supported beam. In Case No. 4, the load is in the middle of the beam. The start-point of the beam has been fixed and the endpoint is able to move because the endpoint is a sliding hinge support. Sliding hinge support represents a constraint that only provides vertical support, but does not provide lateral constraints or bending moment constraints. That means it only constrains the displacement of the member towards the support surface along the support surface normally. Of course, in engineering design, the endpoint of the beam does not have to be

equipped with wheels, but there must be room for deformation. It is mainly used for the articulation of building nodes, especially for the articulation of steel structures or steel-concrete membrane structure nodes in airports, stations, subway facilities, stadiums, halls and exhibition halls, etc., and can also meet the needs of bridge shock absorption. It can ensure the free deformation of the structure under the action of live load, temperature change, concrete shrinkage, and creep (see Figure. 4-12).

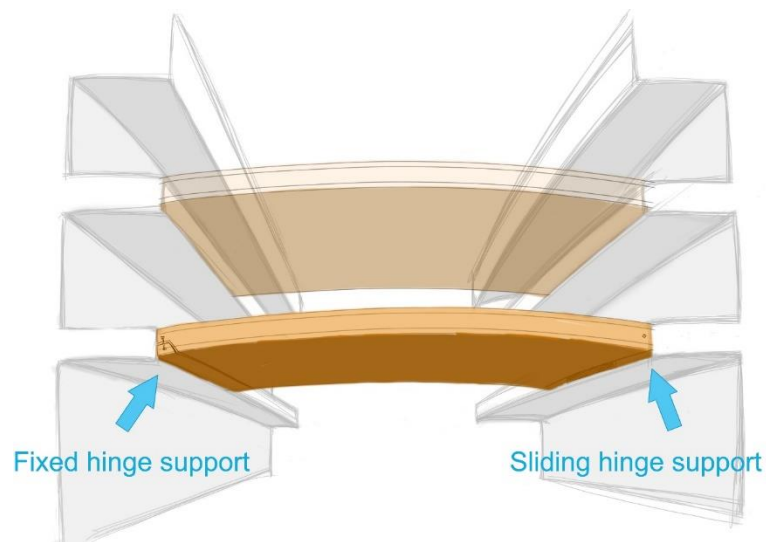


Figure 4-12. This is an example - the sketch by Han Liu - of the simply supported beam with Fixed hinge support and Sliding hinge support in engineering. The types of Sliding hinge support are various in practical applications. In this example, there is a corridor between the two buildings. Since the deformation of the two buildings is not consistent, the corridor is made into a simply supported beam, one end is Fixed hinge support, and the other end is Sliding hinged support.

Apart from the explanation of the example, the comparison of Case No. 4 and NURBS is shown by the simulation. The corridor is assumed to be steel, and the parameter is Steel 40X40X1000 5000N. This means that the cross-section is a square 40mm × 40mm, the total length is 1000mm, and the load in the middle is 5000N. Based on these boundary conditions, the stress analysis of the steel beam is shown (see Figure. 4-13).

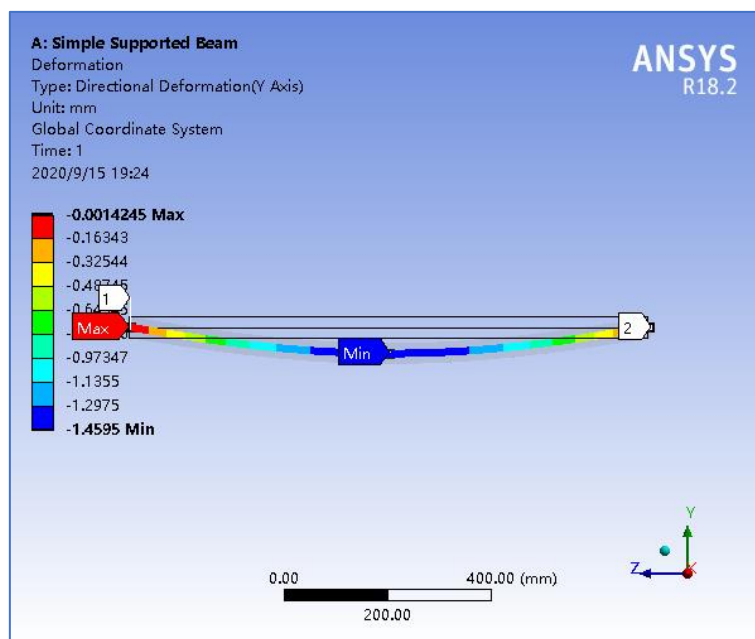


Figure 4-13. The simulation result of the steel beam

From the simulation result, it is clear that the deformation in the middle of the beam is the most because of the location of the load. On the one hand, the simulation result clearly shows the steel beam bent to curvy from straight due to the load on it. On the other hand, this image is a schematic diagram only, and the specific numbers of deformations are listed on the left side. That means

the beam in the image is not drawn by the parameters of the deformations. So, to compare with the curved beam and NURBS, the curve drawn with deformations and NURBSs are put together (see Figures. 4-14 to 4-16).

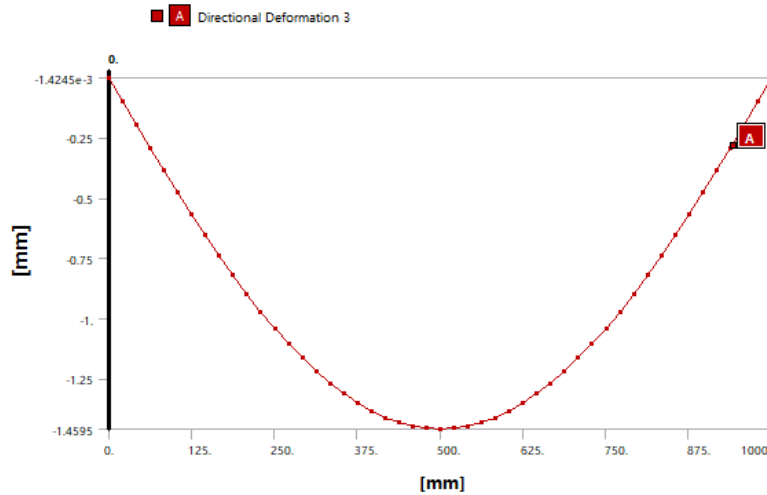


Figure 4-14. The curve is drawn by directional deformations of the beam. A is the third directional deformation.

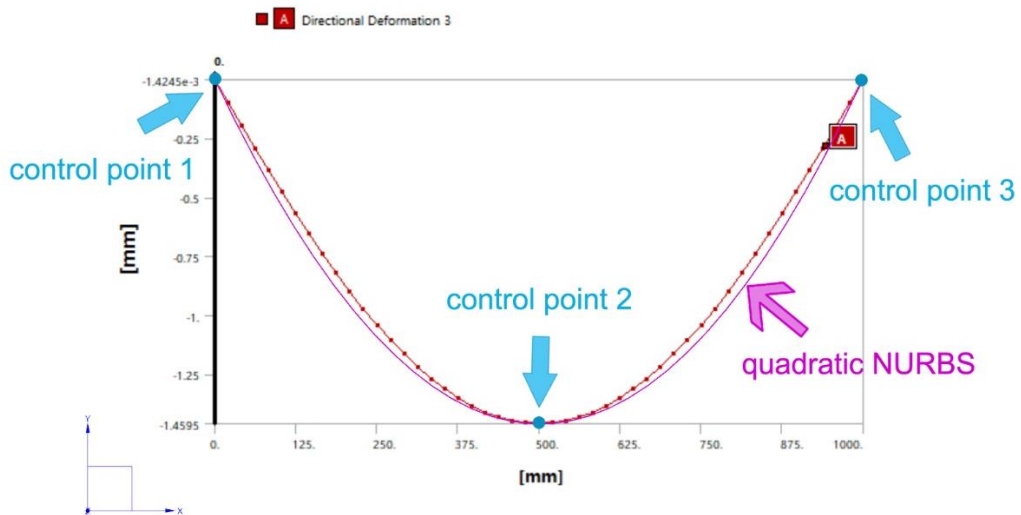


Figure 4-15. The comparison of the deformations and quadratic NURBS

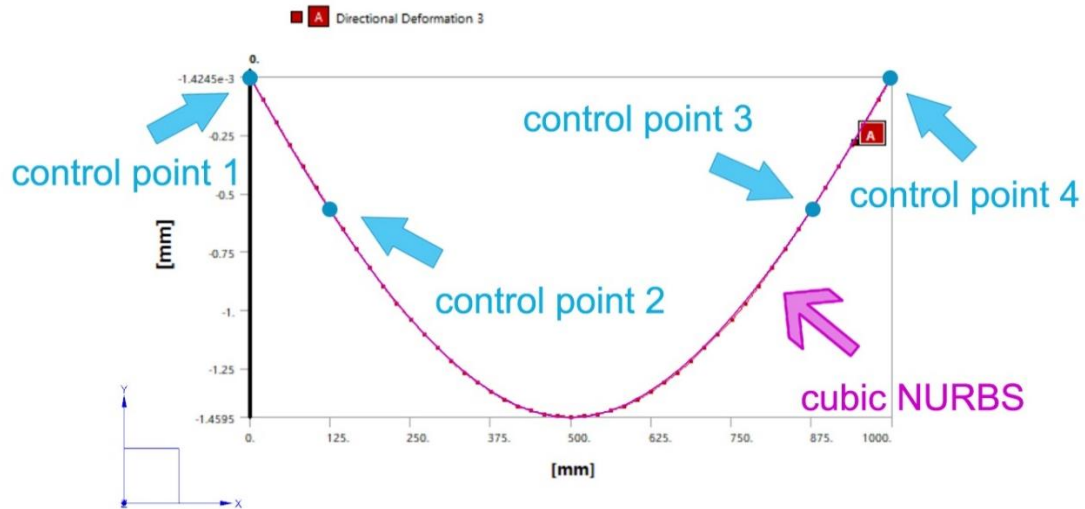


Figure 4-16. This is the comparison of the deformations and cubic NURBS. Because the deformation curve is a parabola, the locations of the control points need to be mirrored.

4.2.2. Using dimensionless quantity to bridge NURBS and beam bending in mathematics

In this part of the study, the three cases including Case No.1, Case No.2 and Case No.4 are mathematically fitted with cubic NURBS, and the mathematical connection – the dimensionless quantity – between the beam bending function and NURBS has been found. Case No.1 is a cantilever beam and its deformation changes as the load at the endpoint changes. Case No.2 is also a cantilever beam and its deformation changes as the load on the whole body changes. Case No.4 is a simply supported beam and its deformation changes as the load in the middle or to the left of the midpoint changes. The Beam Deflection and Slopes form shows the possible forms of beams and loading (see Figure. 4-17). The functions of NURBS and the three beam bendings are

analysed mathematically, resulting in a mathematical relation. The Case No.5 is not included in this part of the analysis.

APPENDIX C Beam Deflections and Slopes

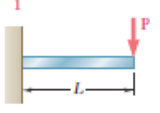
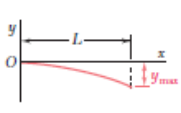
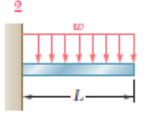
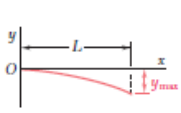
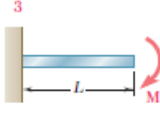
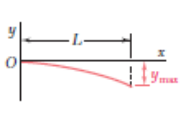
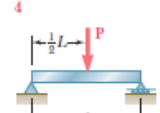
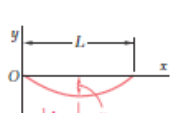
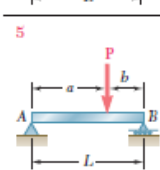
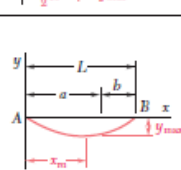
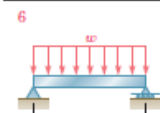
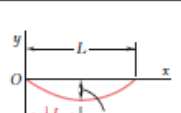
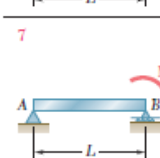
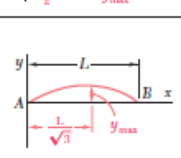
Beam and Loading	Elastic Curve	Maximum Deflection	Slope at End	Equation of Elastic Curve
		$-\frac{PL^3}{3EI}$	$-\frac{PL^2}{2EI}$	$y = \frac{P}{6EI}(x^3 - 3Lx^2)$
		$-\frac{wL^4}{8EI}$	$-\frac{wL^3}{6EI}$	$y = -\frac{w}{24EI}(x^4 - 4Lx^3 + 6L^2x^2)$
		$-\frac{ML^2}{2EI}$	$-\frac{ML}{EI}$	$y = -\frac{M}{2EI}x^2$
		$-\frac{PL^3}{48EI}$	$\pm \frac{PL^2}{16EI}$	For $x \leq \frac{1}{2}L$: $y = \frac{P}{48EI}(4x^3 - 3L^2x)$
		For $a > b$: $-\frac{Pb(L^2 - b^2)^{3/2}}{9\sqrt{3}EIL}$ at $x_m = \sqrt{\frac{L^2 - b^2}{3}}$	$\theta_A = -\frac{Pb(L^2 - b^2)}{6EIL}$ $\theta_B = +\frac{Pa(L^2 - a^2)}{6EIL}$	For $x < a$: $y = \frac{Pb}{6EIL}[x^3 - (L^2 - b^2)x]$ For $x = a$: $y = -\frac{Pa^2b^2}{3EIL}$
		$-\frac{5wL^4}{384EI}$	$\pm \frac{\Sigma L^3}{24EI}$	$y = -\frac{w}{24EI}(x^4 - 2Lx^3 + L^3x)$
		$\frac{ML^2}{9\sqrt{3}EI}$	$\theta_A = +\frac{ML}{6EI}$ $\theta_B = -\frac{ML}{3EI}$	$y = -\frac{M}{6EIL}(x^3 - L^2x)$

Figure 4-17. The Beam Deflection and Slopes¹⁵⁷

Based on the findings in fitting beam bending with NURBS in 4.2.1, the cubic NURBS is utilised in the following study, because the cubic NURBS fitted the deformation curve best. Further, there is a possibility of fitting the beams with cubic NURBSs in an easy way, even automatically obtaining the location of the control points.

4.2.2.1. Cantilever beam in Case NO. 1, NURBS, and dimensionless quantity

The first cantilever beam in Case NO.1 and dimensionless quantity is discussed in this part. Since Case No.1 is a cubic function, it can be exactly replicated by a segment of cubic B-Splines, which is a simplified NURBS.¹⁵⁸ The question is then where the four control points should be so that the cubic B-Splines can represent the beam deflection. The B-Splines that are defined by four control points $\mathbf{P}_0, \mathbf{P}_1, \mathbf{P}_2, \mathbf{P}_3$ is

$$\mathbf{C}(t) = \frac{1}{6}(1-t)^3\mathbf{P}_0 + \frac{1}{6}(3t^3 - 6t^2 + 4)\mathbf{P}_1 + \frac{1}{6}(-3t^3 + 3t^2 + 3t - 1)\mathbf{P}_2 + \frac{1}{6}t^3\mathbf{P}_3, \text{ Equation 4-1}$$

Here \mathbf{C} is the B-Splines curve, t is the variable, and $\mathbf{P}_0, \mathbf{P}_1, \mathbf{P}_2, \mathbf{P}_3$ are the four control points.

with $t \in [0,1]$. t can be written as a polynomial function of t :

$$\mathbf{C}(t) = \alpha_0 + \alpha_1 t + \alpha_2 t^2 + \alpha_3 t^3, \text{ Equation 4-2}$$

Where

$$\alpha_0 = \frac{1}{6}(\mathbf{P}_0 + 4\mathbf{P}_1 + \mathbf{P}_2)$$

$$\alpha_1 = -\frac{1}{2}(\mathbf{P}_0 - \mathbf{P}_2)$$

$$\alpha_2 = \frac{1}{2}(\mathbf{P}_0 - 2\mathbf{P}_1 + \mathbf{P}_2)$$

$$\alpha_3 = -\frac{1}{6}(\mathbf{P}_0 - 3\mathbf{P}_1 + 3\mathbf{P}_2 - \mathbf{P}_3)$$

Suppose the coordinates of the four control points $\mathbf{P}_0, \mathbf{P}_1, \mathbf{P}_2, \mathbf{P}_3$ on a Cartesian are $(x_0, y_0), (x_1, y_1), (x_2, y_2)$ and (x_3, y_3) . The curve can be then described by a parametric function of $x(t)$ and $y(t)$, $0 \leq t \leq 1$. First, we can write $x(t)$ as

$$x(t) = a_0 + a_1t + a_2t^2 + a_3t^3 \quad \text{Equation 4-3}$$

Where

$$a_0 = \frac{1}{6}(x_0 + 4x_1 + x_2)$$

$$a_1 = -\frac{1}{2}(x_0 - x_2)$$

$$a_2 = \frac{1}{2}(x_0 - 2x_1 + x_2)$$

$$a_3 = -\frac{1}{6}(x_0 - 3x_1 + 3x_2 - x_3)$$

For $x(t)$, its form can be as simple as possible, for example, $x(t) \propto t$, and $x(0) = 0$, $x(1) = L$, where L is the length of the beam. Then the x values of the four control points can be obtained as:

$$a_2 = \frac{1}{2}(x_0 - 2x_1 + x_2) = 0 \Rightarrow x_1 = \frac{1}{2}(x_0 + x_2)$$

$$a_3 = -\frac{1}{6}(x_0 - 3x_1 + 3x_2 - x_3) = 0 \Rightarrow x_2 = \frac{1}{2}(x_1 + x_3) \quad \text{Equation 4-4}$$

$$x(0) = a_0 = \frac{1}{6}(x_0 + 4x_1 + x_2) = 0 \Rightarrow x_1 = 0$$

$$x(1) = a_0 + a_1 = l \Rightarrow -\frac{1}{3}x_0 + \frac{2}{3}x_2 = L$$

Or,

$$x_0 = -L$$

$$x_1 = 0$$

$$x_2 = L$$

Equation 4-5

$$x_3 = 2L$$

$$x(t) = Lt$$

Similar to $x(t)$, the $y(t)$ function of the curve is:

$$y(t) = b_0 + b_1t + b_2t^2 + b_3t^3$$

Equation 4-6

Where

$$b_0 = \frac{1}{6}(y_0 + 4y_1 + y_2)$$

$$b_1 = -\frac{1}{2}(y_0 - y_2)$$

$$b_2 = \frac{1}{2}(y_0 - 2y_1 + y_2)$$

$$b_3 = -\frac{1}{6}(y_0 - 3y_1 + 3y_2 - y_3)$$

For the beam under load case 1, the caps flecion follows $y = \frac{P}{6EI}(x^3 - 3Lx^2)$.

Substituting x with $x(t) = Lt$, the parametric function of $y(t)$ can then be written as

$$y(t) = \frac{P}{6EI}(L^3t^3 - 3L^3t^2) = \frac{PL^3}{6EI}(t^3 - 3t^2)$$

Equation 4-7

Here P is the force/load, L is the length of the beam, E means the materials, and intersection shapes defined as I .

The coefficients can be matched to polynomial terms to Equation 4-8:

$$b_0 = \frac{1}{6}(y_0 + 4y_1 + y_2) = 0$$

$$b_1 = -\frac{1}{2}(y_0 - y_2) = 0$$

$$b_2 = \frac{1}{2}(y_0 - 2y_1 + y_2) = -3\frac{PL^3}{6EI} = -3A \quad \text{Equation 4-8}$$

$$b_3 = -\frac{1}{6}(y_0 - 3y_1 + 3y_2 - y_3) = \frac{PL^3}{6EI} = A$$

$$\text{where } A = \frac{PL^3}{6EI}$$

Therefore,

$$y_0 = -2A$$

$$y_1 = A$$

$$y_2 = -2A \quad \text{Equation 4-9}$$

$$y_3 = -5A$$

and when $t = 1$, the maximum deflection is:

$$y(1) = -\frac{PL^3}{3EI} = -2A \quad \text{Equation 4-10}$$

Suppose an artist selects two points $(0, 0)$ and $(L, -D)$ to draw the deflected beam, and based on (10), $y(1) = -2A = -D$, the four points the artist should

choose are $(-L, -D)$, $(0, 0.5D)$, $(L, -D)$, and $(2L, -2.5D)$, so that the defined cubic B-spline/NURBS curve will match the beam deflection exactly. If we assume $L = 1$ (so that D is equal to the ratio of the endpoint beam length), the four points become $(-1, -D)$, $(0, 0.5D)$, $(1, -D)$, and $(2, -2.5D)$.

More generally, a dimensionless position can be defined as $x' = x/L$ and a dimensionless deflection as $y' = y/L$, and

$$y'(t) = \frac{PL^2}{6EI}(x'^3 - 3x'^2) \quad \text{Equation 4-11}$$

The dimensionless quantity $\frac{PL^2}{6EI}$ characterizes the beam deflection with different load (P), length of the beam (L), materials (E), and intersection shapes (I). If the dimensionless quantities are the same for two beams, the dimensionless deflections will follow the same parametric function.

4.2.2.2. Cantilever beam in Case NO. 7 and NURBS

As the deflection for Case NO.7 is also a cubic function,

$$y = -\frac{ML^2}{6EI}(x^3 - L^2x) \quad \text{Equation 4-12}$$

the same methodology in Case NO.1 can be applied to Case NO.7 as well, in which the location of the four control points is derived based on the deflection

formula.

The x coordinates are the same as Eqn. (5), where $x(t) = Lt$. Therefore, the deflection function can be written as:

$$y = -\frac{M}{6EI}(t^3 - t) \quad \text{Equation 4-13}$$

The coefficients can be matched to polynomial terms to Eq. (6):

$$\begin{aligned} b_0 &= \frac{1}{6}(y_0 + 4y_1 + y_2) = 0 \\ b_1 &= -\frac{1}{2}(y_0 - y_2) = \frac{ML^2}{6EI} \\ b_2 &= \frac{1}{2}(y_0 - 2y_1 + y_2) = 0 \\ b_3 &= -\frac{1}{6}(y_0 - 3y_1 + 3y_2 - y_3) = -\frac{ML^2}{6EI} \end{aligned} \quad \text{Equation 4-14}$$

Therefore,

$$\begin{aligned} y_0 &= -A \\ y_1 &= 0 \\ y_2 &= A \\ y_3 &= -4A \end{aligned} \quad \text{Equation 4-15}$$

$$\text{where } A = \frac{ML^2}{6EI}$$

The maximum deflection is located at $x = L/\sqrt{3}$ and $y_{max} = \frac{ML^2}{9\sqrt{3}EI}$. Therefore,

if an artist selects two points $(0, 0)$ and $(L/\sqrt{3}, D)$ to draw the beam with the load in NO.7, the four points the artist should choose are $(-L, -\frac{3/\sqrt{3}}{2}D)$, $(0, 0)$, $(L, \frac{3/\sqrt{3}}{2}D)$, and $(2L, -6\sqrt{3}D)$, so that the defined cubic B-spline/NURBS curve will match the beam deflection exactly.

Similarly, a dimensionless deflection function can be given if $x' = x/L$ and $y' = y/L$ are plugged into Equation 4-16:

$$y' = -\frac{ML}{6EI}(x'^3 - x') \quad \text{Equation 4-16}$$

In this case, the quantity $\frac{ML}{6EI}$ characterizes the beam deflection with different torque (M), length of the beam (L), materials (E), and intersection shapes (I).

4.2.2.3. Cantilever beam in Case NO. 3 and NURBS

The deflection equation in Case NO.3 is a quadratic function, which is easier to generate the exact quadratic B-Spline match:

$$y = -\frac{M}{2EI}x^2 \quad \text{Equation 4-17}$$

Three control points $\mathbf{P}_0, \mathbf{P}_1, \mathbf{P}_2$, or $(x_0, y_0), (x_1, y_1), (x_2, y_2)$ in a Cartesian coordinate, can define a quadratic B-Spline curve:

$$\mathbf{C}(t) = \frac{1}{2}(1-t)^2\mathbf{P}_0 + \frac{1}{2}(-2t^2 + 2t + 1)\mathbf{P}_1 + \frac{1}{2}t^2\mathbf{P}_2 \quad \text{Equation 4-18}$$

The equation can be written as a polynomial of t :

$$C(t) = t^2 \left(\frac{1}{2}P_0 - P_1 + \frac{1}{2}P_2 \right) + t(-P_0 + P_1) + \frac{1}{2}(P_0 + P_1) \quad \text{Equation 4-19}$$

Similarly, matching coefficients in Equation 4-18 to $x = Lt$, it can be derived that:

$$\frac{1}{2}x_0 - x_1 + \frac{1}{2}x_2 = 0$$

$$x_1 - x_0 = L$$

$$x_1 + x_0 = 0$$

Therefore,

$$x_0 = -\frac{1}{2}L, x_1 = \frac{1}{2}L, x_2 = \frac{3}{2}L \quad \text{Equation 4-20}$$

Plugging $x = Lt$ into Equation 4-16 and again matching coefficients to Equation 4-18, it can be derived that:

$$\frac{1}{2}y_0 - y_1 + \frac{1}{2}y_2 = -\frac{ML^2}{2EI}$$

$$y_1 - y_0 = 0$$

$$y_1 + y_0 = 0$$

Therefore,

$$y_0 = y_1 = 0, y_2 = -\frac{ML^2}{EI} \quad \text{Equation 4-21}$$

The maximum deflection is located equal $x = L$ and $y_{max} = -\frac{ML^2}{EI}$. Therefore, if an artist selects two endpoints $(0, 0)$ and $(L, -D)$ to draw the beam with the load in NO.3, the three points the artist should choose are $(-\frac{1}{2}L, 0)$, $(\frac{1}{2}L, 0)$, and $(\frac{3}{2}L, -2D)$, so that the defined quadratic B-spline/NURBS curve will match the beam deflection exactly.

The dimensionless deflection function can be given if $x' = x/L$ and $y' = y/L$ are plugged into Equation 4-16:

$$y' = -\frac{ML}{2EI}x'^2 \quad \text{Equation 4-22}$$

In this case, the quantity $\frac{ML}{2EI}$ characterizes the beam deflection with different torque (M) on the end, length of the beam (L), materials (E), and intersection shapes (I).

The mathematical analysis and conclusion of the three cases show that NURBS (or B-Spline, the simplified NURBS) has the same mathematical form as several common beam bending. Therefore, NURBS is able to show the rigidity of bodies by exactly matching commonly observed bending curves with carefully selected control points.

4.2.2.4. Approximation of Cantilever beam with NURBS

In theory, Case NO.2 and NO.6 can also be exactly matched with higher order NURBS or B-Splines. However, due to the mathematical complexity, in this section, the approximation of beam bending curves is discussed as an alternative way to simulate beam bending. It also provides a more flexible way than looking for the exact match where it may become not universally available for complicated cases, for example bending with loading in several points or different weights in control points.

We start with the second cantilever beam- Case NO.2- to introduce the idea of approximation of beam bending and the optimization method involved. In this section, the entire bending curve is approximated by NURBS, with the first and the last control points being the two endpoints, rather than in previous sections in which the control points are not on the curve. For simplicity, a dimensionless equation of deflection is used:

$$y' = -\frac{\omega L^3}{24EI}(x'^4 - 4x'^3 + 6x'^2) \quad \text{Equation 4-23}$$

Additional two points will be needed to define the cubic NURBS to approximate the bending curve. Their coordinates are (x_1, y_1) and (x_2, y_2) . The question is then how to choose their location so that the defined NURBS will best match the bending curve.

To solve for (x_1, y_1) and (x_2, y_2) , the optimization tool in Matlab is used in which the optimization target is the integration of the square of the difference between two curves, similar to the idea of the sum of the square of errors in linear regressions:

$$\int_0^1 (y' - y_{NURBS})^2 dx$$

Equation 4-24

The detailed procedure and code are attached in the Appendix. In the case where the endpoint deflection is -0.15 ($\frac{\omega L^3}{24EI} = 0.05$), the optimized location for (x_1, y_1) and (x_2, y_2) are obtained as $(0.126, -0.0014)$ and $(0.415, -0.0326)$. Based on the different terms, a similarity between two curves can be defined as:

$$Similarity = 1 - \frac{\sqrt{\int_0^1 (y' - y_{NURBS})^2 dx}}{\int_0^1 y' dx + \sqrt{\int_0^1 (y' - y_{NURBS})^2 dx}}$$

Equation 4-25

The similarity approaches to 1 if two curves are more similar and 0 if two curves are totally different from each other. For the obtained results, the similarity between the NURBS approximation and deflection curve is 0.99917, or 99.917%.

To achieve even better results, the two control points may have different weights so that the shape of NURBS can be slightly adjusted to better fit the deflection curve. If the weights are optimized simultaneously with the location of control points, the result is $(0.206, -0.0030)$ with the weight of 0.815 for (x_1, y_1) , and $(0.563, -0.0625)$ with the weight of 1.160 for (x_2, y_2) . The similarity is now improved to 99.938%.

A comparison of fitted NURBS and deflection curve and the location of optimized control points are shown in Figure. 4-18. It is clear that NURBS, with or without applying weight in control points, can approximate the bending curve

with high accuracy and the difference is hardly visible to human eyes. The result without control point weight is sufficient for practical purposes while that with weight further improves the similarity and adds more flexibility.

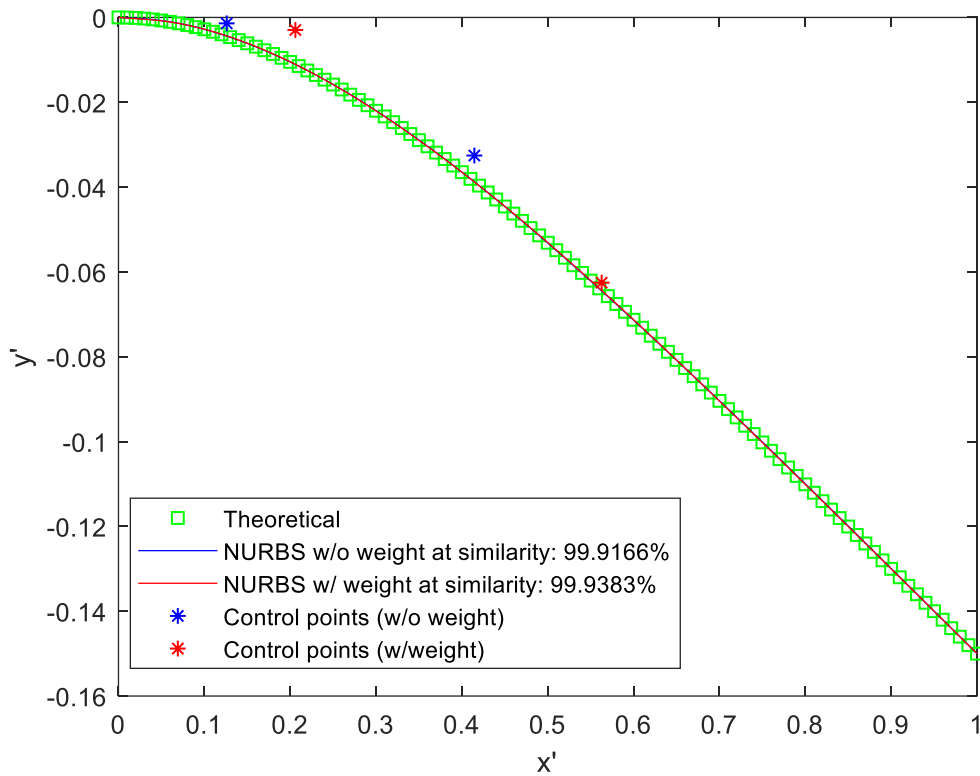


Figure 4-18. The comparison of fitted NURBS and deflection curve for Case NO. 2. The blue and red lines overlap.

The same approach can be applied to Case NO. 4. In this case, on the far left of the beam is a fixed hinge support and a sliding hinge support is on the far right. The load can move from the far left to the midpoint. Here the load is assumed to be at the midpoint.

Due to the symmetry of the bending curve (the symmetry axis is $x=0.5$), only the location of one control point is needed, (x_1, y_1) , and the second control point

would be $(1 - x_1, y_1)$. The dimensionless equation for this case is:

$$y' = \frac{PL^2}{48EI} (4x'^3 - 3x'), \text{ for } x \leq \frac{1}{2}L \quad \text{Equation 4-26}$$

In the case where the maximum deflection is -0.1 ($\frac{PL^2}{48EI} = 0.1$), the optimized control points are (0.351, -0.1042) and (0.649, -0.1042) with a similarity of 99.853%. The result with control point weight is quite close, and the control points are (0.351, -0.1047) and (0.649, -0.1047) with equal weights of 0.915 and a similarity of 99.903%. The result comparison is shown in Figure. 4-19.

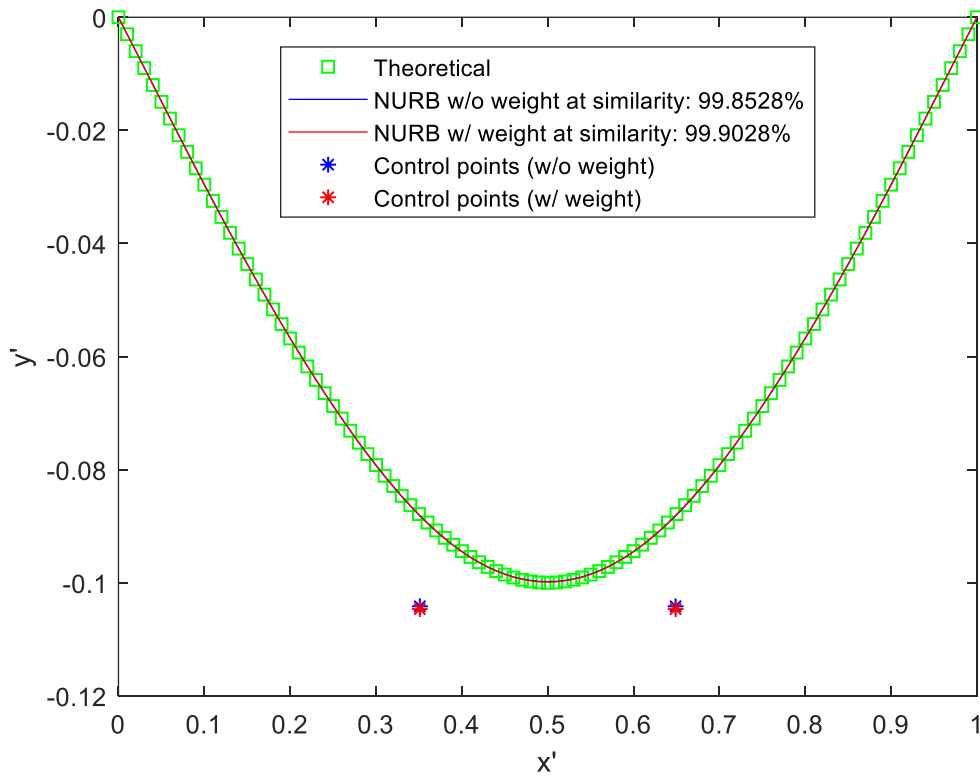


Figure 4-19. The comparison of fitted NURBS and deflection curve for Case NO. 4. The blue and red lines overlap.

The same approach can also be applied to Case NO. 6. In this case, the beam

support is the same as NO. 4, but the load is assumed to be uniform on the beam.

Again, due to the symmetry of the bending curve (the symmetry axis is $x=0.5$), only the location of one control point is needed, (x_1, y_1) , and the second control point would be $(1 - x_1, y_1)$. The dimensionless equation for this case is:

$$y' = -\frac{\omega L^3}{24EI} (4x'^3 - 2x'^3 + x') \quad \text{Equation 4-27}$$

In the case where the maximum deflection is -0.0313 ($\frac{\omega L^3}{24EI} = 0.1$), the optimized control points are $(0.330, -0.0326)$ and $(0.670, -0.0326)$ with a similarity of 99.864%. Control points with weight are nearly identical $(0.330, -0.0327)$ and $(0.670, -0.0327)$ with equal weights of 0.919, and the similarity improves a little bit to 99.927%. The result comparison is shown in Figure. 4-20.

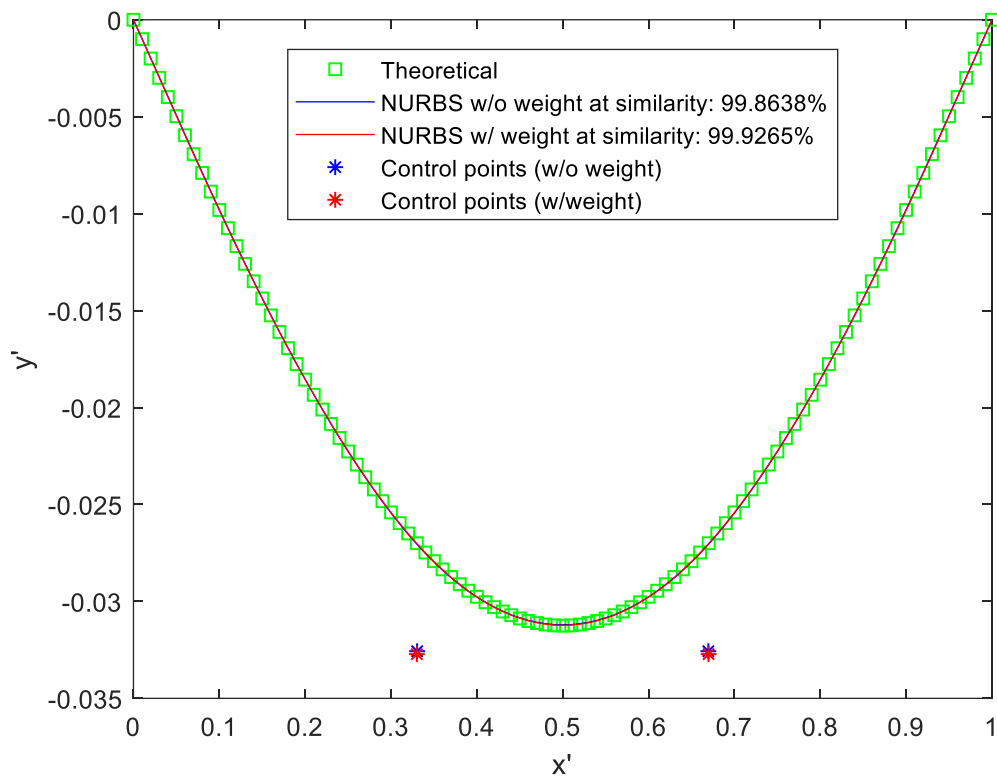


Figure 4-20. The comparison of fitted NURBS and deflection curve for Case NO. 6. The blue and red lines overlap.

4.3. Application of the rigidity of NURBS in art (Chinese calligraphy)

4.3.1. The power and toughness in Chinese calligraphy

All of the findings and methods about the rigidity of NURBS are valuable for

applications, even in art creations. In art, curves play significant roles in representing the soft texture of materials, the gentle character of a creature, and the smoothness of surfaces. Conversely, straightforward elements such as solid bodies, sharp angles, and straight lines generally indicate powerful visual impact or balanced objects or compositions. However, the rigidity of NURBS can be used in representing the power and balance of curves too. Chinese calligraphy is a good example that can show the application of the method.

Chinese calligraphy is the art of handwriting. Chinese calligraphy was once considered an art that evolved well after the period of written history. Some recent research shows that the art of the brush began in the formative stage of Chinese society, as early as the Neolithic age.¹⁵⁹ Yee Chiang points out that the written form of Chinese characters not only serves the purpose of conveying thought but also expresses, in a peculiar visual way, the beauty of a thought.¹⁶⁰ From the beginning to the present, various fonts of Chinese calligraphy have been created. Many beautiful ones, including Zhuan Shu, Li Shu, Kai Shu, Xing Shu and Shou Jin Ti, have played a major role in the development of Chinese calligraphy. Chinese calligraphy is inseparable from beautiful characters; beautiful characters are composed of a multitude of different good-looking strokes.¹⁶¹

In Chinese calligraphy, there are several basic strokes. The “Eight Laws of Yung” was widely used for practising brush strokes (see Figure. 4-21). Based on the rules of stroke classification in “Xiandai Hanyu Tongyongzi Bishun Guifan”, the “Eight Laws of Yung” can be summarized as six basic strokes, including “丶 (Dian)”, “一(Heng)”, “丨 (Shu)”, “丿 (Pie)”, “㇇ (Na)” and “ノ(Ti)”. In 1988, the basic strokes are defined as five, which are: “一”, “丨”, “丿”, “㇇” and “一”(Hengzhe).¹⁶² The other strokes are the derivatives and variations of the basic stroke. The stroke “丶” looks like a “dot” in calligraphy and does not have much curvy variation. So, only “一”, “丨”, “丿”, “㇇” -one variation of “丶”- and “ノ” -one variation of “一”- will be analysed in this chapter.¹⁶³

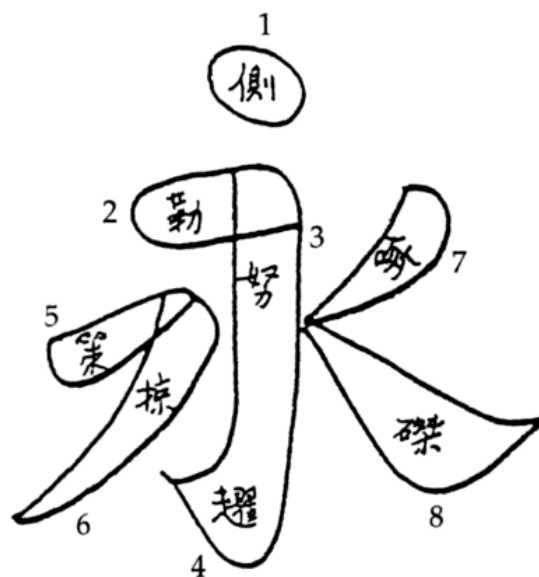


Figure 4-21. The eight components of the character Yong

In Chinese calligraphy, both straight and curvy strokes can be visually powerful. For example, the inscriptions on the tablets in the period of the Han, Wei, Jin and Northern and Southern dynasties (a major period in Chinese history between the Han and Sui dynasties from 202 B.C. to 589 A.D.) show beauty and power with straight strokes (see Figures. 4-22 and 4-23). Different from the inscriptions, Song Huizong's (Ji Zhao) handwriting shows strong and toughness using curves (see Figure. 4-24).



Figure 4-22. Both straight and curvy strokes were used in He Yang Ling Cao Quan Bei made in Han Dynasty (185 A.D.). In its rubbing, the characters represent both power and rigidity. The curvy strokes do not seem to follow certain rules of change, and the straight strokes had not been curved

much.¹⁶⁴



Figure 4-23. The straight strokes were used in Han Gu Gu Cheng Chang Dang Yin Ling Zhang Jun Biao, also called Zhang Qian Bei, made in Han Dynasty (186 A.D.).¹⁶⁵ In its rubbing, straight strokes show the power and hardness of the characters. Every word looks approximately square.



Figure 4-24. In this piece of Hui Zong's calligraphy named Run Zhong Qiu Yue Tie (1110 A.D.), every stroke seems curved, and the changes in the strokes seem to follow specific rules. All the changes make the characters represent the beauty of slimness and elegance. The work is now preserved in the Palace Museum in Beijing.¹⁶⁶

4.3.2. The rigidity of strokes in Huizong's Shou Jin Ti

Despite being a total failure in running state and military affairs, Huizong is probably one of the greatest patrons of art any nation ever had, and also a great artist. He excelled in painting birds and flowers and also produced worthy poetry. His paintings are considered to be China's greatest surviving masterpieces. His unique calligraphy became an independent style known as the "Slender Gold" style (Shou Jin Ti). The name "Slender Gold" came from the fact that Huizong's writing resembled gold filament, twisted and turned. This style of calligraphy is a sharp diversion from anything seen before and, in a way, demonstrates that although Huizong was not very courageous on the battlefield, he certainly dared to innovate in the field of aesthetics. His calligraphy, even more celebrated than his painting, is extremely unconventional and original, the strokes are stretched to their extreme limits and the result is a fascinating dynamism that still stands out as an independent and striking interpretation of Chinese characters.¹⁶⁷

In Huizong's Shou Jin Ti, the strokes are visually similar to the bent beams discussed above. There were many Shou Jin Ti calligraphy works created by Huizong during his life. In this chapter, Run Zhong Qiu Yue Tie is selected to be analysed as a sample. All the basic strokes can be found in this piece of

calligraphy work. The five basic strokes - “一”, “丨”, “丿”, “㇇” and “ノ”- from the characters in this artwork are highlighted (see Figures. 4-25 to 4-27).

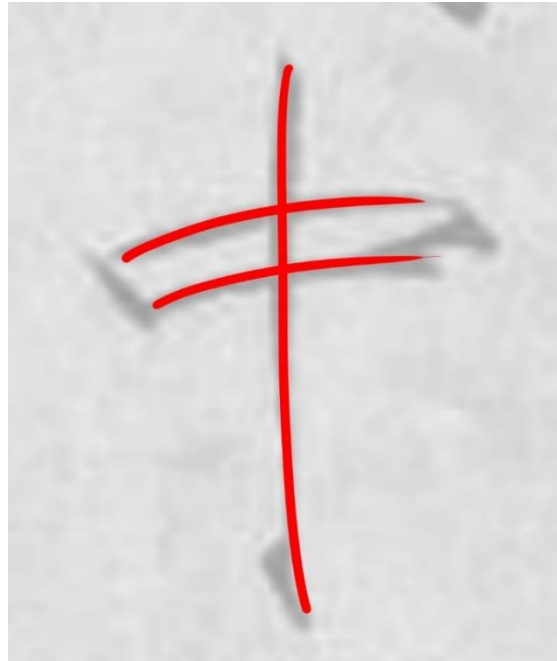


Figure 4-25. In the character “Zhong” from Run Zhong Qiu Yue Tie, the basic strokes “一” and “丨” have been highlighted in red.

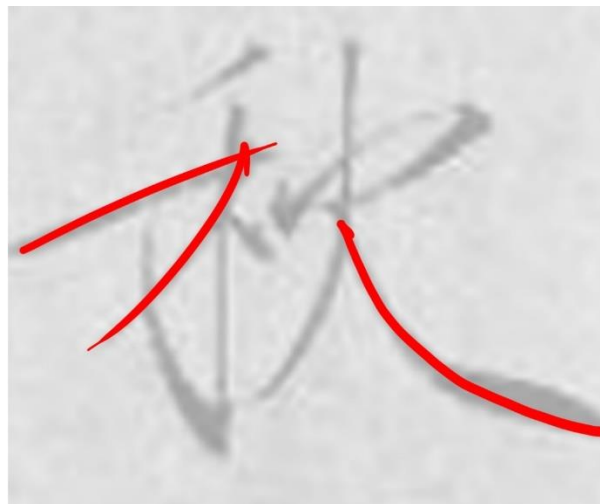


Figure 4-26. In the character “Qiu”, the basic strokes “一”, “丿” and “㇇” have been highlighted in red.



Figure 4-27. In the character “Di”, the basic strokes “—”, “|” and “丿” have been highlighted in red.

In Chinese calligraphy, even if the strokes look like bent beams, it is not feasible to use the method of rigidity of NURBS directly, because the deformations in stroke curves are changeable. For example, in different characters, the same strokes are often not identical. Even in the same character, generally, the same strokes are slightly varied. That means the shape of the stroke will be non-identical, resulting in different deformations in stroke curves. Also, strokes are not metal beams, and they do not have Young’s modulus which is a mechanical property that measures the tensile or compressive stiffness of a solid material when a load is applied lengthwise.¹⁶⁸ That means that the only way to fit the curve of the stroke with NURBS is to keep changing the parameter in the code in 4.2 until the NURBS fitted the stroke shape visually. The samples also show that it is not easy to use the calculation and get the four control points, because

the load, which causes the deformation is not directly given. Also, no artist wants to spend large amounts of time on mathematical calculation and learning piecewise functions. What the artist wants most is a way to get the whole curve with just one click, knowing the locations of the two endpoints only. That means the method can be more practical in the application if the NURBS curves can be drawn just with one click, and only the start point and endpoint are given. So, the code needs to be rewritten for easy use in stroke drawings.

The code aims to provide a convenient approach to producing NURBS curves based on the condition and parameter, including the beam type and the endpoint location of the beam curve. The beam types include Case No.1, No.2, No.3, No.4, No.6 and No.7. Case No.5 is not included due to the big difference in the mathematical function. Also, in Case No.3 and Case No.7, because the pressure or the load is not perpendicular to the beam in the X-Y plane, these two cases do not apply to the content studied in this chapter. So, only Cases NO.1, NO.2, NO.4 and NO.6 are discussed. Here the cubic NURBS has been used. The code is shown in Appendix.

The codes can produce cubic NURBS curves with simple settings. First, the case type needs to be selected and put the number of the case behind the

“beam_case=”. For example, if the condition fits in Case No.1, then put 1 in the equation and make it “beam_case=1”. Second, put the maximum deformation behind the “end_point_y =”. For example, if the maximum deformation is 0.05 of 1.00, then make it “end_point_y = 0.05”. Technically, the result can show the curve drawn with NURBS after the code is run successfully (see Figure. 4-28).

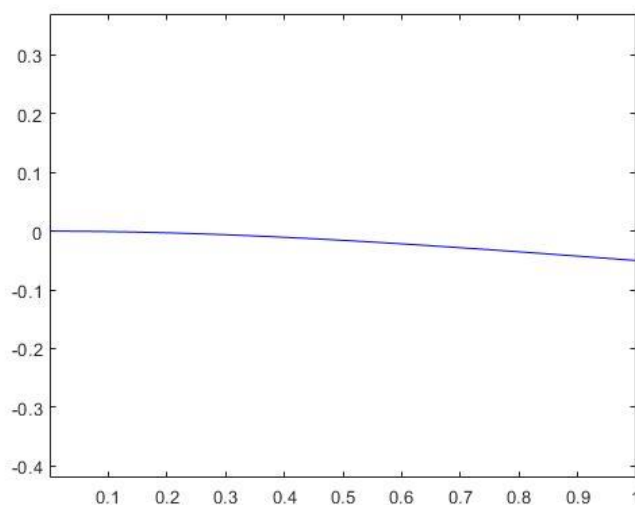


Figure 4-28. The beam in Case NO.1 fitted by cubic NURBS with a -0.05-unit deformation.

To fit Huizong’s stroke with the produced cubic NURBSs easily, the basic strokes are picked out from Huizong’s calligraphy one for each. Although the same type of strokes in handwriting cannot be exactly the same, the difference is not too significant. For example, the two “一” in the character “Zhong” have different and ungiven deformation and cannot use the fitting code in 4.2 directly. But the bending trends of the strokes look similar. So, the curves formed by the same

type of strokes can be seen as the same beam bending. That means the same type of stroke can be fitted with the same case of beam bending using NURBS. Then based on the manner of stroke selection, all the highlighted basic strokes can be simplified and reduced to five samples. Because the basic strokes studied in this chapter are “一”, “丨”, “丿”, “㇇” and “ノ”, the five typical strokes are found and extracted from Run Zhong Qiu Yue Tie (see Figures. 4-29 to 4-32).



Figure 4-29. In the character of Zhong, the first basic stroke “一” is extracted and highlighted in orange.



Figure 4-30. The second basic stroke “ | ” is extracted and highlighted in orange.



Figure 4-31. In the character of Qiu, the third and fourth basic strokes “ J ”, and “ ㄣ ” are extracted and highlighted.



Figure 4-32. In the character of Di, the fifth basic stroke “丿” is extracted and highlighted in orange.

The next step is to test and see which case of beam bending fits each stroke best. That means all cases of beam bending except Cases No.3, No.5 and No.7 are utilised in the stroke fitting. For example, with an unchanged deformation, four cubic NURBSs are produced after the code in 4.3, “The code in the analysis of the rigidity of strokes in Huizong’s Shou Jin Ti”, runs successfully. Compared with the first basic stroke “一” in the character “Zhong”, the most similar NURBS curve can be found. Because the code in 4.3 has been linked to the code in 4.2, the results in this section can represent the rigidities of the curves. Then the curve that can both represent rigidity and show the track of the stroke is found. The deformation starts from 0.01 units or an approximate numerical value and changes at 0.01 every time if needed.

For easier comparison, the five basic strokes -“一”, “丨”, “丿”, “㇇” and “㇏”- are

picked out and drawn in a simple cartesian coordinate (the X-Y coordinates) with a zoom in or out proportionally. Then the approximate numerical value can be shown in the images.

The analysis of the five basic strokes includes three steps. First, to simulate the cases of beam bending, the basic strokes are put in a cartesian coordinate, and the start point of the strokes is located at “0”. Then an approximate deformation can be found. Second, the code in 4.3 is run using the type of cases and the parameter of approximate deformation. If the code runs successfully, a cubic NURBS can be plotted out in a cartesian coordinate. Third, the strokes and the generated NURBS curves are put together and compared. Then the NURBS curves that fit the basic strokes best can be found. That means the most suitable cases and relevant deformation parameters for the strokes can be picked out.

In the analysis of the first basic stroke, the stroke “一 (heng)” from Run Zhong Qiu Yue Tie is put in a cartesian coordinate (see Figures. 4-33 and 4-34).

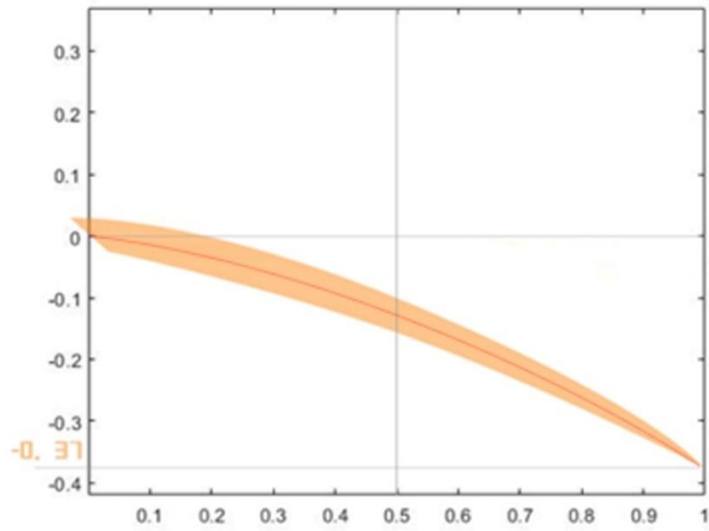


Figure 4-33. To simulate Cases NO.1 and NO.2, the basic stroke “—” is put in a Cartesian coordinate and the approximate deformation shows as -0.37 unit.

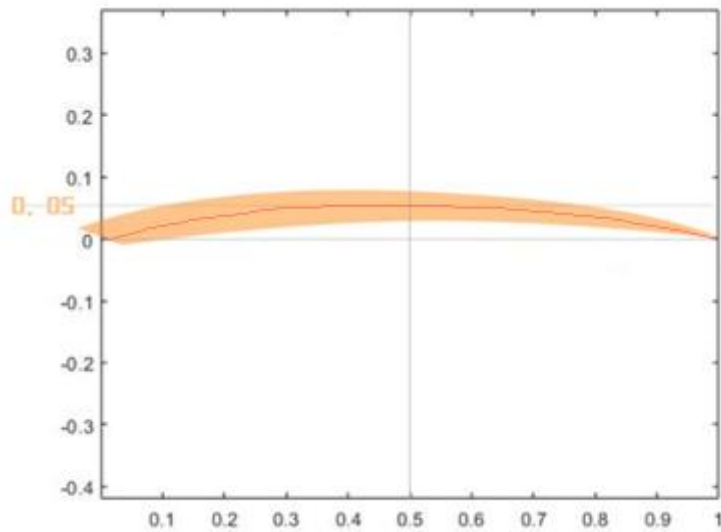


Figure 4-34. To simulate Cases NO.4 and NO.6, the basic stroke “—” is put in a Cartesian coordinate and the approximate deformation shows as 0.05 unit.

The code ran successfully, and the results show the NURBS curves with different cases and the deformation (see Figure. 4-35 to 4-38).

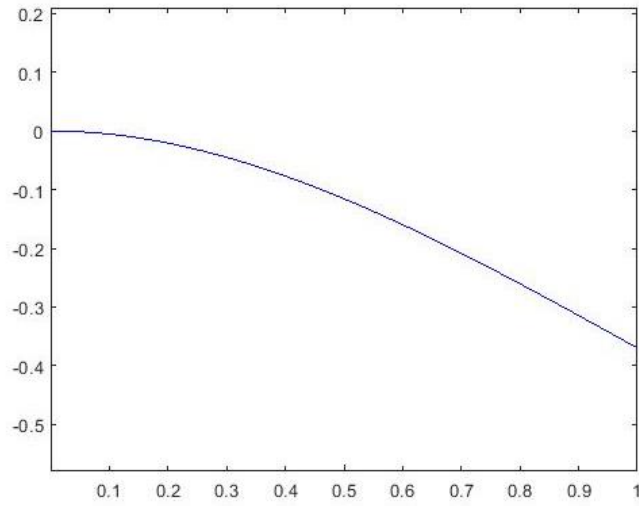


Figure 4-35. In Case NO.1, the cubic NURBS curve is produced based on the given deformation (-0.37).

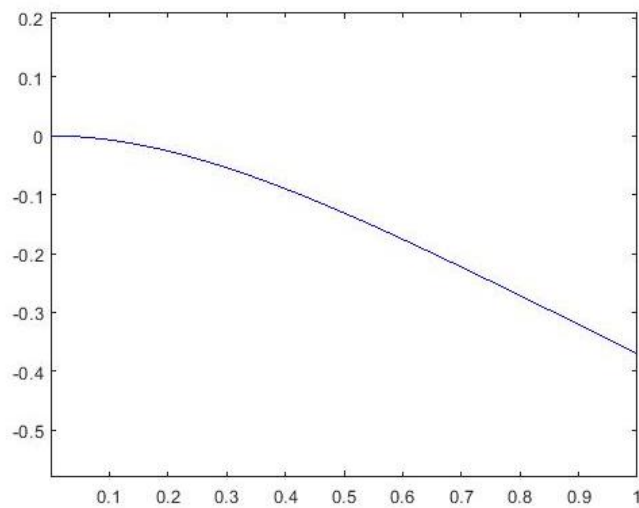


Figure 4-36. In Case NO.2, the cubic NURBS curve is produced based on the given deformation (-0.37).

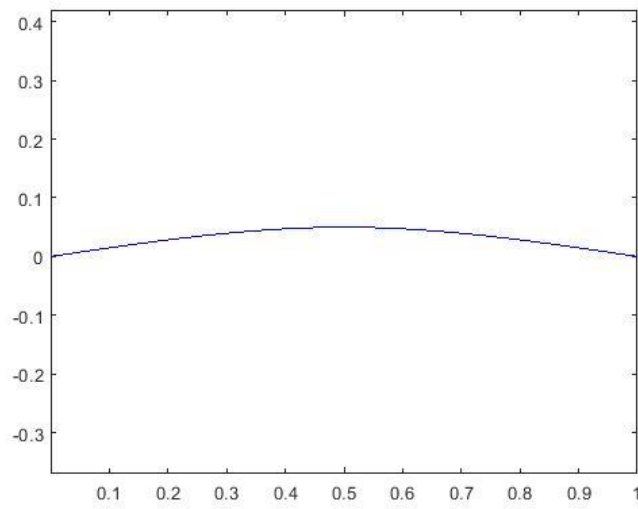


Figure 4-37. In Case NO.4, the cubic NURBS curve is produced based on the given deformation

(0.05).

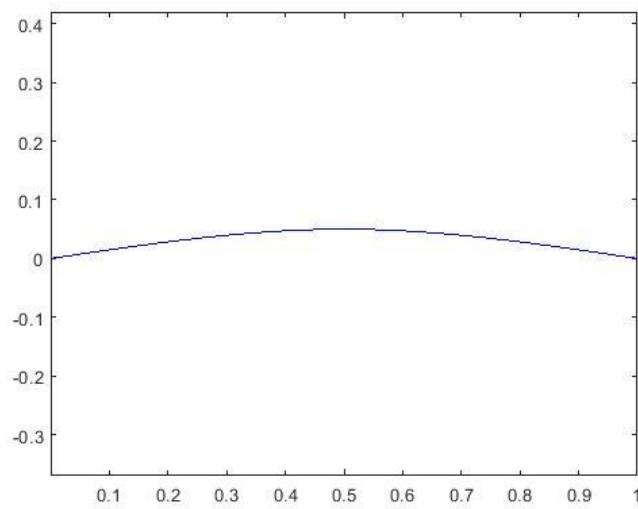


Figure 4-38. In Case NO.6, the cubic NURBS curve is produced based on the given deformation

(0.05).

In the analysis of the second basic stroke, the stroke “ | (shu)” from Run Zhong Qiu Yue Tie is put in a cartesian coordinate (see Figures. 4-39 and 4-40).

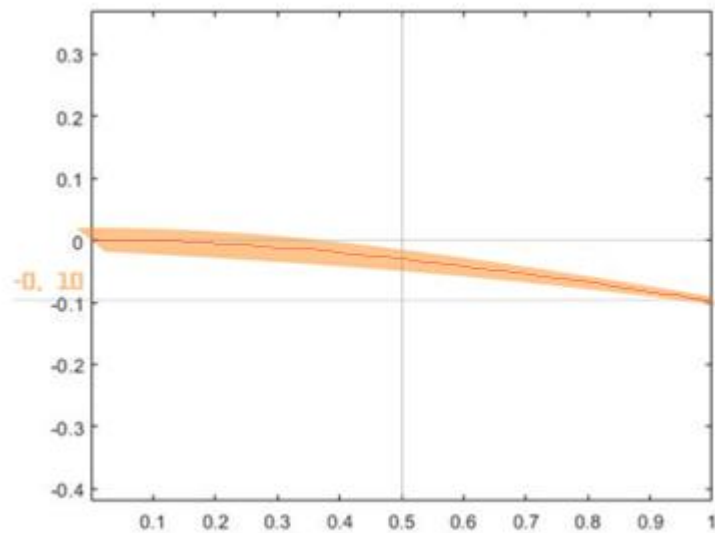


Figure 4-39. To simulate Cases NO.1 and NO.2, the basic stroke “ | ” is put in a Cartesian coordinate and the approximate deformation shows as -0.10 unit.

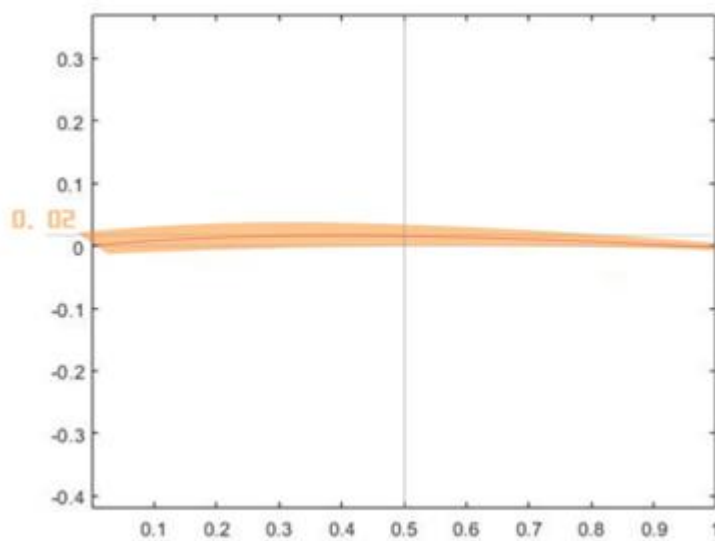


Figure 4-40. To simulate Cases NO.4 and NO.6, the basic stroke “ | ” is put in a Cartesian coordinate and the approximate deformation shows as 0.02 unit.

The code ran successfully, and the results show the NURBS curves with different cases and the deformation (see Figures. 4-41 to 4-44).

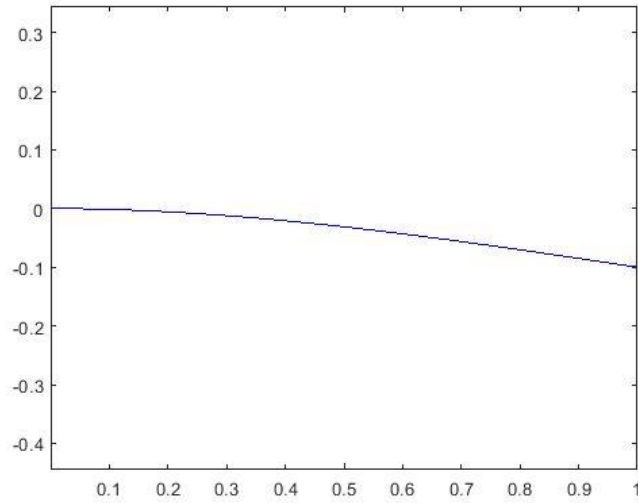


Figure 4-41. In Case NO.1, the cubic NURBS curve is produced based on the given deformation (-0.10).

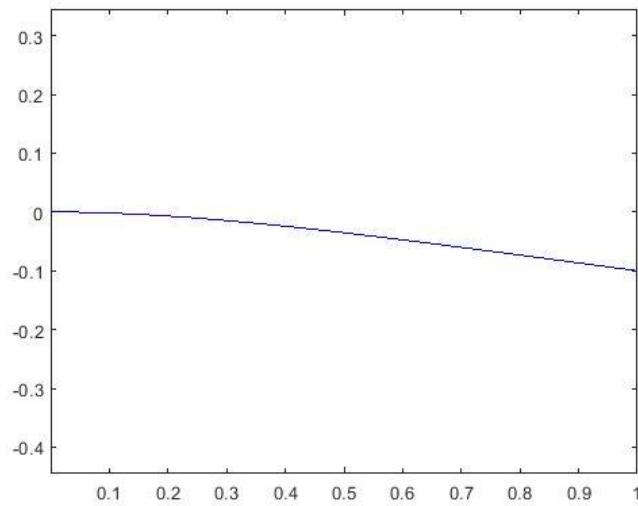


Figure 4-42. In Case NO.1, the cubic NURBS curve is produced based on the given deformation (-0.10).

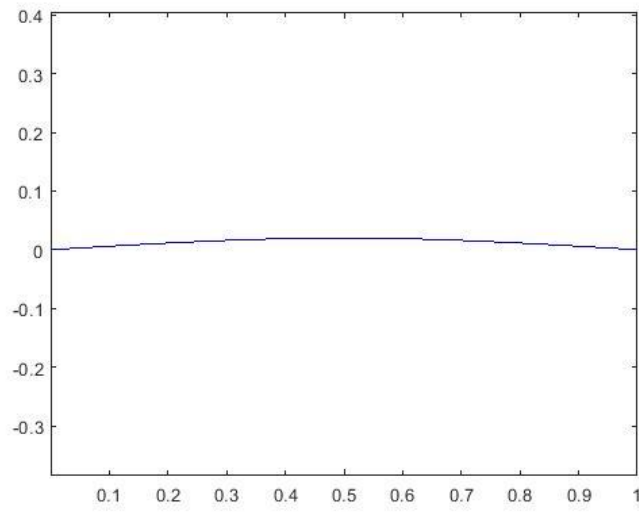


Figure 4-43. In Case NO.4, the cubic NURBS curve is produced based on the given deformation (0.02).

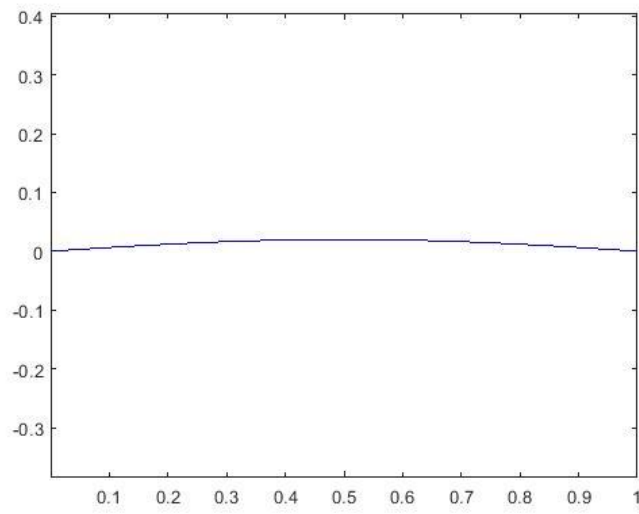


Figure 4-44. In Case NO.6, the cubic NURBS curve is produced based on the given deformation (0.02).

In the analysis of the third basic stroke, the stroke “丿 (pie)” from Run Zhong Qiu Yue Tie is put in a cartesian coordinate (see Figures. 4-45 and 4-46).

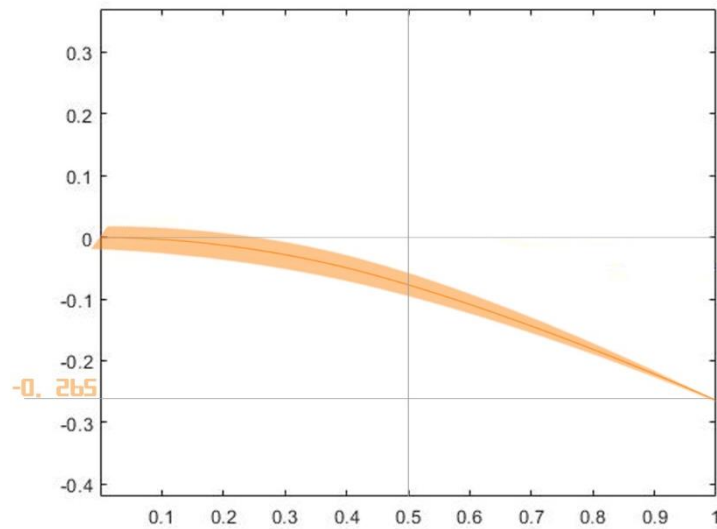


Figure 4-45. To simulate Cases NO.1 and NO.2, the basic stroke “丿” is put in a Cartesian coordinate and the approximate deformation shows as -0.265 unit.

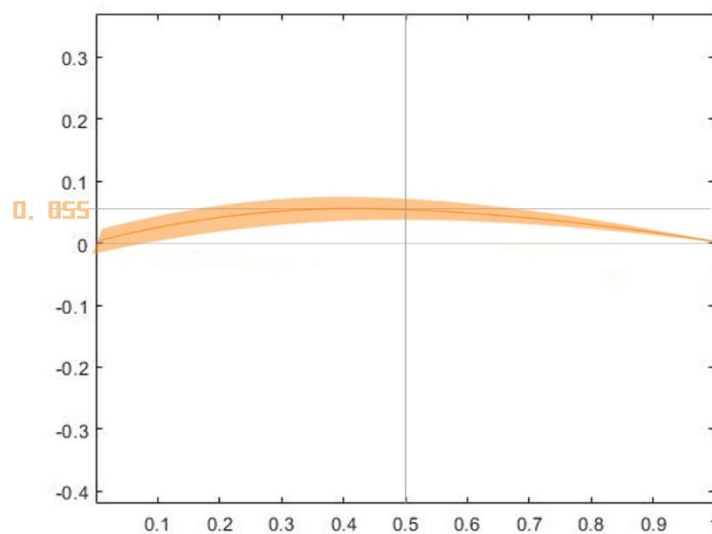


Figure 4-46. To simulate Cases NO.4 and NO.6, the basic stroke “丿” is put in a Cartesian coordinate and the approximate deformation shows as 0.055 unit.

The code ran successfully, and the results show the NURBS curves with different cases and the deformation (see Figures. 4-47 to 4-50).

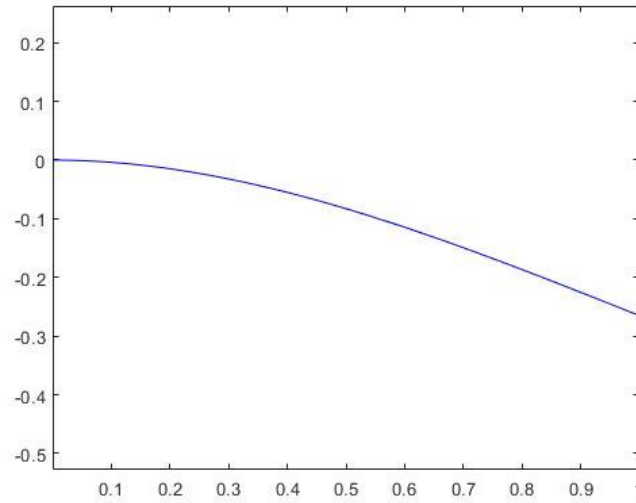


Figure 4-47. In Case NO.1, the cubic NURBS curve is produced based on the given deformation (-0.265).

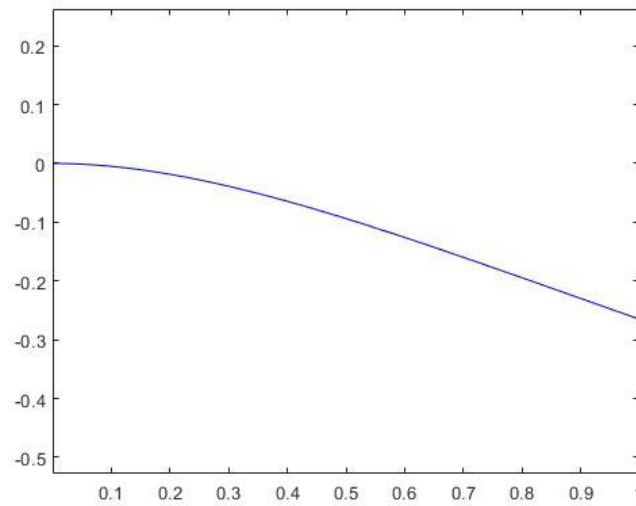
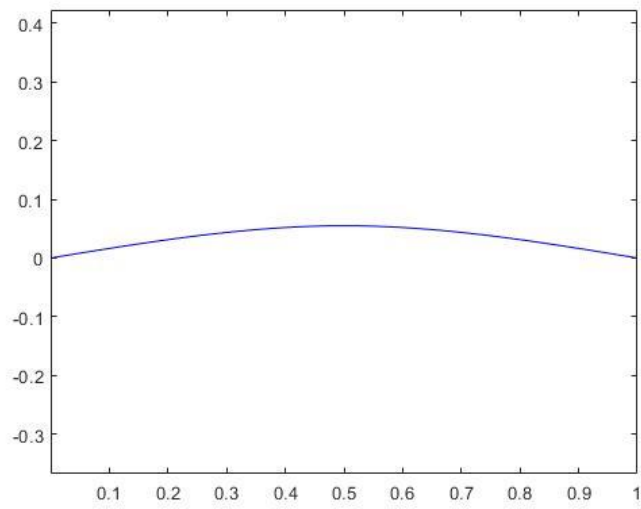
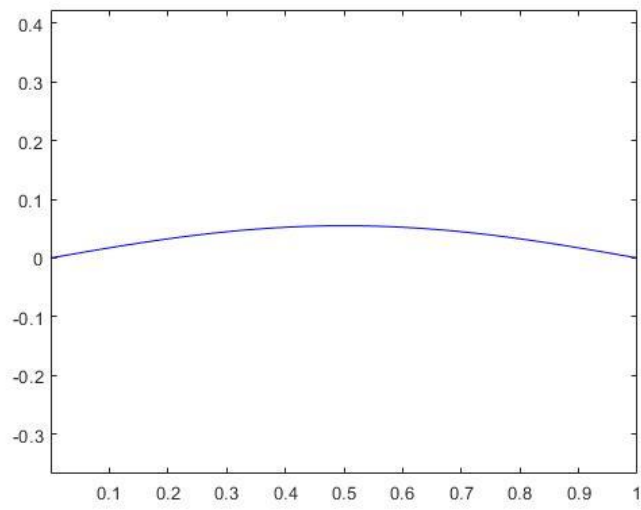


Figure 4-48. In Case NO.2, the cubic NURBS curve is produced based on the given deformation (-0.265).



*Figure 4-49. In Case NO.4, the cubic NURBS curve is produced based on the given deformation
(0.055).*



*Figure 4-50. In Case NO.6, the cubic NURBS curve is produced based on the given deformation
(0.055).*

In the analysis of the fourth basic stroke, the stroke “ㄣ” from Run Zhong Qiu Yue Tie is put in a cartesian coordinate (see Figures. 4-51 and 4-52).

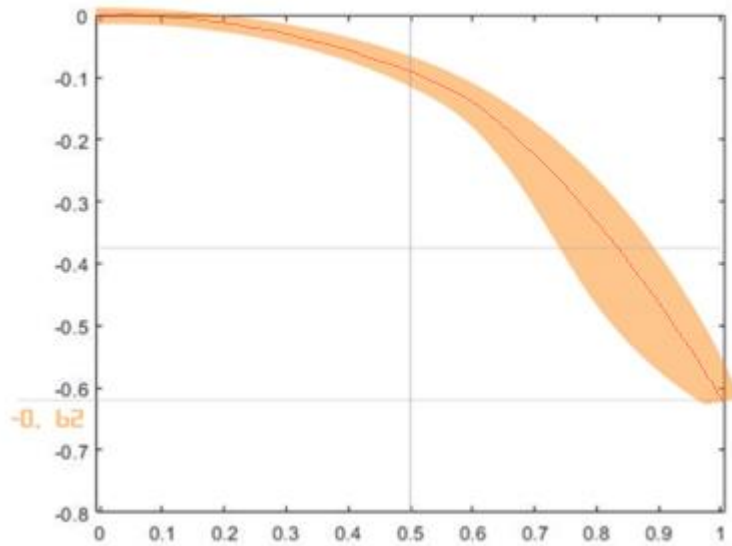


Figure 4-51. To simulate Cases NO.1 and NO.2, the basic stroke “ㄣ” is put in a Cartesian coordinate and the approximate deformation shows as -0.62 unit.

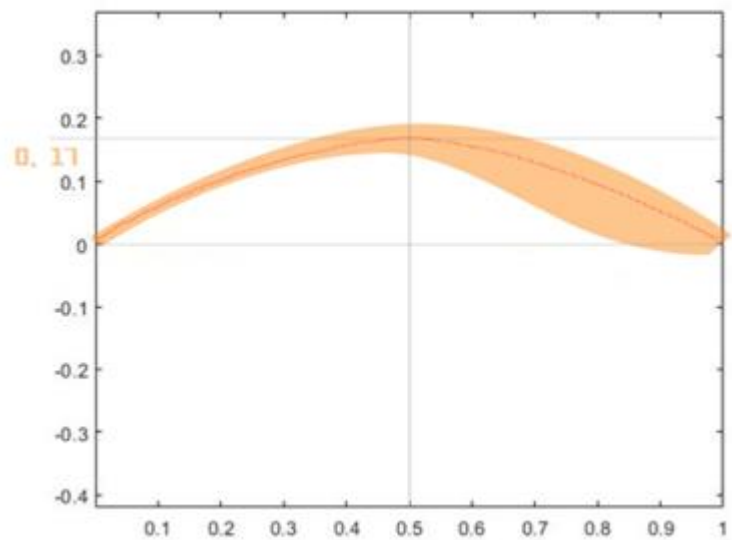


Figure 4-52. To simulate Cases NO.4 and NO.6, the basic stroke “ㄣ” is put in a Cartesian coordinate and the approximate deformation shows as 0.17 unit.

The code ran successfully, and the results show the NURBS curves with different cases and the deformation (see Figures. 4-53 to 4-56).

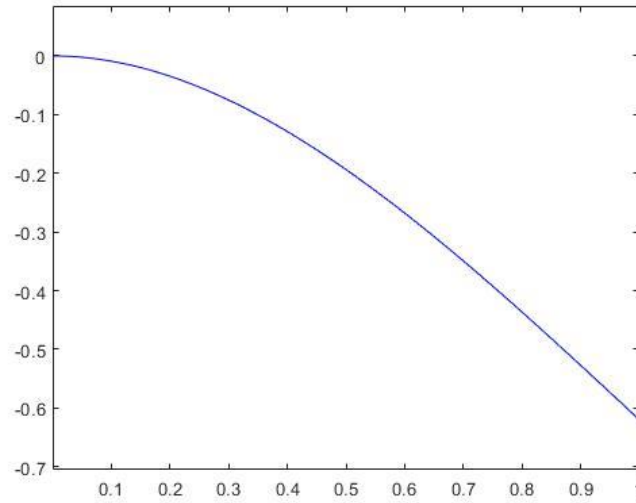


Figure 4-53. In Case NO.1, the cubic NURBS curve is produced based on the given deformation (-0.62).

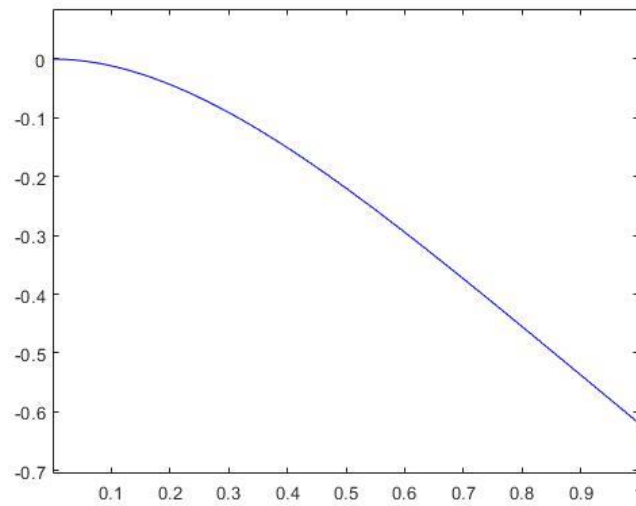


Figure 4-54. In Case NO.2, the cubic NURBS curve is produced based on the given deformation (-0.62).

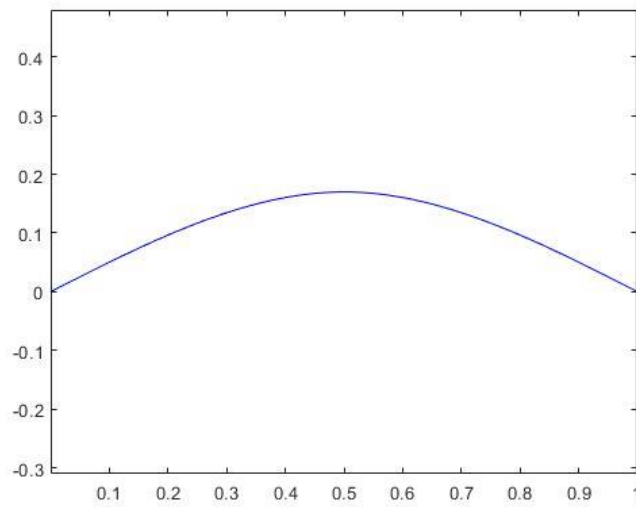


Figure 4-55. In Case NO.4, the cubic NURBS curve is produced based on the given deformation

(0.17).

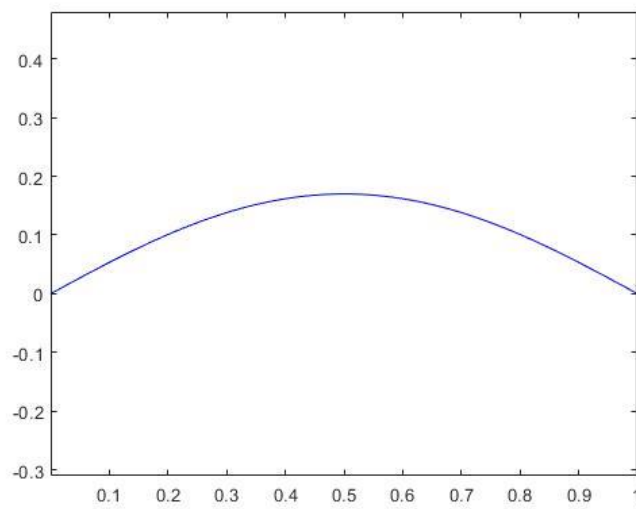


Figure 4-56. In Case NO.6, the cubic NURBS curve is produced based on the given deformation

(0.17).

In the analysis of the fifth basic stroke, the stroke “ノ” from Run Zhong Qiu Yue Tie is put in a cartesian coordinate (see Figures. 4-57 and 4-58).

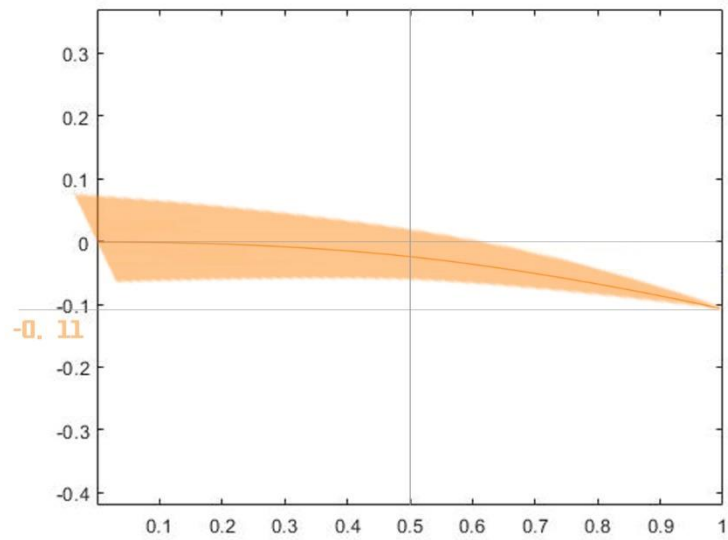


Figure 4-57. To simulate Cases NO.1 and NO.2, the basic stroke “ノ” is put in a Cartesian coordinate and the approximate deformation shows as -0.11 unit.

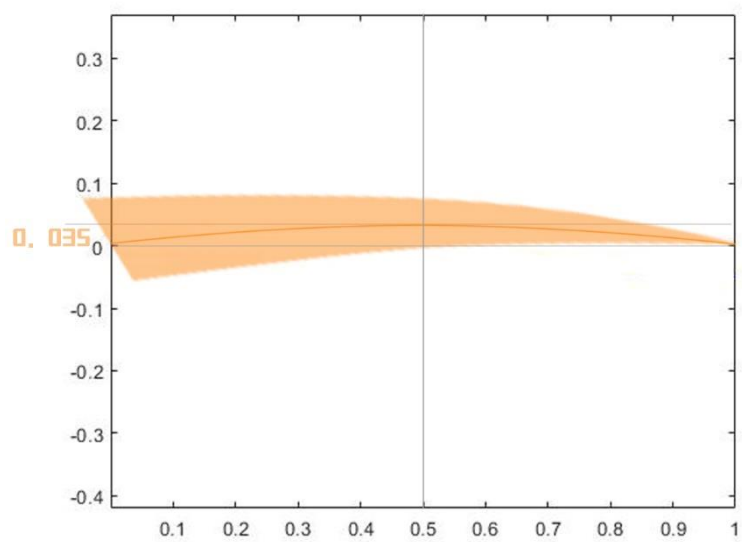


Figure 4-58. To simulate Cases NO.4 and NO.6, the basic stroke “ノ” is put in a Cartesian coordinate and the approximate deformation shows as 0.035 unit.

The code ran successfully, and the results show the NURBS curves with different cases and the deformation (see Figures. 4-59 to 4-62).

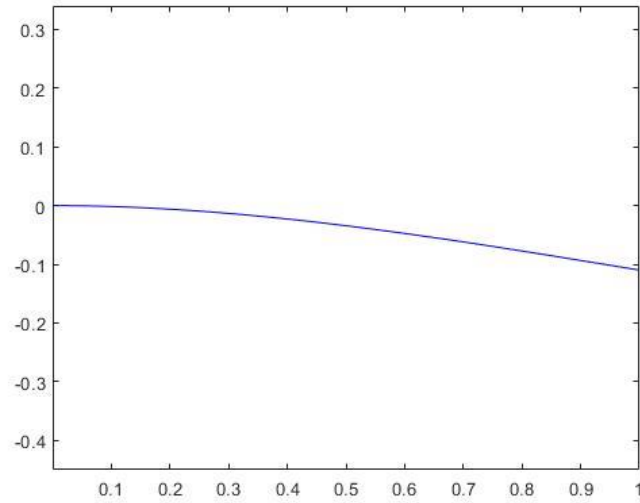


Figure 4-59. In Case NO.1, the cubic NURBS curve is produced based on the given deformation (-0.11).

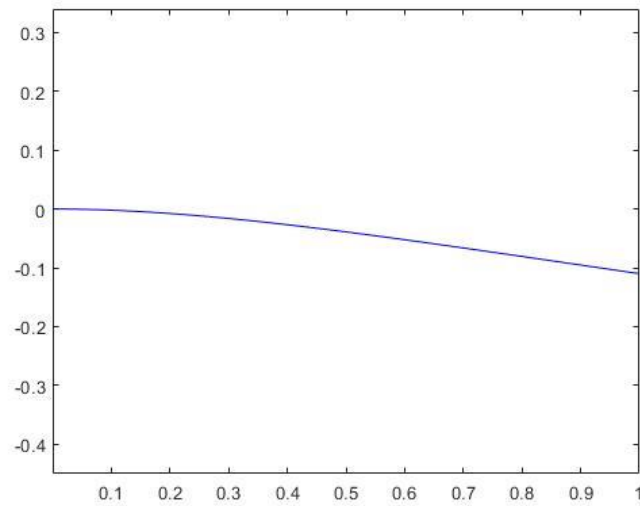


Figure 4-60. In Case NO.2, the cubic NURBS curve is produced based on the given deformation (-0.11).

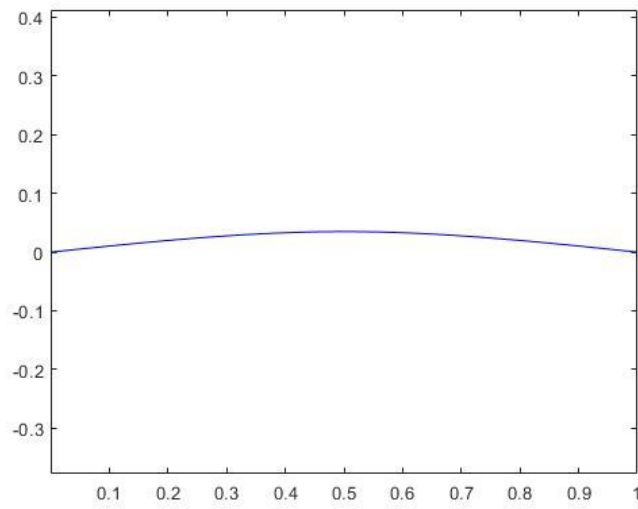


Figure 4-61. In Case NO.4, the cubic NURBS curve is produced based on the given deformation

(0.035).

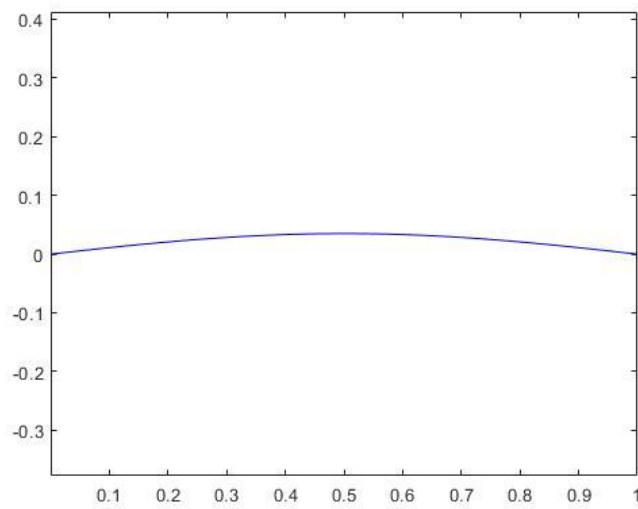


Figure 4-62. In Case NO.6, the cubic NURBS curve is produced based on the given deformation

(0.035).

All the NURBS curves have been generated by the code in different cases. The next is to compare the similarity between the basic strokes and the generated NURBS curves. After comparing the stroke with the four different bending beams, in turn, the NURBS curve with the highest coincidence can be found. That means the best NURBS curve for each basic stroke can be found.

4.4. Results

4.4.1. The rigidity of NURBS and dimensionless quantity

It is visually easier to compare the two by putting the bent beams and NURBSs together. In Case No.1, there is not much difference between comparisons with the platform bending and NURBSs. The lateral view of a movement in springboard diving is used in the analysis. Three NURBS curves in different orders including quadratic, cubic and quartic NURBS are drawn in UG-NX and compared with the bent beam in the photo (see Figures. 4-63 to 4-65). There are some slight differences between the results, but not significant at all.



Figure 4-63. The comparison between the platform and the fitted quadratic NURBS curve.

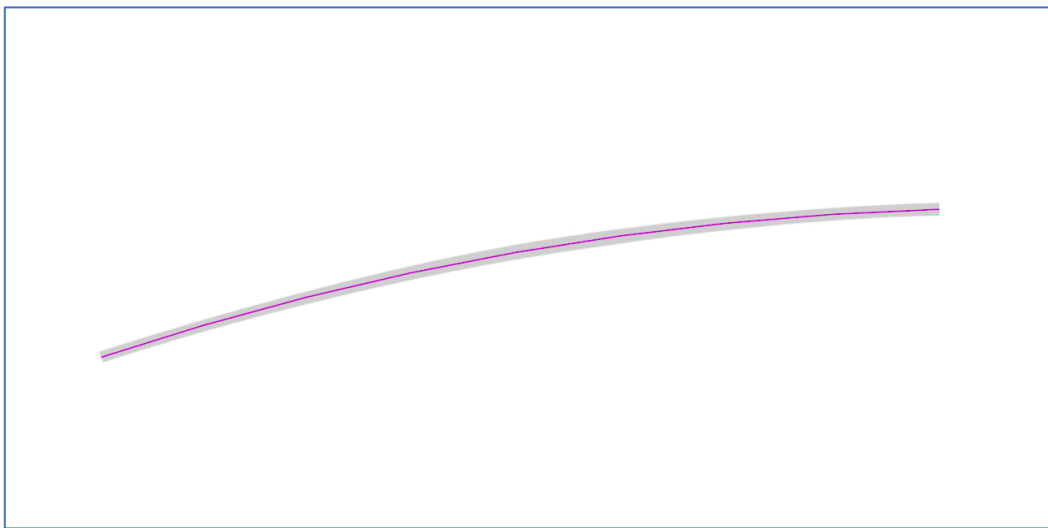


Figure 4-64. The comparison between the platform and the fitted cubic NURBS curve.

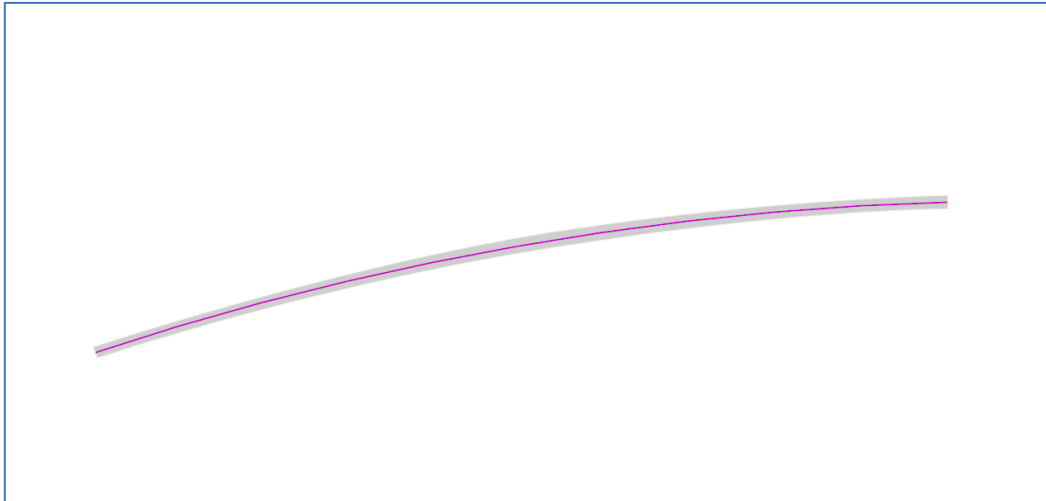


Figure 4-65. The comparison between the platform and the fitted quartic NURBS curve.

In Case No.4, as a result, quadratic NURBS and cubic NURBS can visually fit the deformation well. From the comparisons, the quadratic NURBS is defined by three control points, and it looks similar to the deformation. But there are still slight differences between the two curves. After all, they don't seem to coincide exactly. Differently, the cubic NURBS is defined by four control points, and it fits the deformation curve very well.

However, fitting well visually is not sufficient and only means that NURBS can draw a curve which looks like the deformation curves of beams well. The key is to find a way to connect the deformation and NURBS in mathematics, resulting in a practical approach to locating the control points automatically. Then designers or artists can use the parameters/location of the control points to

draw NURBS in a very easy way.

Here the concept of dimensionless quantity becomes significant. The dimensionless quantity is defined as $\frac{PL^2}{6EI}$ and it can be used to characterize the beam deflection with different loads, materials, and intersection shapes. Using the dimensionless quality, Case No.1, Case No.2 and Case No.4 are analysed mathematically and discussed.

In Case No.1, as the output, given the start point and the endpoint, artists or art designers can have the whole curve from an image and the specific coordinates of the four control points automatically, and the cubic curve (NURBS) fits the beam 100% (see Figures. 4-66 to 4-68).

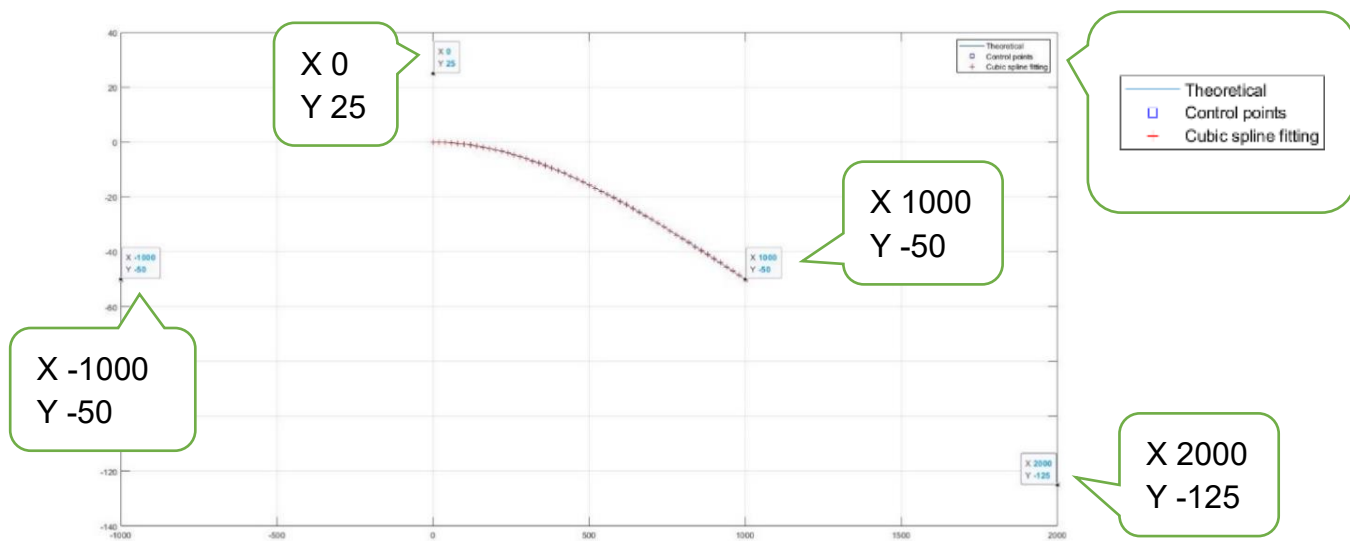


Figure 4-66. The output shows the cubic curve (NURBS), the curve of the bent cantilever beam, and the control points. In this image, the blue line is the theoretical beam bending curve, the blue squares are the control points (there are four in total), and the red cross is the points of the cubic spline (NURBS) fitting.

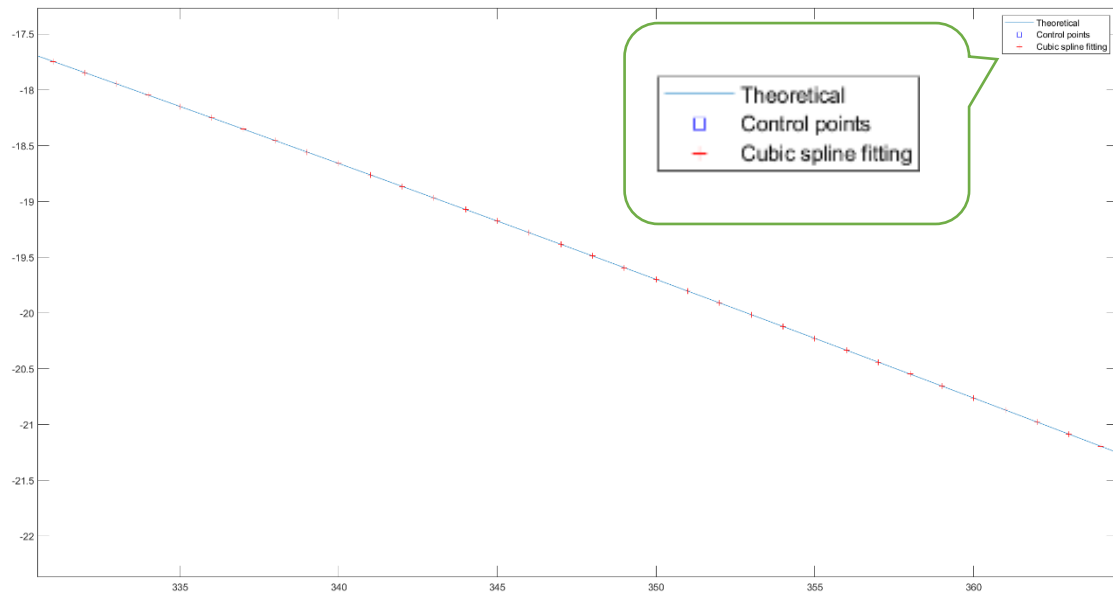


Figure 4-67. The zoomed-in Figure 4-66 shows the fitting is very good visually. From this image, it is clear that all the red cross points - the points of the cubic spline (NURBS) fitting - are on the theoretical beam bending curve.

1000x1 double			
	1	2	:
1	-1.8198e-04		
2	-7.2767e-04		
3	-0.0016		
4	-0.0029		
5	-0.0045		
6	-0.0065		
7	-0.0089		
8	-0.0116		
9	-0.0147		
10	-0.0181		
11	-0.0219		
12	-0.0261		
13	-0.0306		
14	-0.0355		
15	-0.0408		
16	-0.0464		
17	-0.0523		
18	-0.0586		
19	-0.0653		
20	-0.0723		
21	-0.0797		

(A)

1001x2 double				
	1	2	3	
1		0	0	
2		1	-1.8198e-04	
3		2.0000	-7.2767e-04	
4		3	-0.0016	
5		4	-0.0029	
6		5.0000	-0.0045	
7		6.0000	-0.0065	
8		7	-0.0089	
9		8	-0.0116	
10		9.0000	-0.0147	
11		10.0000	-0.0181	
12		11.0000	-0.0219	
13		12	-0.0261	
14		13	-0.0306	
15		14.0000	-0.0355	
16		15.0000	-0.0408	
17		16.0000	-0.0464	
18		17	-0.0523	
19		18.0000	-0.0586	
20		19.0000	-0.0653	
21		20	-0.0723	

(B)

Figure 4-68. The comparison has shown the equivalence between the y- coordinates of the theoretical beam bending curve (the group A of the parameter) and the y- coordinates of the cubic fitting curve (the group B of the parameter). Here for the parameter comparison, only a small group of the units is selected because there are 1000 points, and it is not necessary to show all the numbers.

In Case No.2, similarly, given the start point and the endpoint, artists or art designers can have the whole curve from an image and the specific coordinates of the four control points automatically, and the cubic curve (NURBS) fits the

beam very well (see Figures. 4-69 to 4-71).

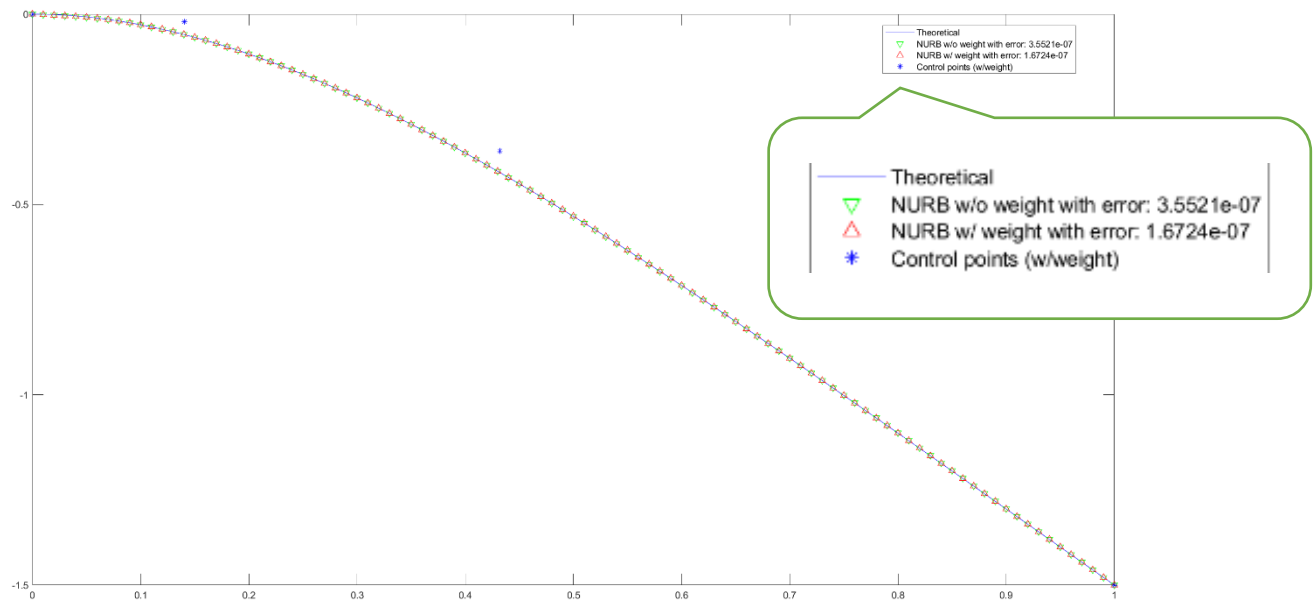


Figure 4-69. The output shows the cubic curve (NURBS), the curve of the bent cantilever beam, and the control points. In this image, the blue line is the theoretical beam bending curve, the green triangle is the points of the cubic NURBS without weight fitting and the error is $3.5521e-07$, the red triangle is the points of the cubic NURBS with weight fitting and the error is $1.6724e-07$, and the blue star means the control points of the cubic NURBS curve. This image shows the fitting is very good visually. From this image, it is clear that all the green and red triangles look appear to overlap, and on the theoretical beam bending curve.

101x1 double		
	1	2
1		0
2	-2.9801e-04	
3	-0.0012	
4	-0.0026	
5	-0.0047	
6	-0.0073	
7	-0.0104	
8	-0.0140	
9	-0.0182	
10	-0.0229	
11	-0.0281	
12	-0.0337	
13	-0.0398	
14	-0.0464	
15	-0.0535	
16	-0.0610	
17	-0.0689	
18	-0.0773	
19	-0.0861	
20	-0.0952	
21	-0.1048	

(A)

101x1 double		
	1	2
1		0
2	-0.0014	
3	-0.0028	
4	-0.0043	
5	-0.0061	
6	-0.0084	
7	-0.0112	
8	-0.0146	
9	-0.0186	
10	-0.0232	
11	-0.0282	
12	-0.0338	
13	-0.0398	
14	-0.0464	
15	-0.0534	
16	-0.0609	
17	-0.0687	
18	-0.0770	
19	-0.0858	
20	-0.0950	
21	-0.1045	

(B)

Figure 4-70. The comparison has shown the similarity between the y- coordinates of the theoretical beam bending curve (the group A of the parameter) and the y- coordinates of the cubic fitting curve (no weight) (the group B of the parameter). Here for the parameter comparison, only a small group of the units is selected because there are 100 points. So, it is not necessary to show all the numbers.

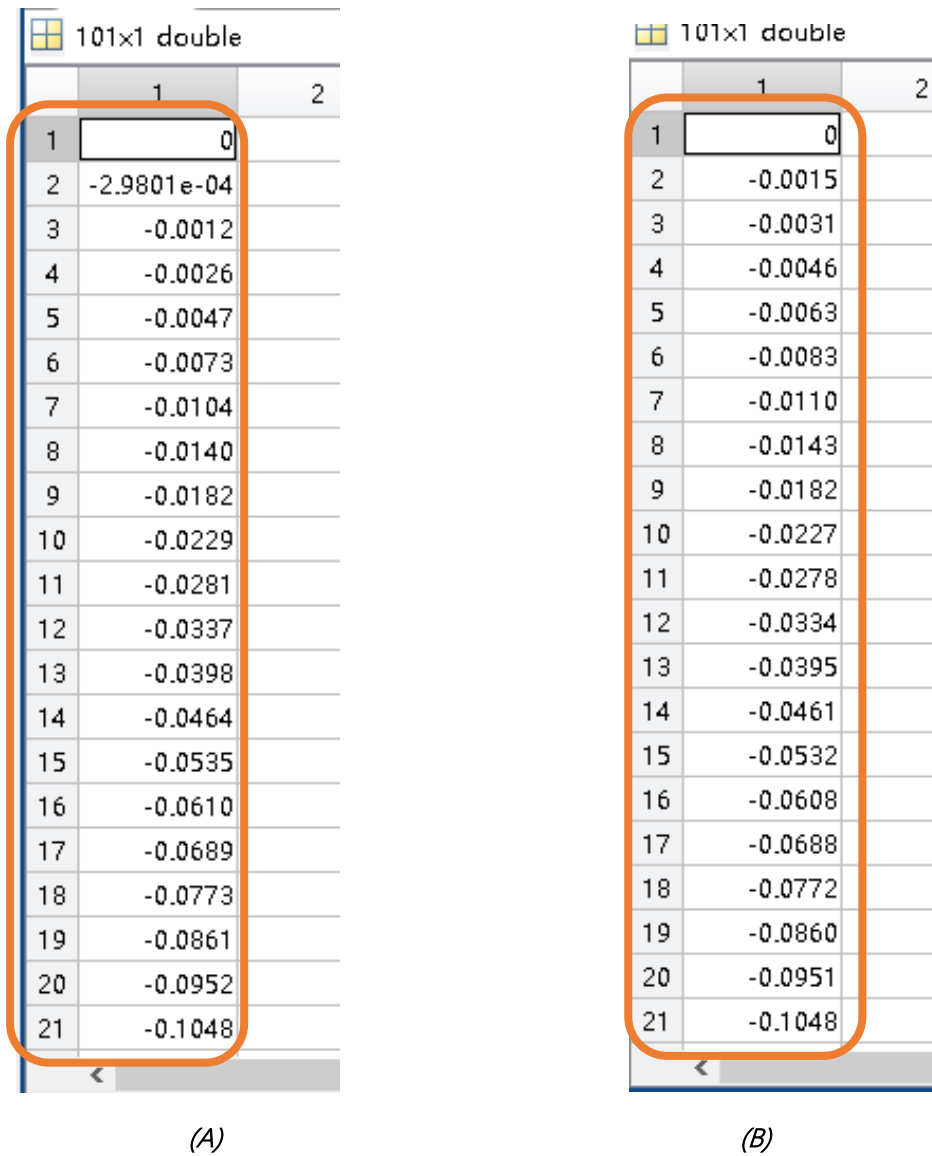


Figure 4-71. The comparison has shown the similarity between the y- coordinates of the theoretical beam bending curve (the group A of the parameter) and the y- coordinates of the cubic fitting curve (with weight) (the group B of the parameter). Same to the previous comparison, only a small group of the units is selected.

In Case N0.4 as well, given the start point and the endpoint, people can have the whole curve from an image and the specific coordinates of the four control points automatically, and the cubic curve (NURBS) fits the beam with high

accuracy (see Figures. 4-72 to 4-74).

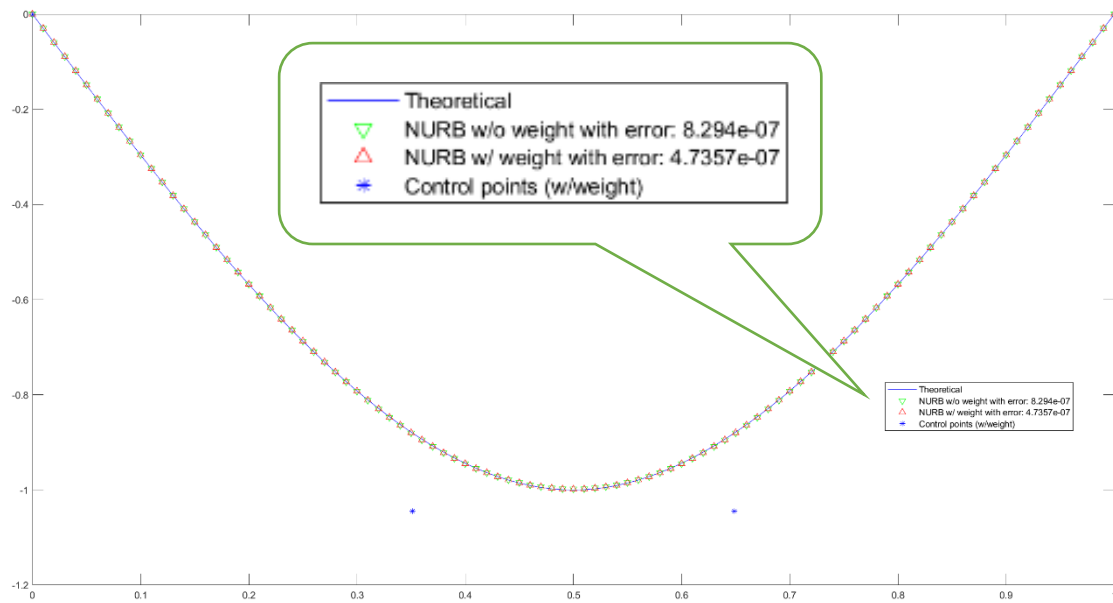


Figure 4-72. The output shows the cubic curve (NURBS), the curve of the bent simply supported beam, and the control points. In this image, the blue line is the theoretical beam bending curve, the green triangle is the points of the cubic NURBS without weight fitting and the error is $8.294e-07$, the red triangle is the points of the cubic NURBS with weight fitting and the error is $4.7357e-07$, and the blue star means the control points of the cubic NURBS curve. This image shows the fitting is very good visually. In this image, all the green and red triangles look appear to overlap, and on the theoretical beam bending curve.

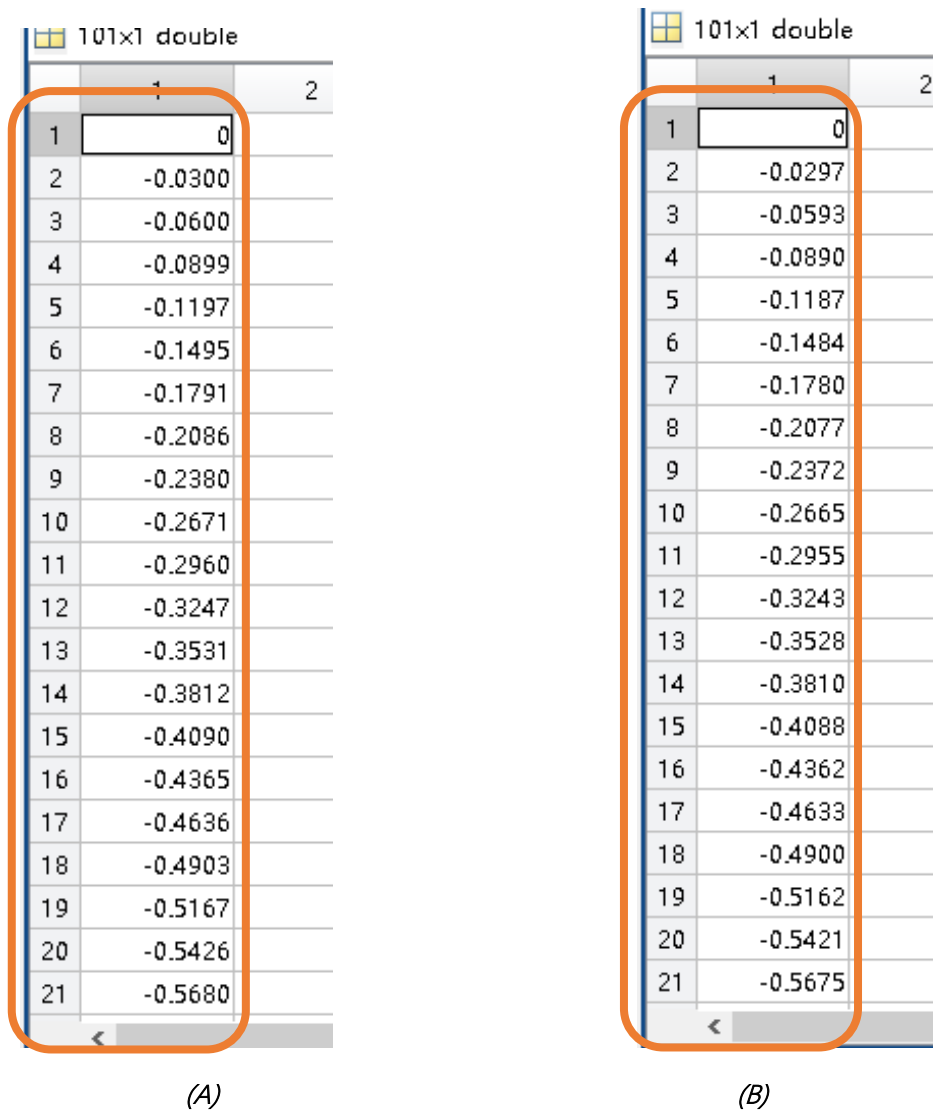
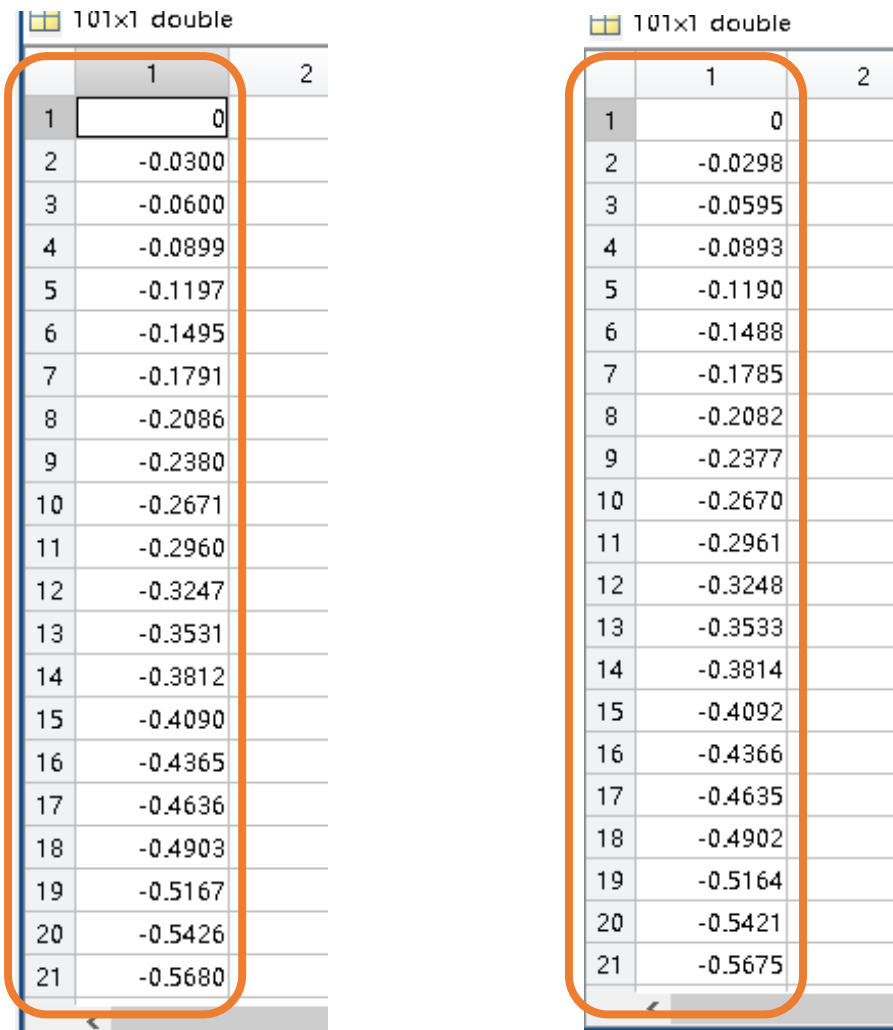


Figure 4-73. The comparison has shown the similarity between the y- coordinates of the theoretical beam bending curve (the group A of the parameter) and the y- coordinates of the cubic fitting curve (no weight) (the group of B the parameter). Here for the parameter comparison, only a small group of the units is selected because there are 100 points. So, it is not necessary to show all the numbers.



(A)

(B)

Figure 4-74. The comparison has shown the similarity between the y- coordinates of the theoretical beam bending curve (the group A of the parameter) and the y- coordinates of the cubic fitting curve (with weight) (the group B of the parameter). Same to the previous comparison, only a small group of the units is selected.

4.4.2. Application of the rigidity of NURBS in art (Chinese calligraphy)

This analysis shows, then, that the rigidity of NURBS can be applied in Chinese calligraphy through the use of dimensionless quality. The method is based on the connection between NURBS and statics, and uses a simple cubic NURBS to draw the bone and strength, also called the “soul”, of the stroke. For example, the calligraphy in the “Slender Gold” style (Shou Jin Ti) by Ji Zhao (Song Huizong) has been analysed using engineering solid mechanics and dimensionless quantity. Other handwriting works have been compared with that of Huizong, including the Huizong-like font automatically generated by online software and my own Shou Jin Ti practice works. The results show how superb Huizong’s calligraphy is and why others look imperfect.

The results of the comparison show that Huizong’s strokes are well-matched to the NURBS curves generated by the code in 4.3 in some conditions. The similarities between the basic strokes -“一”, “丨”, “丿”, “㇇” and “ノ”- and NURBS-fitted curves generated based on the four cases - Cases No.1, No.2, No.4 and No.6 - of beam bending are different. But there is a curve that visually fits the stroke better than the others. The comparisons are the following:

The first stroke “—” and the generated NURBS curves from Cases No.1, No.2, No.4 and No.6 are put together and compared (see Figures. 4-75 to 4-78).

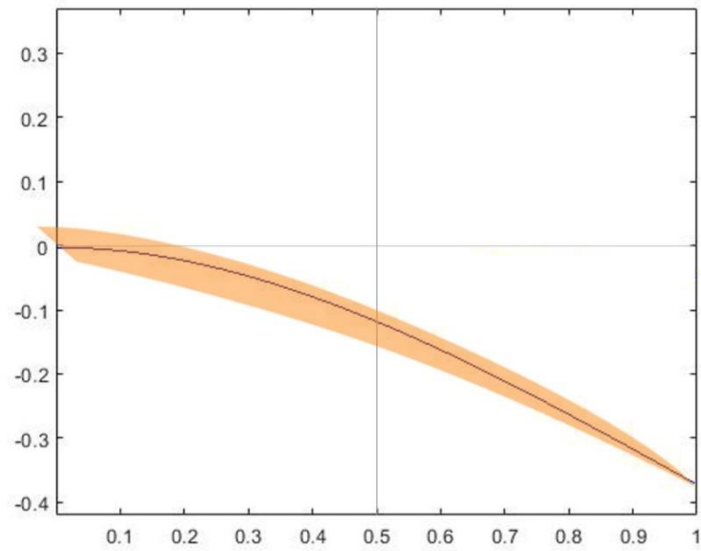


Figure 4-75. In Case NO.1, the basic stroke “—” is fitted by the cubic NURBS curve with the given deformation (-0.37).

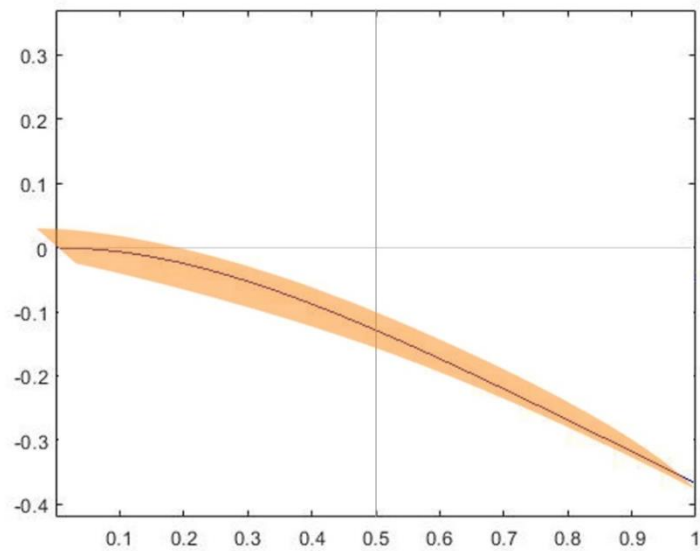


Figure 4-76. In Case NO.2, the basic stroke “—” is fitted by the cubic NURBS curve with the given

deformation (-0.37).

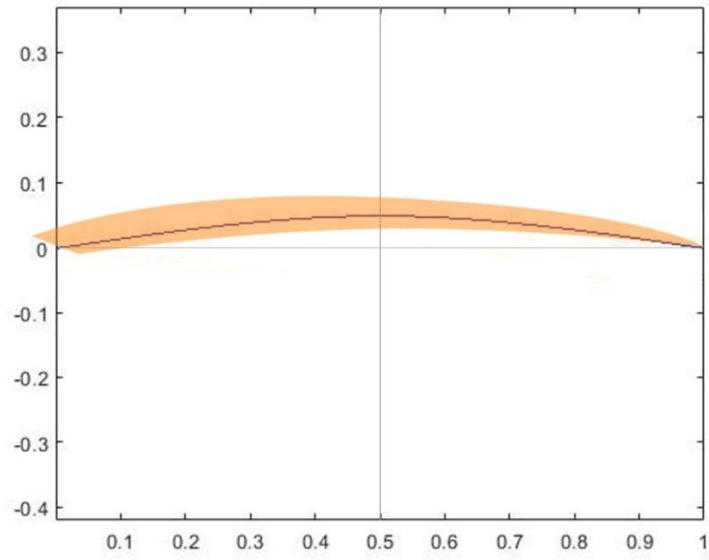


Figure 4-77. In Case NO.4, the basic stroke “—” is fitted by the cubic NURBS curve with the given

deformation (0.05).

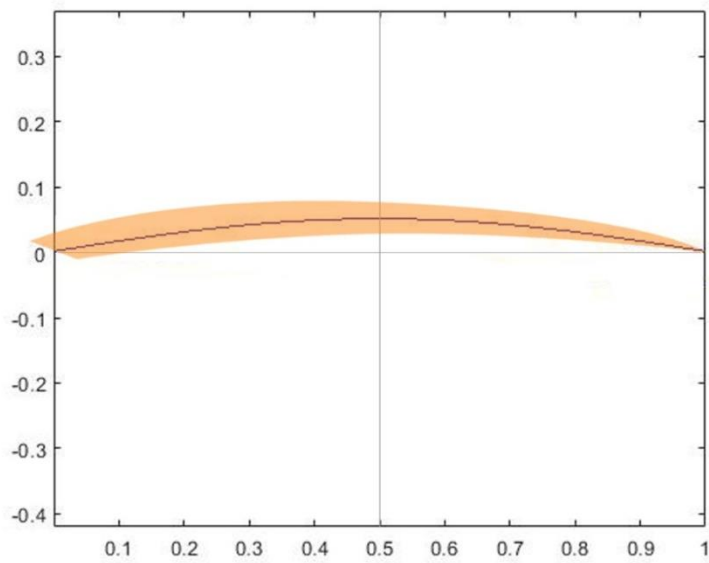


Figure 4-78. In Case NO.6, the basic stroke “—” is fitted by the cubic NURBS curve with the given

deformation (0.05).

The comparison shows that in Case No.6, the generated NURBS curve goes through the middle of the stroke. In the other cases, the NURBS curve does not follow the midline of the stroke well. That means the NURBS in Case NO.6 fit the basic stroke “—” best.

The second stroke “|” and the generated NURBS curves from the four cases are put together and compared (see Figures. 4-79 to 4-82).

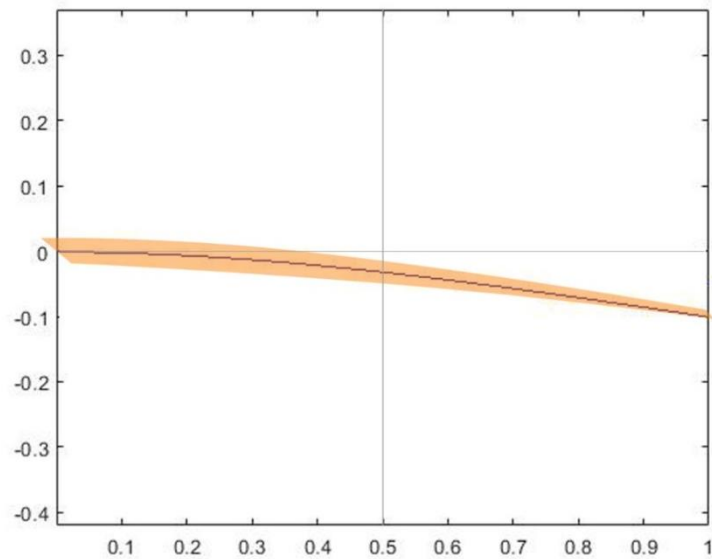


Figure 4-79. In Case NO.1, the basic stroke “|” is fitted by the cubic NURBS curve with the given deformation (-0.10).

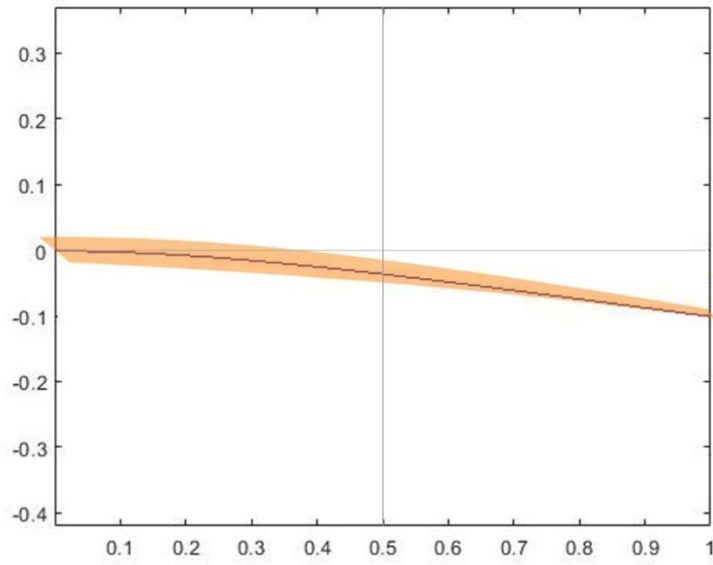


Figure 4-80. In Case NO.2, the basic stroke " I " is fitted by the cubic NURBS curve with the given deformation (-0.10).

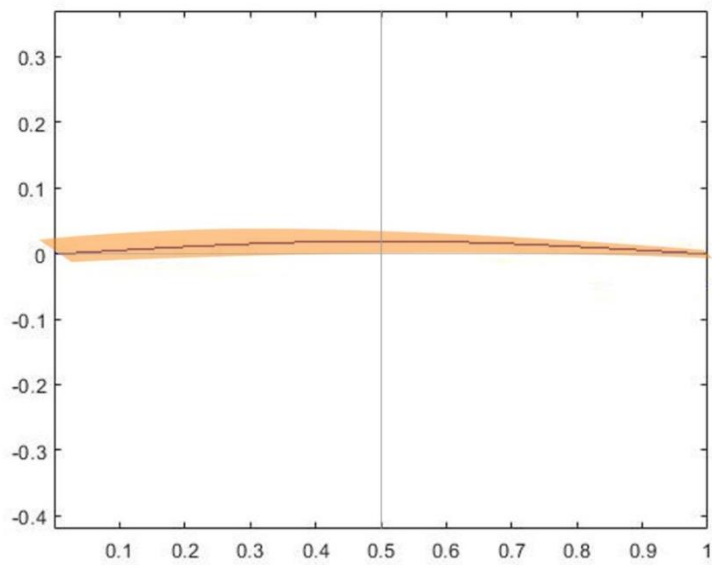


Figure 4-81. In Case NO.4, the basic stroke " I " is fitted by the cubic NURBS curve with the given deformation (0.02).

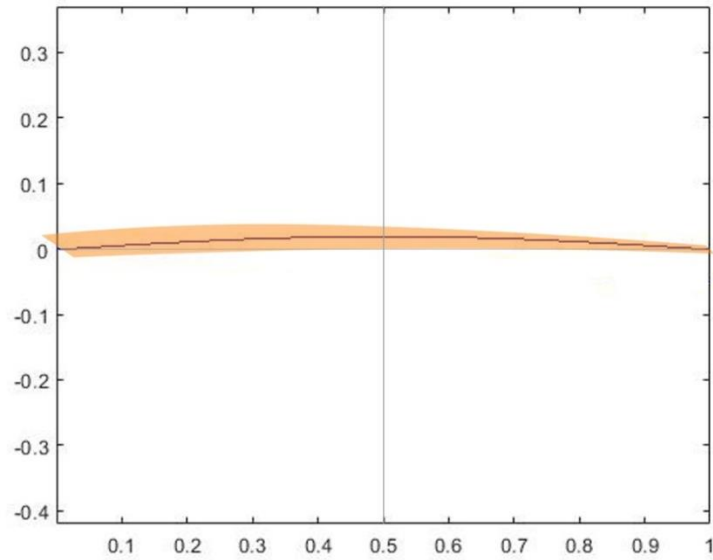


Figure 4-82. In Case NO.6, the basic stroke “ | ” is fitted by the cubic NURBS curve with the given deformation (0.02).

The comparison shows that in Case No.2, the generated NURBS curve goes through the middle of the stroke. In the other cases, the NURBS curve does not follow the midline of the stroke well. That means the NURBS fits the basic stroke “ | ” best in Case NO.2. Notably, even in Case NO.2, the fitting is not perfect because the endpoints of the NURBS curve and the end of the stroke do not coincide. The reason is that the endpoint -the deformation- of the NURBS curve is selected with an approximation. The more accurate value of the deformation here should be 0.09 or 0.095. The fitting gets much better when the deformation is changed to 0.095 in Case No.2 (see Figure. 4-83).

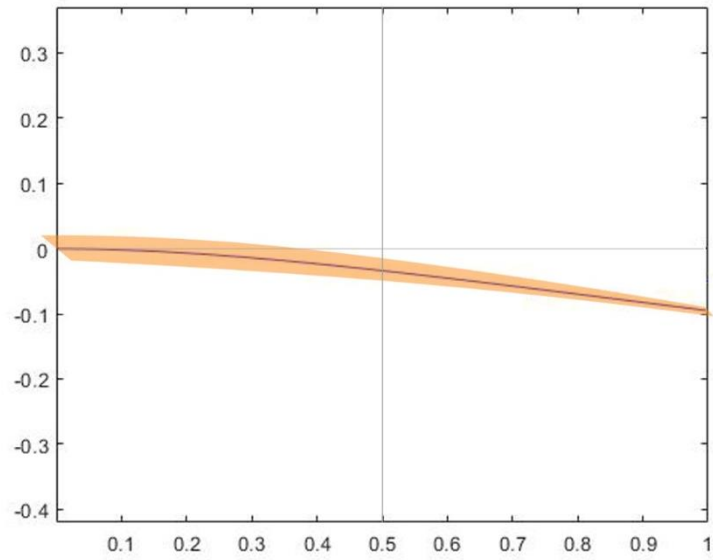


Figure 4-83. In Case NO.2, the basic stroke “ I ” is fitted by the cubic NURBS curve with the given deformation (-0.095).

The third stroke “ J ” and the generated NURBS curves from the four cases are put together and compared (see Figures. 4-84 to 4-87).

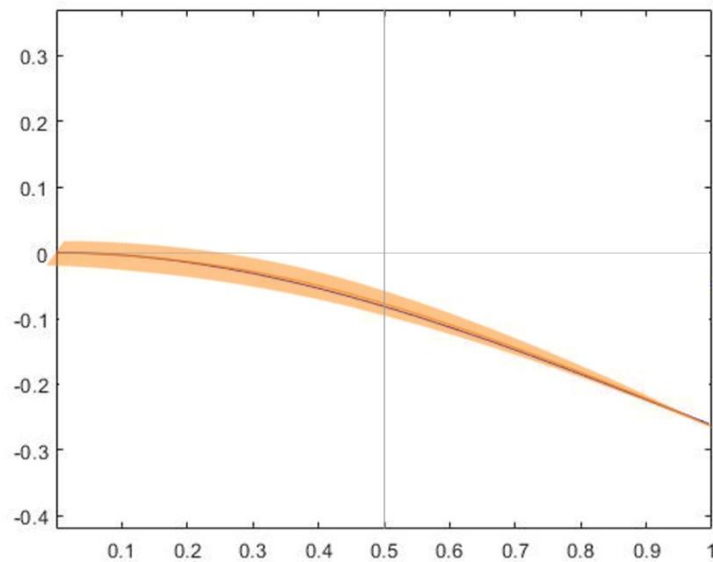


Figure 4-84. In Case NO.1, the basic stroke “ J ” is fitted by the cubic NURBS curve with the given deformation (-0.265).

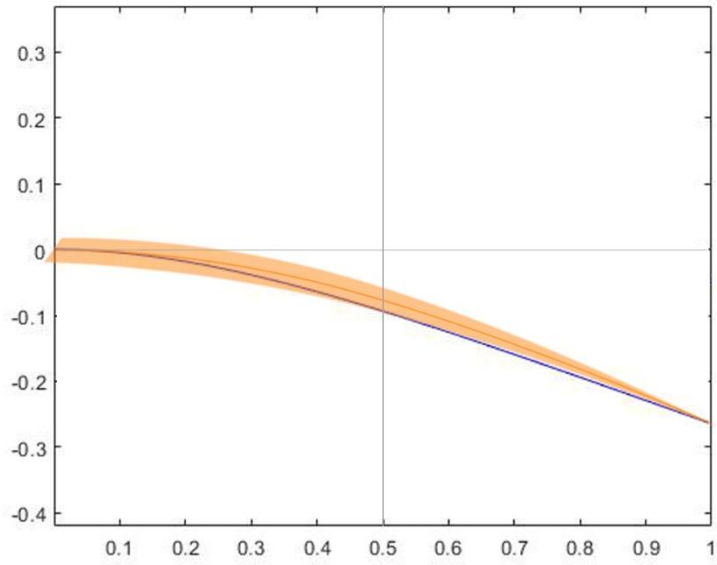


Figure 4-85. In Case NO.2, the basic stroke "J" is fitted by the cubic NURBS curve with the given deformation (-0.265).

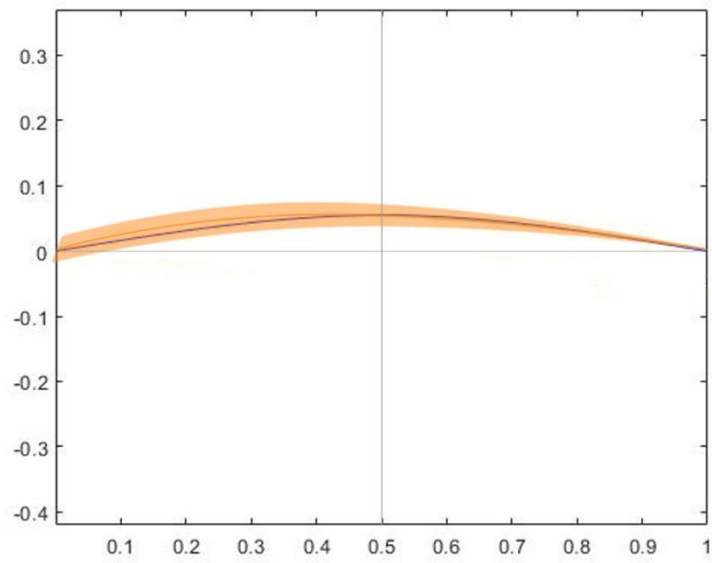


Figure 4-86. In Case NO.4, the basic stroke "J" is fitted by the cubic NURBS curve with the given deformation (0.055).

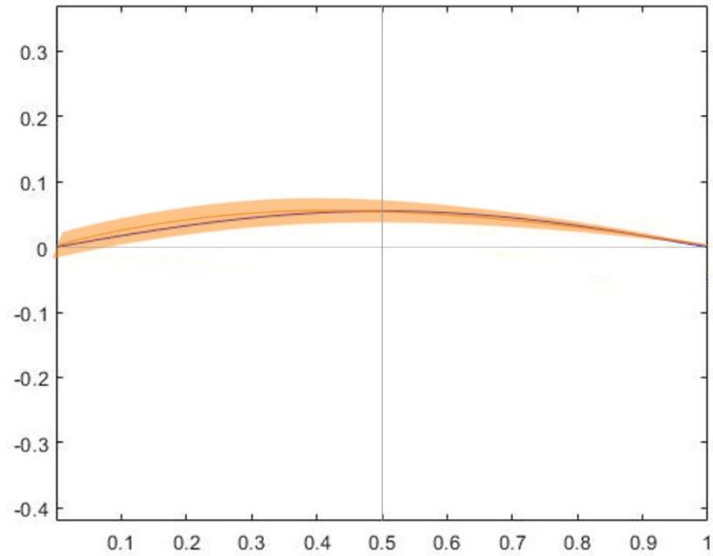


Figure 4-87. In Case NO.6, the basic stroke “J” is fitted by the cubic NURBS curve with the given deformation (0.055).

The comparison shows that in Case N0.1, the generated NURBS curve goes through the middle of the stroke. In the other cases, the NURBS curve does not follow the midline of the stroke well. That means the NURBS in Case No.1 fits the basic stroke “J” best.

The fourth stroke “\” and the generated NURBS curves from the four cases are put together and compared (see Figures. 4-88 to 4-91).

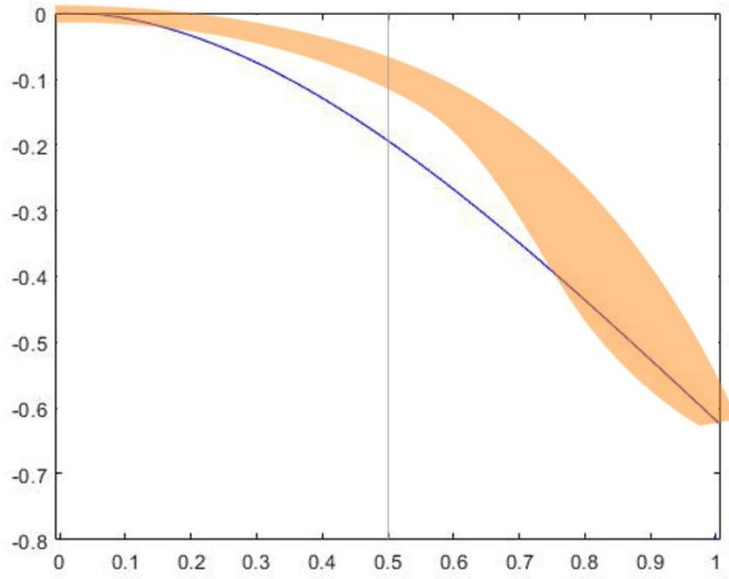


Figure 4-88. In Case NO.1, the basic stroke “ㄣ” is fitted by the cubic NURBS curve with the given deformation (-0.62).

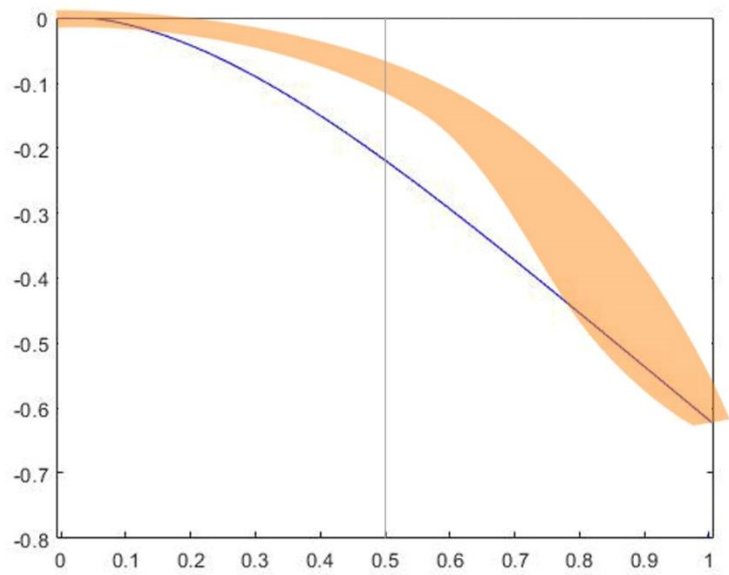


Figure 4-89. In Case NO.2, the basic stroke “ㄣ” is fitted by the cubic NURBS curve with the given deformation (-0.62).

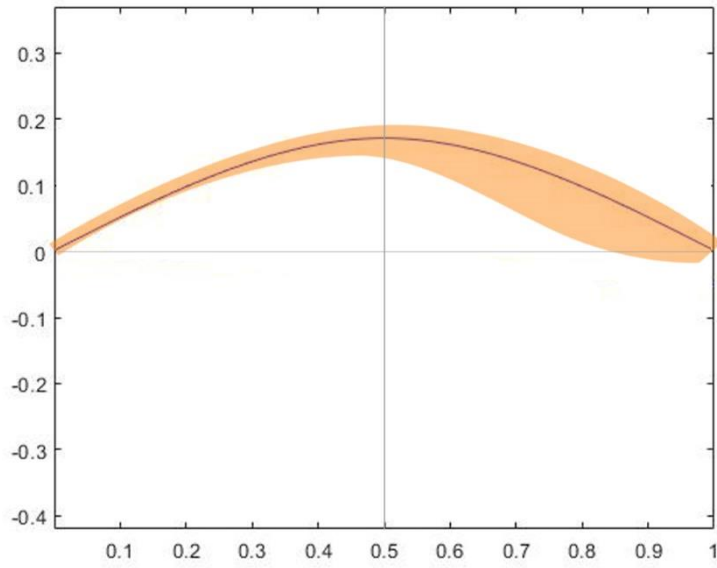


Figure 4-90. In Case NO.4, the basic stroke “ㄣ” is fitted by the cubic NURBS curve with the given deformation (0.17).

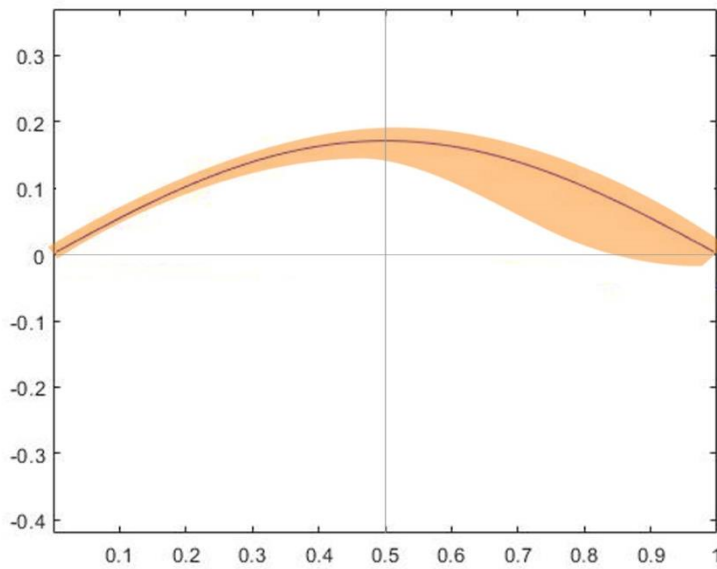


Figure 4-91. In Case NO.6, the basic stroke “ㄣ” is fitted by the cubic NURBS curve with the given deformation (0.17).

The comparison shows that in Cases No.4 and No.6, the generated NURBS

curve goes through the middle of the stroke. Compared with Case NO.4, the NURBS curve from Case NO.6 fits the stroke slightly better. In Cases No.1 and No.2, the NURBS curve does not follow the midline of the stroke at all. That means the NURBS in Case NO.6 fit the basic stroke “\” best.

The fifth stroke “/” and the generated NURBS curves from the four cases are put together and compared (see Figures. 4-92 to 4-95).

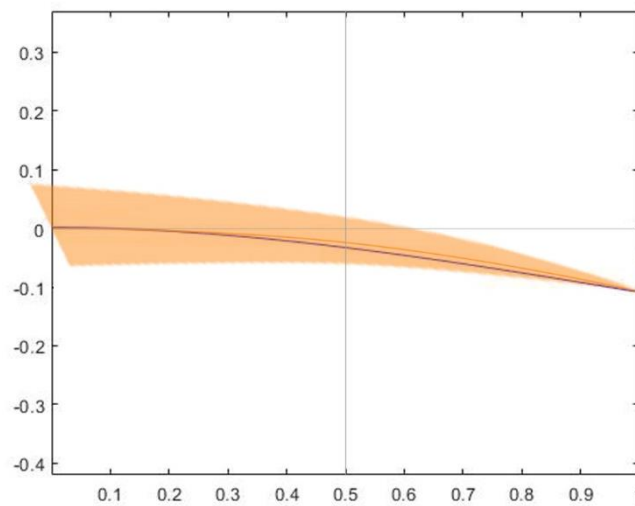


Figure 4-92. In Case NO.1, the basic stroke “/” is fitted by the cubic NURBS curve with the given deformation (-0.11).

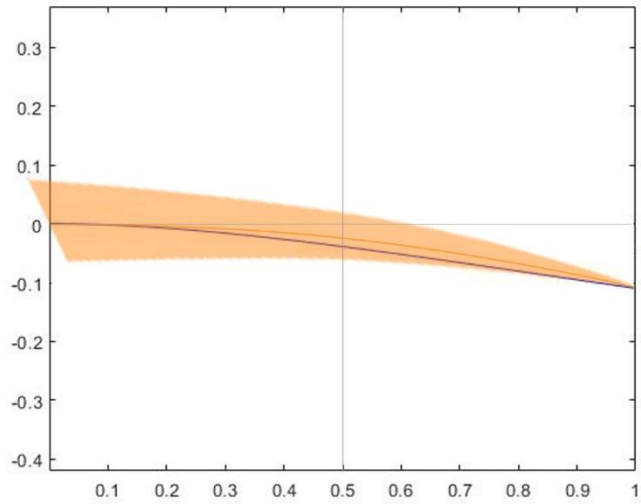


Figure 4-93. In Case NO.2, the basic stroke “↗” is fitted by the cubic NURBS curve with the given deformation (-0.11).

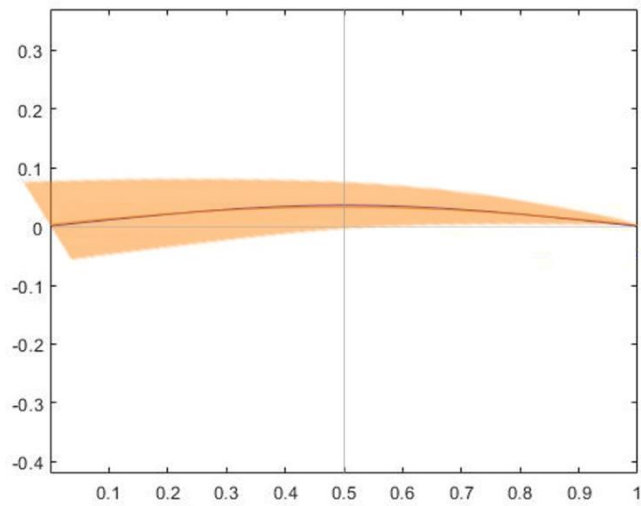


Figure 4-94. In Case NO.4, the basic stroke “↗” is fitted by the cubic NURBS curve with the given deformation (0.035).

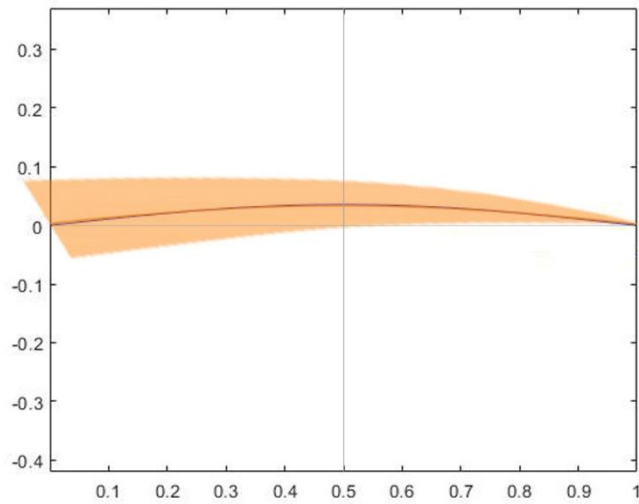


Figure 4-95. In Case NO.6, the basic stroke “↗” is fitted by the cubic NURBS curve with the given deformation (0.035).

The comparison shows that in Cases N0.4 and N0.6, the generated NURBS curve goes through the middle of the stroke. Compared with Case No.4, the NURBS curve from Case No.6 fits the stroke slightly better. In Cases No.1 and No.2, the NURBS curve does not follow the midline of the stroke very well. That means the NURBS in Case NO.6 fit the basic stroke “↗” best.

4.5. Conclusions

In this part of the study, the connection between NURBS, the dimensionless quantity, and its application in art have been discussed. The relationship

between beam bending and NURBS is explained mathematically, resulting in a dimensionless quantity which describes the rigidity of NURBS. The rigidity of NURBS can be used in the art of Chinese calligraphy to analyse the strokes, to understand, learn and, in turn, create.

Having found the relationship between NURBS and the bending of the beams, artists and even amateurs can use the contribution -the rigidity of NURBS – as a new practical and reliable approach to guide art creation. For example, if artists or designers want to draw a curve that looks like a bending beam, that means there is a straight line bent due to stress or load, they can use the dimensionless quantity to gain the curve they want easily. Similarly, people can use the relationship to test and verify whether curves are reasonable in scientific theory or not. Following this guide, artists and designers can make their creations and designs satisfy both functional engineering and artistic requirements.

For Chinese calligraphy, the method can provide an approach to using NURBS to draw the rigidity and strength of Chinese calligraphy. The study is focused on the five basic strokes in Chinese characters, which also show the core of Chinese calligraphy. The bent beams are compared with handwriting by the

most influential Chinese calligraphy artist, Huizong, and the results show the rigidity of Huizong's strokes. Four cases of beam bending -Cases No.1, No.2, No.4 and No.6- are utilised in this chapter. The five basic strokes -“一”, “|”, “丿”, “㇇” and “㇏”- in Chinese calligraphy are picked out and found in Huizong's Run Zhong Qiu Yue Tie. Comparison with the NURBS curves generated by the code using the method in 4.3 shows that there is a high similarity between the NURBS curves and Huizong's strokes. That means the generated NURBS curves can show the rigidity of Huizong's strokes and the rigidity also show the strength and hardness of Chinese calligraphy. Summarising the results of the comparisons, the NURBS in Case No.6 fits the basic stroke “一” best; the NURBS in Case No.2 fits the “|” best; the NURBS in Case No.1 fits the “丿” best, and the NURBS in Case No.6 fits the basic stroke “㇇” and “㇏” best. The study posts a possibility that people can follow the rules of the method in this study and draw beautiful Chinese strokes like Huizong in calligraphy learning and practice easily. This method also produces a new approach to help amateurs and calligraphy artists to improve their understanding and skills of Chinese calligraphy art.

4.6. Discussion, extensions, and implications

In this chapter, the concept of the rigidity of NURBS and its application in Chinese art is shown and discussed. Many studies about the properties of NURBS such as the *local support*, *continuity* and so on. However, its rigidity is rarely explored academically. The idea of discovering NURBS's rigidity is from human daily life. For example, in natural phenomena, the shape of the branches swaying in the wind looks similar to a NURBS curve. Also, in engineering projects, the outline of an arch bridge looks like one too. Similarly, there seems to be a connection between the bent beams and the curves generated by NURBS. The study in this chapter discovered the rigidity of NURBS using engineering solid mechanics and dimensionless quantity, contributing to a practical approach to Chinese art.

The method in this chapter may be used in the learning of Chinese calligraphy. For now, generally, learning Chinese calligraphy is robotic, and beginners have to copy from valuable references like a machine. In the early stages of learning Chinese calligraphy, the importance of practising following some traditional rules should not be denied. However, art creation needs to remain the centrals despite the repetitive practice necessary. Chinese calligraphy cannot be

learned and passed on with copying only because it is a traditional art in Chinese culture with a long story and history, and it needs its strength and tenacity to represent the core. People can learn how to draw the core of Chinese calligraphy following the rules mentioned in this chapter. This theory can be used not only to analyse the strokes in Chinese handwriting but also to teach and practice calligraphy.

The potential application in different fonts of Chinese calligraphy is worthy of attention. There are many different fonts (Ti) that have been handed down to the present in Chinese calligraphy. For example, Xing Ti is a well-known famous font and is best known for Xizhi Wang (303-361)'s work such as "Lan Ting Ji Xu" (see Figure. 4-96). In addition to this, Kai Ti, is another popular one in China and is best known for Zhenqing Yan (709-784)'s work (see Figure. 4-97). In their works, the characters are beautiful and the strokes are strong but not visually overweight. Unlike some famous calligraphers in China nowadays, almost no one said Xizhi Wang and Zhenqing Yan's calligraphy were bad or not good enough. In the modern age, it is a controversial topic whether Moruo Guo's handwriting could be called artwork or opportunistic calligraphy in the world.¹⁶⁹ Even in China, many people questioned his handwriting level and skill. The font of his handwriting is unique, but that does not mean it is excellent. At

least, compared with Huizong, there is a lack of strength and beauty. For the lack, the method in this chapter may play an innovative role in the improvement of handwriting. Perhaps, a small change can make a big difference and significantly improve a work of calligraphy.

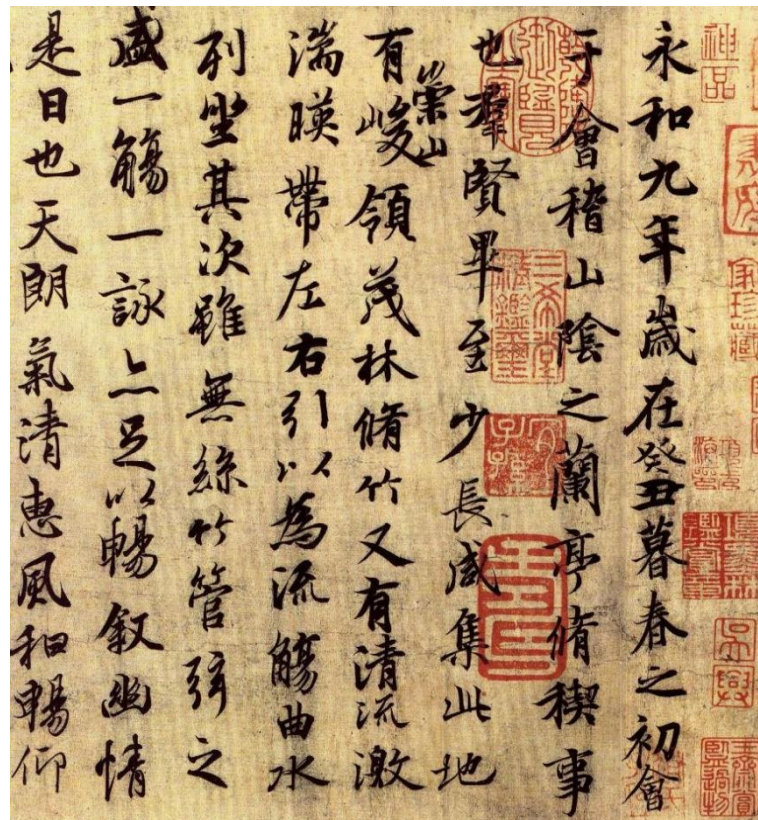


Figure 4-96. A part of Xizhi Wang's calligraphy work "Lan Ting Ji Xu" in 353.



Figure 4-97. A part of Zhenqing Yan's calligraphy work "Duo Bao Ta Bei" in 752.

Moruo Guo's handwriting is studied by many institutions and universities due to his reputation and the popularity of his art. Moruo Guo (1892-1978) was a Chinese author, poet, historian, archaeologist, and government official.¹⁷⁰ This chapter only discusses his handwriting; it does not include a moral critique of him, nor a discussion of his change in political standpoints to save his life, and the reasons why his handwriting became famous. In the studies on his calligraphic works, it is pointed out that Moruo Guo laid a solid foundation for calligraphy since childhood and one of the extraordinary features in his handwriting is the beauty of "overmuch".¹⁷¹ His lack of Kai Ti -a famous font of Chinese calligraphy- has been discussed and it has been pointed out that his

Yan Kai, the Kai Ti from Zhenqing Yan, skills are not as good as Xun Ouyang and Mengfu Zhao's. To put it bluntly, he is not proficient enough in Yan Kai's techniques and essence.¹⁷² From the point of view of this chapter, his handwriting looks weak or coreless because his strokes have not demonstrated the requirement of rigidity (see Figure. 4-98).



Figure 4-98. Two pieces of handwriting by Moruo Guo

Even though different fonts make the style of the characters vary visually, the core of Chinese calligraphy cannot be ignored. That means the characters should be beautiful in general, look “healthy” and not “sick”, balanced and stable.

The strokes need to be strong but not overweight, smooth but not weak. Based on the study in this chapter, some characters from Moruo Guo's handwriting may look better if some basic but important strokes such as “ノ” are drawn using the approach here.

Nowadays, there are many auto-generated fonts by computer programs that look similar to Chinese calligraphy, but are not as good as the famous handwriting. Undeniably, it is beneficial to try to create famous calligraphy with coding. Then everyone can make what they typed to be a Huizong-style, Zhenqing Yan-style or Xizhi Wang-style. However, unlike the features on the face, it is not easy to catch the core of the calligraphy works. So, the generated Huizong-style font may be similar to Shou Jin Ti, but there is still a big gap between his works. Compared with the Huizong-style font generated by an online program,¹⁷³ Huizong's calligraphy looks slim but strong and more beautiful. Even the auto-generated characters are similar to Huizong's style visually, but the core of the stroke is missed (see Figure. 4-99).



Figure 4-99. From the comparison between the generated Huizong-style font (left) and Huizong's art (right), it is not difficult to find the difference. In the characters generated by a computer program, the strokes look different from Huizong's calligraphy, especially in curves relevant to the basic strokes which have been highlighted in orange. The differences make the generated characters miss the core and the most important "soul" of Huizong's art.

The analysis in Chapter 3 explained how NURBS and CFD can be used and benefit art appreciation and creation. This chapter brings NURBS into fine art using the concept of rigidity. In the next chapter the utilisations of NURBS and CFD in product and visual design are considered.

CHAPTER 5. METHOD APPLICATIONS IN DESIGNS

5.1. Introduction

The previous two chapters tested the usefulness of NURBS and CFD for art evaluation and creation, with reference to the scene of fluid flow in realistic art and the curve of the five basic strokes in Chinese calligraphy. In this chapter, the focus now turns to how and why the combination of CFD and NURBS can benefit product development and visual design. The method developed in previous chapters is tested and utilised in engineering projects, the development of new products, and the exploration of visual design, and provides a new approach to higher efficiency performance and a higher quality of design. NURBS is a convenient tool to draw a curve and it is also commonly utilised in the design. CFD is a scientific approach to testing and analysing working efficiency. In this chapter, several different types of products are analysed as samples, from simple to complex.

The first product analysed is pipe design. As an industrial product with a simple

structure, pipes are commonly utilised in fluid transmission. The shape of the pipe directly affects the energy loss; less energy loss means higher working efficiency. In this section, the relationship between energy loss and the change in total pressure is explained and linked. Since there is no difference between straight pipes of the same diameter, only the energy loss of the curved pipes is different. Therefore, the energy loss in different shapes of curved pipes is compared using CFD. The results show that the energy loss can be reduced if the shape of the pipe is drawn by NURBS.

Based on the results from pipe design studies, NURBS and CFD are, in the second example, utilised in an existing engineering project. The project is the development of a new turbo engine range extender named TREx. One part of TREx - the inlet air duct - is redesigned using the combination of NURBS and CFD. In the process of redesign, the model of the inlet air duct is rebuilt with UG-NX. The shapes of the duct are drawn by NURBS. CFD is used for the simulation of air flowing through the duct. The shape of the inlet air duct is changed several times following the result of the simulation, and then the best shape of the duct is found. Two parts of TREx are designed using NURBS including the inlet air duct and the casing of TREx, resulting in a more visually tense and higher quality design. The latter is shown and described in the section

about visual design.

Thirdly, and based on the previous studies in this chapter, the method is utilised in car design. Cars are more complex products and need good shapes for the requirements of functions and aesthetics. Due to the requirements of functions, the profile of a sedan, especially a sports car, should be curvy and streamlined, resulting in less drag. In this section, the key points of a car's profile have been located in a side view. The key points are then joined with different lines, including straight lines, quarter circles and NURBSs. The models of the bodies made of different shapes are built in UG-NX. After that, the moving scenes of the models are simulated with Ansys Workbench. All the information in the movements is represented in the analysis reports, especially the drag. The results show that the drag can be reduced significantly using NURBS in the outline design of a sedan.

Not only did NURBS play a significant role in the field of engineering or product development but also in visual design. The visual design includes the look of the product and poster design. The features of NURBS - the continuity and rigidity - are used in two cases of design. The productions are submitted for some popular international design competitions and exhibitions. Some of the

designs are manufactured and put into the market. The acceptance of these designs by professionals reflects the utility of this theory.

5.2. NURBS and CFD in pipe design

It is useful to begin by utilizing the combination of NURBS and CFD in products with simpler structures such as pipes, rather than with complex products like engines and vehicles. The pipe is a common industrial product and pervades our lives. In general, straight lines and curves are the two basic shapes of pipes. Its structure is widely used in industrial or product designs which are relevant to fluid. For example, we use the pipe to transport oil, water, gas, air and so on. The outline of the pipe plays a significant role in transporting efficiency, and the combination of NURBS and CFD can be used in the design of the pipe's outline to achieve a higher efficiency during transportation. In this section the profiles of pipeline structures are designed and drawn with NURBS, modelled with GUNX (version 10.0) and the status of utilisation is analysed with CFD via Ansys Workbench (version 18.2).

The less energy loss, the higher the efficiency of the pipe, And the shape of the pipe affects the energy loss directly. So, designers and engineers pay careful

attention to the profile of their pipes and attempt to reduce the energy loss during the transmission. There are two openings on a pipe: the entrance and the exit. The entrance of the pipe is named inlet and the exit is named outlet in this study. The working efficiency can be seen as the ratio of the energy at the outlet to the energy at the inlet in percentage. Which is: $(Energy_{outlet} / Energy_{inlet}) \times 100\%$. The energy loss is the difference between the energy at the inlet and the energy at the outlet, which is: $Energy_{inlet} - Energy_{outlet}$. Since the change of energy can also be translated into the change in total pressure, the energy loss is also: $Total\ Pressure_{inlet} - Total\ Pressure_{outlet}$, and the working efficiency is $(Total\ Pressure_{outlet} / Total\ Pressure_{inlet}) \times 100\%$. For example, if the total pressure at the inlet of the pipe is 1.0 bar and 0.9 bar at the outlet, the energy loss in this pipe is $(Total\ Pressure_{inlet} - Total\ Pressure_{outlet}) = (1.0 - 0.9) \text{ bar} = 0.1 \text{ bar}$. The working efficiency of the pipe is $(Total\ Pressure_{outlet} / Total\ Pressure_{inlet}) \times 100\% = (0.9 / 1.0) \times 100\% = 90\%$. Consequently, the smaller the total pressure changes, the higher the efficiency. In the two basic profiles of pipes, only the curved ones are analysed in this section. For straight pipes, the difference in total pressures at the inlet and outlet is negligible.

The shapes of the pipes can easily be drawn using the UG-NX. For instance,

to draw a quadratic NURBS curve, at least three control points are required, and UG-NX can automatically generate one with three given control points. Here the quadratic NURBS is utilised for analysis. The three control points are the three tops of an isosceles right triangle (see Figure. 5-1).

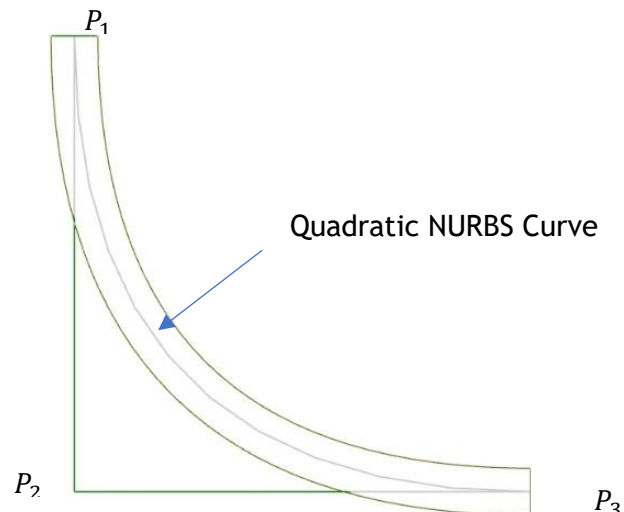


Figure 5-1. The shape of the pipe is made of quadratic NURBS. The plane where the point P_1 is located and the plane where the point P_2 are the inlet and outlet of the pipe. Because $\Delta P_1 P_2 P_3$ is an isosceles right triangle, so the length of $P_1 P_2$ is equivalent to that of $P_2 P_3$, the $\angle P_1 P_2 P_3 = 90^\circ$.

There are three other essential factors in pipe design: the length of the sides which are $P_1 P_2$ and $P_2 P_3$, the angle $\angle P_1 P_2 P_3$, and the diameters of the pipe openings. In this case, the two legs and $\Delta P_1 P_2 P_3$ are set to be equal and the length is between 500mm to 5000mm because a difference of ten times is sufficient to see the changes. Technically, in a design of a curvy pipe, the angle of $\angle P_1 P_2 P_3$ is greater than 0° but smaller than 180° . But in practice, the

range is not that large. So, the range of $\angle P_1P_2P_3$ is as between 70° to 110° which means there is a difference of 40° and is sufficient to see the differences. The sizes of the diameters are from 50 mm to 190 mm. The aim here is not to find the relationship between the change of key parameters and working efficiency, only the feasibility and advantages of NURBS in the design of pipes. Therefore, the parameters are given randomly and close to practical applications.

In modelling, the parameters are selected from the given ranges. The lengths of the sides are set as 500 mm, 1000 mm, 2500 mm and 5000 mm. The angles of $\angle P_1P_2P_3$ are set as 70° , 80° , 90° , 100° and 110° . The sizes of the diameters are set as 50 mm, 80 mm, 150 mm, 180 mm and 190 mm. The NURBS shape is fixed, which means all the curves are drawn by NURBS.

The boundary conditions of the simulations –the inlet, outlet, fluid, pressures and the type of analysis – are set as follows: The plane where P_1 is located set to the inlet, and the opening where P_3 is located is set to the outlet. The fluid is set to clean air, and it enters the inlet and flows out from the outlet. The *Total Pressure_{inlet}* is given as 2.0 bar and *Static Pressure_{outlet}* is fixed as 1.0 bar. The pipe is only filled with air which means that the occupancy rate of

air is always 100% in the pipe. So, unlike in the study in Ingres and Raphael, the method of Volume of Fluid is not applicable. Consequently, the simulations can show the changes in the total pressure between the inlets and outlets of the pipes.

After the simulations run successfully, the energy loss in different shapes of curved pipes can be compared. Analogue software, ANSYS CFX, is used, in order to more easily obtain data (ANSYS CFX is a high-performance CFD software tool that delivers reliable and accurate solutions quickly and robustly across a wide range of CFD and Multiphysics applications¹⁷⁴). The data is shown in analysis reports. For easier comparison, all the data is collected and put in charts. Then the change of the parameters, the data from the simulations, and the connection between both can be read clearly.

As the results, Tables 5-1 to 5-3 show the change in the working efficiency of the pipeline under different conditions.

MODEL SIZE: Diameter=50mm; $\angle=90^\circ$; L=Length

Boundary Conditions

Inlet: Total Pressure (Stable) =2 bar

Outlet: Static Pressure=1 bar

Efficiency=Outlet/Inlet (total pressure)

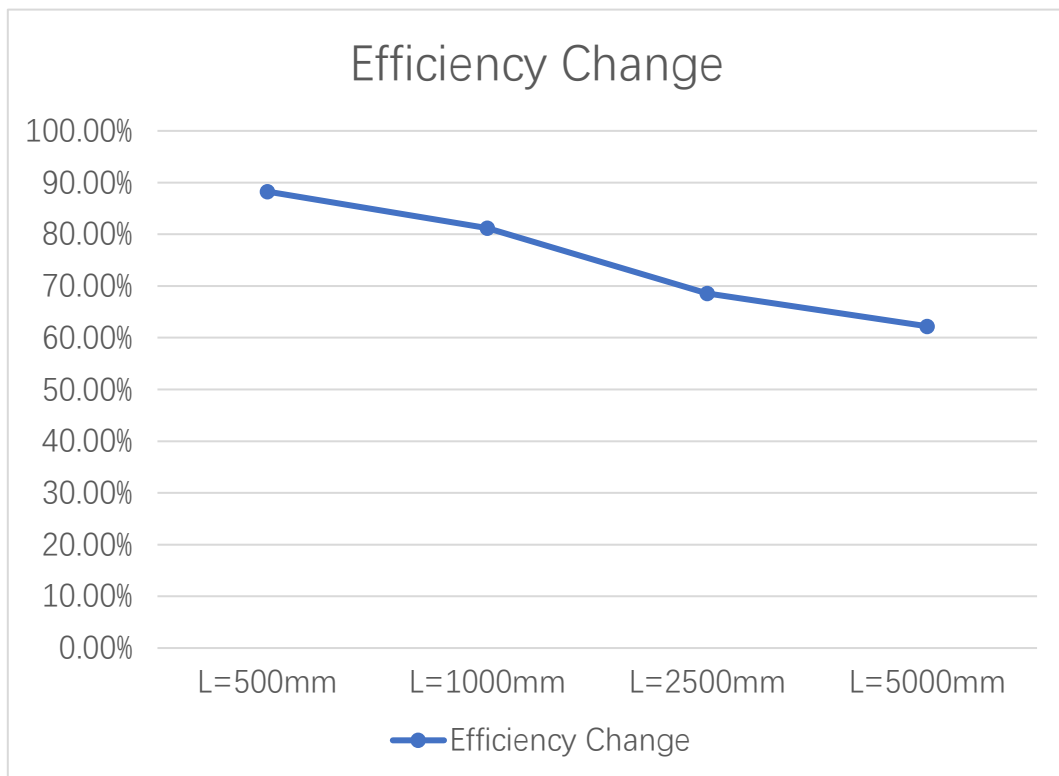


Table 5-1. The working efficiency of the pipe changes while the length increases.

MODEL SIZE: Diameter=50mm; Length=500mm; \angle =Angle

Boundary Conditions

Inlet: Total Pressure (Stable) =2 bar

Outlet: Static Pressure=1 bar

Efficiency=Outlet/Inlet (total pressure)

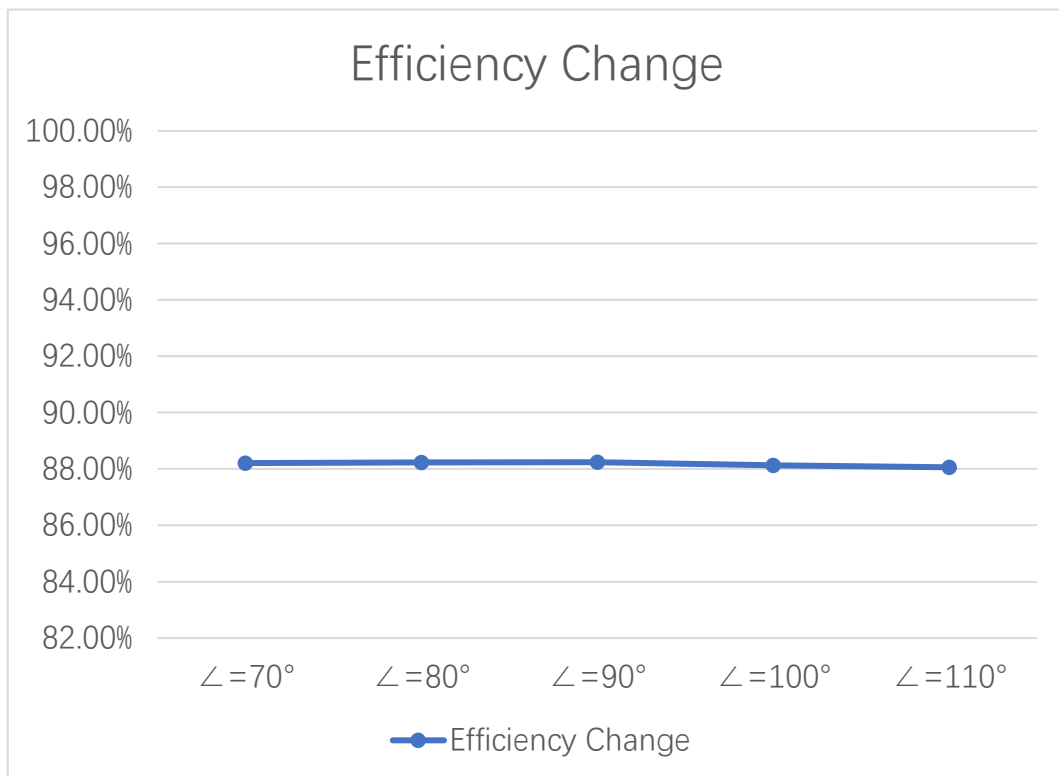


Table 5-2. The working efficiency of the pipe changes while the angle increases.

MODEL SIZE: Length=500mm; $\angle=90^\circ$; D=Diameter

Boundary Conditions

Inlet: Total Pressure (Stable) =2 bar

Outlet: Static Pressure; 1 bar

Efficiency=Outlet/Inlet (total pressure)

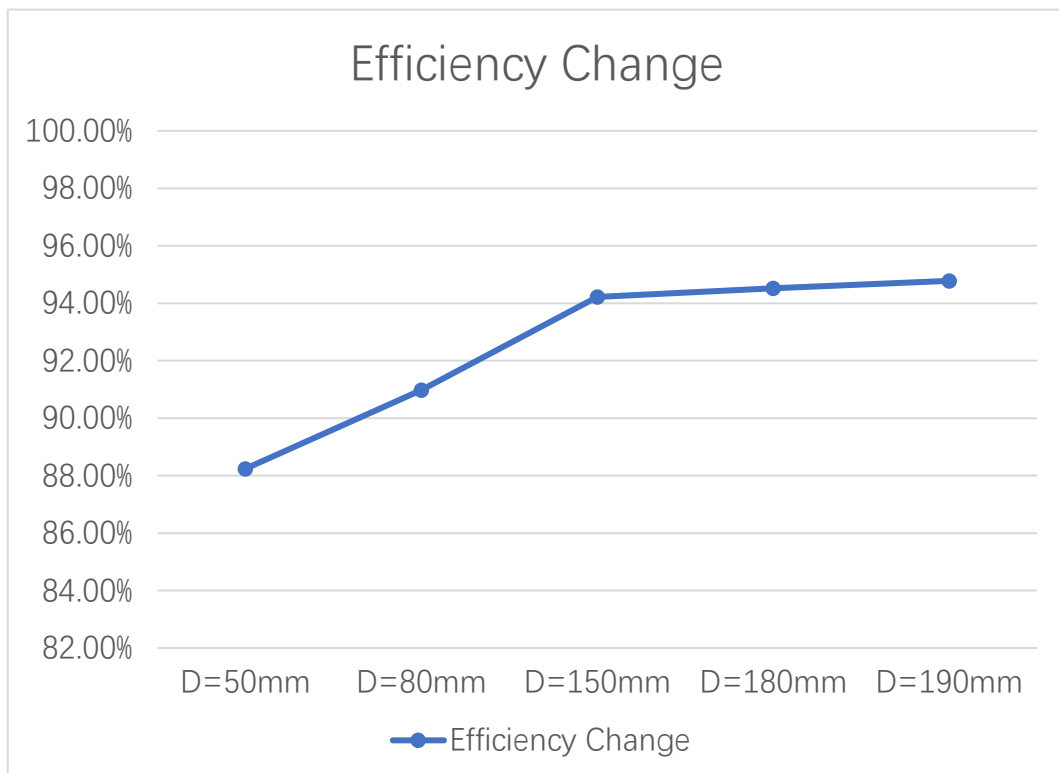


Table 5-3. The working efficiency of the pipe changes while the diameter increases.

The data from Table. 5-1 to 5-3 show how the efficiency of the pipe is affected by changes in leg length, angle or diameter. When the boundary conditions are fixed, the working efficiency of the pipe decreases if the length of the two right-angled sides becomes longer. The working efficiency does not change

significantly when the angle opens from 70 to 110 degrees. The working efficiency increases if the diameter of the pipe gets larger. The importance of these results will be discussed in more depth further on.

The utilisation of NURBS in pipe design has the potential to be used in other design fields and brings more possibilities to design. This means that if the NURBS can provide a stable working efficiency in pipe design, then it can also benefit the design of some industrial components with a simple structure, even guiding the redesign of products.

5.3. NURBS, CFD, and the design of industrial product components

This section considers how the combination of NURBS and CFD can benefit simple product components, resulting in a better design that meets its requirements in function and aesthetics. First, good performance is always essential in product development. For those products or components that need to use fluid, such as air ducts, the shape directly affects their functionality. Second, in most cases of design, the parts need to be relevant to the main body in the outlook. It means that there should be some elements linked or similar

between the parts and the main body. For example, if the main body of a product such as a kettle is a cylinder, the lid should be rounded, not a pentagon or a trapezoidal since it will otherwise not meet the requirements of general aesthetics. To match and combine the duct and casing design, NURBS is applied to the profile design of the duct in this part of the study.

To further expand the research on producing functional and appropriate shapes, the inlet air duct of the TREx engine needs to be redesigned using NURBS and CFD. TREx is a new and environmentally friendly engine. Compared with other engines nowadays, it improves combustion efficiency and reduces the internal loss of energy through radical engine configuration and design. So, it is important that every process can minimize energy loss, including inconspicuous parts such as the inlet air duct. The previous design of the inlet air duct is designed following the feature and the shape of the main body of TREx. However, it had not been verified if the previous design can meet the functional requirements (see Figure. 5-2). The shape of the previous design is made of straight lines and fillets only, and no NURBSs and any other curvy lines are utilised. The model is built with UG-NX, and the side view is shown (see Figure. 5-3).

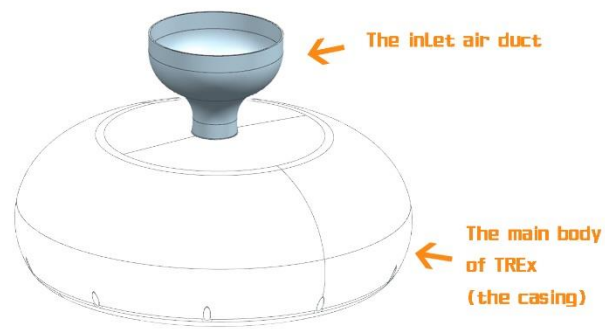


Figure 5-2. The image shows both the inlet air duct and the main body of TREx have curvy shapes.

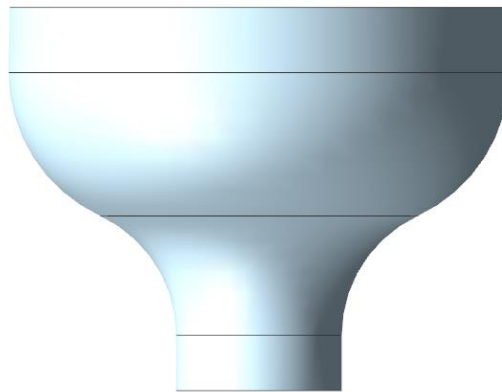


Figure 5-3. The side view of the previous design of the inlet air duct.

To test the fluid flow inside the inlet duct, ANSYS CFX is used for simulation. ANSYS CFX is recognized for its outstanding accuracy, robustness and speed when simulating turbomachinery, such as pumps, fans, compressors and gas and hydraulic turbines¹⁷⁵. This software can be used to analyse whether the model can maximize product productivity under specific boundary conditions. Similar to the previous study in the design of pipes, the method of Volume of

Fluid is not applicable. When the engine is working, only air goes through from the top to the bottom of the duct. The boundary condition at the top is static pressure with 1 bar and total pressure with 3 bars at the bottom. Because the bottom connects the compressor of the engine which is the part that can compress and bring the air into the combustion chambers. With the original design of the inlet air duct, the simulation shows that there may be some turbulence and the fluid flow is not very smooth. Figure. 5-4 illustrates the simulation result of the previous design.

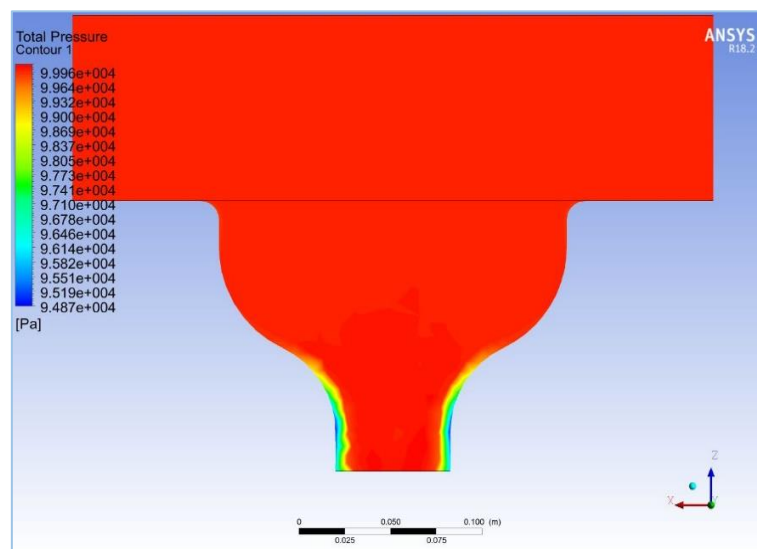


Figure 5-4. The simulation result of the previous design of the compressor inlet air duct.

Based on the previous model, NURBS is used in the redesign of the inlet air duct. In this section, the quadratic NURBS is utilised to draw the new shape of the air duct. By changing the coordinate position of the control points and the diameter of the top opening, a relatively aesthetically pleasing range of values

is obtained. As previously, the model of the new design is built in GU-NX (see Figure. 5-5).

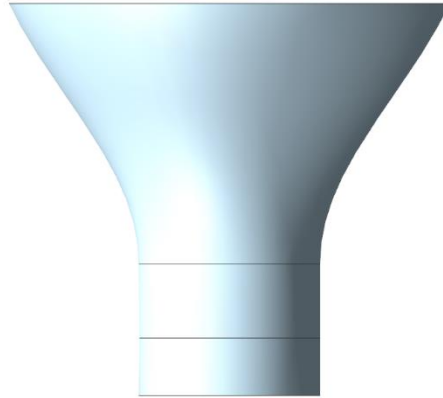


Figure 5-5. The side view of the optimised design of the inlet air duct.

Under the premise of invariant boundary conditions, the simulation results are optimised by changing the key points of the quadratic NURBS, and the optimal design of the inlet is obtained. Figure. 5-6 illustrates the optimised design of the inlet air duct.

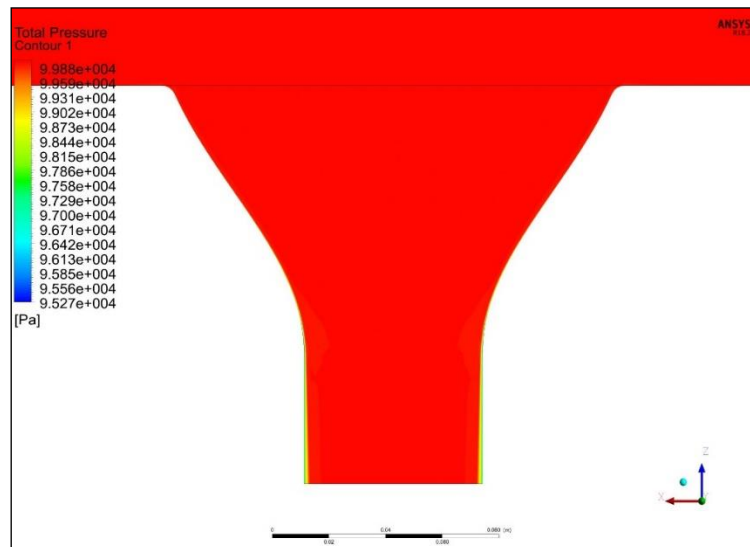


Figure 5-6. The simulation result of the optimised design of the compressor inlet air duct.

The difference between Figure. 5-4 and Figure. 5-6 shows how the total pressure near the bottom of the air ducts changes. When the boundary conditions are fixed, the change in the Total Pressure near the bottom is significant. In Figure. 5-4, the data shows the area close to the wall that has a visible reduction in Total Pressure, from $9.996e+004$ to $9.487e+004$. In Figure. 5-6, even though the reduction in Total Pressure still exists, the size of the area is much smaller and even can be ignored, and the change in the Total Pressure is not that significant. That means the shape of the lower part of the air duct plays a key role in working efficiency. The importance of these results will be discussed further on.

Generally, for the design of pipes or other industrial products with simple

structures, designers or engineers do not need to pay much attention to the appearance. Sometimes the functional requirements are the needs in engineering projects. For example, people don't care if the pipes buried in the ground look good or not. Similarly, the parts which cannot affect the main body too much also don't require too much design in appearance. Like the inlet air duct of the TREx engine, compared with its appearance, the merging with the main body and the function or its working efficiency are more important.

5.4. A guide to the sedan design

Even though the function is essential in product design, if the part is the main body or the cover of the main body of the product, its appearance becomes critical as the main body or casing of the product gives people their first impression before use. For example, in car/sedan design, the profile and the appearance play a key role in its popularity. Popularity directly determines the sales volume, and a good sales volume reflects the success of the design.

This section involves the numerical modelling of the standard sedan, with various outlines made of different curves. First, the profile of the sedan is drawn by straight-line, and polyline based on the necessary conditions and

fundamental standards of sedan design. The basic outline of a sedan shows every key turning point of the profile via CAD. Second, the outline changes due to the different connecting methods. This means the turning points are replaced by a rounded design or strung together with quadratic NURBS separately, resulting in two outlines: one changes little, except that the angle will become more rounded, and the other looks significantly different. Third, different orders of NURBS are utilised to fit the sedan's profile and cause changes in the outline. Then, based on the different profiles, the corresponding models are built using UG-NX. Subsequently, the models are imported to Ansys Workbench for running the simulations - the simulation of how they run on the road - and then the results of the simulations are compared and contrasted with the popular aesthetic.

5.4.1. Using NURBS to fit the outline of the car and build the model via CAD

Before fitting the profile with NURBS, the general structure of a car needs to be described. There are some basic rules in sedan design, including fundamental sizes, the position of people and so on. The most important parts of vehicle

design - the appearance of the vehicle - are the engine and relevant components, the dashboard, the steering system, the transmission system, the chassis, the wheels, the seats and the casing. Because those above are all related to the space of the car. The standard requirements of the sedan design are also shown in the image (see Figure. 5-7). The approximate necessary space for a car is highlighted too (see Figure. 5-8).

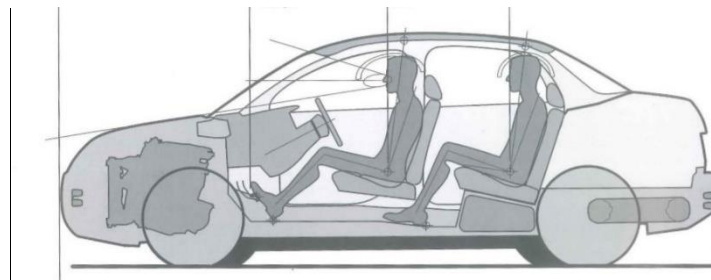


Figure 5-7. The general structure of the sedan is shown. In this image, the engine and relevant components, the dashboard, the steering wheel, the wheels, the seats, the people with an appropriate ratio, the chassis and a general casing are found. The positions of all the essential components of the car are reliable and ergonomic.

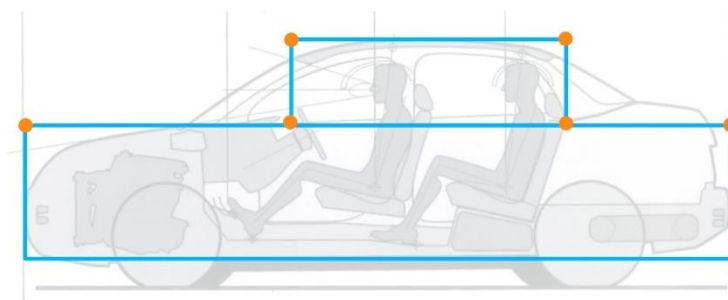


Figure 5-8. The blue boxes are the approximate necessary space for a car. The orange dots are the key inflexion points.

In product design, NURBS is used often, especially in sketching and modelling.¹⁷⁶ The vehicles are a sort of product, and their design includes cars, sedans, trucks, Special Operation Vehicles, etc. In the car and sedan design, except for the chassis, the profile of a car can be compared to a more complex curve, similar to NURBS, as a piecewise function. So, the profile of a car can also be drawn with one NURBS function in the early stage of design, which is sketching.

After locating the key points of the car, the general outlines of the car are fitted with different orders of NURBS, including Quadratic NURBS, Cubic NURBS, Quartic NURBS and Quintic NURBS. The purple lines are the NURBS curves in different orders (see Figures. 5-9 to 5-12).

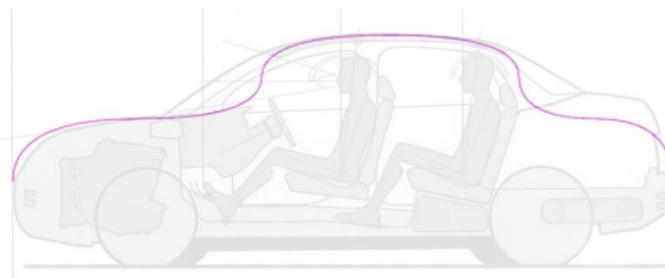


Figure 5-9. The general outline is fitted by quadratic NURBS.

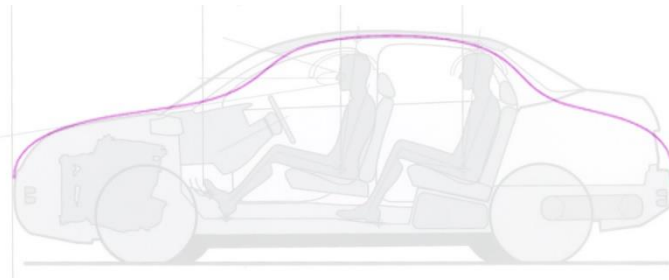


Figure 5-10. The general outline fitted by cubic NURBS.

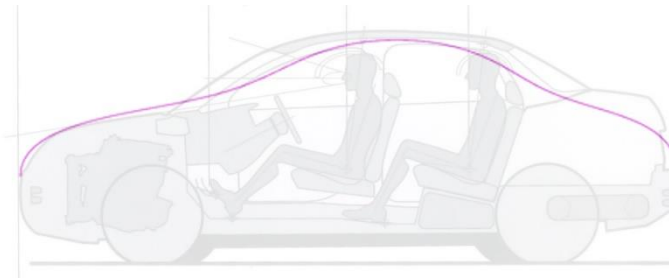


Figure 5-11. The general outline is fitted by quartic NURBS.

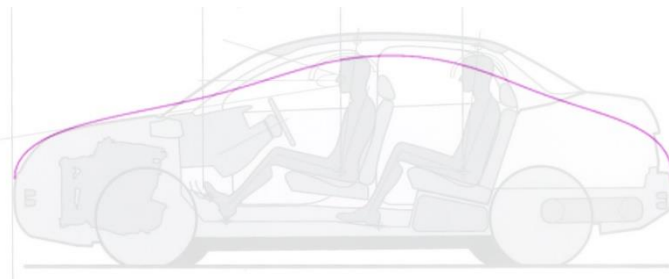


Figure 5-12. The general outline fitted by quintic NURBS.

From the result of fittings, it is clear that quartic and quintic NURBS cut too much and are not suitable to make a profile of a sedan as there is insufficient space for people. Even though the size of the engine and other larger components can be shrunk due to rapidly advancing technology, the space required for the people is fixed. So, the people sitting in the back seats do not have enough space in the outlines drawn by quartic and quintic NURBS.

Comparatively, the outlines fitted with quadratic and cubic NURBS do not have this problem.

5.4.2. Using CFD to simulate the running and calculate the drag

The performance of the outlines drawn with different NURBS can be tested using CFD. The performance in this case is reflected by the drag, which means that the less drag there is, the higher the performance is. The CFD simulation can be run in Ansys Workbench. When a car is moving at a high speed, it is also can be described as a static object staying in a wind tunnel, with high wind speed. In Ansys Workbench, the CFX is a suitable tool to analyse the performance and the drag can be calculated automatically.

The models of the profiles drawn with different NURBSs are built with UG-NX. The model includes the profile of the car and enough space for the flowing air. There needs to be more room above the car in the air tunnel because, in reality, cars run on the road with almost no obstruction above the casing. Also, there is a gap between the body of the sedan and the ground (see Figure. 5-13).

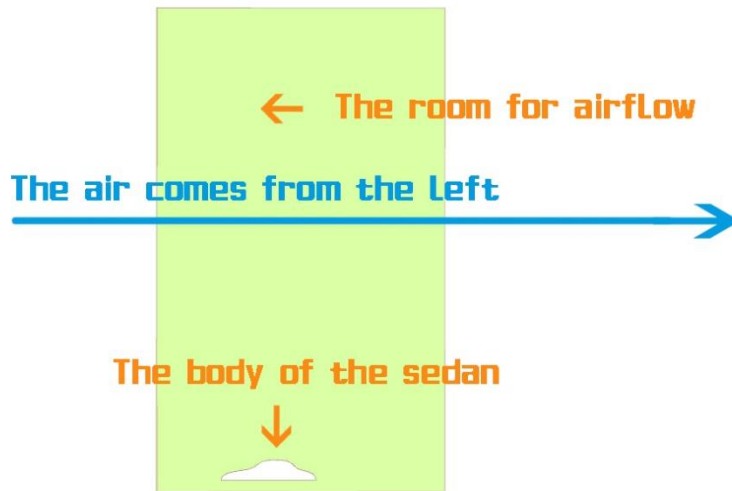


Figure 5-13. In the model for the simulation, the green area is the room for airflow; there is a gap between the chassis of the sedan and the ground; the air comes from the left and goes through to the right. The profile of the sedan in this image is drawn with cubic NURBS. Then the model now meets the requirements of the simulation.

The model of the simulation is built following the wind tunnel testing rules. The sedan is set as staying in the middle, and the air flows from the left to the right. The speed of the airflow is set as 100km/h. From the simulation, the velocities can be shown (see Figures. 5-14 to 5-17) and the pressures are shown (see Figures. 5-18 to 5-21). In terms of speed, the maximum speed around is close to 140 km/h, which is because the speed soars when the wind blows over the body.

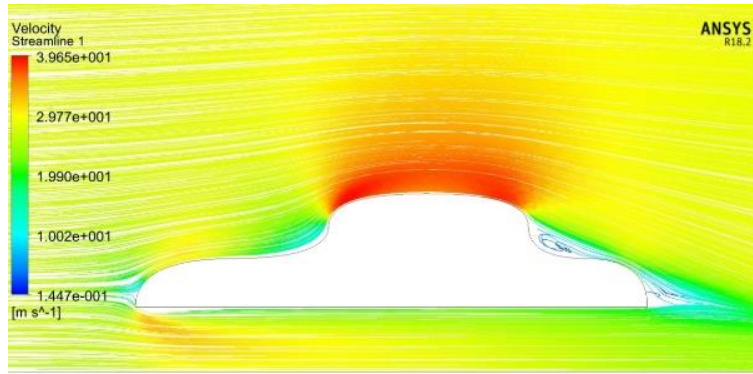


Figure 5-14. The velocity of the quadratic outline

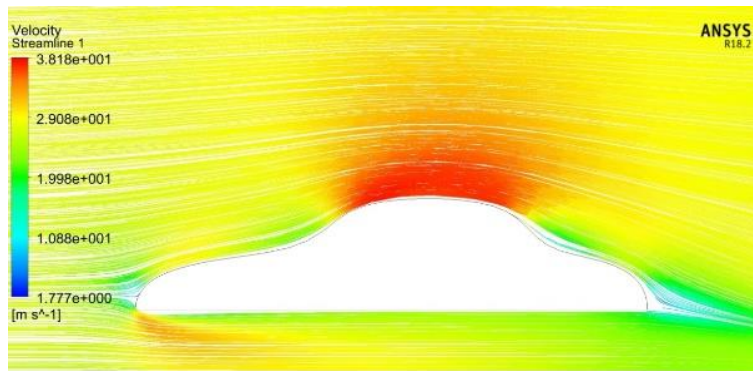


Figure 5-15. The velocity of the cubic outline

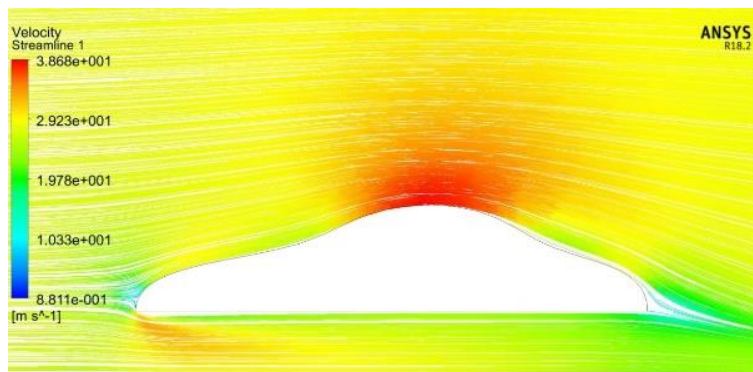


Figure 5-16. The velocity of the quartic outline

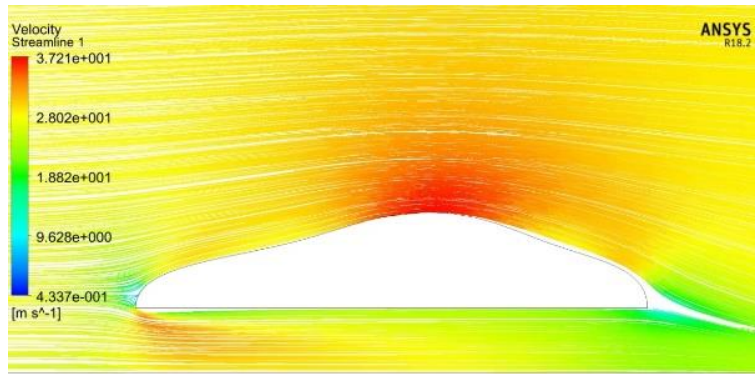


Figure 5-17. The velocity of the quintic outline

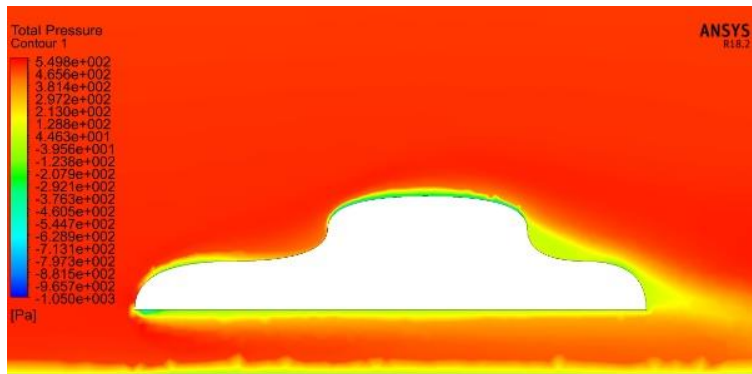


Figure 5-18. The total pressure of the quadratic outline

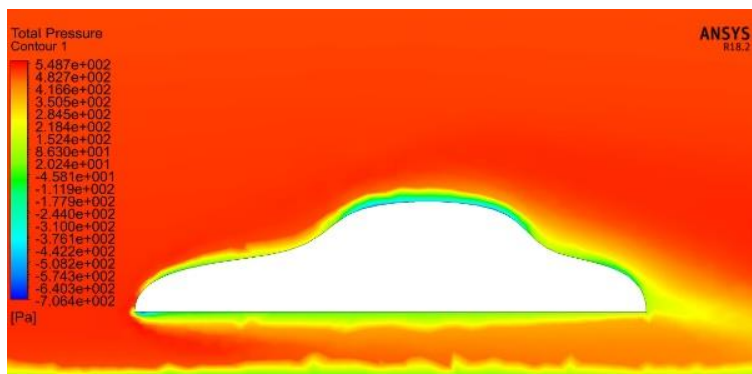


Figure 5-19. The total pressure of the cubic outline

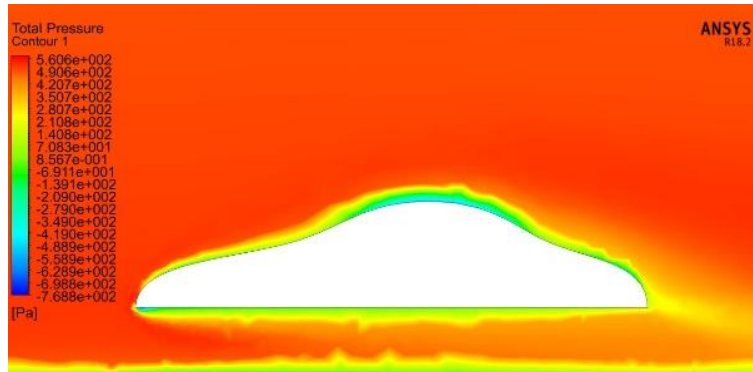


Figure 5-20. The total pressure of the quartic outline

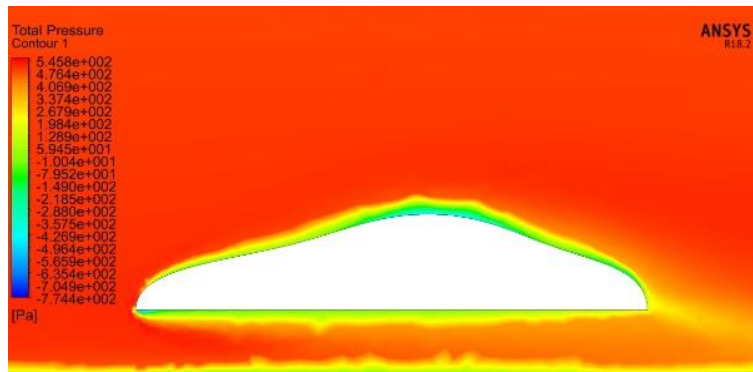


Figure 5-21. The total pressure of the quintic outline

From the images showing the velocity, it is clear the airflow velocity changes with the shape change. It is shown that the air is turbulent behind the car in Figure. 5-14. There is no big difference between Figure. 5-16 and Figure. 5-17.

From the images showing the total pressure, the total pressure has changed with the shape change. Similar to that of velocity, there is no significant

difference between Figure. 5-19, Figure. 5-20 and Figure. 5-21.

The drag on the car changes due to the order of NURBS. From the calculation in Ansys Workbench, the drag on the quadratic outline is -778.490 N, the drag on the cubic outline is -648.785[N], the drag on the quartic outline is -593.652 N, and the drag on the quintic outline is -552.977 N. From the simulation results, a rule can be found between the order of NURBS and drag. The drag will be reduced when the order of NURBS increases.

Because the quartic outline and the quintic outline are not suitable in this case, the comparison is limited to the quadratic outline and the cubic outline. The numbers show that the drag on the cubic outline was reduced by 19.999% more than that of the quadratic outline.

If the connection between two end-to-end structure lines is changed from the right angle to a rounded design, the model of the body is built in UG-NX (see Figure. 5-22 and 5-23). The simulation results for the velocity of airflow and the total pressure around the sedan are shown in Figure. 5-24 and Figure. 5-25.

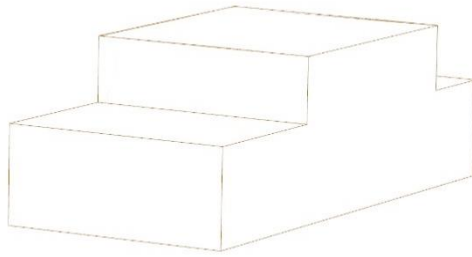


Figure 5-22. The sedan's body with a right-angle design

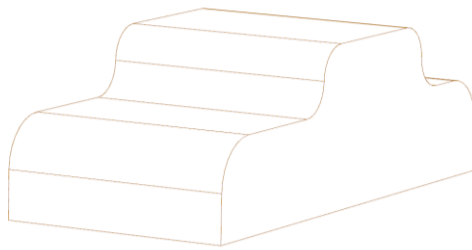


Figure 5-23. The sedan's profile with a rounded design

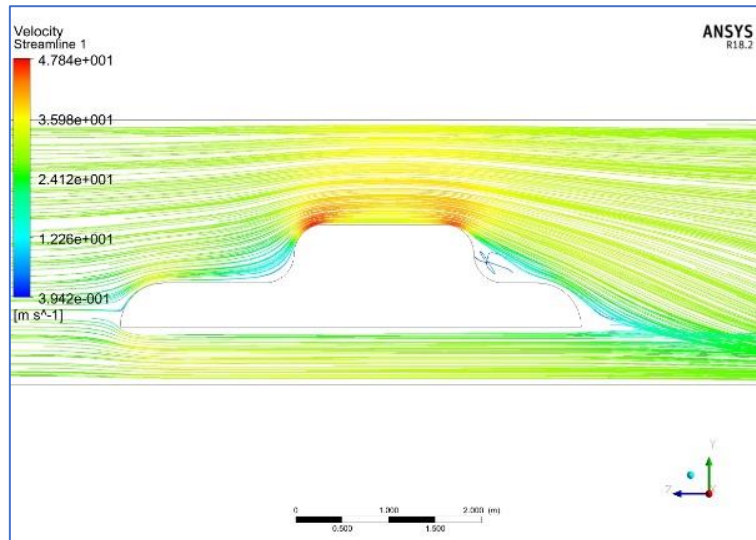


Figure 5-24. The velocity of the rounded design outline

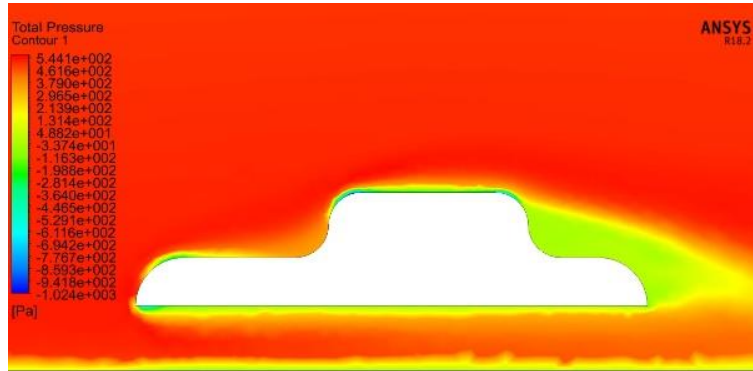


Figure 5-25. The pressure of the rounded design outline

From the calculation in Ansys Workbench, the drag on the rounded design outline is -828.465 N. Compared with the rounded design, the drag on the cubic outline has been reduced by 22%.

Coincidentally, the outline fitted with cubic NURBS (drawn by the yellow line) looks similar to the profile of the 2018 PORSCHE 911 (see Figure. 5-26).



Figure 5-26. The comparison of the 2018 PORSCHE 911 and cubic outline (yellow line).

5.5. The other cases of design using the application of NURBS

Except for the utilisation of NURBS in pipe design, the design of the inlet air duct, and the sedan design, some more cases used NURBS. In the first case, the casing of TREx is redesigned using NURBS. In the second, a poster about the product of TREx and the research is designed and drawn. Third, NURBS is used in a package design of a Chinese wine product. The last case, a poster for an international conference, is designed and drawn by NURBS.

5.5.1. The redesign of the casing of TREx

As noted earlier, TREx (Turbo Range Extender)¹ is a recent radical design of

¹ TREx is a revolution in engine design. It is registered in international patent PCT. The development of the TREx has been funded by Innovate UK projects 104021 and 72086, Department for Transport T-TRIG project 2020.

the gas turbine. It can be used for electric vehicles to eliminate range concerns, and for drones with up to 100 kg payload and 2-hour flight time capability. The new design decouples the constraint between the compressor and combustion chamber and enables a compact size. It also improves combustion efficiency and reduces internal loss. Its advanced air bearing system brings out the benefits of fast response, high power output, a 30% improvement in compression ratio, long lifespan, and low maintenance. The radical and compact design enables the engine to be contained in a space as small as a spare tyre. The design is optimised with NURBS and computational fluid dynamics for enhanced airflow efficiency in the casing, the inlet/outlet air ducts, and the turbine wheel. The new configuration has been proven a success in fire tests.

As a part that can leave an important impression, the casing of TREx is redesigned with NURBS. The design of the casing needs to satisfy not only the technical characteristics and main functions of TREx but also the general aesthetic. First, the overall shape is curvy instead of right-angled or anything with sharp edges, because TREx is an environmentally friendly engine product and curves tend to convey a sense of more geniality and smoothness to people. The main shape of the new casing is drawn with NURBS. Due to the rigidity of

NURBS, the shape made of NURBS can provide a strong but soft profile. There are some links between the main function of TREx and the features on the casing. For example, the two concave structural changes represent that TREx is a product related to fluid flow and mechanics. The materials in rendering are Aluminum alloy (the upper half) and stainless steel (the lower half) because the temperatures of airflow are different at the inlet and outlet air ducts. Considering assembly, more details need to be further designed. For example, the docking of the upper and lower parts and the number and position of bolts. The main colours are silver and Prussian Blue - a famous pigment that was synthesised for the first time in Berlin in the early 1700s - to reflect its sense of technology and metal texture.¹⁷⁷ The sketches are drawn with Photoshop using the pen tablets (Wacom Intuos Pro M). The model is built in UG-NX and rendered in Keyshot (10.0 version) (see Figures. 5-27 to 5-32).



Figure 5-27. From the main view of the new casing of TREx, the inlet air duct, the upper and lower half of the main body, the concave structures and the bolts for assembling can be found. The outlet air duct is not shown due to the angle of the view.



Figure 5-28. The image of the front display



Figure 5-29. The image of the top display

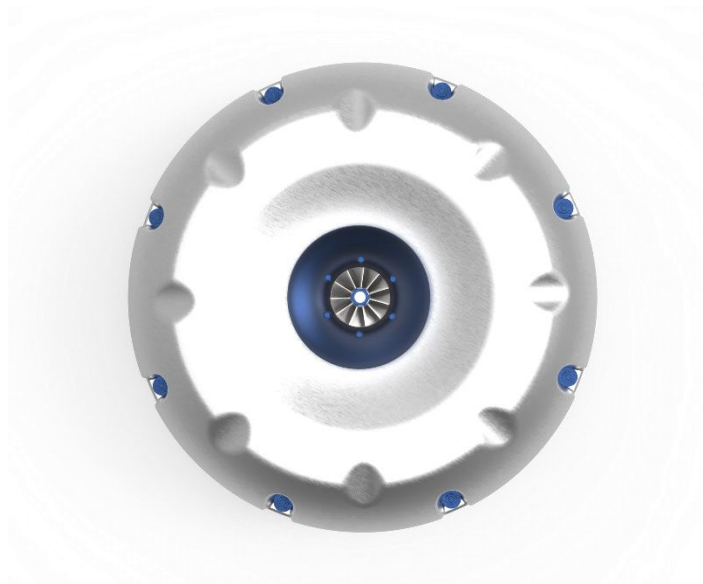


Figure 5-30. The image of the bottom display



Figure 5-31. The inlet air duct, the main body of the casing and the outlet air duct are shown in this image.



Figure 5-32. The image of the status of use

The overall appearance is rounded to match the internal structure of this new turbocharged engine. The curve on the side of the casing is drawn with NURBS to meet the requirements of both the function - a compact design - and

aesthetics. On the upper half of the casing, two scalloped concave feature surfaces that are axisymmetric with each other can be seen. These two characteristics are created using product semantics to reflect the technical characteristics of the engine and high work efficiency.

5.5.2. A poster design about TREx

The posters about TREx (Note-1) were designed and drawn for an international conference. In the posters, NURBS is used in the combination between the profile of TREx and the features of the leaves of the lotus. The high continuity of NURBS (cubic NURBS or other NURBS with higher order) makes curves visually smooth. So, it can be utilised in some elements representing something gentle, friendly or soft. The plants are parts of nature and are environmentally friendly. The lotus is a plant and generally means *clean* due to the fact that such clean, pure colours grow in the mud. The NURBS curves are drawn in UG-NX first and then illustrated in Photoshop. The posters are a series of designs which includes three pages (see Figures 5-33 to 5-35).

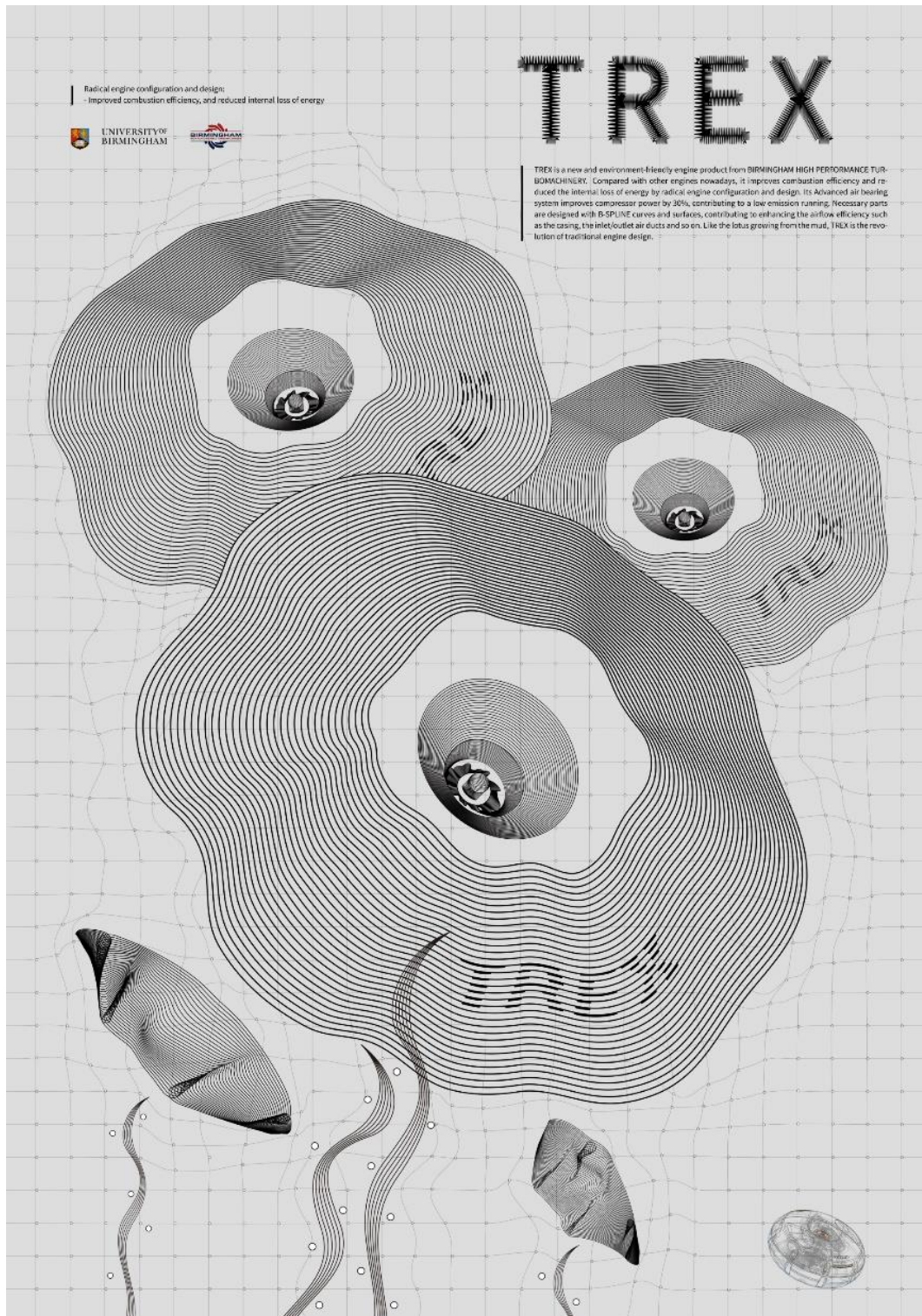


Figure 5-33. Page one of the designs of TREX posters



Figure 5-34. Page two of the designs of TREX posters

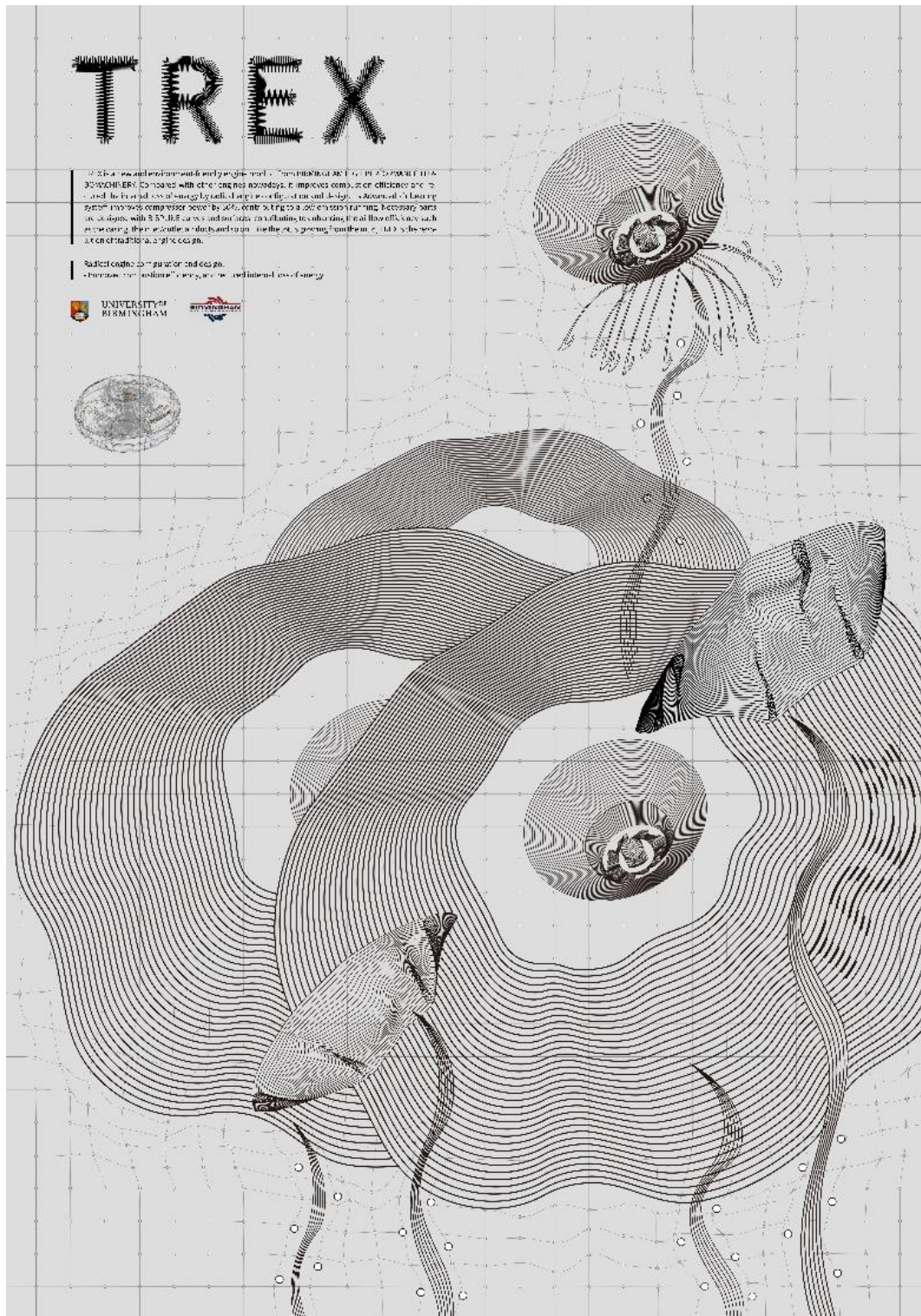


Figure 5-35. Page three of the designs of TReX posters.

The poster illustrates a new generation turbine engine product and the applications of NURBS and computational fluid dynamics. Compared with other engines nowadays, TREx, the environment-friendly engine, improves combustion efficiency and reduces the internal loss of energy by radical engine configuration and design. Like the lotus growing in the pond, TREx is the revolution of traditional engine design.

5.6. Results

5.6.1. NURBS and CFD in pipe design

From the results, it can be found that the efficiency decreases when the length of the pipe increases, the efficiency rises when the diameter increases, and the efficiency don't change much as the angle increases. Among them, the most efficient simulation result is 94.78%. The conditions are:

MODEL SIZE: Length=500mm; $\angle=90^\circ$; Diameter=190mm

Boundary Conditions

Inlet: Total Pressure (Stable) =2 bar

Outlet: Static Pressure=1 bar

Efficiency: 94.78%

Furthermore, the analysis in pipe design shows a potential application of NURBS. The working efficiency of the pipe changes significantly when the length of the sides or the diameter of the inlet and outlet change. The changes are likely to be visually linear. It is normal for the working efficiency to reduce while the length increases, as the longer the pipe, the more energy loss will occur. Also, if the total pressure at the inlet is fixed, the larger the diameter of the inlet and outlet, the higher the working efficiency. These results are not unique, only to be found in pipes made of NURBS. The change also commonly exists in most pipes from the market. However, the difference is that the working efficiency does not change significantly when the angle changes from 70° to 110° . The working efficiency hovers at 88%, which is the peak of its efficiency. The change is so insignificant that it can even be ignored. However, it also means that the change of angle (in a range of differences) does not affect the working efficiency much in the pipes which have a shape made of NURBS. This means that using pipes with NURBS curves reduces energy loss during transmission.

5.6.2. NURBS, CFD, and the design of industrial product components

In the previous design of the inlet air duct, the fluid is shown to be not very smooth as indicated by the colour of the total pressure changes near the bottom of the inlet air duct. In other words, the total pressure changes significantly when the air goes through the neck. That means the air cannot flow smoothly along the shape of the inlet duct.

Compared with the previous design, it is clear that the total pressure does not change significantly in the optimised design. That means the airflow in the new design of the inlet duct is smoother than that of the previous one.

5.6.3. A guide to the sedan design

Based on the room limitation and the general structure of a sedan, the profile of the sedan is drawn by a rounded-corner design, the quadratic NURBS, cubic NURBS, quartic NURBS and quintic NURBS. The velocity of airflow and the total pressure around the sedan are shown in the simulation results. The

difference in the results is visible. The drag can be calculated in Ansys Workbench.

The results show that outer coverings made of quadratic and cubic NURBS can ensure the basic design requirements. More specifically, cubic NURBS not only fulfil the basic requirements, but are also more aesthetically pleasing. Next, the running states of the sedan with different outlines are simulated using CFD. It is found that the outline fitted by cubic NURBS can reduce the drag on the sedan by over 20% more than that of a rounded design and fast cars need high-order smoothness, and high-order NURBS have the required property.

5.6.4. The other cases of design using the application of NURBS

The casing of TREx is redesigned using NURBS in this section. The profile of the redesigned casing meets the requirements of the function and general aesthetics. The casing is manufactured, and the main material is aluminium alloy. In post-processing, the surface is oxidized to make it more industrial and advanced (see Figure. 5-36 and 5-37).



Figure 5-36. The assembled casing



Figure 5-37. The inlet air duct (left) and outlet air duct (right)

Three posters about TREx are designed and drawn using NURBS. The series design is designed from the characteristics of environmental protection and higher performance. The combination of the lotus and the profile of TREx represents its environmental friendliness and low-carbon emissions. The designs are submitted for the A' Design Award -a popular and high-level international design competition - and won a Silver Winner of A' Design Award

5.7. Conclusions, extensions, and implications

This part of the study has tested and proved the advantages of NURBS in engineering and design. The difference between the two areas is that CFD is only used in engineering projects for testing efficiency. The design targets visualisation and does not need large amounts of scientific analysis to support it. But the study of the rigidity of NURBS can be utilised in design directly.

The combination of NURBS and CFD provides a potential application in pipe design, resulting in a stable working efficacy even though the range of angle change is up to 40° (70° to 110°). The application is potential because the method has its limitation. First, the angle changes from 0° to 70° and 110° to 180° have not been tested and simulated. For pipe design, only two sorts of structures are used, which are the straight ones and the curvy ones at the corners. These two ranges of angle change had not been involved in the study because the angle would be too small or too large for practical use. So long as the angle of the corner is not too small or too big, the range of angle change could be widened further.

NURBS simplified the redesign of the inlet air duct, and the effect is tested by CFD. The duct is an industrial component with a simple structure. So, it is not too difficult to change the shape of the duct and find the best solution. However, it can be simple to find a better shape which meets the requirements of function and general aesthetics using NURBS. The optimal solution is then found through CFD and fine-tuning of the control points, following the result of the simulation. Even though NURBS has been used in 3D modelling for over ten years, especially in product design, a convenient guide using NURBS can still save time for designers.

Furthermore, with NURBS, the early stage of car design can also be simplified. Nowadays, designers use their experience, imagination, and older products to design new ones. For example, streamlines are used in the appearance design of most sedans. But it will speed up the whole design process if designers can follow a reliable rule in sketching or other early stages of design. The utilisation of NURBS provided in this chapter gives designers a model when they are creating a new appearance for a car or sedan. Surely, this is not limited to vehicle design, but applies to any object moving at high speed in space and fluid, including aircraft, submarines and space vehicles. Locating the key points

(the control points), designers can draw one cubic NURBS as the overall profile of the product, ensuring that the outline meets the functional requirements. The parts or components on the casing can then be designed, following the NURBS shape.

The redesign of the TREx casing and the poster about TREx provide more possibilities for NURBS to be used in product and visual design. Here the casing of TREx is a sort of product, and unlike the inside parts, such products always have a visual impact. The issue is that the appearance of a product will often not be given the serious consideration that it deserves in the early stage of design. That is because designers do not have good design guidelines in shape drawing. A better shape has to be picked out from many sketches. It is not bad to draw more sketches, it can diverge the designer's thinking. However, sketching with a good guide can make a satisfactory solution emerge more quickly. The rigidity of NURBS can be used in sketching and makes the curve meets scientific explanation and aesthetics at the same time. This means that in product design, the curves can simultaneously look powerful, strong, balanced and smooth using the rigidity of NURBS. The design of the posters also shows that NURBS can benefit the visual design. The higher order of NURBSs - higher than quadratic NURBS - make the curves smoother due to

the higher continuities. More designs won a prize in popular international competitions and those have been listed in the Appendix. The approval of the design by experts proves that the application of NURBS in visual design is feasible.

The study concludes that, being tested with CFD, NURBS can provide streamlined curves and easily meet the functional requirements. Also, NURBS can benefit visual design because of its rigidity. The combination of NURBS and CFD is a new guideline for designers. Although there are similar tools in Photoshop, Illustrator and other 2D image editing software and the curvature of the drawn curve are easy to control. However, the guidelines for curve change can make the curve be edited freely and follow to specific scientific basis at the same time. Then the working efficiency of the design can be enhanced, and time can be saved.

CHAPTER 6. CONCLUSIONS AND FUTURE WORK

6.1. Introduction

This chapter presents the conclusions from this study; followed by the novel contributions of this PhD research. Suggestions for future research projects are given in the last section.

6.2. Conclusions

The overall aims of this research were to explore the utilisations of engineering solid mechanics and CFD in art, engineering and design. The main conclusions of this study are listed below:

- 1) The application of CFD in the analysis of Raphael and Ingres' paintings provides a reliable approach to artistic design and art creation. The study delivers that in art or artistic design, people do not have to find a real existing object as a fluid container and use a camera or other photography device to record the fluid flows. Today, even though cameras can help people during drawing and painting, still not every

object and scene can be photographed, especially considering fluid flows. Undeniably, Artificial Intelligence (AI) starts to play a dramatic role in generating images with simple descriptions. However, the limitation and similarities of AI cannot be ignored. So, the combination of CAD and CFD simulation can be seen as a practical and feasible way to change the scene of fluid flow from the imagination into a reality.

2) The engineering solid mechanics can be used in Chinese calligraphy. In this part of the study, NURBS and beam bending were connected, and the feasibility of the utilisation of engineering solid mechanics in calligraphy was explained. The relationship between the cubic NURBS curve and the five different beam bending functions was represented, resulting in a dimensionless quantity which describes the rigidity of NURBS. The fundamental strokes in Huizong's calligraphy artworks were fitted by cubic NURBSs and analysed. The results also suggest that Huizong's strokes, perhaps, meet the laws of nature and scientifically regular patterns.

3) The engineering solid mechanics can be used in Chinese calligraphy. In this part of the study, NURBS and beam bending were connected, and the feasibility of the utilisation of engineering solid mechanics in

calligraphy was explained. The relationship between the cubic NURBS curve and the five different beam bending functions was represented, resulting in a dimensionless quantity which describes the rigidity of NURBS. The fundamental strokes in Huizong's calligraphy artworks were fitted by cubic NURBSs and analysed, with the result, again, that Huizong's strokes could be said to meet the laws of nature and scientifically regular patterns.

- 4) CFD and NURBS can be used in different fields and design tasks. In the pipe design, the application of NURBS and CFD provides a potential approach to keeping stable work efficiency. From the case of the inlet air duct, the combination of NURBS and CFD benefits the design of simple industrial product components. The study in this part presented a scientific analysis of the fluid dynamics and aesthetic rules of NURBS in sedan design. Then two designs relevant to TREx, both highly praised by experts from the same area.

6.3. Summary of novel contributions to knowledge

The novel contributions of this PhD research can be listed as follows:

-
- 1) The study in Chapter 3 provides infinite possibilities for the artist's creation. It is the first time CFD and NURBS are used to explore the research of Raphael and Ingres. In the future, more and more CAD tools can be applied to combine CFD in arts. Technically, every scene of fluid flow can be verified if the painting or drawing is in the classic style. Then both the accuracy and the inaccuracy can be found and shown visually.
 - 2) Through the link between NURBS and beam bending, it is the first time the rigidity of NURBS is explained mathematically. The analysis in Huizong's calligraphy shows that the rigidity of NURBS can be used in the art of Chinese calligraphy to analyse the strokes, to understand, learn and create.
 - 3) There is a potential application in pipe design, resulting in a stable working efficacy even though the range of angle change is up to 40° (70° to 110°). That means the fault tolerance or the design flexibility for the pipe-like structure is enhanced.
 - 4) It has also been found that the outline fitted by cubic NURBS can reduce the drag on the sedan by over 20% more than that of a rounded design. The results show that the overall profile of a product with a high-moving speed requirement can be designed with cubic or higher-order NURBSs during the stage of sketching for a larger drag reduction.
 - 5) The cubic or a higher order NURBS can easily draw a smooth streamline in product design and graphic creation. For example, if the concept of a

product or a part of that is friendly, soft, gentle, flexible or high-tech, then the profile design it will very likely benefit from NURBS. The challenge of this might be how to locate the control points more efficient.

6.4. Proposal for future work

It is proposed that the future development of research from this study could include one of the following topics:

- 1) Explore potential applications of CFD and NURBS in arts.

The combination-utilisation of NURBS and CFD could have great potential for art appreciation. For example, the accuracy of any scene of fluid flow from classic or Neoclassical paintings can be analysed using the method. Also, many artworks such as *Susanna at Her Bath* by Han Liu can be created with high accuracy.

- 2) Explore potential applications of the rigidity of NURBS in the teaching and learning of the calligraphy.

More potential utilisations of the rigidity of NURBS can be utilised in the study of Chinese calligraphy. For example, not only Huizong's *Shou Jin Ti*,

but also other styles of handwriting such as *Li Shu* and *Kai Ti* in Chinese calligraphy can be analysed with the theory in Chapter 4. In addition, because it is one piece of evidence to prove Huizong's masterly skill in calligraphy, the rigidity of NURBS can be used in teaching people how to draw a strong but slim stroke.

3) Further integration of the codes for curve drawing.

In this study, the integration of the code in Chapter 4 can be used in drawing a beam-like curve. That means the code that links beam bending and cubic NURBS provides an approach to drawing a curve which looks natural and meets the scientific basis. After an integration, everyone can use the code easily for drawing the curves.

4) Further specific analysis of CFD in design with NURBS.

In the pipe design, the effect of angle change with a NURBS shape can be further analysed. A more accurate range of the angle change can be verified.

APPENDIX

1. The code in the analysis of approximation of Cantilever beam with NURBS

```
function [curve_cords] = draw_cubic_spline(xy,N)

% Draw cubic spline based on control points

% Must have at least 4 sets of control points

% Draw each segment based on 4 sets of control points, 1-4, 2-5, 3-6
etc..

if length(xy)<4

    fprintf('Less than 4 points!');

    return

end

A=[-1 3 -3 1;3 -6 3 0;-3 0 3 0;1 4 1 0]/6;

curve_cords = zeros(N*(length(xy)-3)+1,2);

% Starting point of curve, use t=0 and first 4 points

curve_cords(1,:) = [0 0 0 1]*A*xy(1:4,:);

% The coordinates of each curve as t goes from 0 to 1 in eash
```

```

segment.

    for i = 1:length(xy)-3

        points=xy(i:i+3,:);

        for t = 1:N

            curve_cords(t+(i-1)*N+1,:)=[(t/N)^3 (t/N)^2 (t/N)

1]*A*points;

            end

        end

    end

end

```

The elastic curve connecting

```

clear;

clc;

%% Define beam values

L = 1000;           % the length of the beam, unit in mm

E = 2060*100000;   % Youngs modulus, unit in N/mm^2

I = 160000/12;     % the moment of Inertia, unit mm^4

% define load value

P = 200;           % the force load on the beam, unit in N

```

```

user_is_artist = true;      % True if the user is an artist who knows
nothing about physics and only set the location of the tip

                                % False if the user knows beam load

physcis

if user_is_artist

    D = 50;                    % Maximum deflection at the tip (L,-D),
determined by artist

    A = D/2;

else

    A = P*L^3/(6*E*I);

    D = P*L^3/(3*E*I);        % Maximum deflection, determined by
physical parameters

end

% t goes from 0 to 1. We draw 100 equally spaced points on the beam.

t = zeros(101,1);

for i = 0:100

    t(i+1) = i/100;

end

```

```

%% Theoretical deflection

x = t*L;          % x coordinates of points on the beam

with load

y = A*(t.^3-3*t.^2); % y coordinates of points (deflection at
x) on the beam with load , based on theoretical solution Eq. (6)

%% Plot the theoretical curve and set figure options

figure(1);

clf;

plot(x,y);

grid on;

%% Select the four points that define the spline curve

N=50;          % Number of points on the spline curve

xs=[-1 0 1 2]*L; % x coordinates of the four points

ys=A*[-2 1 -2 -5]; % y coordinates of the four points

xy=[xs;ys]';

%% Calculate the spline curve defined by the four points

%Control point matrix is n-by-2, [x0 y0; x1 y1; x2 y2; ...]

```

```

%N is the number of points per segment, the greater N is the smoother
the plotted line is

spline_curve_cords = draw_cubic_spline(xy,N);

%% Plot the four points and the spline curve

hold on

plot(xs,ys,'bs');

plot(spline_curve_cords(:,1),spline_curve_cords(:,2),'r+')

legend('Theoretical','Control points','Cubic spline fitting')

```

2. The code in the analysis of cantilever beam of Case 2&6 and NURBS

```

%% Theoretical solution

x_t = (0:0.01:1)';

A = -0.5;

y_t = zeros(length(x_t),1);

for i = 1:length(x_t)

    y_t(i) = A*(x_t(i)^4-4*x_t(i)^3+6*x_t(i)^2);

```

```

end

y_t = y_t(:);

%% Optimization with uniform weight (no weight)

% For this case we need to choose two points in addition to the two
endpoints, let p(1),p(2) be x-cords for the two points, and p(3),p(4)
be y-cords

% The two endpoints are (0,0) and (1,-3A), so the x-cords of the
four control points are [0,p(1),p(2),1] and y-cords are
[0,p(3),p(4),-3A], here y_t(end)=-3A

% Define error function, see comments in "curve_nurb_fit.m" file,
here

% value fun wraps curve_nurb_fit function, assembling p and other
fixed parameters

valuefun=@(p) (curve_nurb_fit([0 p(1) p(2) 1],[0 p(3) p(4)
y_t(end)],x_t,y_t,[1 1 1 1]));

% Set optimization option

optionscon = optimoptions(@fmincon,'Algorithm','interior-
point','Display','iter');

% Set initial two points to (0.25,y_t(end)*0.25) and

```

```

(0.75,y_t(end)*0.75) and run the optimization

[p,fval_no]=fmincon(valuefun,[0.25 0.75 y_t(end)*0.25
y_t(end)*0.75],[[],[],[],[],[],[0 0 y_t(end) y_t(end)],[1 1 0
0],[[],optionscon)];

% Print result

fprintf('\nFitted result (no weight):');

for i = 1:length(p)

    fprintf('\t%.3f',p(i));

end

fprintf('\t at error: %.7f\n',fval_no);

% Store the y cords of the fitted NURB curve. x-cords are the same as
theoretical

fitted_y_noweight = curve_nurb_fit_result([0 p(1) p(2) 1],[0 p(3)
p(4) y_t(end)],x_t,[1 1 1 1]);

%% Optimization with different weights, the p(1),p(2) are x-cords for
the two points, and p(3),p(4) are y-cords for the two points, p(5),
p(6) are their weights

valuefun=@(p)(curve_nurb_fit([0 p(1) p(2) 1],[0 p(3) p(4)
y_t(end)],x_t,y_t,[1 p(5) p(6) 1]));

```

```

[pw,fval]=fmincon(valuefun,[0.25 0.75 y_t(end)*0.25 y_t(end)*0.75 1
1],[[],[],[],[],[],[0 0 y_t(end) y_t(end) 0.5 0.5],[1 1 0 0 1.5
1.5],[[],optionscon)];

fprintf('\nFitted result (w/ weight):');

for i = 1:length(pw)

    fprintf('\t%.3f',pw(i));

end

fprintf('\t at error: %.7f\n',fval);

fitted_y_weight = curve_nurb_fit_result([0 pw(1) pw(2) 1],[0 pw(3)
pw(4) y_t(end)],x_t,[1 pw(5) pw(6) 1]);

%% Plot the theoretical, NURB without weight, NURB with weight, and
control points for NURB with weight

figure(1)

clf;

plot(x_t,y_t,'b-

',x_t,fitted_y_noweight,'gv',x_t,fitted_y_weight,'r^',[0 p(1) p(2)
1],[0 p(3) p(4) y_t(end)],'b*')

hold on

```

```
legend('Theoretical', ['NURB w/o weight with error: '
num2str(fval_no)], ['NURB w/ weight with error: '
num2str(fval)], 'Control points (w/weight)', 'Location', 'best')
```

3. The code in the analysis of simply supported beam of Case 4 and NURBS

```
clear;

clc;

x_t = (0:0.01:1)';

A = 1;

y_t = zeros(length(x_t),1);

for i = 1:ceil(length(x_t)/2)

    y_t(i) = A*(4*x_t(i)^3-3*x_t(i));

end

for i = ceil(length(x_t)/2):length(x_t)

    y_t(i) = A*(-4*x_t(i)^3+12*x_t(i)^2-9*x_t(i)+1);

end

y_t = y_t(:);
```

```

% x=[0 0.25 0.75 1];

% y=[0 -1 -1 0];

valuefun=@(x) (curve_nurb_fit([0 x(1) 1-x(1) 1],[0 x(2) x(2)
0],x_t,y_t,[1 x(3) x(3) 1]));

optionscon = optimoptions(@fmincon,'Algorithm','interior-
point','Display','iter');

[x,fval_no]=fmincon(valuefun,[0.25 -1 1],[[],[],[],[],[0 -1.5*A
0.99999],[1 0 1.00001],[],optionscon);

fprintf('\nFitted result (no weight):');

for i = 1:length(x)

    fprintf('\t%.3f',x(i));

end

fprintf('\t at error: %.7f\n',fval_no);

fitted_y_noweight = curve_nurb_fit_result([0 x(1) 1-x(1) 1],[0 x(2)
x(2) 0],x_t,[1 x(3) x(3) 1]);

[x,fval]=fmincon(valuefun,[0.25 -1 1],[[],[],[],[],[0 -1.5*A 0.9],[1 0
1.1],[],optionscon);

fprintf('\nFitted result (w/ weight):');

```

```

for i = 1:length(x)

    fprintf('\t%.3f',x(i));

end

fprintf('\t at error: %.7f\n',fval);

fitted_y_weight = curve_nurb_fit_result([0 x(1) 1-x(1) 1],[0 x(2)
x(2) 0],x_t,[1 x(3) x(3) 1]);

figure(1)

clf;

plot(x_t,y_t,'b-
',x_t,fitted_y_noweight,'gv',x_t,fitted_y_weight,'r^',[0 x(1) 1-x(1)
1],[0 x(2) x(2) 0],'b*')

hold on

legend('Theoretical',[ 'NURB w/o weight with error: '
num2str(fval_no)],[ 'NURB w/ weight with error: '
num2str(fval)], 'Control points (w/weight)', 'Location', 'best')

```

4. The code in the analysis of the rigidity of strokes in Huizong's Shou Jin Ti

```
clear;

clc;

%% All equations are substituted with  $x'=x/L, y'=y/L$  so that  $x\_points$ 
is always from 0 to 1.

x_points = 0:0.01:1;

%%  $y\_points$  are determined in each case, choose a case number, modify
end_point_y as needed. Case 5 is not complete yet.

beam_case = 1;

switch beam_case

    case 1

        end_point_y = -0.05; %% at  $x'=1$ , we have  $PL^2/(6EI)*(-2) =$ 

end_point_y

        y_points = -0.5*end_point_y*(x_points.^3-3*x_points.^2);

    case 2

        end_point_y = -0.05; %% at  $x'=1$ , we have  $-wL^3/(24EI)*3 =$ 
```

```

end_point_y

    y_points = end_point_y/3*(x_points.^4-
4*x_points.^3+6*x_points.^2);

    case 3

        end_point_y = -0.05; %% at x'=1, we have -ML/(2EI)*1 =

end_point_y

    y_points = end_point_y*(x_points.^2);

    case 4

        end_point_y = -0.05; %% at x'=1/2, we have PL^2/(48EI)*(-1) =

end_point_y

    y_points = -end_point_y*(4*x_points.^3-3*x_points);

    for i = ceil(length(x_points)/2):length(x_points)

        y_points(i) = y_points(length(x_points)+1-i);

    end

    case 5

        y_points = x_points*0;

    case 6

        end_point_y = -0.05; %% at x'=1/2, we have -w/(24EI)*(5/16) =

end_point_y

    y_points = end_point_y*16/5*(x_points.^4-

```

```

2*x_points.^3+x_points);

    case 7

        end_point_y = 0.05; %% at x'=1/sqrt(3), we have -ML/(6EI)*(-
2/(3*sqrt(3)))=end_point_y

        y_points = end_point_y*(-3*sqrt(3)/2)*(x_points.^3-x_points);

    end

%% Plot a figure with the axis shown and an equal axis

figure(1)

plot(x_points,y_points,'b-');

axis equal

%% Plot and save a figure without an axis for comparison with
handwritings

figure(2)

plot(x_points,y_points,'b-');

axis equal

axis off

print('curve_example','-dpng','-r300')

```

REFERENCES

- ¹ Silva M N, Marques M M, Teixeira P J. Testing theory in practice: The example of self-determination theory-based interventions[J]. *European Health Psychologist*, 2014, 16(5): 171-180. 171
- ² Ede S. *Art and science*[M]. Bloomsbury Publishing, 2012. 26
- ³ Neer R. *The emergence of the classical style in Greek sculpture*[M]//*The Emergence of the Classical Style in Greek Sculpture*. University of Chicago Press, 2010. 150
- ⁴ Ede S. *Art and science*[M]. Bloomsbury Publishing, 2012. 26-29
- ⁵ Kemp M. *The science of art: Optical themes in western art from Brunelleschi to Seurat*[J]. 1990.
- ⁶ Yang H M, Lu J J, Lee H J. A Bezier curve-based approach to shape description for Chinese calligraphy characters[C]//*Proceedings of sixth international conference on document analysis and recognition*. IEEE, 2001: 276-280.
- ⁷ Loncaric S. A survey of shape analysis techniques[J]. *Pattern recognition*, 1998, 31(8): 983-1001.
- ⁸ Angel E. *Interactive Computer Graphics: A top-down approach with OpenGL*[M]. Addison-Wesley Longman Publishing Co., Inc., 1996.
- ⁹ Strosberg E. *Art and science*[M]. WW Norton, 2013.
- ¹⁰ Buchanan R. Wicked problems in design thinking[J]. *Design issues*, 1992, 8(2): 5-21.
- ¹¹ Bates J. *Virtual reality, art, and entertainment*[J]. *Presence: Teleoperators & Virtual Environments*, 1992, 1(1): 133-138.
- ¹² Li W. *Chinese writing and calligraphy*[M]. University of Hawaii Press, 2010. 19
- ¹³ Martin Kemp. (1998). *Kemp's conclusions*. Nature Publishing Group. *Nature* vol. 392 iss. 6679.

875. DOI: 10.1038/31829

¹⁴ Irene Plonczak and Susan Goetz Zwirn, "Understanding the Art in Science and the Science in Art through Crosscutting Concepts," *Science Scope* 38, no.7 (2015): 58.

¹⁵ Bruce Cole and Adelheid M. Gealt, *Art of the Western World: From Ancient Greece to Post Modernism* (New York: Simon and Schuster, 1991), 100.

¹⁶ Cole and Gealt, *Art of the Western World*, 15.

¹⁷ Art and Anatomy in Renaissance Italy. Bernard Schulz

¹⁸ Domenico Laurenza. *Art and Anatomy in Renaissance Italy: Images from a Scientific Revolution* (2012, Metropolitan Museum of Art)

¹⁹ Clive Ashwin. *Encyclopaedia of Drawing: Materials, Technique and Style*, (London: B.T. Batsford, 1982), 15.

²⁰ Clive Ashwin. *Encyclopaedia of Drawing: Materials, Technique and Style*, (London: B.T. Batsford, 1982), 22.

²¹ Martin Kemp, *The Science of Art: Optical Themes in Western Art from Brunelleschi to Seurat*. (London: Yale University Press, 1990), 9.

²² Martin Kemp, "Leonardo Da Vinci's Laboratory: Studies in Flow," *Nature* 571 (2019): 322, <https://doi.org/10.1038/d41586-019-02144-z>.

²³ Ginn S R, Lorusso L. *Brain, mind, and body: interactions with art in renaissance Italy*[J]. *Journal of the History of the Neurosciences*, 2008, 17(3): 295-313. 308

²⁴ Sheldon Peck, Leena Peck. (1995). *Selected Aspects of the Art and Science of Facial Esthetics. Seminars in Orthodontics, Vol I, No 2 (June), 1995: pp 105-126. P. 112*

²⁵ Panofsky E. *Galileo as a critic of the arts: Aesthetic attitude and scientific thought*[J]. *Isis*, 1956, 47(1): 3-15. 3

²⁶ Heilbron, J. L. (2012 June 26). *Book Review Renaissance and Reformation. Between Raphael and*

Galileo. Mutio Oddi and the Mathematical Culture of Late Renaissance Italy. Annals of Science vol. 71 iss. 1. P 140. DOI: 10.1080/00033790.2011.653584

²⁷ *Wendy Leeks. (1986). Ingres Other-Wise. Oxford Art Journal, Vol. 9, No. 1 (1986), Oxford University Press. P. 32. Stable URL: <https://www.jstor.org/stable/1360370>*

²⁸ *Werner, Alfred. 2020. "Monsieur Ingres- Magnificent t ' Reactionary " 26 (4): 491–500. 497.*

²⁹ *Etro, Federico, Silvia Marchesi, and Elena Stepanova. 2020. "Liberalizing Art. Evidence on the Impressionists at the End of the Paris Salon." European Journal of Political Economy 62 (February): 101857. <https://doi.org/10.1016/j.ejpoleco.2020.101857>. 3*

³⁰ *Strobel H A. Reflections: Personal Essays[M]. Henry Strobel Publisher, 1999. 62*

³¹ *Baker C H C. Reflections on the Ingres Exhibition[J]. The Burlington Magazine for Connoisseurs, 1921: 36-42. 36-37*

³² *Leeks W. Ingres Other-Wise[J]. Oxford Art Journal, 1986, 9(1): 29-37.*

³³ *Bear, Greg. 2004. "Science in Culture." Nature 430 (6996): 147–147. <https://doi.org/10.1038/430147a>.*

³⁴ *Cynthia M. Pyle. The Art and Science of Renaissance Natural History. P.265.*

³⁵ *Xia B, Sun D W. Applications of computational fluid dynamics (CFD) in the food industry: a review[J]. Computers and electronics in agriculture, 2002, 34(1-3): 5-24. 5*

³⁶ *Moin P, Kim J. Tackling turbulence with supercomputers[J]. Scientific American, 1997, 276(1): 62-68.*

³⁷ *Schaldach G, Berger L, Razilov I, et al. Computer simulation for fundamental studies and optimisation of ICP spray chambers[J]. ISAS (Institute of Spectrochemistry and Applied Spectroscopy) Current Research Reports, Berlin, Germany, 2000.*

³⁸ *Mills D. Development and validation of a preliminary model for optimisation of baking ovens[J]. The Food and Packaging Cooperative Research Centre Annual Report (1998-1999), Australia, 1998.*

-
-
- ³⁹ Wilcox D C. *Turbulence modeling for CFD*[M]. La Canada, CA: DCW industries, 1998. 53-58
- ⁴⁰ Slotnick J P, Khodadoust A, Alonso J, et al. *CFD vision 2030 study: a path to revolutionary computational aerosciences*[R]. 2014. 1.37.
- ⁴¹ Yu Y, Pu G, Jiang T, et al. *Discontinuous grooves in thrust air bearings designed with CAPSO algorithm*[J]. *International Journal of Mechanical Sciences*, 2020, 165: 105197.
- ⁴² Han Y, Zhang X, Liu H, et al. *Structural design, numerical examination and experimental approach of the multi-powder mixer for directed energy deposition*[J]. *Powder Technology*, 2022, 398: 117144.
- ⁴³ Kumar A. *Numerical investigation of secondary flows in helical heat exchangers*[C]//Institute of Food Technologists Annual Meeting. Anaheim, CA, USA. 1995: 148.
- ⁴⁴ Norton T, Sun D W. *Computational fluid dynamics (CFD)—an effective and efficient design and analysis tool for the food industry: a review*[J]. *Trends in Food Science & Technology*, 2006, 17(11): 600-620.
- ⁴⁵ Martin Kemp, "Leonardo Da Vinci's Laboratory: Studies in Flow," *Nature* 571 (2019): 323, <https://doi.org/10.1038/d41586-019-02144-z>.
- ⁴⁶ Carola S. König, "Correlations between Art and CFD through Colour and Shape," *Optics and Laser Technology* 43, no. 2 (2011): 354, <https://doi.org/10.1016/j.optlastec.2009.08.022>.
- ⁴⁷ König, Carola S. 2011. "Correlations between Art and CFD through Colour and Shape." *Optics and Laser Technology* 43 (2): 348–57. <https://doi.org/10.1016/j.optlastec.2009.08.022>.
- ⁴⁸ Han Liu, Vincent van Bever Donker and Kyle Jiang. (June 2020). A SCIENTIFIC STUDY OF JEAN AUGUSTE DOMINIQUE INGRES' LA SOURCE. AMPS PROCEEDINGS SERIES 20.2. ISSN 2398-9467. P 223-234. <http://architecturemp.com/wp-content/uploads/2021/03/Amps-Proceedings-Series-20.2.pdf>
- ⁴⁹ Hoang M L, Verboven P, De Baerdemaeker J, et al. *Analysis of the air flow in a cold store by means of computational fluid dynamics*[J]. *International Journal of Refrigeration*, 2000, 23(2): 127-140.

-
-
- ⁵⁰ Verboven P, Scheerlinck N, De Baerdemaeker J, et al. Computational fluid dynamics modelling and validation of the temperature distribution in a forced convection oven[J]. *Journal of food engineering*, 2000, 43(2): 61-73.
- ⁵¹ Kondjoyan A, Daudin J D. Optimisation of air-flow conditions during the chilling and storage of carcasses and meat products[J]. *Journal of food engineering*, 1997, 34(3): 243-258.
- ⁵² Jiang T, Jiang K. Numerical analysis of a hydrodynamic air bearing with electromagnetic assistance[J]. *Proceedings of the Institution of Mechanical Engineers, Part J: Journal of Engineering Tribology*, 2022: 13506501221100617.
- ⁵³ Shigley J E. *Shigley's mechanical engineering design [M]*. Tata McGraw-Hill Education, 2011. 5-6
- ⁵⁴ Groover M, Zimmers E. *CAD/CAM: computer-aided design and manufacturing[M]*. Pearson Education, 1983. 58
- ⁵⁵ Shigley J E. *Shigley's mechanical engineering design [M]*. Tata McGraw-Hill Education, 2011. 4
- ⁵⁶ Myers W. Interactive Computer Graphics: Flying High-Part I[J]. *Computer*, 1979, 12(07): 8-17.
- ⁵⁷ Groover M, Zimmers E. *CAD/CAM: computer-aided design and manufacturing[M]*. Pearson Education, 1983. 59
- ⁵⁸ Groover M, Zimmers E. *CAD/CAM: computer-aided design and manufacturing[M]*. Pearson Education, 1983. 57-64
- ⁵⁹ Brown P. CAD: Do computers aid the design process after all? [J]. *Intersect: The Stanford Journal of Science, Technology, and Society*, 2009, 2(1): 52-66.
- ⁶⁰ Valdez-Tullett, Joana. 2019. "An Integrated Methodology for the Study of Atlantic Rock Art." *Quaternary International*, no. April: 0-1. <https://doi.org/10.1016/j.quaint.2019.10.006>.
- ⁶¹ Ontañón, Roberto, Vicente Bayarri, Elena Castillo, Ramón Montes, José Manuel Morlote, Emilio Muñoz, and Eduardo Palacio. 2019. "New Discoveries of Pre-Magdalenian Cave Art in the Central Area of the Cantabrian Region (Spain)." *Journal of Archaeological Science: Reports* 28 (November): 102020. <https://doi.org/10.1016/j.jasrep.2019.102020>.

⁶² Jones, Huw. 1998. "Trends in Computer-Mediated Art and Design: Examples from the Centre for Electronic Arts." *Computer Networks* 30 (20–21): 1951–60. [https://doi.org/10.1016/s0169-7552\(98\)00221-9](https://doi.org/10.1016/s0169-7552(98)00221-9).

⁶³ *Tactile 3D bas-relief from single-point perspective paintings a computer based method* P5668-5679

⁶⁴ Furferi R, Governi L, Volpe Y, et al. *From 2D to 2.5 D ie from painting to tactile model*[J]. *Graphical Models*, 2014, 76(6): 706-723. 708-723

⁶⁵ Shi J, Pan Z. *China: Computer graphics is fastest developing computer application*[J]. *Acm Siggraph Computer Graphics*, 1996, 30(2): 11-14.

⁶⁶ Piegel L A. *Ten challenges in computer-aided design*[J]. *Computer-aided design*, 2005, 37(4): 461-470.

⁶⁷ Krikke J. *Axonometry: A matter of perspective*[J]. *IEEE Computer Graphics and Applications*, 2000, 20(4): 7-11. 8

⁶⁸ Elman B A. *On their own terms: Science in China, 1550-1900*[M]. Harvard University Press, 2005. XXV

⁶⁹ Chiang Y. *Chinese calligraphy: An introduction to its aesthetic and technique*[M]. Harvard University Press, 1973. 1.

⁷⁰ Chiang Y. *Chinese calligraphy: An introduction to its aesthetic and technique*[M]. Harvard University Press, 1973. 14.

⁷¹ Elman B A. *On their own terms: Science in China, 1550-1900*[M]. Harvard University Press, 2005. 19.

⁷² Li W. *Chinese writing and calligraphy*[M]. University of Hawaii Press, 2010. 12

⁷³ Atsuji Tetsuji. *Tushuo hanzi de lishi 图说汉字的历史 (An illustrated history of Chinese characters)*. Translation into Chinese by Gao Wenhan. Shandong Huabao Chubanshe, 2005.

-
-
- ⁷⁴ Li W. *Chinese writing and calligraphy*[M]. University of Hawaii Press, 2010. 13
- ⁷⁵ Chiang Y. *Chinese calligraphy: An introduction to its aesthetic and technique*[M]. Harvard University Press, 1973. 189-193
- ⁷⁶ Wenhua Liu, Haiyang Xue. *Li Qi Bei*. He Nan Mei Shu Chu Ban She. 2007. ISBN 978-7-5401-1594-4.
- ⁷⁷ Shuang Yang, Zhang Qian Bei. *Hu Bei Mei Shu Chu Ban She*. 2014. ISBN 978-7-5394-6968-3
- ⁷⁸ Leping Shen, Yihua Wang, Lin Ji, Xiaomian Lou, Mengxia Cai. *7000 HAN ZI WU TI MAO BI SHU FA ZI DIAN*. Zhejiang Gu Ji Chu Ban She. 2005. ISBN 978-7-80715-083-1
- ⁷⁹ Chiang Y. *Chinese calligraphy: An introduction to its aesthetic and technique*[M]. Harvard University Press, 1973. 196
- ⁸⁰ Sun Y, Qian H, Xu Y. *A geometric approach to stroke extraction for the Chinese calligraphy robot*[C]//2014 IEEE International Conference on Robotics and Automation (ICRA). IEEE, 2014: 3207-3212.
- ⁸¹ Mi X F, Tang M, Dong J X. *Droplet: a virtual brush model to simulate Chinese calligraphy and painting*[J]. *Journal of Computer Science and Technology*, 2004, 19(3): 393-404.
- ⁸² Wong H T F, Ip H H S. *Virtual brush: a model-based synthesis of Chinese calligraphy*[J]. *Computers & Graphics*, 2000, 24(1): 99-113.
- ⁸³ Xu S, Lau F C M, Cheung W K, et al. *Automatic generation of artistic Chinese calligraphy*[J]. *IEEE Intelligent Systems*, 2005, 20(3): 32-39.
- ⁸⁴ Xu S, Jiang H, Lau F C M, et al. *An intelligent system for Chinese calligraphy*[C]//AAAI. 2007, 7: 1578-1583.
- ⁸⁵ Chao F, Lv J, Zhou D, et al. *Generative adversarial nets in robotic Chinese calligraphy*[C]//2018 IEEE International Conference on Robotics and Automation (ICRA). IEEE, 2018: 1104-1110.
- ⁸⁶ Jian M, Dong J, Gong M, et al. *Learning the traditional art of Chinese calligraphy via three-dimensional reconstruction and assessment*[J]. *IEEE Transactions on Multimedia*, 2019, 22(4): 970-

979.

⁸⁷ Iguchi T. *Reconsideration of the World Design Conference 1960 in Tokyo and the World Industrial Design Conference 1973 in Kyoto: Transformation of Design Theory[C]//5th International Congress of International Association of Societies of Design Research. 2013.*

⁸⁸ Baxter, M. (1995). *Product Design: Practical methods for the systematic development of new products.* London, UK: Chapman & Hall.

⁸⁹ Cawthon, N., Moere, A. (2007). *The Effect of aesthetic on the usability of data visualization. 11th International Conference Information Visualization, Washington, DC, USA, 637–648.*

⁹⁰ Sauer, J., & Sonderegger, A. (2009). *The influence of prototype fidelity and aesthetics of design in usability tests: Effects on user behaviour, subjective evaluation, and emotion. Applied Ergonomics, 40, 670–677.*

⁹¹ Sauer, J., & Sonderegger, A. (2011). *The influence of product aesthetics and user state in usability testing. Behaviour & Information Technology, 30(6), 787–796.*

⁹² Seva, R. R. Gosiaco, K. G. T., Santos, M. C. E. D., & Pangilinan, D. M. L. (2011). *Product design enhancement using apparent usability and effective quality. Applied Ergonomics, 42, 511–517.*

⁹³ Veryzer, R. W. (1993). *Aesthetic Response and the Influence of Design Principles on Product Preferences. Journal of Consumer Research, 20, 224–228.*

⁹⁴ MacDonald, A. S. (2000). *Aesthetic intelligence: optimizing the user-centred design. Journal of Engineering Design, 12(1), 37–45.*

⁹⁵ Bloch, P. H., Brunel, F. F., & Arnold, T. J. (2003). *Individual Differences in the Centrality of Visual Product Aesthetics: Concept and Measurement. Journal of Consumer Research, 29, 551–565.*

⁹⁶ Khalighy, Shahabeddin (2015) *Product design methodology supporting aesthetic evaluation. PhD thesis.*

⁹⁷ Kenya, H. (2003). *Conferência designer Hara Kenya na FAUUSP. Pós. Revista do Programa de Pós-Graduação em Arquitetura e Urbanismo da FAUUSP, 13(0), p.156. 31–33*

-
-
- ⁹⁸ Hara, K. (n.d.). *White*. (2009). P. 34-35.
- ⁹⁹ Chikit K. Au and Matthew Ming-Fai Yuen, "Unified Approach to NURBS Curve Shape Modification," *Computer-Aided Design* 27, no. 2 (February 1995): 85, [https://doi.org/10.1016/0010-4485\(95\)92148-L](https://doi.org/10.1016/0010-4485(95)92148-L).
- ¹⁰⁰ Terzopoulos D, Qin H. *Dynamic NURBS with geometric constraints for interactive sculpting*[J]. *ACM Transactions on Graphics (TOG)*, 1994, 13(2): 103-136. 103-104
- ¹⁰¹ Piegl L, Tiller W. *The NURBS book*[M]. Springer Science & Business Media, 1996. 117-118
- ¹⁰² Sanchez-Reyes J. *A simple technique for NURBS shape modification*[J]. *IEEE Computer Graphics and Applications*, 1997, 17(1): 52-59. 53
- ¹⁰³ Piegl L, Tiller W. *The NURBS book*[M]. Springer Science & Business Media, 1996. 120
- ¹⁰⁴ TzuYi Yu and Bharat K. Soni, "Application of NURBS in Numerical Grid Generation," *Computer-Aided Design* 27, no. 2 (February 1995): 147, [https://doi.org/10.1016/0010-4485\(95\)92154-K](https://doi.org/10.1016/0010-4485(95)92154-K).
- ¹⁰⁵ Piegl L, Tiller W. *The NURBS book*[M]. Springer Science & Business Media, 1996. 592
- ¹⁰⁶ Piegl L, Tiller W. *The NURBS book*[M]. Springer Science & Business Media, 1996. 432, 471
- ¹⁰⁷ *On continuous modelling of smooth contact surfaces using NURBS and application to 2D problems* P2177-2199
- ¹⁰⁸ Yongjie Zhang, Yuri Bazilevs, Samrat Goswami, Chandrajit L. Bajaj and Thomas J.R. Hughes, "Patient-Specific Vascular NURBS Modeling for Isogeometric Analysis of Blood Flow," *Computer Methods in Applied Mechanics and Engineering* 196, no. 29 (2007): 2946, <https://doi.org/10.1016/j.cma.2007.02.009>.
- ¹⁰⁹ Kemp, Martin, and William Buckland. 2004. "Animated Animals." *Nature*, no. 1997: 2004-2004. P 398
- ¹¹⁰ Piegl L, Tiller W. *The NURBS book*[M]. Springer Science & Business Media, 1996. FOREWORD
- ¹¹¹ Warwick A. *Master of Theory: Cambridge and the rise of mathematical physics*[M]. University

of Chicago Press, 2003. 86-88

¹¹² Kunes J. *Dimensionless physical quantities in science and engineering*[M]. Elsevier, 2012. 1

¹¹³ Kunes J. *Dimensionless physical quantities in science and engineering*[M]. Elsevier, 2012.

¹¹⁴ Cooke P. *Gustave Moreau and Ingres*[J]. *Burlington Magazine*, 2014, 156(1333): 219-227. 221

¹¹⁵ Bell J C. *Light and color in caravaggio's" supper at emmaus"*[J]. *Artibus et historiae*, 1995: 139-170. 173

¹¹⁶ Jean Auguste Dominique Ingres, *The Spring, 1820-1856, Oil on canvas, H. 163; W. 80 cm., Paris, Musée d'Orsay*

¹¹⁷ Kleinbub C K. *Vision and the Visionary in Raphael*[M]. Penn State Press, 2011. Chapter 4

¹¹⁸ Honour H, Fleming J. *A world history of art*[M]. Laurence King Publishing, 2005. 357

¹¹⁹ Ian Chilvers - *The Concise Oxford Dictionary of Art and Artists (1991, The Concise Oxford Dictionary of Art and Artists)*. 383

¹²⁰ Honour H, Fleming J. *The visual arts: A History* [M]. Pearson Education, 2010. 361

¹²¹ <http://www.hellenicaworld.com/Greece/Science/en/SchoolAthens.html>

¹²² Honour H, Fleming J. *The visual arts: A history*[M]. Pearson Education, 2010. 362

¹²³ <https://www.museivaticani.va/content/museivaticani/en/collezioni/musei/stanze-di-raffaello/stanza-della-segnatura/scuola-di-atene.html> (accessed at 12/10/2022)

¹²⁴ Kemp M. *Leonardo da Vinci: The 100 Milestones*[M]. Union Square & Co., 2019. 114

¹²⁵ Farling S. *1001 Paintings you must see before you die*[J]. 2016. 139,147,151,152

¹²⁶ <https://www.wikiart.org/en/raphael>

¹²⁷ Farling S. *1001 Paintings you must see before you die*[J]. 2016. 16-18

-
-
- ¹²⁸ Shearman J. Raphael as architect[J]. *Journal of the Royal Society of Arts*, 1968, 116(5141): 388-409. 389-391
- ¹²⁹ Rowland I D. Raphael, Angelo Colocci, and the genesis of the architectural orders[J]. *The Art Bulletin*, 1994, 76(1): 81-104
- ¹³⁰ Chilvers, I. (Ed.). (1996). *The concise Oxford dictionary of art and artists*. Oxford University Press, USA. 382
- ¹³¹ Honour H, Fleming J. *The visual arts: A history*[M]. Pearson Education, 2010. 362
- ¹³² Hoeniger C. Christian K. Kleinbub. *Vision and the Visionary in Raphael*. University Park: The Pennsylvania State University Press, 2011. xiii+ 208 pp. index. illus. bibl. \$89.95. ISBN: 978-0-271-03704-2[J]. *Renaissance Quarterly*, 2011, 64(4): 1219-1220.
- ¹³³ Octave Uzanne, *JEAN-AUGUSTE-DOMINIQUE INGRES: PAINTER*. The BALLANTYNE PRESS. VII
- ¹³⁴ Werner A. Monsieur Ingres-Magnificent" Reactionary"[J]. *The Antioch Review*, 1966, 26(4): 491-500. 497
- ¹³⁵ Etro F, Marchesi S, Stepanova E. Liberalizing art. Evidence on the Impressionists at the end of the Paris Salon[J]. *European Journal of Political Economy*, 2020, 62: 101857
- ¹³⁶ Octave Uzanne, *JEAN-AUGUSTE-DOMINIQUE INGRES: PAINTER*. The BALLANTYNE PRESS. XVIII
- ¹³⁷ Kenneth Clarke cited in Henry A. Strobel, *Reflections: Personal Essays* (Thomson-Shore, 1999), 62.
- ¹³⁸ C. H. Collins Baker, "Reflections on the Ingres Exhibition," *The Burlington Magazine for Connoisseurs* 39, no. 220 (1921): 41, www.jstor.org/stable/861323.
- ¹³⁹ Wendy Leeks, "Ingres Other-Wise," *Oxford Art Journal* 9, no. 1 (1986): 31. www.jstor.org/stable/1360370.
- ¹⁴⁰ <https://www.wikiart.org/en/raphael/all-works#!#filterName:all-paintings->

[chronologically,resultType:masonry](#)

¹⁴¹ <https://www.wikiart.org/en/raphael/jacob-s-encounter-with-rachel-1519>

¹⁴² Sanzio R, Joannides P. *The drawings of Raphael: with a complete catalogue*[M]. Univ of California Press, 1983. 52

¹⁴³ Alexandre Cabanel, *The Birth of Venus, 1820-1856, Oil on canvas, H. 130; W. 225 cm., Paris, Musée d'Orsay.*

¹⁴⁴ Furferi R, Governi L, Vanni N, et al. *Tactile 3D bas-relief from single-point perspective paintings: a computer-based method*[J]. *Journal of Information & Computational Science*, 2014, 11(16): 5667-5680. 5668-5679

¹⁴⁵ Furferi R, Governi L, Volpe Y, et al. *From 2D to 2.5 D ie from painting to tactile model*[J]. *Graphical Models*, 2014, 76(6): 706-723. 708-723

¹⁴⁶ Steckel R H. *New light on the "Dark Ages": the remarkably tall stature of northern European men during the medieval era*[J]. *Social Science History*, 2004, 28(2): 211-229

¹⁴⁷ VAN ZANDEN J L. *Wages and the standard of living in Europe*[J]. *European Review of Economic History*. 1500–1800

¹⁴⁸ Clement Kleinstreuer, *Two-Phase Flow: Theory and Applications (London: Taylor and Francis, 2003), 77-79.*

¹⁴⁹ Zhang Y, Bazilevs Y, Goswami S, et al. *Patient-specific vascular NURBS modeling for isogeometric analysis of blood flow*[J]. *Computer methods in applied mechanics and engineering*, 2007, 196(29-30): 2943-2959. 2949.

¹⁵⁰ Kemp M. *Luold Looking: David Hockney's drawings using the camera lucida*[J]. *NATURE-LONDON-*, 1999: 524-524.

¹⁵¹ Piegl L, Tiller W. *The NURBS book*[M]. Springer Science & Business Media, 1996. 117-120

¹⁵² Gruber T R, Olsen G R. *An ontology for engineering mathematics*[C]//*Principles of Knowledge Representation and Reasoning*. Morgan Kaufmann, 1994: 258-269.

-
-
- ¹⁵³ Li W. *Chinese writing and calligraphy*[M]. University of Hawaii Press, 2010. 52, 178
- ¹⁵⁴ Li W. *Chinese writing and calligraphy*[M]. University of Hawaii Press, 2010. 41,107,173
- ¹⁵⁵ Chiang Y. *Chinese calligraphy: An introduction to its aesthetic and technique*[M]. Harvard University Press, 1973. 107
- ¹⁵⁶ Ferdinand P. Beer, E. Russell Johnston, Jr., John T. DeWolf, David F. Mazurek. *STATICS AND MECHANICS OF MATERIALS*. McGraw-Hill. 692. ISBN 978-0-07-338015-5
- ¹⁵⁷ Ferdinand P. Beer, E. Russell Johnston, Jr., John T. DeWolf, David F. Mazurek. *STATICS AND MECHANICS OF MATERIALS*. McGraw-Hill. 692. ISBN 978-0-07-338015-5
- ¹⁵⁸ Piegl L, Tiller W. *The NURBS book*[M]. Springer Science & Business Media, 1996. 119
- ¹⁵⁹ Yuho Tseng, Youhe Zeng (1993). *A History of Chinese Calligraphy*. The Chinese University Press. p. xxv. ISBN 962-201-426-7
- ¹⁶⁰ Yee, Chiang (1974). *Chinese Calligraphy: An Introduction to Its Aesthetic and Technique, Third Revised and Enlarged Edition*. Harvard University Press. p. 1-2. DOI: 10.2307/j.ctvjghxvf
- ¹⁶¹ Yee, Chiang (1974). *Chinese Calligraphy: An Introduction to Its Aesthetic and Technique, Third Revised and Enlarged Edition*. Harvard University Press. p. 151. DOI: 10.2307/j.ctvjghxvf
- ¹⁶² Yuho Tseng, Youhe Zeng (1993). *A History of Chinese Calligraphy*. The Chinese University Press. p. 228. ISBN 962-201-426-7
- ¹⁶³ State Language Commission (1997). *Xiandai Hanyu Tongyongzi Bishun Guifan*. Yuwen Chubanshe. 2
- ¹⁶⁴ Unknown (185). *He Yang Ling Cao Quan Bei*.
- ¹⁶⁵ Unknown (186 A.D.). *Han Gu Gu Cheng Chang Dang Yin Ling Zhang Jun Biao*.

-
-
- ¹⁶⁶ Ji Zhao (1110 A.D.). <https://www.dpm.org.cn/lemmas/240221.html>
- ¹⁶⁷ Patricia Buckley Ebrey, Maggie Bickford, Peter K. Bol, John W. Chaffee, ShShin-Yihao, Ronald C. Egan, Asaf Goldschmidt, Charles Hartman, Tsuyoshi Kojima, Joseph S. C. Lam, Ari Daniel Levine, Paul Jakov Smith, Stephen H. West Emperor Huizong and Late Northern Song China: The Politics of Culture and the Culture of Politics. Harvard University Asia Center. 4, 20, 260, 262. ISBN: 0674021274; 9780674021273
- ¹⁶⁸ Jastrzebski, D. (1959). *Nature and Properties of Engineering Materials* (Wiley International ed.). John Wiley & Sons, Inc.
- ¹⁶⁹ Harrist Jr R E. *The Art of Calligraphy in Modern China*[J]. 2003. 406
- ¹⁷⁰ Kraus, R. C. (1991). *Brushes with power: Modern politics and the Chinese art of calligraphy*. University of California Press. 117
- ¹⁷¹ 曾韶翔 (2010). 郭沫若书法艺术的美学特征探析. *China Academic Journal Electronic Publishing House*. 63. DOI: 10.16142/j.cnki.gmrkx.2010.04.012
- ¹⁷² 徐立昕, 宣海生 (2012). 郭沫若楷书研究. *China Academic Journal Electronic Publishing House*. 63-64. 1003- 7225 (2012) 01- 0062- 05
- ¹⁷³ <https://www.diyiziti.com/Builder/123>
- ¹⁷⁴ Wang L, Li X, Lin J, et al. *Studies of modeling and simulation method of temperature rise in medium-voltage switchgear and its optimum design*[J]. *IEEE Transactions on Components, Packaging and Manufacturing Technology*, 2017, 8(3): 439-446.
- ¹⁷⁵ Kim K Y, Samad A, Benini E. *Design Optimization of Fluid Machinery: Applying Computational Fluid Dynamics and Numerical Optimization*[M]. John Wiley & Sons, 2019.
- ¹⁷⁶ Ye X, Liu H, Chen L, et al. *Reverse innovative design—an integrated product design methodology*[J]. *Computer-aided design*, 2008, 40(7): 812-827.
- ¹⁷⁷ Bartoll J. *The early use of Prussian blue in paintings*[C]//*Proceedings of the 9th International Conference on NDT of Art*. 2008. 5-6
- ¹⁷⁸ <https://competition.adesignaward.com/gooddesign.php?ID=90333>